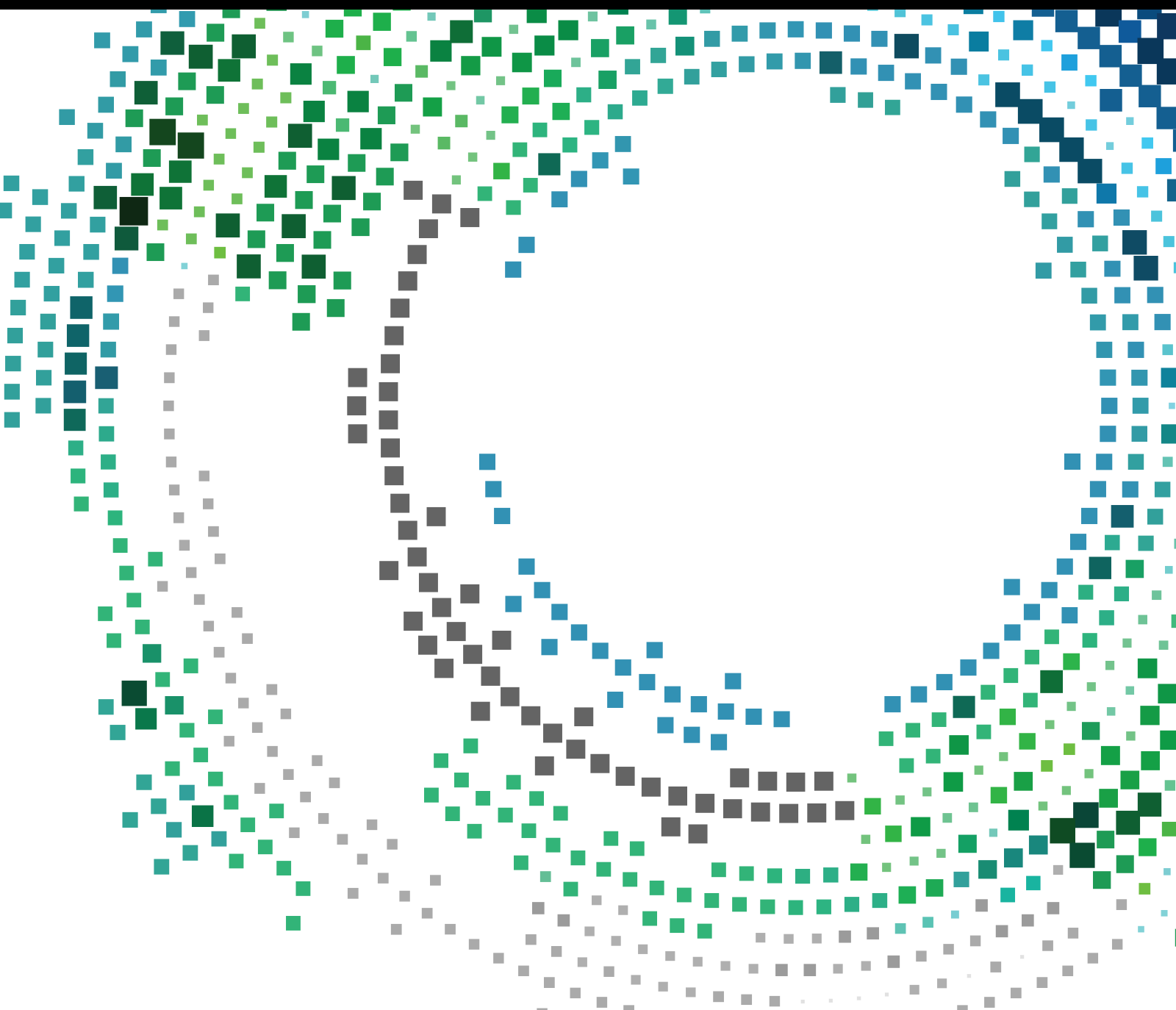


# Enabling Technologies for Smart Mobile Services 2020

Special Issue Editor in Chief: Peter Brida

Guest Editors: Ondrej Krejcar and Stavros Kotsopoulos





---

# **Enabling Technologies for Smart Mobile Services 2020**

Mobile Information Systems

---

## **Enabling Technologies for Smart Mobile Services 2020**

Special Issue Editor in Chief: Peter Brida

Guest Editors: Ondrej Krejcar and Stavros  
Kotsopoulos



---

Copyright © 2022 Hindawi Limited. All rights reserved.

This is a special issue published in "Mobile Information Systems." All articles are open access articles distributed under the Creative Commons Attribution License, which permits unrestricted use, distribution, and reproduction in any medium, provided the original work is properly cited.



# Chief Editor

Alessandro Bazzi, Italy

## Editorial Board

Hammad Afzal, Pakistan  
Ramon Agüero, Spain  
Sikandar Ali, China  
Markos Anastassopoulos, United Kingdom  
Marco Anisetti, Italy  
Claudio Agostino Ardagna, Italy  
DR. ASHISH BAGWARI, India  
Jose M. Barcelo-Ordinas, Spain  
Luca Bedogni, Italy  
Paolo Bellavista, Italy  
Dr. Robin Singh Bhadoria, India  
Nicola Bicocchi, Italy  
Peter Brida, Slovakia  
Carlos Tavares Calafate, Spain  
María Calderon, Spain  
Juan-Carlos Cano, Spain  
Salvatore Carta, Italy  
Yuh-Shyan Chen, Taiwan  
Pengyun Chen, China  
Wenchi Cheng, China  
Massimo Condoluci, Sweden  
Almudena Díaz Zayas, Spain  
Ahmed Farouk, Canada  
Filippo Gandino, Italy  
Jorge Garcia Duque, Spain  
L. J. García Villalba, Spain  
Romeo Giuliano, Italy  
Francesco Gringoli, Italy  
Rutvij Jhaveri, India  
Wei Jia, China  
Adrian Kliks, Poland  
Dr. Manoj Kumar Kumar, India  
Quanzhong Li, China  
Ding Li, USA  
Jian-Xun Liu, China  
Juraj Machaj, Slovakia  
Mirco Marchetti, Italy  
Elio Masciari, Italy  
Eduardo Mena, Spain  
Massimo Merro, Italy  
Aniello Minutolo, Italy  
Jose F. Monserrat, Spain  
Raul Montoliu, Spain  
Mario Muñoz-Organero, Spain





HAMAD NAEEM, China, China  
Giovanni Nardini, Italy  
Mehrbakhsh Nilashi, Malaysia  
Francesco Palmieri, Italy  
José J. Pazos-Arias, Spain  
Marco Picone, Italy  
Alessandro Sebastian Podda, Italy  
Amon Rapp, Italy  
Michele Ruta, Italy  
Neetesh Saxena, United Kingdom  
Filippo Sciarrone, Italy  
Florian Scioscia, Italy  
Dr. Mueen Uddin, Brunei Darussalam  
Michael Vassilakopoulos, Greece  
Ding Xu, China  
Laurence T. Yang, Canada  
Kuo-Hui Yeh, Taiwan  
Yugen Yi, China  
Jianming Zhu, China

# Contents



## **Enabling Technologies for Smart Mobile Services 2020**

Peter Brida , Ondrej Krejcar , and Stavros Kotsopoulos  
Editorial (3 pages), Article ID 9870706, Volume 2022 (2022)

## **Impact of GPS Interference on Time Synchronization of DVB-T Transmitters**

Juraj Machaj , Peter Brida , Norbert Majer , and Roman Sčehovič   
Research Article (11 pages), Article ID 8812333, Volume 2021 (2021)





## **Mobile Coverage in Rural Sweden: Analysis of a Comparative Measurement Campaign**

P. G. Sudheesh  and Jaap van de Beek   
Research Article (13 pages), Article ID 8869534, Volume 2021 (2021)


## **An Adaptive Grid and Incentive Mechanism for Personalized Differentially Private Location Data in the Local Setting**

Kangsoo Jung and Seog Park   
Research Article (12 pages), Article ID 8898223, Volume 2020 (2020)



## **User Acceptance of Internet of Vehicles Services: Empirical Findings of Partial Least Square Structural Equation Modeling (PLS-SEM) and Fuzzy Sets Qualitative Comparative Analysis (fsQCA)**

Yikai Liang , Guijie Zhang , Feng Xu , and Weijie Wang   
Research Article (22 pages), Article ID 6630906, Volume 2020 (2020)


## **A Smart System for Sitting Posture Detection Based on Force Sensors and Mobile Application**

Slavomir Matuska , Martin Paralic, and Robert Hudec  
Research Article (13 pages), Article ID 6625797, Volume 2020 (2020)

## **Research and Development of Palmprint Authentication System Based on Android Smartphones**

Xinman Zhang , Kunlei Jing , and Guokun Song  
Research Article (16 pages), Article ID 8846192, Volume 2020 (2020)


## **A Method to Diagnose, Improve, and Evaluate Children's Learning Using Wearable Devices Such as Mobile Devices in the IoT Environment**

Mohammad Moradi  and Kheirollah Rahsepar Fard  
Research Article (25 pages), Article ID 8850244, Volume 2020 (2020)

## **A Smart Parking System Based on Mini PC Platform and Mobile Application for Parking Space Detection**

Vladimir Sobeslav  and Josef Horalek   
Research Article (15 pages), Article ID 8875301, Volume 2020 (2020)

## **Smart Radio Resource Management for Content Delivery Services in 5G and Beyond Networks**

Dominik Neznik, Lubomir Dobos, and Jan Papaj   
Research Article (14 pages), Article ID 8898798, Volume 2020 (2020)

## Editorial

# Enabling Technologies for Smart Mobile Services 2020

**Peter Brida** <sup>1</sup>, **Ondrej Krejcar** <sup>2</sup>, and **Stavros Kotsopoulos**<sup>3</sup>

<sup>1</sup>University of Zilina, Zilina, Slovakia

<sup>2</sup>University of Hradec Králové, Hradec Králové, Czech Republic

<sup>3</sup>University of Patras, Patras, Greece

Correspondence should be addressed to Peter Brida; [peter.brida@fel.uniza.sk](mailto:peter.brida@fel.uniza.sk)

Received 9 March 2022; Accepted 9 March 2022; Published 20 April 2022

Copyright © 2022 Peter Brida et al. This is an open access article distributed under the Creative Commons Attribution License, which permits unrestricted use, distribution, and reproduction in any medium, provided the original work is properly cited.

Mobility of people (users) plays an important role in day-to-day life, and currently these users are overwhelmed by a variety of services. Mobile services belong to an essential segment of modern communication services, and new trends in these consist of smart services, defined as a variety of context-aware services. Additionally, smart mobile devices (smartphones) can fulfil an astonishingly wide range of demands of users and providers. One of the reasons behind mobile development is the ever-growing computing power and communication capabilities of mobile devices. Furthermore, smart mobile devices offer new human-computer interfaces like speech recognition or touchscreens and employ powerful sensors, such as GNSS receivers, inertial sensors, or new communication platforms. The mentioned supporting technologies enable the provision of a completely new spectrum of context-aware, personalized, and intelligent services and applications. This raises device utilization issues, not only from the communication point of view but also for device smartness purposes. Smartphones, in fact, are very powerful devices with constantly increasing processing, communication, and sensing capabilities, and very recently, a large plethora of proposals have emerged to leverage those capabilities to contribute to the information production process. Smart mobile devices can be used in the health care sector and in the transportation sector, and in addition, multimedia services form a very interesting sector.

Because a variety of wireless telecommunication services need position information for real-time service operation, almost all modern devices are equipped with GNSS sensor. However, it cannot always be used due to the corresponding

received signal strength level being too low or there is no signal present at all. In these cases, alternative positioning solutions are available or can be implemented. These alternative positioning solutions mainly utilize the improving mobile device performance such as increasing processing, communication, and sensing capabilities. A challenging wireless mobile environment impacts on the delivering of these services, as each service is sensitive to the immediate status of the radio channel in different ways, and these need to be considered in the services design.

Recently, we are witnessing a dynamic cloud computing evolution in nearly all areas of human activities exploiting information technologies. The implementation of solutions based on the idea of cloud services produces new challenges in areas such as management, security, technical solutions, infrastructure modelling, and mobile devices support.

This Special Issue aims at reporting on some of the recent research efforts on this increasingly important topic. The nine accepted papers in this issue cover interesting research topics: effective radio spectrum allocation, complex outdoor smart parking system based on IoT, utilization of IoT in education process, an effective and full-function palmprint authentication system regarding the application on an Android smartphone, smart chair system for sitting posture detection based on IoT, determination of behavioral intention to accept IoV (Internet of Vehicles) services, privacy issue in location-based services, analysis of mobile signal strength experienced by users, and the impact of the GPS interference caused by jamming and spoofing on the function of the DVB-T SFN network.

The paper entitled “Smart Radio Resource Management for Content Delivery Services in 5G and Beyond Networks” by D. Neznik et al. presents the idea, that effective spectrum allocation to devices is not an option but a requirement in a huge data flow environment of the wireless communications, if one wants to ensure acceptable speed and quality of the connection and to provide adequate quality of the services. Each of the selected methods for radio resource management has some advantages and disadvantages in the evaluation of results. The process of channel allocation with different methods for IEEE 802.11xx networks that are in the focus of our research in the sphere of wireless communication. The proposed and tested algorithms show the effective channel allocation by a method based on Fuzzy Logic, Game Theory, and the Smart Method.

The aim of the paper “A Smart Parking System Based on Mini PC Platform and Mobile Application for Parking Space Detection” by V. Sobeslav and J. Horalek is to propose a complex outdoor smart parking IoT system based on the mini PC platform with the pilot implementation, which would provide a solution for the aforementioned problem. Current outdoor car park management is dependent on human personnel keeping track of the available parking lots or a sensor-based system that monitors the availability of each car. The proposed solution utilizes a modern IoT approach and technologies such as mini PC platform, sensors, and IQRF. When compared to a specialized and expensive system, it is a solution that is cost-effective and has the potential in its expansion and integration with other IoT services.

The purpose of the paper “A Method to Diagnose, Improve, and Evaluate Children’s Learning Using Wearable Devices Such as Mobile Devices in the IoT Environment” by M. Moradi and K. Rahsepar is to transform the traditional classroom into a modern classroom in order to increase the ease and efficiency of the teaching process. The method includes phases of diagnosis and improvement. In the diagnose phase, the classroom is equipped with modern items such as Internet of Things (IoT) and game-based learning. In the improvement phase, the field method is used to extract and weight the effective criteria in improving the educational status. As a result, the proposed educational method can increase the learning performance of children.

The paper entitled “Research and Development of Palmprint Authentication System Based on Android Smartphones” by X. Zhang et al. presents the development an effective and full-function palmprint authentication system regarding the application on an Android smartphone, which bridges the algorithmic study and application of palmprint authentication. In more detail, an overall system framework is designed with complete functions, including palmprint acquisition, key points location, ROI segmentation, feature extraction, and feature coding. Basically, we develop a palmprint authentication system having user-friendly interfaces and good compatibility with the Android smartphone. Authors provide an open technology to extend the biometric methods to real-world applications. On the public PolyU databases, simulation results suggest that the improved algorithm outperforms the original one with a promising accu-

racy of 100% and a good speed of 0.041 seconds. In real-world authentication, the developed system achieves an accuracy of 98.40% and a speed of 0.051 seconds. All the results verify the accuracy and timeliness of the developed system.

The paper “A Smart System for Sitting Posture Detection Based on Force Sensors and Mobile Application” by S. Matuska et al. presents a smart system for sitting posture detection based on force sensors and mobile application. The major problem is the spinal pain caused by the poor sitting posture on the office chair. The smart chair has six flexible force sensors. The IoT node based on Arduino connects these sensors into the system. The system detects wrong seating positions and notifies the users. In advance, authors develop a mobile application to receive those notifications. The user gets feedback about sitting posture and additional statistical data. The data from smart chairs are collected by a private cloud solution from QNAP and are stored in the MongoDB database. The Node-RED application was used for the whole logic implementation.

The paper entitled “User Acceptance of Internet of Vehicles Services: Empirical Findings of Partial Least Square Structural Equation Modeling (PLS-SEM) and Fuzzy Sets Qualitative Comparative Analysis (fsQCA)” by Y. Liang et al. presents the study that identifies the determinants of behavioral intention to accept IoV (Internet of Vehicles) services by using an integrated model that combines UTAUT, perceived risk theory, and initial trust theory. The study uses Partial Least Square Structural Equation Modeling (PLS-SEM) and Fuzzy Sets Qualitative Comparative Analysis (fsQCA) methods to explore the role of determinants in consumers’ intention to accept and purchase IoV-based services. Specifically, the net effects of each antecedent factor on intention are analyzed by conventional correlational techniques (PLS-SEM). The direct effects of performance expectancy, price value, habit, and initial trust on intention are found to be significant. Despite the determinants (e.g., effort expectancy, social influence, facilitating conditions, hedonic motivation, and perceived risk) are found to be nonsignificant effects on intention, however, it cannot be said they are not important to intention to accept IoV-based services, due to the existence of causal complexity. For the high levels of causal complexity, fsQCA provides a more nuanced understanding of how these antecedent conditions fit together to affect consumers’ intention to accept and purchase IoV-based services. The results from fsQCA provide twelve different configurations to achieve high levels of behavioral intention to accept IoV services and eight causal paths equifinally to lead to the negation of behavioral intention to accept IoV services. The findings provide relevant insights and marketing suggestions for incentivizing consumers to accept IoV-based services.

For the growth of the location-based services, more accurate and various types of personal location data are required. However, concerns about privacy violations are a significant obstacle to obtain personal location data. In paper “An Adaptive Grid and Incentive Mechanism for Personalized Differentially Private Location Data in the Local Setting” by K. Jung and S. Park, authors propose a local

differential privacy scheme in an environment where there is no trusted third party to implement privacy protection techniques and incentive mechanisms to motivate users to provide more accurate location data. The proposed local differential privacy scheme allows a user to set a personalized safe region that he/she can disclose and then perturb the user's location within the safe region. It is the way to satisfy the user's various privacy requirements and improve data utility. The proposed incentive mechanism has two models, and both models pay the incentive differently according to the user's safe region size to motivate to set a more precise safe region. We verify the proposed local differential privacy algorithm and incentive mechanism can satisfy the privacy protection level while achieving the desirable utility through the experiment.

The paper titled "Mobile Coverage in Rural Sweden: Analysis of a Comparative Measurement Campaign" by P. G. Sudheesh and J. Beek presents a framework for analyzing mobile signal strength experienced by users. Based on measured signal strength, a coverage map has been made via IDW interpolation. Various analyses are carried out on signal strength over residential areas and roads of Norrbotten. Further, measurements are compared to those of Östergötland and it was found that both municipalities have almost similar measurements. By analyzing coverage across all 14 municipalities of Norrbotten, in contrast to the suspicion that rural areas have poor signal strength, we found that 2G and 4G provide satisfactory results. However, 3G fails to provide coverage in some areas. This is worse in some areas, resulting in more than 50% of areas to be outside coverage area at some places. These areas are mostly near the Finland border, which results in the fact that roaming and additional charges may be applicable to the 3G user in these areas.

In the paper titled "Impact of GPS Interference on Time Synchronization of DVB-T Transmitters" by J. Machaj et al., the impact of the GPS (Global Positioning System) interference caused by jamming and spoofing on the function of the DVB-T SFN network was investigated. The transmitters in DVB-T SFN use GPS signals for synchronization of data in the network, to avoid interference and sustain the quality of received signals. With an increased number of GPS interference caused by jammers, it is required to understand how DVB-T transmitters can cope with the affected GPS signals. We have performed experiments in two scenarios: in the first scenario, the GPS receiver at one of the transmitters was affected by jamming and in the second scenario by spoofing of GPS signals. Based on achieved results, it can be concluded that the DVB-T SFN network is able to cope with the jamming of GPS signals, in case that it does not last too long. From the results, it is obvious that the SNR of the received DVB-T signal was reduced, resulting in increased BER. However, the receiver was still able to decode the video stream without any significant decrease in quality.

## Conflicts of Interest

The authors declare no conflict of interest.

## Acknowledgments

Finally, guest editors of this Special Issue would like to thank all authors who have submitted their manuscripts for considering the Sensors journal and the reviewers for their hard work during the review process. We hope that the readers enjoy reading the articles within this Special Issue. Finally, the guest editors wish to acknowledge the partial support from the Slovak Grant Agency, Project No. 1/0626/19 "Research of mobile objects localization in IoT environment".

*Peter Brida  
Ondrej Krejcar  
Stavros Kotsopoulos*

## Research Article

# Impact of GPS Interference on Time Synchronization of DVB-T Transmitters

Juraj Machaj <sup>1,2</sup>, Peter Brida <sup>1,2</sup>, Norbert Majer <sup>3</sup>, and Roman Sčehovič <sup>3</sup>

<sup>1</sup>Department of Multimedia and Information-Communication Technology,  
Faculty of Electrical Engineering and Information Technology, University of Zilina, Žilina 010 26, Slovakia

<sup>2</sup>University Science Park, University of Zilina, Žilina 010 26, Slovakia

<sup>3</sup>Research Institute of Posts and Telecommunications, Banská Bystrica 974 05, Slovakia

Correspondence should be addressed to Juraj Machaj; [juraj.machaj@fel.uniza.sk](mailto:juraj.machaj@fel.uniza.sk)

Received 17 September 2020; Revised 5 October 2020; Accepted 31 March 2021; Published 15 April 2021

Academic Editor: Adrian Kliks

Copyright © 2021 Juraj Machaj et al. This is an open access article distributed under the Creative Commons Attribution License, which permits unrestricted use, distribution, and reproduction in any medium, provided the original work is properly cited.

Nowadays, the Global Positioning System (GPS) is widely used in all aspects of our lives. GPS signals are not used only in positioning and navigation applications and services in transport and military, but, thanks to quite precise information about time, also for synchronization of world trade and synchronization of wireless transmitters. However, with the recent spread of location-based services, a large number of GPS jammers had appeared. Use of these jammers is prohibited by law; however, their use is gaining popularity especially in the transport segment since jammers can be used to trick vehicle onboard units and help avoid paying toll fees on highways or avoid tracking of company cars when used privately. In this paper, we will investigate the impact of GPS interference caused by jamming and spoofing on the synchronization of Single Frequency Network (SFN) Digital Video Broadcasting–Terrestrial (DVB-T) transmitters. Since GPS signals are used in the DVB-T SFN to provide synchronization which is crucial for the correct network operation, the interference of GPS signals can cause problems with signal distribution. Thus, signals received from a DVB-T SFN network might be out of synchronization and disrupt the service for users.

## 1. Introduction

Recently Global Navigation Satellite System (GNSS) positioning systems are being widely implemented in all areas of our lives. GNSS systems are only not used for positioning and navigation purposes anymore but also for purposes of time synchronization in different applications. However, the GNSS and mainly GPS applications are widespread in all aspects of our daily life, for example, monitoring of company cars movement of tolling systems [1, 2]. Therefore, some people are trying to trick the system and are using GPS jammers. Although the use of GPS jammers is prohibited by the law in the majority of countries, it is relatively easy to get one shipped into any country and start using it.

The use of GPS jammers can potentially cause significant problems in various applications, for example, GPS-like signals are used at airports for air traffic control and

navigation of planes during critical parts of the flight, like landing procedure for example. There have been reported cases when GPS jammer, used to hide the use of company vehicle for personal purposes, has caused disruption of airport services.

Moreover, GPS signals are widely used for time synchronization purposes in wireless networks as well as fixed networks, transport system, and financial transaction systems nowadays.

Recently, there has been a lot of studies focusing on the detection and mitigation of jamming and spoofing interference on GPS signals. A handful of solutions was proposed to detect the interference caused by jammers and spoofers. Jamming detection can be performed relatively easily as jammers transmit signals in the same band as GPS but with a higher amplitude, thus causing higher error rates in the received data or loss of GPS signals.



On the other hand, the detection of spoofing attacks is more complicated since the interference signal is mimicking the signals transmitted by GPS satellites. The solutions for the detection of GPS spoofing are based on monitoring of received power [3], spatial processing [4], Time of Arrival (TOA) Discrimination [5], Signal Quality Monitoring [6], distribution analysis of the correlator output [7], or consistency checks [8, 9]. Nevertheless, these solutions are not widely implemented in the GPS receivers since some special capabilities of the receiver, for example, L2 reception, correlators, multiple antennas, and so forth, are usually required [10].

However, the impact of GPS signal interferences caused by jamming and spoofing on systems used for time synchronization was not studied to a large extent yet. Therefore, we will focus on the impact of GPS attacks on the time synchronization of DVB-T transmitters in SFN configuration in this paper. In DVB-T SFN, it is important to have good synchronization of transmitters so signals can be considered as multipath copies of the same signal. Tight synchronization of the transmitters can be achieved using GPS signals, which can provide time synchronization with accuracy up to nanoseconds, while synchronization required by the DVB-T SFN networks is in microseconds. For the specific implementation of DVB-T SFN in Slovakia, the required synchronization accuracy is  $224\ \mu\text{s}$ , due to the physical separation of transmitters in the range of 64 km as well as setting of the guard interval in OFDM signals.

The main contribution of the paper is the analysis of the DVB-T SFN operation in a situation when one of the transmitters is affected by the interference of GPS signal used for synchronization. The analysis of the results shows that the implementation of some spoofing detection algorithms is required in order to make the system functionality reliable under a spoofing attack. It is important to note here that spoofing attack may be aimed on other applications which, however, can also affect the operation DVB-T SFN network that can be considered a part of the safety infrastructure, as in case of emergency, it can be used to spread safety information among citizens.

The rest of the paper is organised as follows: Section 2 provides an overview of DVB-T SFN networks as well as GPS interferences, Section 3 describes the testing setup, achieved results will be presented in Section 4, and Section 5 will conclude the paper.

## 2. Related Work

With the increased use of GPS systems in our daily life, also the number of so-called attacks on GPS services has increased. These attacks are commonly caused by devices causing interference of GPS signals. Due to increased interference of GPS signals, the attention of the research community was drawn to the development of solutions that are able to detect GPS interferences and thus provide some kind of warning to the users affected. In this section, we will provide an overview of GPS interferences and approaches of their detection, time synchronization using GPS, and a description of the DVB-T SFN network.

*2.1. GPS Interference.* GPS signals are vulnerable to many signals, which is caused by the low power level of signals received by the device. In civil code GPS L1 C/A, the power of the received signal can be as low as  $-158.5\ \text{dBW}$  [11]. The GPS signals can therefore be affected by any transmitter operating at frequencies near to the GNSS bands with high transmission power or because of imperfections of implementation or malfunction of wireless systems [12]. Such interferences are considered to be unintentional and can be caused for example by DVB-T transmitters [13]. A method to assess the robustness of GPS signal in the presence of unintentional interference has been proposed in [14].

Unfortunately, unintentional interference is not the only problem GPS receivers have to face. Intentional GPS jamming can be caused by jammers that transmit noise-like signals on frequencies in the same frequency band as the GPS signals, thus causing loss of GPS signal reception. Jamming can be performed using different types of signals, the most common types of jamming are pulse jamming, spot jamming, barrage noise jamming, sweep jamming, and repeater jamming [15]. However, from the work presented in [16], it seems most of the publicly available jammers use swept tone method for jamming the GPS signals. From the tests, it was also concluded that the effective range of GPS jammers can be from 300 m up to 8.7 km.

On top of these relatively simple jamming approaches, it is possible to perform spoofing attacks on GPS services. Spoofing attacks can be performed in two ways, by re-broadcasting GPS signals recorded at another place or time (called meaconing) and by generating and transmitting modified satellite signals. Spoofing attacks can be much harder to detect since the receiver is still able to decode all GPS data without significant errors; however, these data are faulty. To detect spoofing of the GPS signals, additional features of the GPS receiver have to be implemented. Among approaches proposed to detect GPS spoofing methods like detection of unusual values in power-related parameters, monitoring of time-related parameters, spatial processing, and use of hybrid navigation, for example, GNSS + INS (Inertial Navigation System) in case of navigation services are used [17]. However, these are not suitable for static implementation with a single GPS receiver.

*2.2. Time Synchronization Using GPS.* The GPS signals not only are used for tracking purposes but can provide accurate time information as well. This can be done thanks to the fact that all GPS satellites are tightly synchronized to national and international standards. Therefore, GPS signals can be processed by the master clock, time servers, or reference clocks and thus provide accurate time synchronization to a variety of applications. The accuracy of the GPS synchronization is typically in the range of nanoseconds if devices are synchronized directly by GPS signals, up to milliseconds with accuracy depending on the protocol used to distribute the timing information among the devices [18].

Since GPS can provide accuracy close to atomic clocks and eliminates manual clock setting, it allows correlating events that are time-stamped by different clocks. There is a

vast number of applications that rely on GPS time synchronization including, legally validated time stamps, operational efficiency, regulatory compliance, and secure networking.

Characteristics of the GPS timing modules for accurate time synchronization were investigated in [19]. The authors have used M12M timing receivers to measure relative time error between generated PPS (pulse per second) and 100 PPS signals. The achieved mean timing offset between two receivers was 14 ns with a standard deviation of 13 ns without the implementation of data correction. The authors conclude that the difference might be higher for receivers placed further apart, as in such case, signals from different satellites will be received.

The GPS time synchronization with nanosecond accuracy with receivers in a region within 10 km was described in [20]. The authors were evaluating the impact of imprecise position in fixed position timing application and proposed a weighting algorithm that allowed them to achieve nanosecond level timing accuracy using GPS L1CA signals.

Based on data in [20–23], the influence of different error sources on the timing synchronization is summarized in Table 1.

From the table, it can be seen that the most important sources of errors are user clock bias and the impact of the ionospheric delay [21]. The user clock bias can be solved in the receiver for example by the implementation of advanced signal processing and carrier phase measurements [22].

**2.3. DVB-T SFN Network.** The DVB-T standard specifies characteristics of channel coding, modulation, and framing structure for transmission of digital television signals [24]. The Coded Orthogonal Frequency Division Multiplex (COFDM) with a large number of subcarriers is used to transfer video data streams since it delivers robust signal able to deal with complex radio channel conditions affected by signal fading and multipath propagation.

The use of COFDM with guard interval allows a network of DVB-T transmitters to operate in the SFN mode. The SFN operation allows covering an area with signals transmitted from different geographical sites at the same frequency and this way enhances coverage of the area. When the SFN signals, synchronized at both time and frequency domain, are received by the DVB-T receiver, they can be considered to be “echoes” of the same signal if the time delay between signals is shorter than the guard interval of the OFDM signal. On the other hand, when the delay between signals is higher than the guard interval, the received signal will be affected by ISI (Inter Symbol Interference) resulting in noticeable noise in the receiver [25] causing increased bit error rate (BER).

### 3. Experimental Scenario

Experiments were performed in laboratory conditions. We have used two DVB-T transmitters in a single frequency setup with OFDM modulators being synchronized using GPS receivers. In the experiments, two DVB-T modulators PRO Television TV-05D were used. The main reason for

TABLE 1: Sources of timing errors in GPS.

Source of error	Timing error
User clock bias	10–50 ns
Receiver noise	<1 ns
Residual satellite clock error	<7 ns
Residual of broadcast ephemeris	<7 ns
Residual of tropospheric delay	0.3–2 ns
Residual of ionospheric delay	3–15 ns

using these modulators was their implementation in a real network operating in Slovakia. Real GPS signals were used in the experiments and one of the GPS receivers was affected by an interference signal, caused either by jamming or by spoofing. The block diagram of the experimental setup is shown in Figure 1.

To gather data from the experimental setup and monitor the achieved results, all devices were connected to the network and managed from a PC (Figure 2). In the SFN, it is important to have transmitters synchronized using, for example, GPS receivers. The transmitted data stream was created using camera and data stream coder and Megaframe Initializing Packet (MIP) inserter to provide MIP information required for synchronization of DVB-T modulators.

Measurements of parameters of DVB-T SFN signal was performed on receiver HD TAB 9 which allows measuring received power strength, bit error rate, modulation error ratio, and visualisation of the received signal characteristics including constellation diagram of the modulated signal, the spectrum of the signal, and delay between signals in SFN network.

In the experiment, the video data was transmitted in the MPEG-2 stream to the MIP inserter since MIP information is crucial for the correct operation of DVB-T/H SFN transmitters. To achieve correct operation of the network, MIP has to be tightly synchronized using 10 MHz frequency normal as well as PPS signals derived from GNSS signals. In the experiment, both 10 MHz and PPS signals were generated in the DVB-T transmitter 1, which was not affected by the interference, that is, jamming and spoofing, of GPS signals.

The PPS signal consists of periodic impulses which are shorter than 1 s and repeat every second. The accuracy of the PPS signals generated by internal clocks of the selected DVB-T transmitters is in the range from 12 ps up to microseconds per second, or 2 ns up to a few milliseconds per day. The accuracy of the signal depends on the resolution and accuracy of the signal generator. An example of the PPS signal is shown in Figure 3.

The web interface of the modulators is shown in Figure 4. It can be seen that the data stream with MIP as well as GPS signals are available, that is, highlighted with green colour. The same settings were applied to the second transmitter. Both transmitters operated at the 490 MHz frequency, which represents the TV23 channel. The DVB-T modulators were operating in 8k IFFT OFDM mode with 64 QAM modulation scheme and 1/8 guard interval. The signal was transmitted from both DVB-T modulators with a power of 0 dBm and attenuated by 7 dB in the inserter. Therefore, the signal should be received with the same amplitude from both DVB-T transmitters.



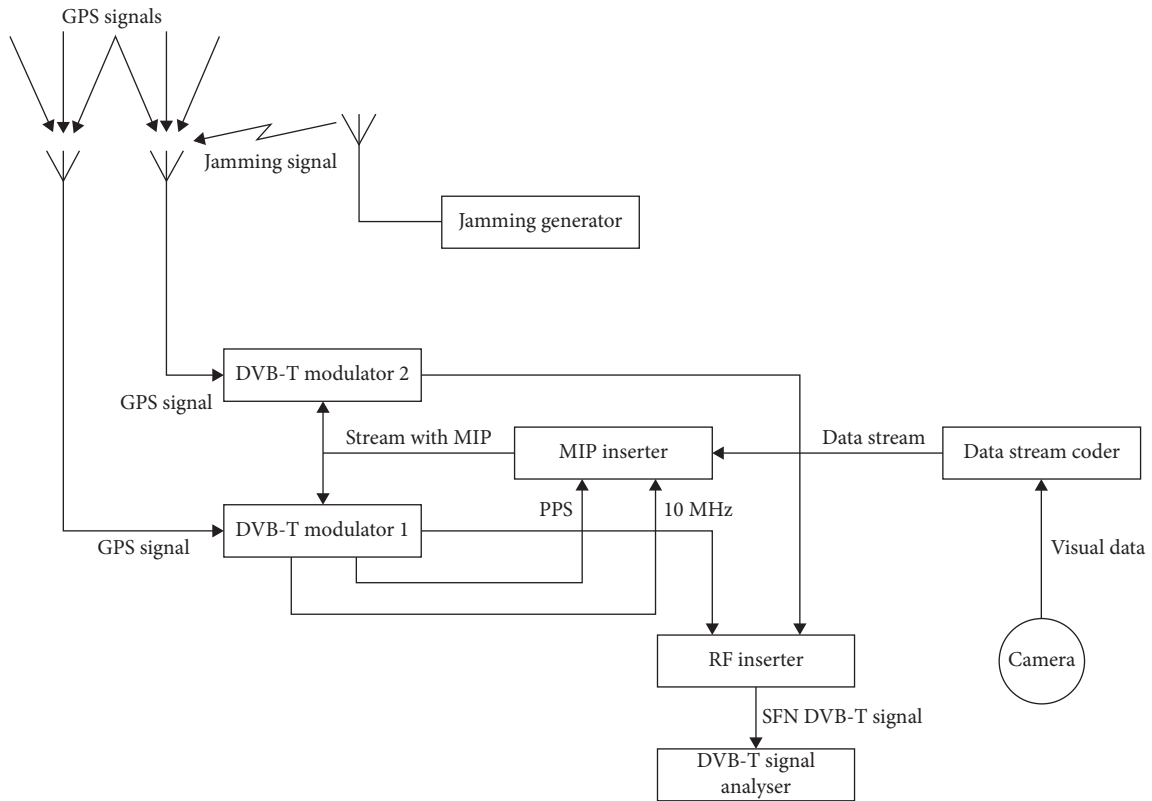


FIGURE 1: Block diagram of the experimental setup.

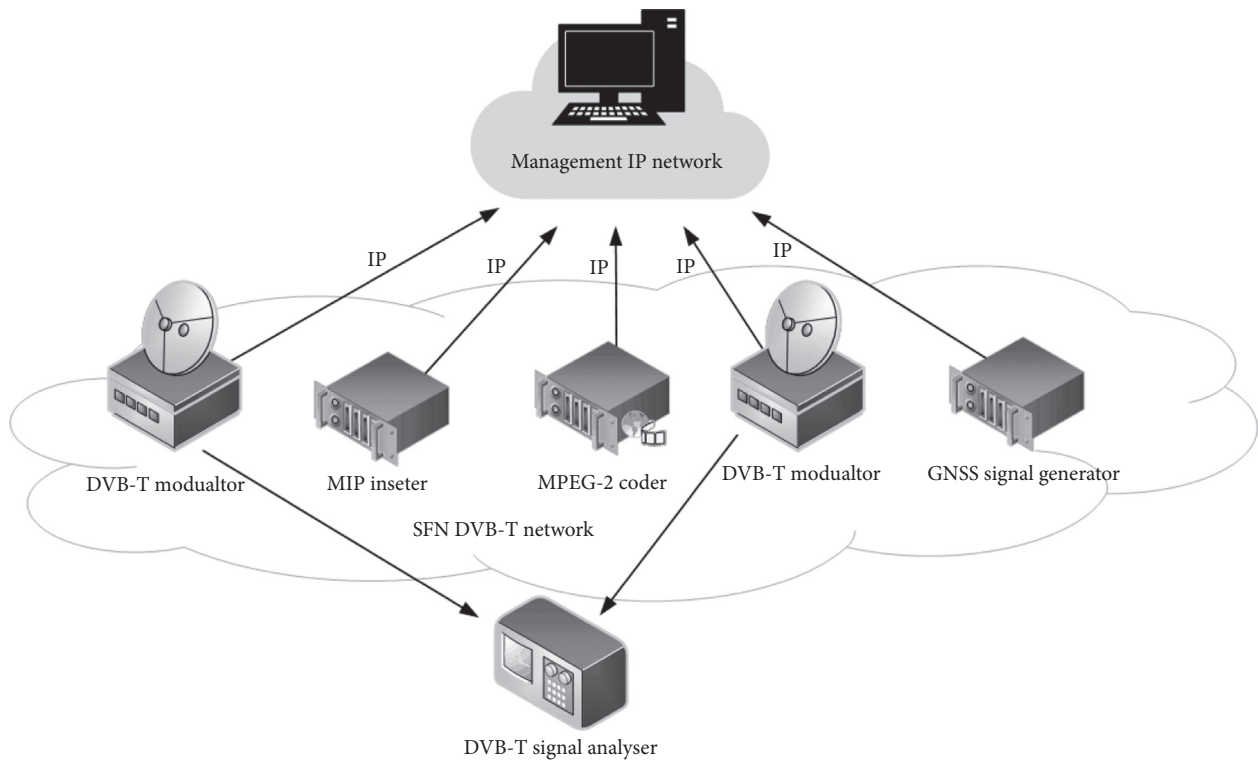


FIGURE 2: Connection of devices into the management network.

The correct function of SFN was verified at the receiver which was used during the experiments. The values shown in Figure 5 are based on signals received from both

transmitters. Without the interference to GPS signals used for synchronization of the second transmitter, the received power is 98.9 dBuV, modulation error ratio is MER >42 dB,

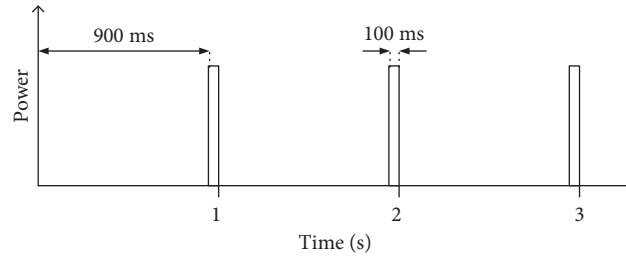
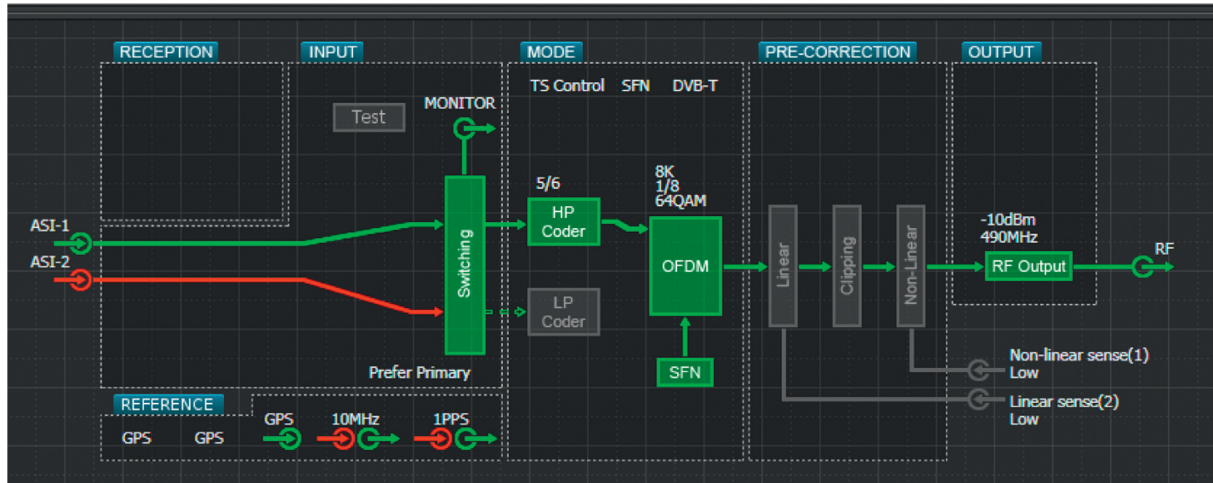
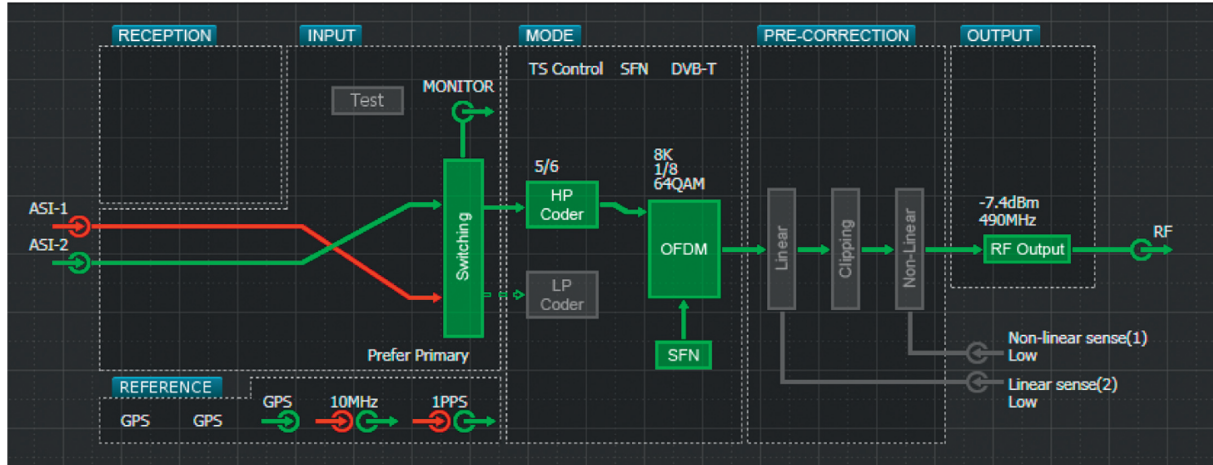


FIGURE 3: Principle of PPS signal timing.



(a)



(b)

FIGURE 4: Web interface of DVB-T modulators.

and the bit error rate after decoding and before correction bBER and bit error rate for evaluation of quality aBER are less than  $10e-6$  and less than  $10-8$ , respectively.

In the experiment, we have considered two scenarios for GPS interference. In the first scenario, a simple GPS jammer was used to interfere with GPS signals, while in the second scenario, a GNSS signal generator was used to generate GPS signals and perform a spoofing attack on the GPS receiver used for the synchronization of the second DVB-T transmitter.

In the beginning, the impact of different power levels of the jammer and distance between the jammer and GPS receiver on detection of GPS jamming was tested. The achieved results can be seen in Figure 6. The blue line in the figure highlights the threshold level of the field strength of the jamming signal equal to 0.77 mV/m that will be detected by the GPS receiver and thus cause an outage of the GPS clock synchronization.

From the figure, it can be seen that a jammer with the 1 mW transmit power can affect the receiver up to the distance of

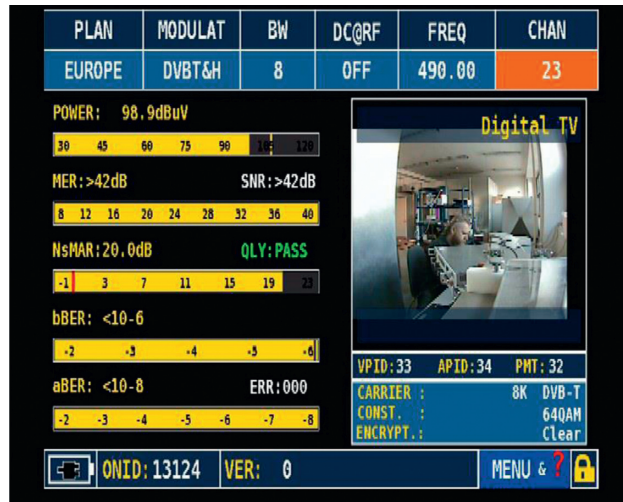


FIGURE 5: Screenshot from the DVB-T analyser without GPS jamming.

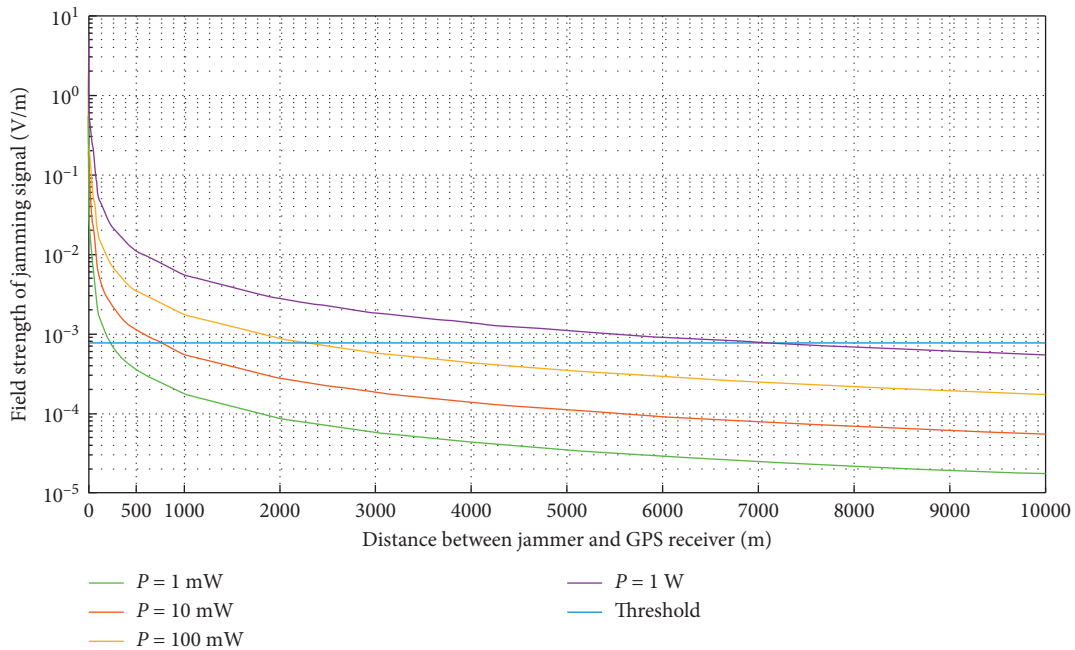


FIGURE 6: Impact of the power level of jammer and distance between jammer and GPS receiver on detection of GPS jamming.

250 m, while with increasing transmit power, the distance between the jammer and GPS receiver can grow up to more than 7 km in the case when transmitting power of the jammer was 1 W. Therefore, using jammers with high transmit powers can disrupt GPS services in a significant range.

In the first scenario, the jamming signal, depicted in Figure 7, was generated by GPS jammer model DHM3659. The antenna of the GPS jammer was deployed in the proximity of the GPS antenna of the second DVB-T transmitter. The power of the GPS jammer was set to value which caused the loss of GPS signals at the DVB-T transmitter.

In the second scenario, the GNSS simulator Spirent GSS6700 was used instead of a jammer to generate fake

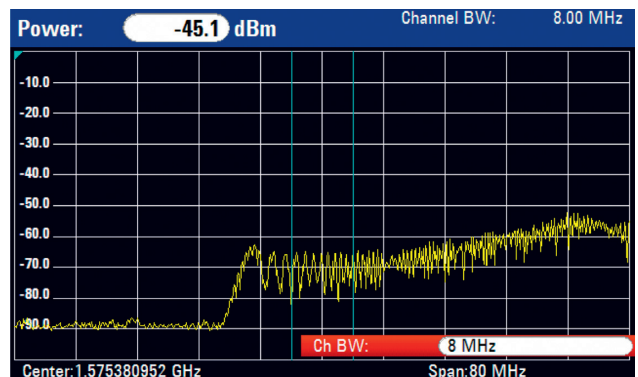


FIGURE 7: Frequency spectrum of the jamming signal.

signals from GPS satellites. The transmitting antenna was placed 1 m from the GPS antenna of the second DVB-T transmitter, similarly to the first scenario. Parameters of the generated GPS signals were chosen as close to real signals as possible. The GPS satellites were simulated with satellite constellation shown in Figure 8, and GPS simulation time was shifted by 1 minute compared to real GPS clocks; therefore, the constellation of satellites in the simulations was close to the real situation.

In this scenario, the power of the spoofing signals was at the beginning set to value 49 dB below the real GPS signals, the power was gradually increased up to the point when the GPS receiver at the DVB-T transmitter picked up the spoofing signal and used it for synchronization purposes. The spoofing signal was picked by the GPS receiver when the received power of the signal was  $-127$  dBm, which is close to the power of the real GPS signals received from the GPS satellites.

#### 4. Discussion of Achieved Results

In the first scenario, the GPS signal used to synchronize the second DVB-T transmitter was affected by a jammer. In this case, the DVB-T modulator is able to detect the problem with GPS signals as can be seen from the yellow label next to GPS input in the web interface of the modulator shown in Figure 9. The yellow colour indicates that the status of the GPS receiver is unlocked; therefore, it cannot be used for synchronization of the transmitter.

The measurements of the quality of the received signal were performed over time to evaluate the impact of GPS jamming on the performance of SFN DVB-T. The impact of GPS jamming on signal parameters can be seen in Table 2. Measurements were performed for a 60-minute period after the start of jamming, since the transmitter will automatically shut down after 60 minutes of running on internal clocks only, in order to prevent interference in the network.

From the table, it can be seen that, with increasing time, the SNR, MER, and BER parameters were negatively affected, and the quality of the received signal was decreasing gradually. The fact that signal parameters are better after 60 minutes from the start of jamming is given by the fact that the transmitter affected by GPS jamming automatically muted the transmission which can be seen from Figure 10 where GPS input, as well as the output of the transmitter, is marked with the red colour. This is given by the fact that the transmitter is set up to mute output in case it lost the time synchronization for a certain period of time, in this case, 60 minutes, in order to avoid interferences in the SFN broadcasting.

Figure 11 shows constellation diagrams of the received signals in time 0 (without GPS jamming) after 30 minutes of jamming and after 50 minutes of jamming. It can be seen that modulation symbols were affected by lack of synchronization in the network; however, the resulting signal was still decoded with minimum errors since the SNR of the received signal is well above the threshold [26] required for successful decoding.

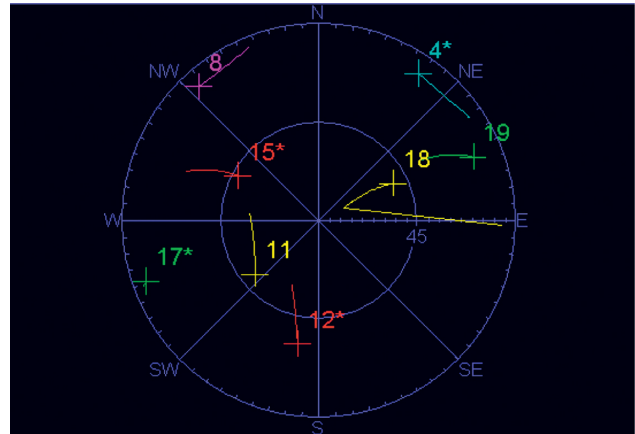


FIGURE 8: Constellation of GPS satellites used for spoofing purposes.

From the results achieved during the first experimental scenario, it can be concluded that when the GPS receiver at the DVB-T transmitter is affected by jamming, the transmitter switches automatically to internal synchronization; however, this is not sufficient for operation over a long period of time. The longer the period without external synchronization, the higher is the interference caused by the transmitter in the SFN network. However, the transmitter will automatically mute after a certain period of time, before it will cause significant interference and loss of signal in the area covered by the affected transmitter. Since the loss of GPS signals was reported in the web interface of the DVB-T transmitter, it is relatively easy to detect the problem thru the management network.

In the second scenario, a spoofing attack on the GPS receiver of the second transmitter was performed. In this case, measurements were performed when spoofing signals were below the power level of real GPS signals and when spoofing signals were higher compared to real signals and therefore were picked up by the GPS receiver. The spoofing signal was picked by the GPS receiver when the received power of the signal was  $-127$  dBm.

When spoofing signals were picked up by the DVB-T transmitter, there was not any indication of a problem, synchronization seems to work fine, and the transmitter is broadcasting at full power, as can be seen from Figure 12. However, from the results below, we can conclude that the SFN network is not working properly as can be seen from the results presented in Figure 13.

From Figure 13, it can be seen that the signal is received with the power of 103.7 dBuV; however, there is no image at the output and values of SNR, MER, bBER, and aBER are signalling that there is significant interference in the received signal since bBER is only  $10^{-2}$ .

In Figure 14, a constellation diagram of the received signal is presented; it can be seen that there is a huge noise in the signal and it is not possible to detect symbols of QAM modulation, which is resulting in high BER and lack of image data at the receiver.



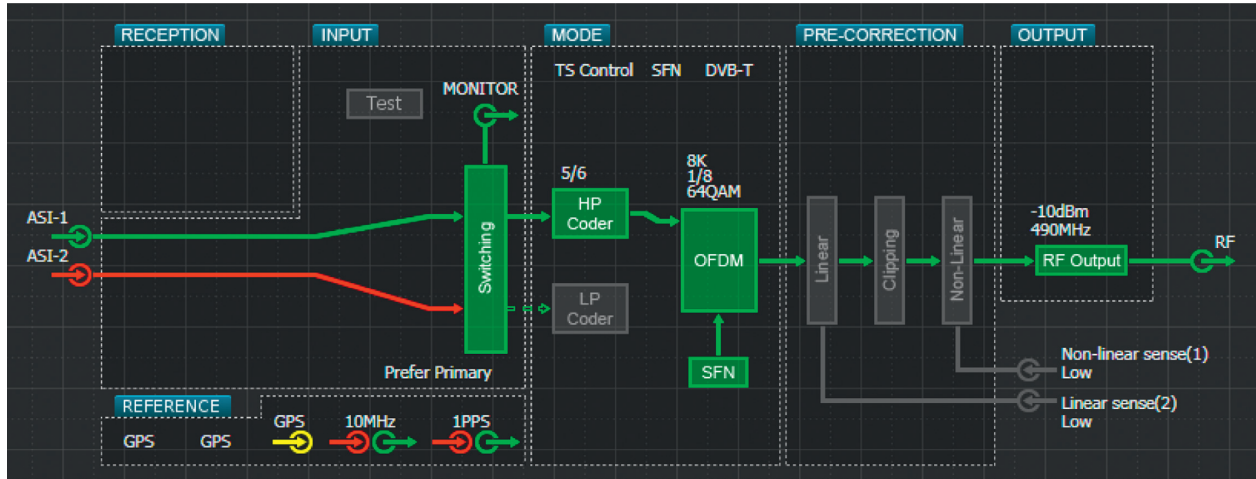


FIGURE 9: Web interface of DVB-T modulator affected by GPS jamming.

TABLE 2: Sources of timing errors in GPS.

Signal parameter	Time (minutes)						
	0	5	10	30	40	50	60
Power (dBuV)	98.9	100.2	105.4	99.1	103.2	103.4	101.6
SNR (dB)	>42	34	35	35	33	28	38
MER (dB)	>42	34.3	34.9	35.3	33.1	28.5	37.7
bBER	$<10e-6$	$2e-4$	$2e-4$	$2e-4$	$3e-4$	$6e-4$	$<10e-6$
aBER	$<10e-8$	$<10e-8$	$<10e-8$	$<10e-8$	$<10e-8$	$5e-07$	$<10e-8$

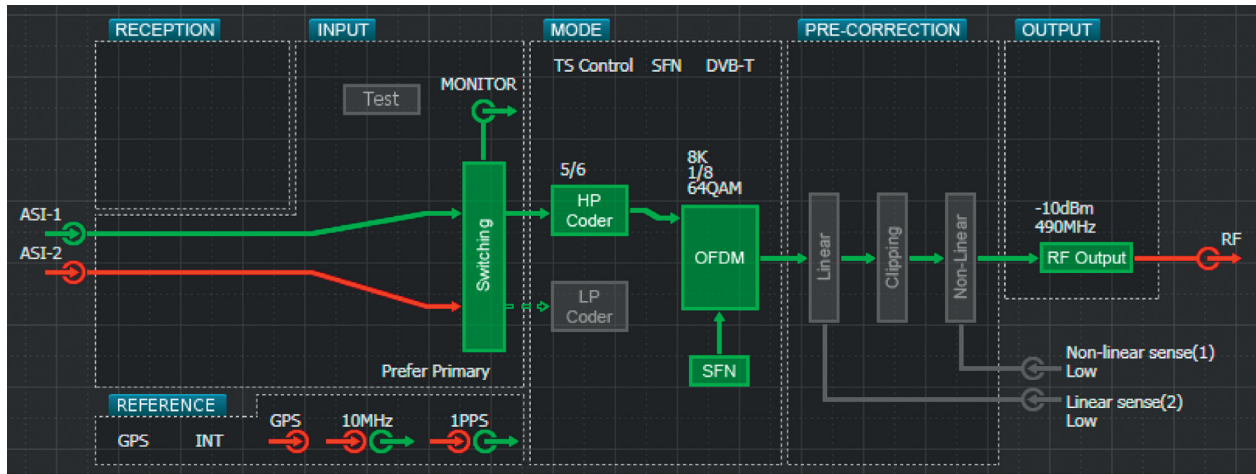


FIGURE 10: Web interface of DVB-T modulator affected by GPS jamming after 60 minutes.

In Figure 15, the time delays of DVB-T signals from transmitters in the SFN are shown. If delays of individual signals are smaller than the guard interval of the signal, then these signals do not cause intersymbol interference and the SFN network is operating correctly.

However, in the second scenario, the DVB-T transmitter affected by spoofed GPS signal caused interference in the whole SFN network. Moreover, it was not possible to detect this problem from the monitoring and management tools as the affected transmitter was not showing any issues with the synchronization and was showing a correct operation in the management web interface.

To reduce the vulnerability of the DVB-T SFN network to GPS spoofing, some algorithms for spoofing detection and spoofing mitigation should be implemented in the GPS receivers. In order to implement spoofing detection with good performance, a GPS receiver with the support of multiple antennas should be implemented. This would help to estimate the direction of arrival of the GPS signal and thus easily detect the spoofing signal since this signal is usually terrestrial [4]. The advantage of multiple GPS receiver antennas is also a possibility to implement spoofing mitigation solutions based on Multiantenna Beam Forming and Null Steering [27] or Vestigial Signal Detection [28].

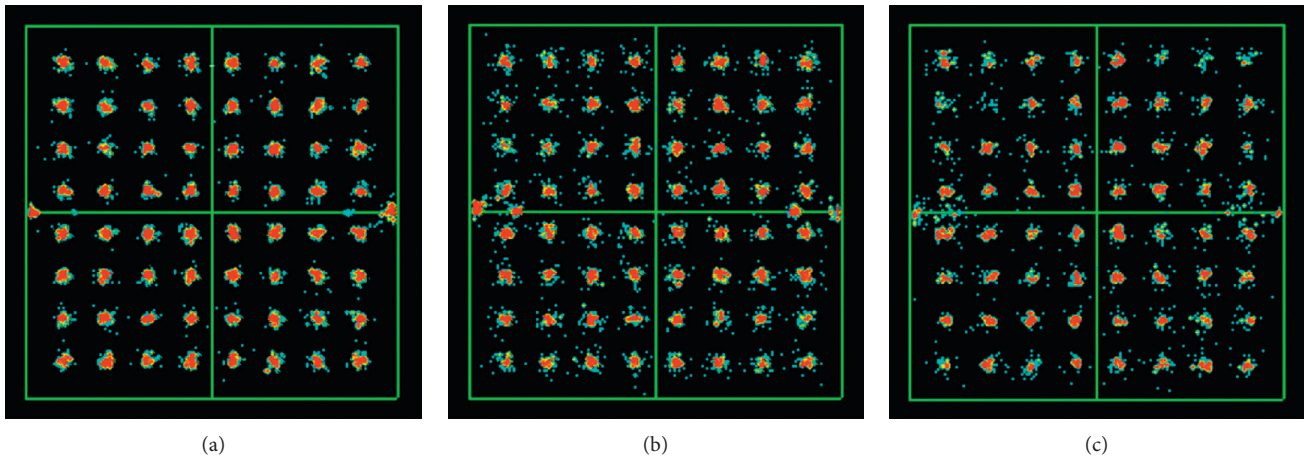


FIGURE 11: Constellation diagrams of received DVB-T signal (a) without GPS jamming, (b) after 30 of GPS jamming, and (c) 50 minutes of GPS jamming.

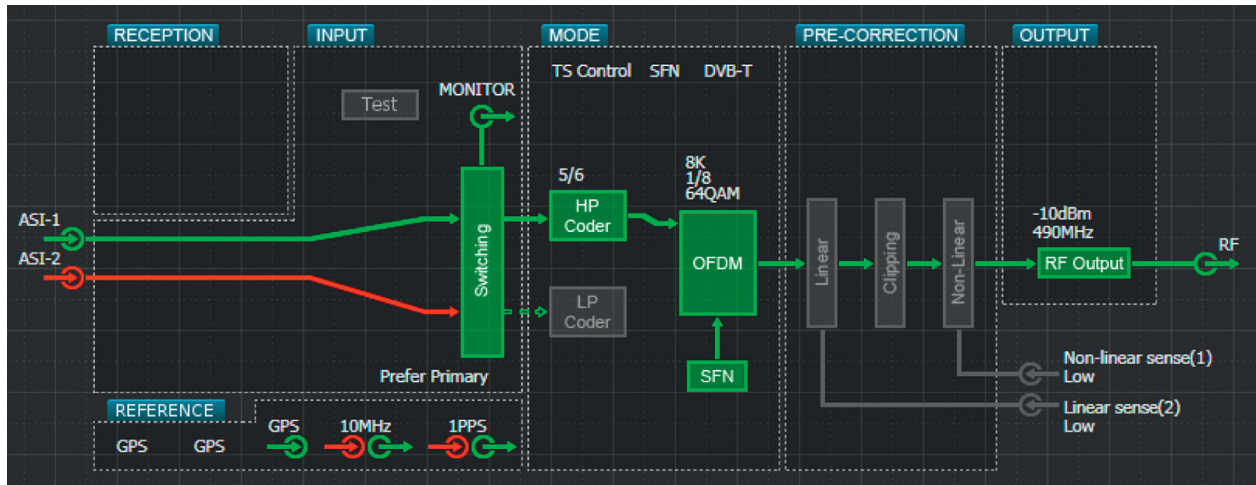


FIGURE 12: Web interface of DVB-T modulator affected by GPS spoofing.

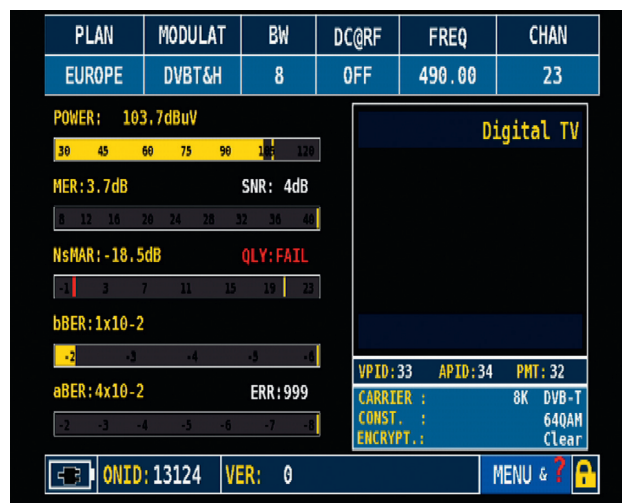


FIGURE 13: Screenshot from the DVB-T signal analyser with active GPS spoofing.

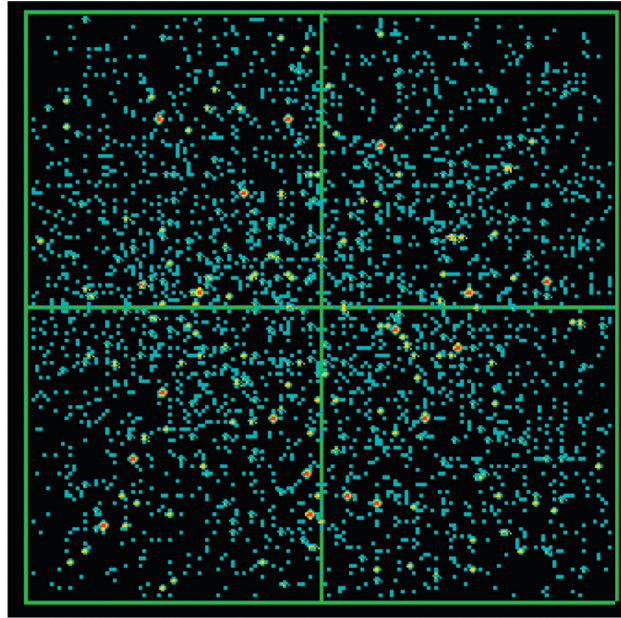


FIGURE 14: Constellation diagrams of the received DVB-T signal with GPS spoofing.

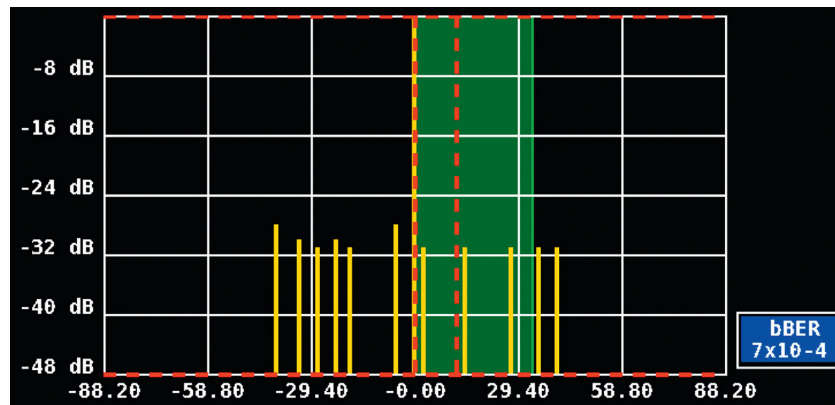


FIGURE 15: Timeshift of received DVB-T signals during GPS spoofing.

## 5. Conclusion

In the paper, the impact of the GPS interference caused by jamming and spoofing on the function of the DVB-T SFN network was investigated. The transmitters in DVB-T SFN use GPS signals for synchronization of data in the network, to avoid interference and sustain the quality of received signals. With an increased number of GPS interference caused by jammers, it is required to understand how DVB-T transmitters can cope with the affected GPS signals. We have performed experiments in two scenarios: in the first scenario, the GPS receiver at one of the transmitters was affected by jamming and in the second scenario by spoofing of GPS signals.

Based on achieved results, it can be concluded that the DVB-T SFN network is able to cope with the jamming of GPS signals, in case that it does not last too long. From the results it is obvious that the SNR of the received DVB-T signal was reduced, resulting in increased BER. However, the

receiver was still able to decode the video stream without any significant decrease in quality.

Moreover, jamming of the GPS signal used for synchronization of the transmitter could be easily detected through the management interface. On the other hand, when one of the transmitters was affected by GPS spoofing, the situation was much worse. The transmitter was out of synchronization, which caused that it was not possible to decode the signal at the receiver. On top of that, the management interface of the affected transmitter did not show any errors since the GPS receiver was receiving a spoofing signal which was decoded correctly, although the time information in the signal was tempered.

## Data Availability

The data supporting the results are presented in the manuscript.



## Conflicts of Interest

The authors declare that they have no conflicts of interest.

## Acknowledgments

This work was partially supported by the Slovak Vega grant agency, project no. 1/0626/19, “Research of Mobile Objects Localization in IoT Environment” and Operational Program Integrated Infrastructure 2014–2020 of the project: Innovative Solutions for Propulsion, Power and Safety Components of Transport Vehicles, code ITMS 313011V334, cofinanced by the European Regional Development Fund.

## References

- [1] J. Ristvej, M. Lacinák, and R. Ondrejka, “On smart city and safe city concepts,” *Mobile Networks and Applications*, vol. 25, no. 3, pp. 836–845, 2020.
- [2] A. Kiritmat, O. Krejcar, A. Kertesz, and M. F. Tasgetiren, “Future trends and current state of smart city concepts: a survey,” *IEEE Access*, vol. 8, pp. 86448–86467, 2020.
- [3] H. Wen, P. Y. R. Huang, J. Dyer, A. Archinal, and J. Fagan, “Countermeasures for GPS signal spoofing,” in *Proceedings of the 18th International Technical Meeting of the Satellite Division of the Institute of Navigation (ION GNSS '05)*, pp. 1285–1290, Long Beach, CA, USA, September 2005.
- [4] C. E. McDowell, “GPS Spoofer and Repeater Mitigation System Using Digital Spatial Nulling,” Rockwell Collins, Cedar Rapids, IA, USA, US Patent 7250903 B1, 2007.
- [5] S. C. Lo and P. K. Enge, “Authenticating aviation augmentation system broadcasts,” in *Proceedings of the IEEE/ION Position, Location and Navigation Symposium (PLANS'10)*, pp. 708–717, Indian Wells, CA, USA, May 2010.
- [6] J. Nielsen, A. Broumandan, and G. Lachapelle, “Spoofing detection and mitigation with a moving handheld receiver,” *GPS World*, vol. 21, no. 9, pp. 27–33, 2010.
- [7] N. A. White, P. S. Maybeck, and S. L. DeVilbiss, “Detection of interference/jamming and spoofing in a DGPS-aided inertial system,” *IEEE Transactions on Aerospace and Electronic Systems*, vol. 34, no. 4, pp. 1208–1217, 1998.
- [8] A. Jafarnia-Jahromi, T. Lin, A. Broumandan, J. Nielsen, and G. Lachapelle, “Detection and mitigation of spoofing attack on a vector based tracking GPS receiver,” in *Proceedings of the International Technical Meeting of the Institute of Navigation*, Newport Beach, CA, USA, January 2012.
- [9] S. Moshavi, “Multi-user detection for DS-CDMA communications,” *IEEE Communications Magazine*, vol. 34, no. 10, pp. 124–136, 1996.
- [10] A. Jafarnia-Jahromi, A. Broumandan, J. Nielsen, and G. Lachapelle, “GPS vulnerability to spoofing threats and a review of antispoofing techniques,” *International Journal of Navigation and Observation*, vol. 2012, Article ID 127072, 16 pages, 2012.
- [11] Interface Specification, IS-GPS-200 Rev.D, IRN-200D-001, 7. March 2006.
- [12] A. Novák, F. Jůn, F. Škultéty, and A. N. Sedláčková, “Experiment demonstrating the possible impact of GNSS interference on instrument approach on RWY 06 LZZI,” *Transportation Research Procedia*, vol. 43, pp. 74–83, 2019.
- [13] D. Borio, S. Savasta, and L. L. Presti, “On the DVB-T coexistence with Galileo and GPS systems,” in *Proceedings of the 3rd ESA Workshop on Satellite Navigation User Equipment Technologies (NAVITEC '06), ESA/ESTEC*, pp. 1–13, Integrated Navigation Systems, Noordwijk, The Netherlands, December 2006.
- [14] S. S. BeatriceMotella and F. D. DavideMargaria, “A method to assess robustness of GPS C/A code in presence of CW interferences,” *International Journal of Navigation and Observation*, vol. 2010, Article ID 294525, 8 pages, 2010.
- [15] E. Elezi, G. Cankaya, B. Ali, and S. Yarkan, “The effect of electronic jammers on GPS signals,” in *Proceedings of the 2019 16th International Multi-Conference on Systems, Signals & Devices (SSD'19)*, Istanbul, Turkey, March 2019.
- [16] R. H. Mitch, “Signal characteristics of civil GPS jammers,” in *Proceedings of the 24th International Technical Meeting of the Satellite Division of The Institute of Navigation (ION GNSS 2011)*, pp. 1907–1919, Portland, OR, USA, September 2011.
- [17] J. Magiera and R. Katulski, “Detection and mitigation of GPS spoofing based on antenna array processing,” *Journal of Applied Research and Technology*, vol. 13, no. 1, pp. 45–57, 2015.
- [18] H. Puttnies, P. Danielis, A. R. Sharif, and D. Timmermann, “Estimators for time synchronization-survey, analysis, and outlook,” *IoT*, vol. 1, no. 2, pp. 398–435, 2020.
- [19] P. Vyskocil and J. Sebesta, “Relative timing characteristics of GPS timing modules for time synchronization application,” in *Proceedings of the 2009 International Workshop on Satellite and Space Communications*, pp. 230–234, Siena, Italy, September 2009.
- [20] W. Liu, H. Yuan, and J. Ge, “Local-area nanosecond-accuracy time synchronisation based on GPS L1 observations,” *IET Radar, Sonar & Navigation*, vol. 13, no. 5, pp. 824–829, 2019.
- [21] B. W. Parkinson, J. J. Spilker, P. Axelrad, and P. Enge, *Global Positioning System: Theory and Applications*, American Institute of Aeronautics and Astronautics, Washington, DC, USA.
- [22] Q. Zhu, Z. Zhao, and L. Lin, “Real time estimation of slant path tropospheric delay at very low elevation based on singular ground-based global positioning system station,” *IET Radar, Sonar & Navigation*, vol. 7, no. 7, pp. 808–814, 2013.
- [23] M. Olynik, “Temporal variability of GPS error sources and their effect on relative positioning accuracy,” in *Proceedings of the Institute of Navigation NTM 2002*, San Diego, CA, USA, January 2002.
- [24] ETSI EN 300 744 v1.4.1 (2001-01). European Standard (Telecommunications series). Digital Video Broadcasting (DVB); Framing structure, channel coding and modulation for digital terrestrial television. ETSI and EBU, 1/2001.
- [25] T. Kratochvil and V. Ricny, “Simulation and experimental testing of the DVB-T broadcasting in the SFN networks,” in *Proceedings of the 2008 18th International Conference Radioelektronika*, pp. 1–4, Prague, Czech Republic, April 2008.
- [26] ETSI TR 101 290 v1.2.1, “Digital video broadcasting (DVB); measurement guidelines for DVB systems ETSI and EBU, 5/2001,” Technical report, 2001–2005, ETSI, Sophia Antipolis, France.
- [27] S. Daneshmand, A. Jafarnia-Jahromi, A. Broumandan, and G. Lachapelle, “A low complexity gnss spoofing mitigation technique using a double antenna array,” *GPS World Magazine*, vol. 22, no. 12, pp. 44–46, 2011.
- [28] T. E. Humphreys, B. M. Ledvina, M. L. Psiaki, B. W. O'Hanlon, and P. M. Kintner, “Assessing the spoofing threat: development of a portable gps civilian spoofer,” in *Proceedings of the 21st International Technical Meeting of the Satellite Division of the Institute of Navigation (ION GNSS '08)*, pp. 2314–2325, Savannah, GA, USA, September 2008.



## Research Article

# Mobile Coverage in Rural Sweden: Analysis of a Comparative Measurement Campaign

P. G. Sudheesh <sup>1</sup> and Jaap van de Beek <sup>2</sup>

<sup>1</sup>Department of Electronics and Communication, Manipal Institute of Technology, MAHE, Udupi, India

<sup>2</sup>Department of Computer Science, Electrical and Space Engineering, Luleå University of Technology, Luleå, Sweden

Correspondence should be addressed to P. G. Sudheesh; pgsudheesh@gmail.com

Received 9 September 2020; Revised 6 November 2020; Accepted 10 December 2020; Published 5 January 2021

Academic Editor: Peter Brida

Copyright © 2021 P. G. Sudheesh and Jaap van de Beek. This is an open access article distributed under the Creative Commons Attribution License, which permits unrestricted use, distribution, and reproduction in any medium, provided the original work is properly cited.

Under the umbrella of 1G to 5G, different technologies have been used to provide mobile communication. Various technologies are being proposed to bring a person in remote area under coverage. However, a statistical analysis on what these users get from already existing technologies has not been carried out. We fill this gap by carrying out such a study using a measurement campaign, where we present a framework for analyzing mobile signal strength experienced at the user end. Measurements are taken throughout the Norrbotten county, the northernmost county in Sweden, using mobile phones recording various parameters at regular intervals. Based on measured signal strength, a coverage map has been made via inverse distance weighting (IDW) interpolation. Based on the coverage map, various analyses are carried out on signal strength over residential areas and roads of Norrbotten. Overall, we lay a framework to analyze and quantify the effect of signal strength on users.

## 1. Introduction

Earlier this year, 3rd Generation Partnership Project (3GPP) released the first versions of its 5G new radio (NR) standard, first as a non-stand-alone mode, and later the stand-alone mode. For a while now, it has become clear that this standard essentially has its focus on the urban areas. Use cases and scenarios invariably address dense network environments, small cells, and a large number of mobile users per unit area.

Naturally, concerns have been raised by stakeholders representing rural values, needs, and interests. With ever-decreasing cell sizes, how will *areal coverage* be guaranteed is based not only on the old standards and systems but also on new essential 5G functionalities as network slicing, ultralow latencies, and massive bandwidth [1].

The first 5G testbed in Norrbotten, Sweden, was tested in June 2019 [2] and, therefore, for majority of population, 5G network is still not accessible. Also, 5G handsets are also not so widely available in the market. Hence, a major portion of the population is still using 2G, 3G, and/or 4G network for mobile communication. Therefore, expanding coverage area

and bringing more people under mobile coverage map require network planning and installing new base stations.

However, installing terrestrial base stations (BS) and providing backhaul are subject to the revenue earned from the mobile users [3]. Therefore, installing a terrestrial base station and associated backhaul in “not so popular” areas is not attractive from an economical point of view. This in turn results in deployment of lesser number of base stations or even absence of base stations in such sparsely populated areas.

As a result, the people in these areas are subjected to poor or absence of coverage. It is widely known that larger operators and stakeholders of telecom industry do not want to put up new base stations in non-profitable areas. In other words, the telecom companies hold the right not to put up new base stations in places that are not profitable to them [4]. It is rather interesting that the notion of *full coverage* is limited only to the areas defined by the operators.

To overcome these limitations and provide full coverage irrespective of population density, different solutions like positioning UAV BS [5] and new allocation spectrum [6] are

considered. Swedish regulators have come up with new 700 MHz band that focuses on lesser coverage areas [6]. To this end, Swedish authorities and especially Norrbotten, the northernmost county in Sweden, wanted to identify and focus on the areas with no or poor coverage [4]. Neither the coverage map from operators nor the location of base stations was available to researchers. To this end, we generate a coverage map generated using crowd sourced measurements across Norrbotten.

It is found in [7] that mobile coverage is directly linked to socioeconomic performance. Therefore, in this paper, we measure the *coverage poverty* experienced by the people. Several attempts have been done to calculate areas without coverage [8, 9]. Effect of mobile coverage on railway network in Norway is studied in [10]. These attempts, however, do not really give an idea of quality of service experienced by the users. Therefore, to quantify the quality of service, the coverage poverty experienced by (a) people living in their apartments and (b) cars plying through the roads of Norrbotten province of Sweden is mathematically calculated.

The paper is organized as follows. A review of techniques used to analyze effect of signal strength in various conditions is provided in Section 2. A detailed explanation of generating coverage map from crowd sourced measurements is provided in Section 3. Section 4 is devoted to result analysis, while conclusions are listed in Section 5.

## 2. Coverage Maps from Scattered Samples

In this section, we elaborate the methods by which the signal strength over the populated areas and roads are analyzed using measured signal strengths. There are different ways of generating a coverage map and analyzing the signal strength: (1) identifying BS and then calculating the signal strength using factors such as path loss [11], (2) finding base station location from manually measured signal strength at different locations [12–14], and (3) generating coverage map from manually measured signal strength values. Since the locations of BS are not disclosed to public, we resort to the third method where we use tens of millions of measurements to generate coverage map. With millions of measurements, it is more likely to get a predicted signal strength than resorting to earlier methods. The signal strength measurements are taken for different operators and radio access technology (RAT) at difference time instances, which are then interpolated to form rectangular zones depicting average signal strength over that area. However, as we are only relying on available signal strength to generate coverage map, we miss lot of area as unmapped region.

*2.1. Generating Coverage Map.* The availability of measurements is limited to GPS coordinates on roads in general. This is because measurements are usually carried out by mobiles that are kept in the vehicles. Therefore, practically it is impossible to measure signal strength throughout the area to be mapped and identify exact signal strength at those locations. Therefore, we use the signal strength from the

available signal strength measurements to calculate signal strength in the rest of the areas.

In order to generate coverage map of various RATs and operators, it is important to separate the measured signals. The measurement from mobile phones contains network type info, operator, and signal strength, based on which it is possible to filter the point to corresponding sets that represent different RATs and operators. Therefore, for each operator, sets of different RATs such as  $S_{LTE}$ ,  $S_{UMTS}$ ,  $S_{GSM}$  can be made. Sets  $S_{LTE}$ ,  $S_{UMTS}$ , and  $S_{GSM}$  represent the sets of measurements under LTE, UMTS, and GSM, respectively. The subscripts to  $S$  represent different RATs.

Interpolation techniques such as kriging and inverse distance weighting [15] are widely used for obtaining coverage area map using measured signal strengths. Although different versions of kriging such as ordinary kriging and universal kriging are popular for crowd sourced measurements, a computationally less complex algorithm is used here as we consider large geographical area. In [16, 17], the authors compare kriging with IDW algorithm and find that kriging provides slightly better results compared to IDW. However, it is mentioned in [17] that the computational complexity for kriging is much higher, which is not a great concern when the area under study is small. But, as the area under study is large, computationally simple IDW algorithm is preferred over kriging to generate coverage maps for all operators and RATs.

IDW algorithm predicts the signal strength in locations where measured points are not available. IDW algorithm makes use of the fact that measurements in the near vicinity contribute better than farther points. Therefore, bigger number of measured signal strength makes the signal strength prediction more closer to a possible real measurement. It is interesting to note that the IDW algorithm produces an averaging effect on measurements that are isolated. However, in case of crowded measurements, the signal strength assigned to the polygon is affected not only by the measurements in it but also by the measurements near to it.

The output of IDW algorithm is a raster map, made up of a grid of points. These points are located at the center of each pixel, which is the basic building block of the raster. To generate a coverage map, a signal strength value is assigned to each point in the grid, based on the available signal strength values. The points in grid and measured point are marked as blue and red dots, respectively, in Figure 1. Although the IDW algorithm does not limit the number of points that are used in order to calculate the signal strength of point in the grid, since the points in the vicinity contribute more to the measurement, we restrict the search to a circle, where each point in the grid is the center of the search circle.

The points in the grid are spaced at distance  $d$ , which is also the length of the edge of each raster (coverage map) cell. Using Tobler’s rule [18], the grid spacing  $d$  is taken as

$$d = \frac{\text{map scale}}{2 \times 1000}, \quad (1)$$

where map scale depends on where the points under study are spread. In effect, the length of edges of raster is dependent on the distance of right-most, left-most, top-most, and bottom-most points among the available points.

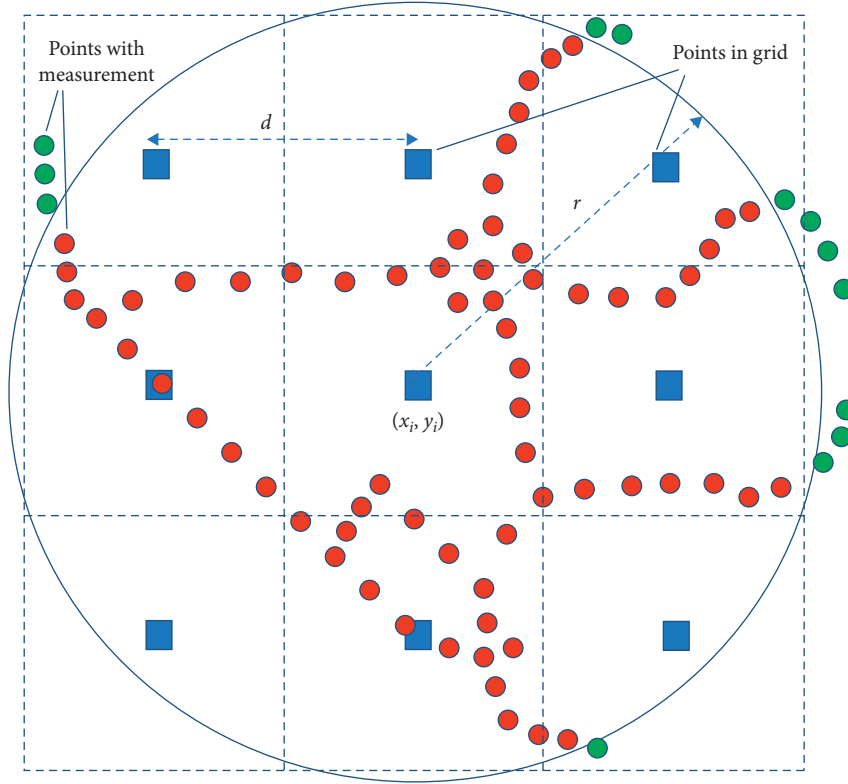


FIGURE 1: Selecting points to run IDW algorithm.

To generate the raster, each pixel or spatial object must hold the value of an element from a set  $\mathbf{M}$ . Therefore, an object  $O$  must have two properties:

- (a) A spatial extent,  $Z_i$
- (b) A function  $f_O$  that assigns a value from set  $\mathbf{M}$  to each point in  $Z_i$

Considering the search radius  $r$ , object  $O$  is defined as

$$O = (Z_i, M_i \Psi_r). \quad (2)$$

Thus, object  $O$  is a tuple  $(Z_i, M_i \Psi_r)$ , where  $M_i \in \mathbf{M}$  and  $Z_i \subseteq \mathbf{R}^2$ . The function  $f_O: Z_i \rightarrow \mathbf{M}$ , where  $\mathbf{M} = \{\mathbf{R}, \text{"NO SIGNAL"}\}$ . In effect, the value  $f_O(x_i, y_i)$  reflects the signal strength to be attributed to  $(x_i, y_i) \in Z_i$ . The distance,  $d$ , between neighbouring points in a raster,  $(x_i, y_i)$ , is obtained from equation (1). The signal strength  $M_i$  for each point in raster at location  $(x_i, y_i)$  is given as

$$M_i = \frac{\sum_{(x_j, y_j) \in \mathbf{S}} S_j \left( (x_i - x_j)^2 + (y_i - y_j)^2 \right)^{-\alpha} \Psi_r(x_j, y_j)}{\sum_{(x_j, y_j) \in \mathbf{S}} \left( (x_i - x_j)^2 + (y_i - y_j)^2 \right)^{-\alpha}}, \quad (3)$$

$$\Psi_r(x_j, y_j) f_O(x_j, y_j) = \begin{cases} f_O(x_j, y_j), & \text{if } \sqrt{(x_i - x_j)^2 + (y_i - y_j)^2} < r, \\ 0, & \text{if } \sqrt{(x_i - x_j)^2 + (y_i - y_j)^2} > r, \end{cases} \quad (4)$$

where  $S_j \in \mathbf{S}$ ,  $\mathbf{S} = \{\mathbf{R}, \text{"NO SIGNAL"}\}$  and  $d_{ij}$  is the Euclidean distance between measured point  $j$  and point  $i$  in the grid.  $\alpha$  denotes the distance exponent or power index, which is taken as 2. The characteristic function  $\Psi_r$  is defined as in equation (4), where  $r$  is the search radius. Hence, after successful implementation of (3) on  $\mathbf{S}_{\text{LTE}}$ ,  $\mathbf{S}_{\text{UMTS}}$ , and  $\mathbf{S}_{\text{GSM}}$ , we get  $\mathbf{M}_{\text{LTE}}$ ,  $\mathbf{M}_{\text{UMTS}}$ , and  $\mathbf{M}_{\text{GSM}}$  representing the coverage map for LTE, UMTS, and GSM, respectively.

**2.2. Coverage Specific Aspects.** To generate coverage map of Telia, Tele2, and Telenor, for each LTE, UMTS, and GSM, IDW algorithm must be carried out to each ensemble of measurements dedicated to each of the above operators and RATs. The IDW applied to each of these groups of measurements is explained in Section 2.1. A simple IDW with all the measurements, where "NO SIGNAL" is also an entry, will generate wrong results and therefore needs to be treated separately.

Here, we formulate a coverage specific approach to generate coverage map, by taking into account both real signal measurements and points with no signal measurements. The algorithm is represented in Figure 2. The first step is to separate points with valid signal measurements and points without signal strengths and generate coverage map for each set. These rasters or grids of points are then converted to polygons. Now, the difference between coverage maps with valid measurements and no signal strengths is created. This output is then merged to the coverage map with valid measurements.

It is still possible to have polygons with more points without signal strength and less points with valid measurements. To address such situations, a final step is required. That is, the polygon is assigned "NO SIGNAL," when the number of points without valid measurements is more even if there is a valid signal strength assigned to it. In the absence of such situations, the signal strength value assigned to the final coverage polygon remains the same as the one from the coverage map generated from valid measurements.

### 3. Practical Case Study

*3.1. Measurements.* In order to generate raster, we measure the signal strengths of various operators and RATs with GPS coordinates and time stamps. The measurement is made by using set of mobile phones, which are locked to specific operators and RATs. The set of mobile phones is kept in a bag as shown in Figure 3, where each phone is locked to a single operator and RAT. To this end, three operators in Sweden are compared, where Tele2 and Telenor share the same infrastructure for 2G (GSM) and 4G (LTE). Therefore, each bag contains 2 phones to measure 2G signal and 3 phones to measure 3G signal and again 2 phones to measure 4G signal, which records measurements at regular intervals.

We consider three operators, Telia, Tele2, and Telenor, over the Norrbotten region, which is the northernmost province in Sweden. The mobile phones that measure signal strengths are enclosed in a bag and are placed in vehicles and boats plying through the area under study. The mobile phones collect data, namely, GPS coordinates, date, time, network type, signal strength, operator, cell identification code (CID), location area code (LAC), and eNode bid at regular intervals. It is worth noting that the measurements from various phones in the bag are not time-synchronized.

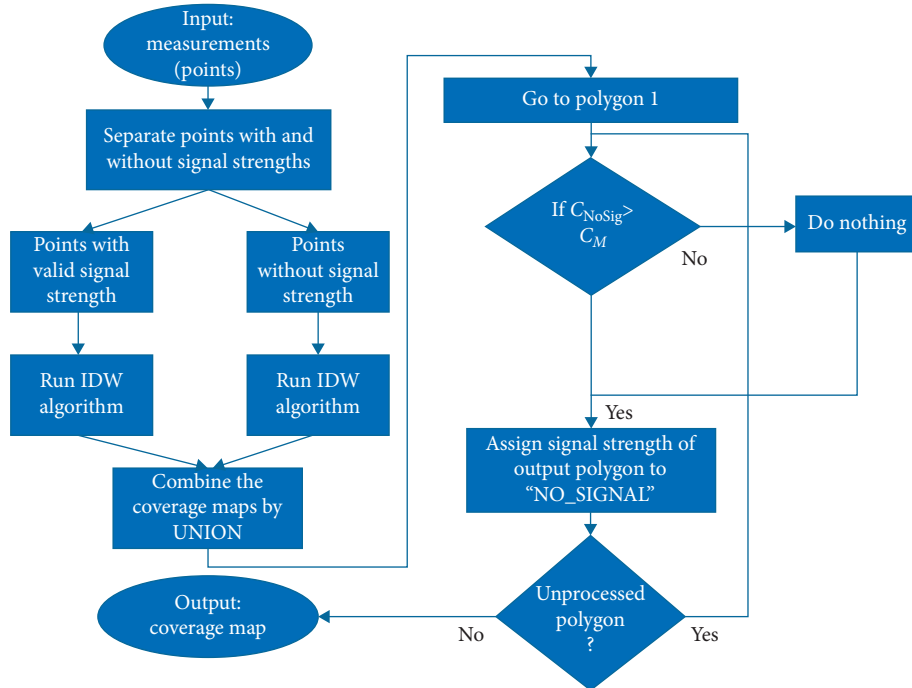
The two GSM phones measure broadcast channel (BCCH) and the signal strength measured in GSM is the received signal strength indicator (RSSI). The 3G RAT used in the phones is universal mobile telecommunications system (UMTS), which is a wideband code division multiple access (WCDMA) system. Therefore, the mobile phones dedicated to measuring 3G signals measure the received power on one code over the primary common pilot channel (CPICH). This value is referred to as the received signal code power (RSCP). The 4G RAT is also known as the long-term evolution (LTE) standard, which uses time-frequency resource block with varying channel size (from 1.4 to 20 MHz). Therefore, the useful power is contributed by different resource blocks, which is measured as reference signal received power (RSRP).

The 2G and 3G phones are locked to 2G and 3G RAT, respectively. This means that the mobile phone cannot perform handover operation from 3G to 2G when it has poor signal strength. However, the 4G mobile phones are not locked to RATs and as a result they switch RAT from LTE to UMTS and then from UMTS to GSM based on the measured signal strength. In other words, the phones that measure LTE signals provide RSRP values in fewer areas, even though there are RSRP values when phone switches to other RATs from LTE.

The number of measurements received per municipality is given in Table 1. In this paper, we study the distribution of signal strength over residential areas and roads. The population and road lengths associated with each of the municipalities are listed in the table. The number of measurements per municipality consists of three RATs and three operators. The population map considered for analysis is a 1 km  $\times$  1 km polygon shape file provided by [19]. The road data is given by [20], which provides information about number of vehicles moving through that particular road.

*3.2. Framework to Analyze the Quality of Service.* With the measurements in hand, this section lays the framework to analyze the distribution of signal strength over residential areas and roads. For this purpose, we use two sets of polygon files, population and road, as a base layer that extracts signal strength from the superimposed coverage map. While the first helps us to study the effect in static users, the latter provides insight into the coverage for mobile users. Further, we define different levels from LTE, UMTS, and GSM signal strength, with which the quality of service enjoyed by the users can be easily identified. The algorithm used for classification of user levels is mentioned in Figure 4. The fact that LTE, UMTS, and GSM offer better service in the respective order is used for forming the algorithm. While RSRP  $> -80$  dBm is an excellent signal strength in LTE,  $-90$  dBm  $<$  RSRP  $< -80$  dBm offers poorer performance than the former [21]. Therefore, we assign the former as level 1 and the latter as level 2. Following the pattern, we assign higher levels to the LTE and lower levels to UMTS [21] as the data rate decreases in UMTS compared to LTE. This pattern is repeated in GSM as well [22].

Note that the points labelled No Signal and NULL are not considered while assigning levels till level 12, where No Signal represents a situation where UEs did not receive any signal, whereas NULL considers a scenario where polygon does not have a signal strength to map to. Level 13 is used to represent the signal strength that is lesser than the minimum required signal strength for a reliable communication. A scenario where the UE cannot make call in any of the RAT is considered in level 14. The difference between level 13 and level 14 is that connection is not possible in level 14, while connection may be possible with possible chance of disconnection in level 13 [21, 23]. For example, if the device under test has LTE signal strength below  $-100$  dBm, UMTS signal strength below  $-85$  dBm, and GSM signal strength below  $-110$  dBm, the signal strength values in mobile



$C_{NoSig}$  = count of points without measurement in polygon  
 $C_M$  = count of points with measurement in polygon

FIGURE 2: Algorithm to generate coverage map.



FIGURE 3: Measurement setup by IQMTEL, Sweden.

phones fall below the minimum recommended signal strength [21, 23]. Such a situation is possible in level 13. Meanwhile, if all devices are not getting any signal from the base station, we assign level 14, which is the worst situation among all. Level 15 does not represent the quality of the signal, as it houses the regions where the measurement campaign was not performed.

TABLE 1: Measurements across municipalities of Norrbotten.

Sl. no.	Municipality	No. of measurements	Area (km <sup>2</sup> )	Population	Road (km)
1	Älvsbyn	708191	1790.4	8256	530.1
2	Arjeplog	887558	14498.3	2903	720.1
3	Arvidsjaur	1826754	6085.7	6490	1019.9
4	Boden	2409219	4277.1	28373	875.9
5	Haparanda	378870	16806.7	9851	284.6
6	Jokkmokk	2089506	933.2	5132	796.3
7	Kalix	940068	19314.4	16240	652.7
8	Luleå	4603223	1850.3	78160	767
9	Pajala	1821622	20642.3	6157	1004.5
10	Piteå	3883938	2155.8	41932	919.6
11	Gällivare	3070680	2913.9	18023	976.6
12	Kiruna	2315800	2515.7	23233	730.1
13	Övertorneå	325123	8103.7	3409	521.7
14	Övertorneå	671210	3246.1	4582	556.1

### 3.2.1. Framework to Analyze Effects in Residential Areas.

In this subsection, we study the effect of signal strength on users in residential areas. Figure 5 demonstrates the extraction of signal strength from the coverage map. The upper layer is the coverage map, which holds the signal strength value. The lower layer, which is population map in this contest, extracts signal strength from the overlapping coverage map and adds the signal strength value  $M_k$  to each polygon of the population or road map.

In order to extract  $M_k$  from an overlapping coverage map, each polygon uses the settings in Table 2, which is executed using QGIS, a free geographic information

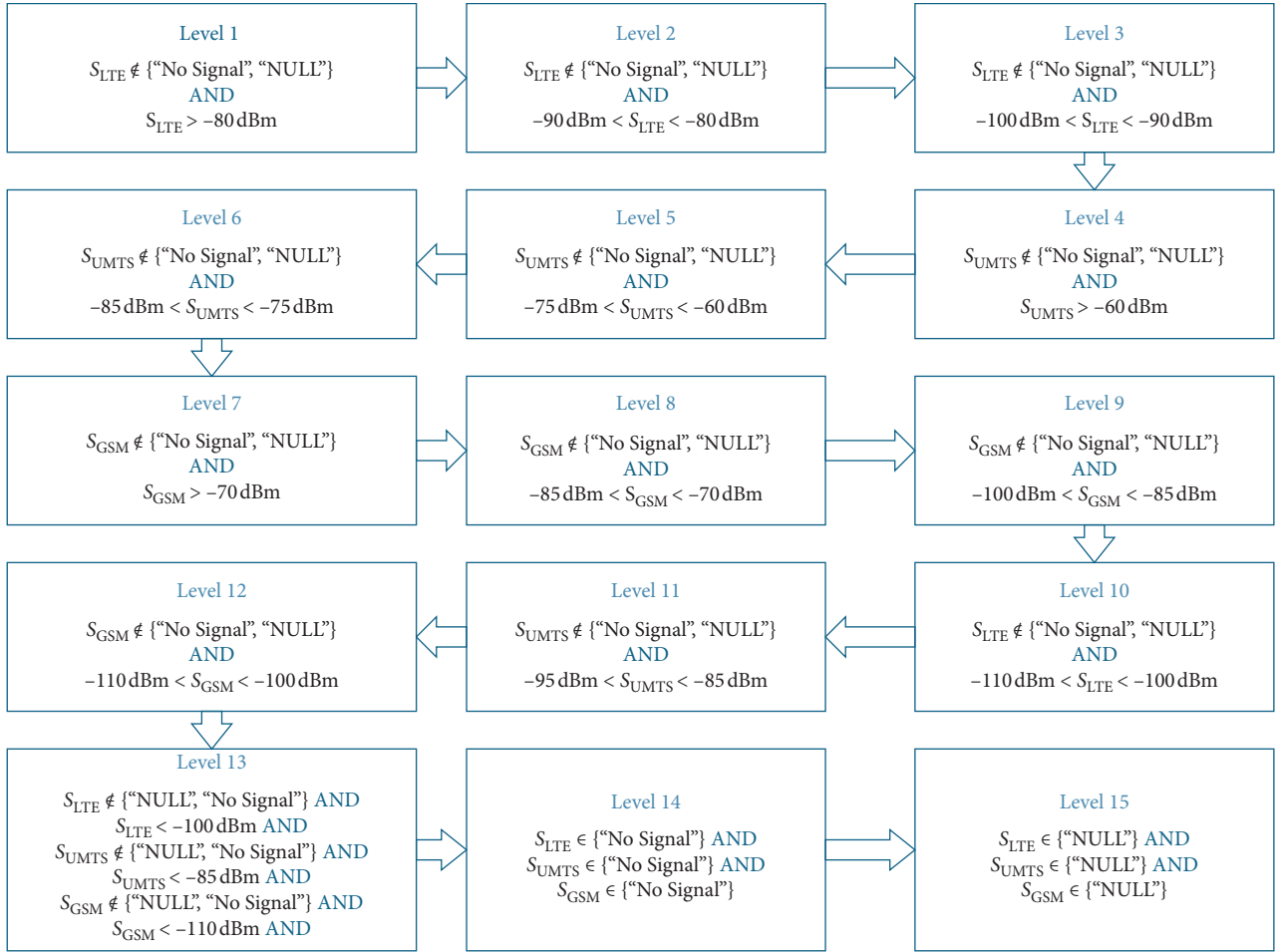


FIGURE 4: Assigning signal levels.

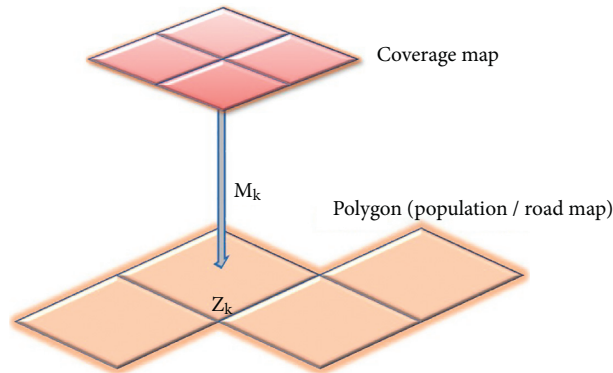


FIGURE 5: Extracting signal strength from coverage map.

system (GIS) software. That is, the polygon in population or road map considers those signal strengths from the overlapping coverage map, when the polygon in coverage map intersects with it. In case the population or road map polygon intersects with multiple polygons of the coverage map, the algorithm selects one random value among them, thereby creating a one-to-one mapping with each polygon in population or road map and signal strength value.

**3.2.2. Framework to Analyze Effects in Roads.** Since the roads can stretch to few kilometers and assigning signal strength to each line is impossible, we split the lines representing roads to segments of 100 m or less, for absorbing information from overlapping coverage map. For example, a road whose length is 1.050 km is divided into 10 units, each of 100 m and one unit of length 50 m. The contribution of the unit of length  $x$ , where  $x < 100$  m, is taken as  $x/100$  while calculating total number of segments

TABLE 2: Feature extraction.

Sl. no.	Option	Setting in algorithm
1	Geometric predicate	Intersect
2	Mapping (join type)	One-to-one
3	Fields to add	Signal strength

in a particular level. Signal strength value is extracted from overlapping coverage map of each RAT,  $S_{LTE}$ ,  $S_{UMTS}$ , and  $S_{GSM}$ , and is assigned to each line segment. As a result, in addition to signal strength value, the line segment object also carries the length of each segment. The line segment extracts signal strength value from overlapped coverage map ( $M$ ) with the settings shown in Table 2. As a result, each line segment object  $q$  is a tuple  $(Z_q, M_q, l_q)$ , where  $l_q$  is the length of the line segment  $q$ .

Furthermore, to analyze the performance of various operators to users on road, we define two variables,  $\lambda_q$  and  $\phi_q$ . The basic logic here is that the coverage poverty experienced by 100 cars in 1 km is the same as that of 1 car in 100 km. Therefore, to quantify the coverage poverty, we multiply the number of cars moving through segment  $q$  with  $l_q$ . Also, to incorporate smaller road segments, we normalize the product by length. Therefore, we define  $\lambda$  for segment  $q$ :

$$\lambda_q = \frac{\text{number of cars through } q \times l_q}{100}. \quad (5)$$

Since different roads have speed limits, we must add this factor into consideration, as the vehicle stays on road for more time in poor coverage areas. Therefore, we define another parameter:

$$\phi_q = \frac{\lambda_q \times 3600}{1000}, \quad (6)$$

where the numerator specifies the speed in (km/hr) and to convert it to (m/s) and we multiply the term by 3.6. These two variables quantify the coverage poverty of absence of coverage to the users.

## 4. Data Analysis

*4.1. Signal Strength across Residential Areas in Municipalities.* Histogram of signal strength is analyzed for various RATs and operators. For the ease of comparison, we consider LTE by Telia in Lulea and Pajala, a comparatively densely populated municipality and a sparsely populated municipality, respectively. Further, the histogram of GSM signal strength is plotted and compared with that of LTE.

Figure 6 shows histogram of GSM signal strength, where the height of each bar shows the percentage of people falling in the respective slot. Both municipalities have maximum number of people in  $-70$  dBm to  $-60$  dBm range for GSM. Also, the range is the same for most of the municipalities.

From Figure 7, we can see that the behaviour in LTE is similar to that of GSM, but majority of people fall in  $-100$  dBm to  $-90$  dBm range. Most of the municipalities show similar behaviour. It is visible that there is a shift in mostly used signal strength in GSM and LTE. That is, from Figure 4, it is known that  $-70$  dBm to  $-60$  dBm range in RSSI

is an excellent GSM signal strength, and  $-100$  dBm to  $-90$  dBm LTE signal strength offers only fair service to the users. On the contrary, the quality of service offered by LTE for signal strength from  $-100$  dBm to  $-90$  dBm is still better than GSM signal strength of  $-70$  dBm to  $-60$  dBm.

*4.2. Signal Strength across Roads in Municipalities.* Figure 8 shows the histogram of signal strength for Telia GSM. For fair comparison of histograms generated for residential areas, we consider the same municipalities, Lulea and Pajala. Unlike residential areas, where both municipalities have maximum number of people in  $-70$  dBm to  $-60$  dBm range for GSM, roads of these municipalities have maximum number of people in  $-90$  dBm to  $-80$  dBm and  $-80$  dBm to  $-70$  dBm ranges, respectively. It is observed that this shift is common for most of the municipalities. Another interesting observation is that the sparsely populated municipality, Pajala, has better signal strength in most of its roads, despite the low population density.

The LTE signal strength in roads of Pajala is reported in Figure 9. Compared to Figure 8, a decrease in signal strength is observed. Although there is a dip in average signal strength in LTE, the performance at the user end is still better than that of GSM. Unlike the histograms of residential areas, where the absence of measurement (“No Data”) is almost zero, the percentage of roads without measurement is bigger. This is mainly due to the mode of measurement, where the measurements are taken by phones placed in mostly public utility vehicles.

*4.3. Effect of Traffic Pattern.* In this subsection, we quantify the effect of 3G signal strength on users on roads. Figure 10(a) plots histogram of  $\lambda$ , where  $\lambda = \{\lambda_q\}$ , for various 3G operators in Jokkmokk. With this approach, the best operator can be identified. Similarly, Figure 10(b) plots histogram of  $\phi$ , where  $\phi = \{\phi_q\}$ , for various 3G operators in Jokkmokk. While the latter gives the idea about temporal signal quality experienced by an average user in car, the former shows the number of cars experiencing the signal strength. However, both figures have more or less the same pattern.

*4.4. Quantifying the Coverage Poverty.* It is quite clear that different municipalities get affected in different levels. A low signal strength in highly populated municipality will have huge impact compared to a less populated area. Figure 11 analyzes average GSM signal strength of Telia on total population of municipalities. While the position of circles represents the mean signal strength and percentage of people without service, the radius of the circles in scatter plot shows



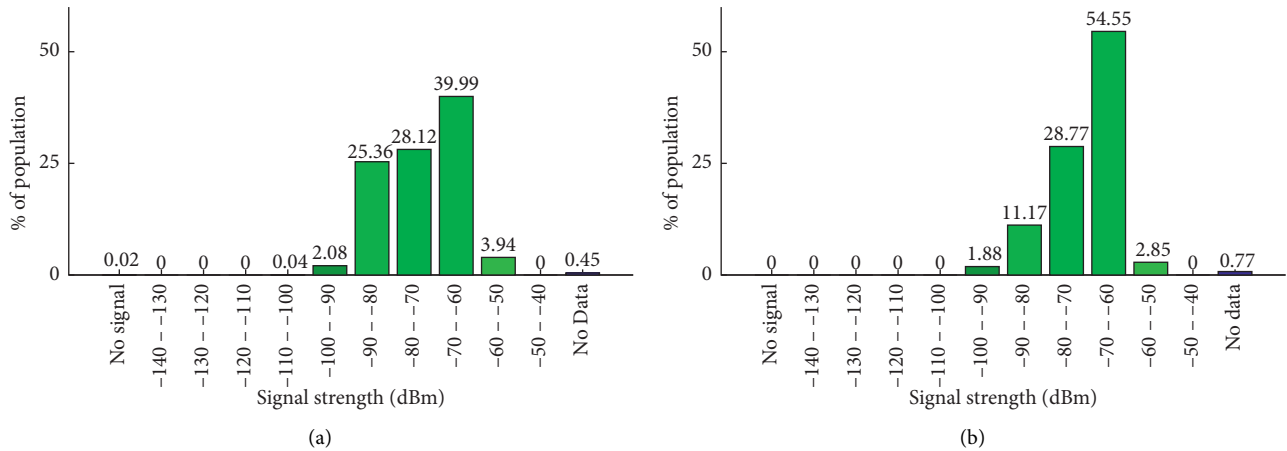


FIGURE 6: GSM coverage in residential areas. (a) Coverage in residential areas of Lulea. (b) 2G Coverage in residential areas of Pajala.

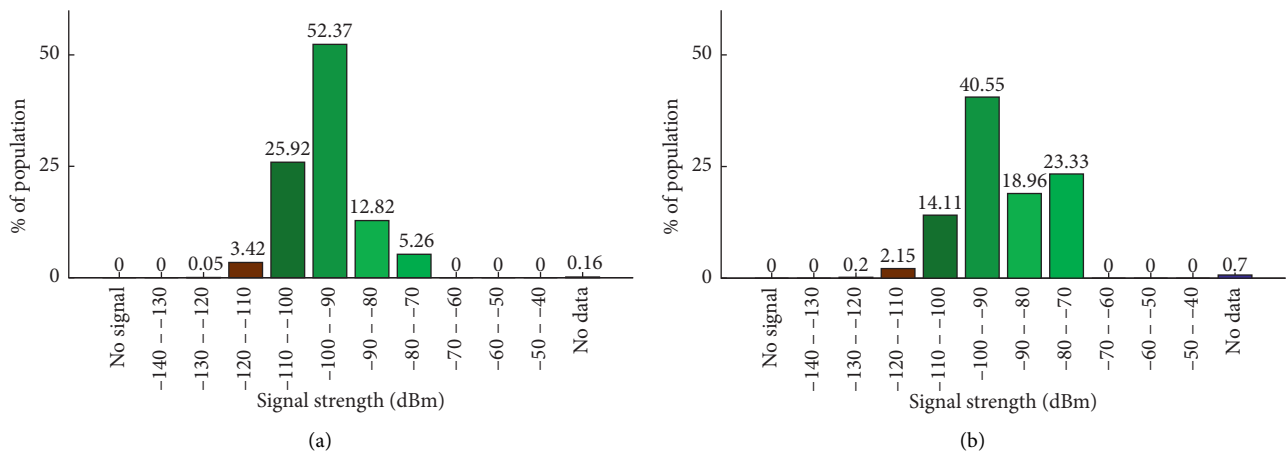


FIGURE 7: LTE coverage in residential areas. (a) 4G coverage in residential areas of Lulea. (b) 4G Coverage in residential areas of Pajala.

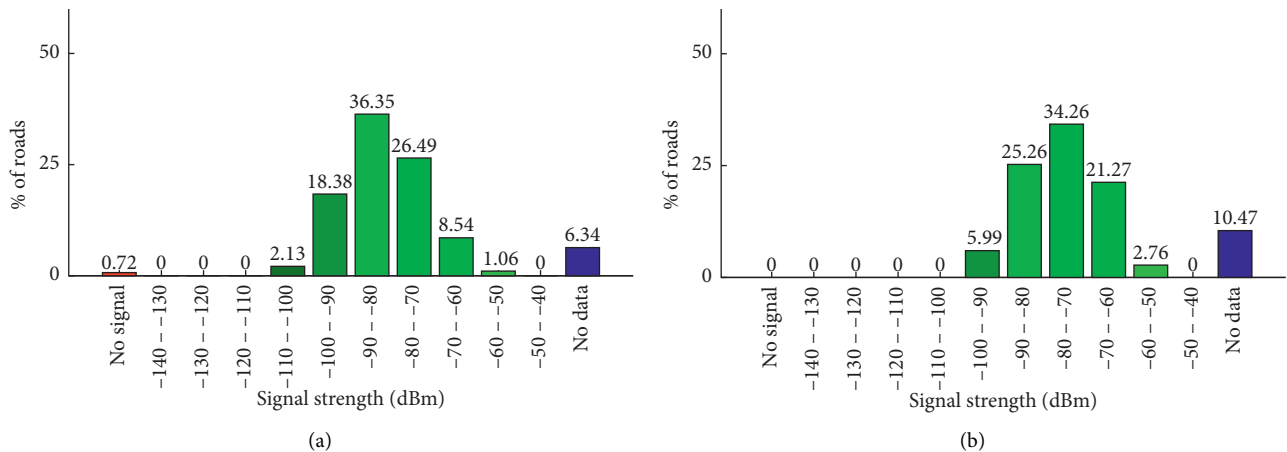


FIGURE 8: GSM coverage on roads. (a) Coverage on roads of Lulea. (b) Coverage on roads of Pajala.

the population or total road length in respective municipalities. Figure 11(a) reports the percentage of population without signal versus mean signal strength with GSM. It is

clear that most of the users in residential areas enjoy fair-quality GSM signal. Most of the populated municipalities have decent signal quality. Also, a very small percentage (less



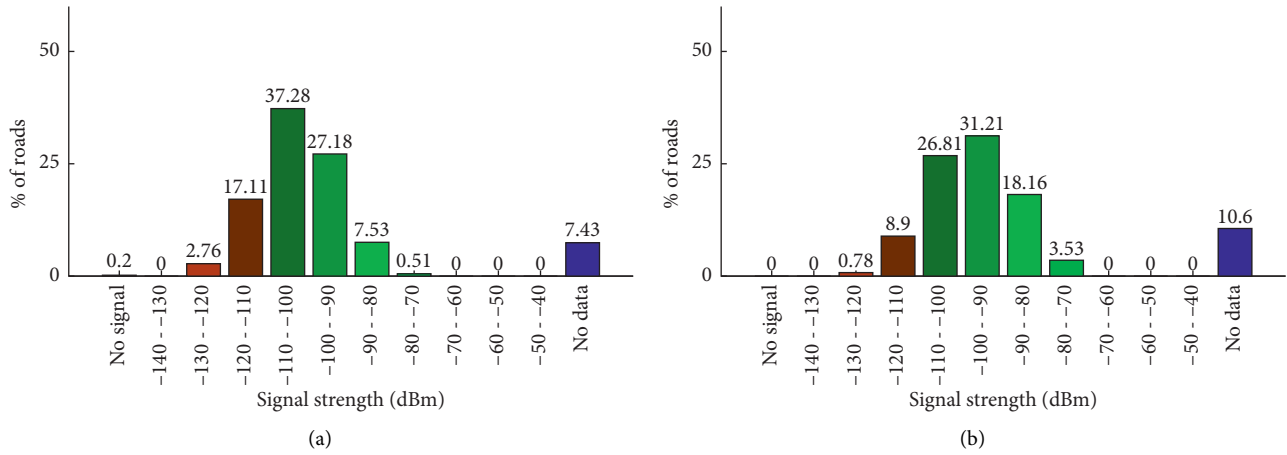


FIGURE 9: LTE coverage on roads. (a) Coverage on roads of Lulea. (b) Coverage on roads of Pajala.

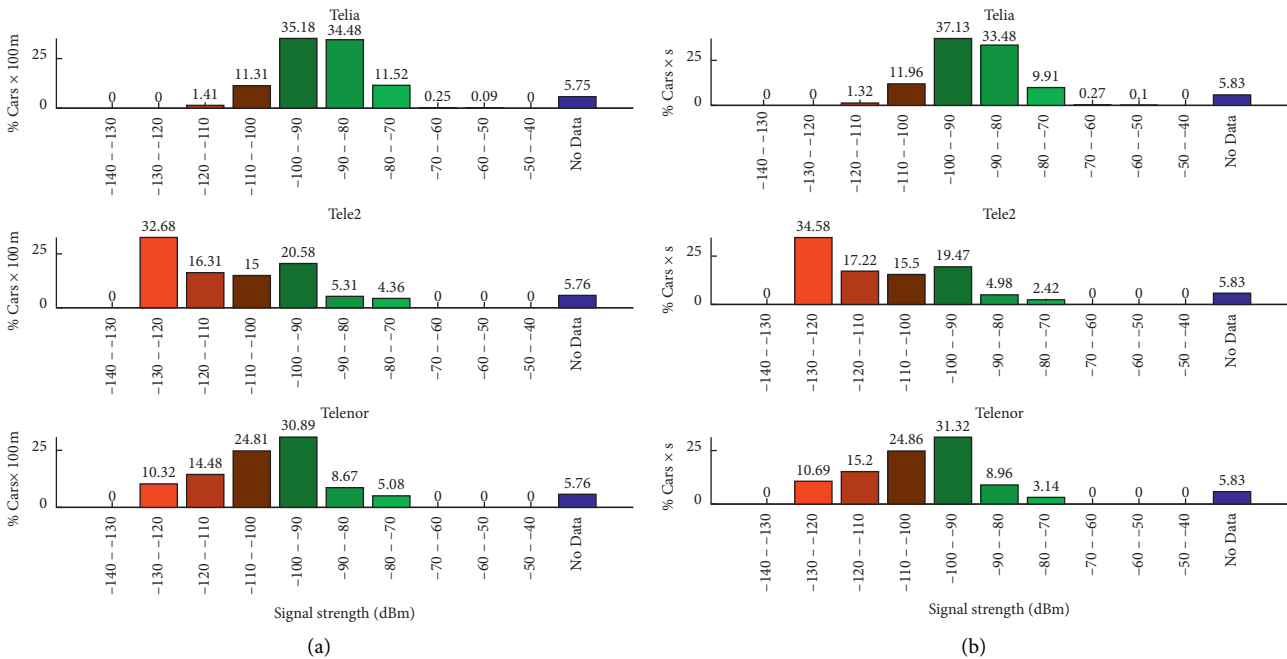


FIGURE 10: Effect of traffic pattern. (a) Cars x 100 m. (b) Cars x sec.

than 1.5) of residential area is not covered. However, on analyzing signal strength on roads, in Figure 11(b), a decline in signal strength is observed. Although majority of municipalities get most of their roads under coverage area, there are municipalities like Övertorneå, where considerable fractions of roads are not covered.

4.5. Signal Strength in Urban, Suburban, and Rest of the Areas.

The effect of signal strength to users in residential areas in urban, suburban, and rest of the areas is reported in Figure 12. The term *rest of the areas* is used to denote residential areas that do not fall under urban or suburban category. The CDF of population is plotted against GSM signal strength. While GSM offers best signal strength in urban areas, the medium and least signal strengths are observed in suburban

areas and rest of the areas, respectively. A fraction of population is under no coverage area of Tele2 and Telenor in suburban areas and *rest of the areas*. However, despite the region classification, Telia offers 1–4 dB better signal to users. It is also important to note that the results in Figure 12 are based only on the available data. We have not considered areas without measurements for analysis.

4.6. Comparison with Another County.

GSM signal strengths of two different counties in Sweden, Norrbotten and Östergötland, are compared in Figure 13. We compare the signal strengths observed in urban and suburban areas of both counties. From Figure 13(a), it is clear that, despite of the county, the signal strength in urban areas remains the same. However, from 13(b), it can be observed that the user

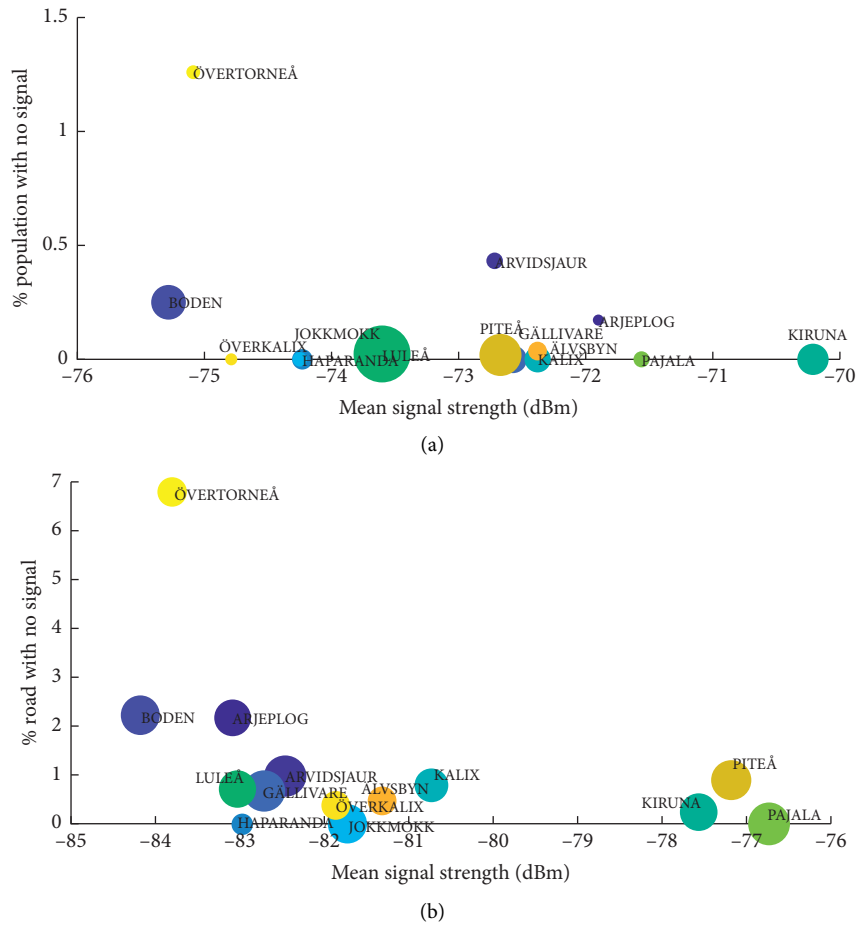


FIGURE 11: Impact on % of roads/population in Telia. (a) Residence area. (b) Roads.

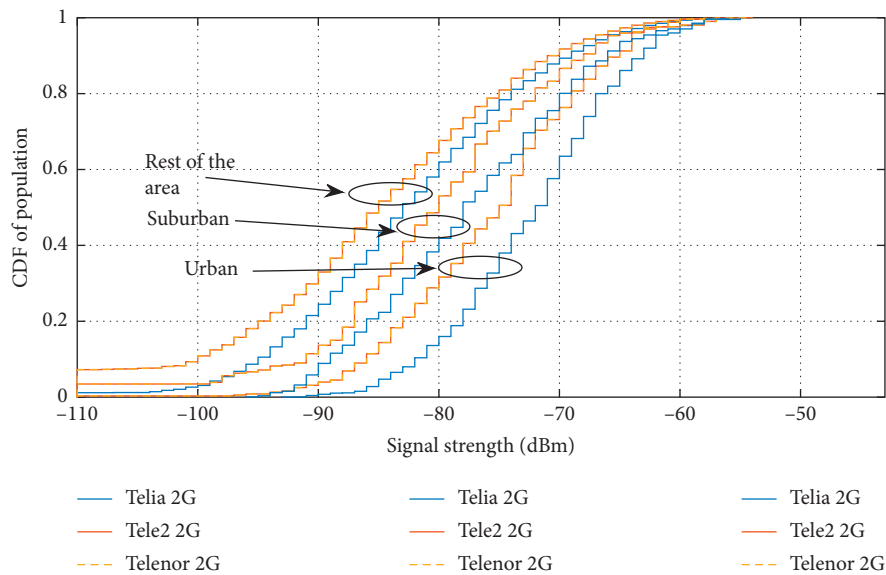


FIGURE 12: Signal strength in urban, suburban, and rest of the areas.

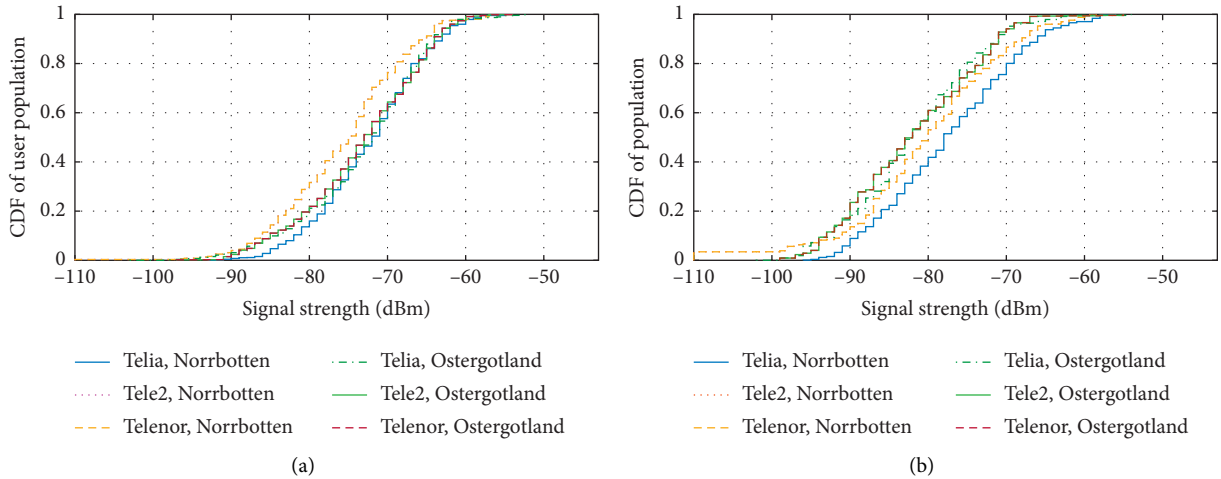


FIGURE 13: Coverage in Norrbotten and Östergötland. (a) Östergötland (urban). (b) Norrbotten (suburban).

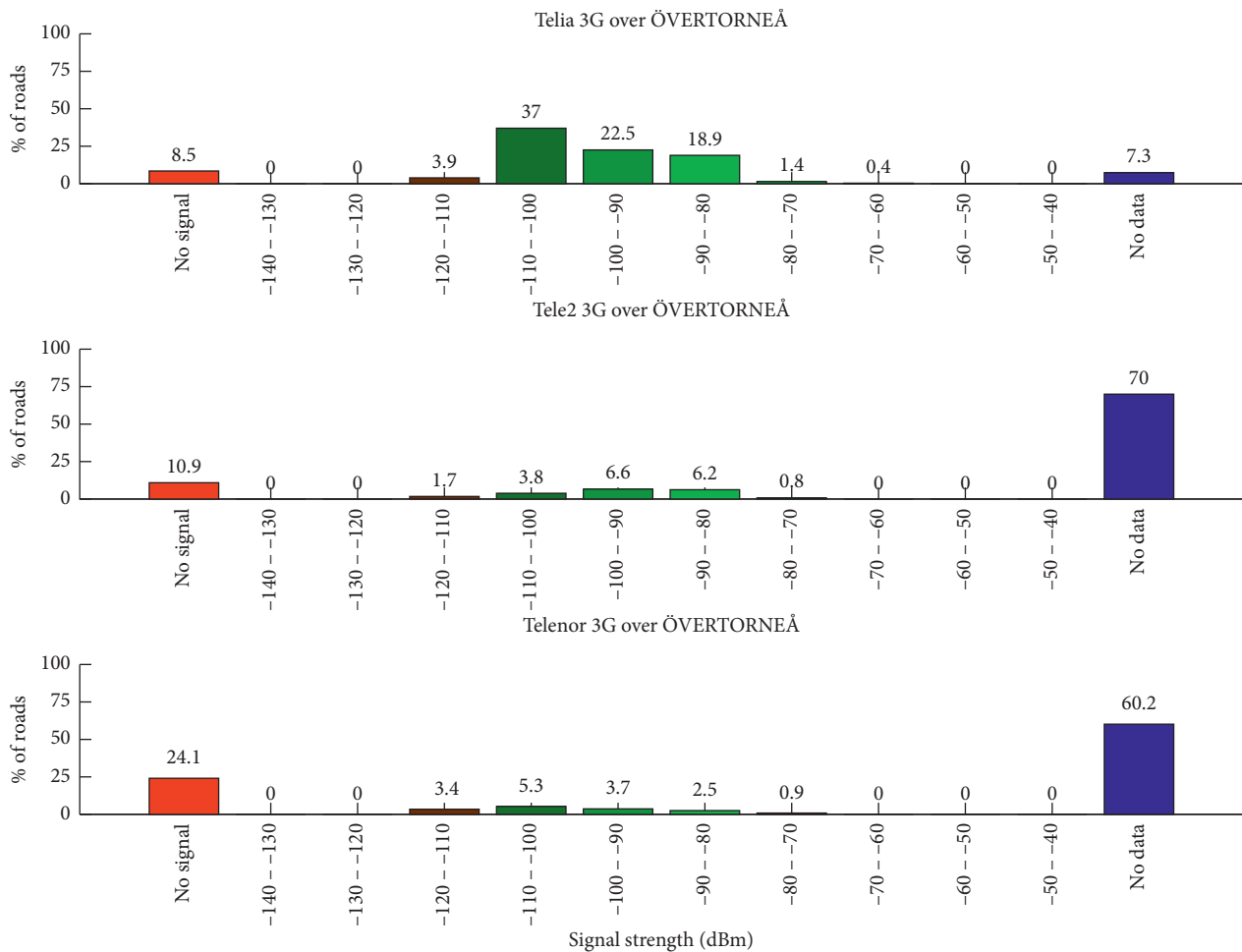


FIGURE 14: Histogram of 3G signal strength in roads of Övertorneå.

gets 5 to 10dB signal strength reduction, when the user moves from urban to suburban area.

4.7. *Effect of Roaming.* It is observed that some areas near Finland are not getting service by Tele2 and Telenor.

Although these areas are in Sweden, Tele2 and Telenor switch the call to another operator from Finland, forming large areas without measurements from Tele2 and Telenor. Telia, on the other hand, offers connectivity from Sweden. Figure 14 shows the histogram of 3G signal strength in roads of Övertorneå. It is seen that 70% of roads and 60.2% of

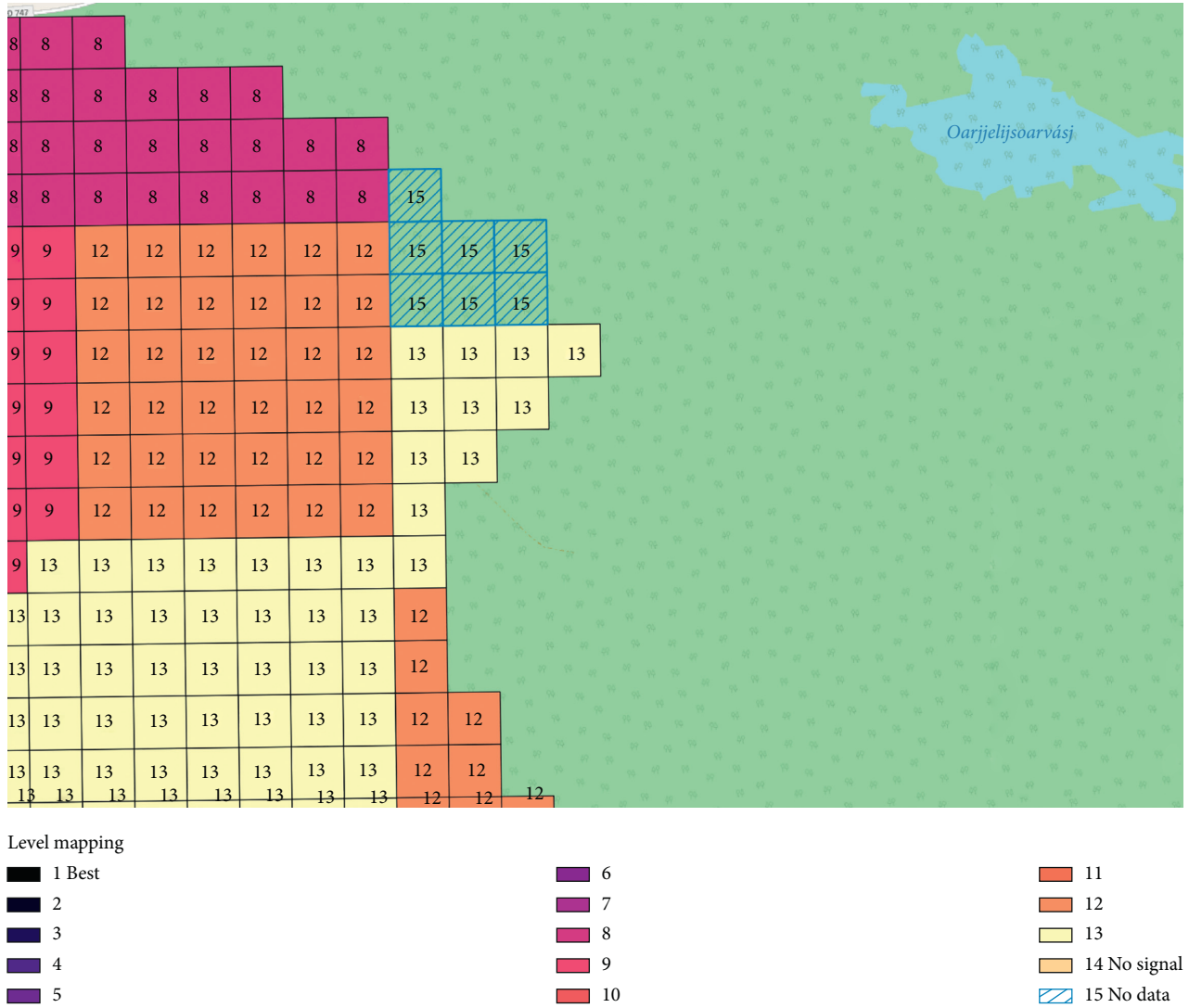


FIGURE 15: Correlation with 700 MHz spectrum’s focus area map.

roads from Tele2 and Telenor are under "No Data" bin. This is because there is no measurement from Tele2 and Telenor in majority of roads and Tele2 and Telenor transfer the call to Elisa, a Finnish operator.

4.8. *Correlation with 700 MHz Spectrum’s Focus Areas.* Recently 700 MHz spectrum has been allocated to certain areas of focus [6]. Figure 15 presents the correlation of Telia’s coverage map developed using algorithm presented in Figure 2 and focus areas of new 700 MHz spectrum, represented by rectangles. Different colours are assigned to each of the locations based on the signal quality, from level 1, which is the best, to level 14, which is the worst. A major portion of the focus area does not intersect with our map due to lack of measurements and is shown in dashed lines. On comparing the focus areas provided with our coverage map, we found that 44.1% of the areas that are intersected with our map experience poor signal (below level 10). Around 54.7% of areas that

are intersected with our map experience below-average signal (level 8–9).

### 5. Conclusions

This paper has presented a framework for analyzing mobile signal strength experienced by users. Based on measured signal strength, a coverage map has been made via IDW interpolation. Various analyses are carried out on signal strength over residential areas and roads of Norrbotten. Further, measurements are compared to those of Östergötland and it was found that both municipalities have almost similar measurements.

By analyzing coverage across all 14 municipalities of Norrbotten, in contrast to the suspicion that rural areas have poor signal strength, we found that 2G and 4G provide satisfactory results. However, 3G fails to provide coverage in some areas. This is worse in some areas, resulting in more than 50% of areas to be outside coverage area at some places. These areas are mostly near the Finland border, which results

in the fact that roaming and additional charges *may* be applicable to the 3G user in these areas.

## Data Availability

The cellular coverage data used to support the findings of this study have not been made available yet, as commercial interests of the supplier prevent this.

## Conflicts of Interest

The authors declare that they have no conflicts of interest.

## Acknowledgments

The authors gratefully acknowledge the financial support for this work from the Norrbotten County Council, along with the relentless efforts from Johanna Lindberg, without whose support this paper would have not been written. The authors also thank here the people involved in the project #full-täckning, with financial support by Vinnova, Norrbotten County Council, and Västerbotten County Council.

## References

- [1] H. Zhang, N. Liu, X. Chu, K. Long, A.-H. Aghvami, and V. C. M. Leung, "Network slicing based 5G and future mobile networks: mobility, resource management, and challenges," *IEEE Communications Magazine*, vol. 55, no. 8, pp. 138–145, 2017.
- [2] "Telia Company and Luleå University of Technology inaugurate 5G-Testbed," 2019, <https://www.teliacompany.com/en/news/news-articles/2019/5g-testbed-lulea/>.
- [3] H. D. Gadi, R. V. Murthy, R. Shanker, and V. Nagadevara, "Antennae location methodology for a telecom operator in India," in *IIM Bangalore Research Paper 454*, 2014.
- [4] J. van de Beek, "Mobile broadband access in Norrbotten," 2019, <https://www.norrbotten.se/publika/lg/regio/Digitalisering/mobile-broadband-access-in-norrbotten-KLAR-NY.pdf>.
- [5] S. A. Hadiwardoyo, C. T. Calafate, J.-C. Cano et al., "Three dimensional uav positioning for dynamic uav-to-car communications," *Sensors*, vol. 20, no. 2, p. 356, 2020.
- [6] "Assignment decision to use radio transmitters in the 700 MHz band," 2019, <https://pts.se/sv/dokument/beslut/radio/2018/tilldelningsbeslut-tillstand-att-anvanda-radiosandare-i-700-mhz-bandet---telia-sverige-ab/>.
- [7] P. Koutroumpis and A. Leiponen, "Crowdsourcing mobile coverage," *Telecommunications Policy*, vol. 40, no. 6, pp. 532–544, 2016.
- [8] D. Baltrunas, E. Ahmed, and A. Kvalbein, "Measuring the reliability of mobile broadband networks," in *Proceedings of the 2014 Conference on Internet Measurement Conference*, pp. 45–58, ACM, Vancouver, Canada, November 2014.
- [9] J. Ponce-Rojas, S. Vidal-Beltrán, M. A. Acevedo-Mosqueda, and M. Jimenez-Licea, "A geographic information system applied to coverage maps of 3g cellular communications networks," *Journal of Geographic Information System*, vol. 03, no. 2, p. 140, 2011.
- [10] A. Lutu, Y. R. Siwakoti, Ö. Alay, D. Baltrūnas, and A. Elmokashfi, "The good, the bad and the implications of profiling mobile broadband coverage," *Computer Networks*, vol. 107, pp. 76–93, 2016.
- [11] X. Chen, H. Wu, and T. M. Tri, "Field strength prediction of mobile communication network based on GIS," *Geo-Spatial Information Science*, vol. 15, no. 3, pp. 199–206, 2012.
- [12] L. Sheynblat and T. Wrappe, "Method and apparatus for determining location of a base station using a plurality of mobile stations in a wireless mobile network," US Patent 7,319,878, 2008.
- [13] W. Riley, R. Girerd, and Z. Biacs, "Use of mobile stations for determination of base station location parameters in a wireless mobile communication system," US Patent 7,127,257, 2006.
- [14] H. Wang, S. Xie, K. Li, and M. Ahmad, "Big data-driven cellular information detection and coverage identification," *Sensors*, vol. 19, no. 4, p. 937, 2019.
- [15] Z. Zhou, M. Zhang, Y. Wang, C. Wang, and M. Ma, "Application of Kriging algorithm based on ACFPSO in geomagnetic data interpolation," *Mathematical Problems in Engineering*, vol. 2019, Article ID 1574918, 14 pages, 2019.
- [16] M. Molinari, M.-R. Fida, M. K. Marina, and A. Pescape, "Spatial interpolation based cellular coverage prediction with crowdsourced measurements," in *Proceedings of the 2015 ACM SIGCOMM Workshop on Crowdsourcing and Crowd-sharing of Big (Internet) Data*, pp. 33–38, ACM, London, UK, August, 2015.
- [17] Z. El-friakh, A. Voicu, S. Shabani, L. Simic, and P. Mahonen, "Crowdsourced indoor wi-fi REMS: does the spatial interpolation method matter?" in *Proceedings of the 2018 IEEE International Symposium on Dynamic Spectrum Access Networks (DySPAN)*, pp. 1–10, IEEE, Seoul, South Korea, October 2018.
- [18] W. Tobler, "Measuring spatial resolution," in *Proceedings of the International Workshop on Geographic Information Systems*, vol. 48, International Geographic Union, Commission on Geographical Information, Beijing, China, 1987.
- [19] "Total Befolkning Per Ruta," 2016, <https://www.scb.se/hitta-statistik/regional-statistik-och-kartor/geodata/oppna-geodata/total-befolkning-per-ruta/>.
- [20] "Norrbotten Trafikdata," 2017, <https://www.trafikverket.se/lastkajen/>.
- [21] "Mobile signal strength recommendations," 2018, [https://wiki.teltonika.lt/view/Mobile\\_Signal\\_Strength\\_Recommendations](https://wiki.teltonika.lt/view/Mobile_Signal_Strength_Recommendations).
- [22] E. Leonard, R. Rainbow, J. Trindall et al., *Accelerating Precision Agriculture to Decision Agriculture: Enabling Digital Agriculture in Australia*, Cotton Research and Development Corporation, Narrabri, Australia, 2017.
- [23] "Electronics communication committee report," 2016, <https://docdb.cept.org/download/494da92a-263a/ECCRep256.pdf>.

## Research Article

# An Adaptive Grid and Incentive Mechanism for Personalized Differentially Private Location Data in the Local Setting

Kangsoo Jung and Seog Park 

*Department of Computer Science and Engineering, Sogang University, Seoul 04107, Republic of Korea*

Correspondence should be addressed to Seog Park; [spark@sogang.ac.kr](mailto:spark@sogang.ac.kr)

Received 10 April 2020; Revised 27 November 2020; Accepted 16 December 2020; Published 30 December 2020

Academic Editor: Peter Brida

Copyright © 2020 Kangsoo Jung and Seog Park. This is an open access article distributed under the Creative Commons Attribution License, which permits unrestricted use, distribution, and reproduction in any medium, provided the original work is properly cited.

With the proliferation of wireless communication and mobile devices, various location-based services are emerging. For the growth of the location-based services, more accurate and various types of personal location data are required. However, concerns about privacy violations are a significant obstacle to obtain personal location data. In this paper, we propose a local differential privacy scheme in an environment where there is no trusted third party to implement privacy protection techniques and incentive mechanisms to motivate users to provide more accurate location data. The proposed local differential privacy scheme allows a user to set a personalized safe region that he/she can disclose and then perturb the user's location within the safe region. It is the way to satisfy the user's various privacy requirements and improve data utility. The proposed incentive mechanism has two models, and both models pay the incentive differently according to the user's safe region size to motivate to set a more precise safe region. We verify the proposed local differential privacy algorithm and incentive mechanism can satisfy the privacy protection level while achieving the desirable utility through the experiment.

## 1. Introduction

With the development of wireless communication technology and widespread of mobile devices, various location-based services are emerging. For example, Dark Sky [1] offers hyperlocal forecasts for an exact address, with down-to-the-minute notifications about changing weather conditions. Curbside [2] is the shopping app using the customer's location information. When the user uses the curbside service, the user gets a notification that the order is ready, and the retailer/restaurant gets an alert when the customer arrives.

There are various techniques [3–8] researched for the proliferation of LBS, and acquiring the good quality of personal location data is one of the essential elements in the LBS. However, there is a risk that personal location data may cause serious privacy violations such as lifestyle exposure or stalking. Users who are threatened by privacy violations do not want to provide their accurate location data. It is one of the biggest obstacles to use more accurate personal location information. Many research studies have been carried out to

solve this privacy violation [9–23], and differential privacy, which is accepted as a de facto standard among the privacy protection techniques, is being studied to protect the privacy of personal location data.

Existing differential privacy is based on the assumption that a trustworthy third party performs the perturbation process. However, it is not suitable for real-world applications because the trusted third party is an overly strong assumption. Therefore, local differential privacy (LDP), in which data owners randomly perturb their data to guarantee the plausible deniability without the trusted data curator, has been proposed. However, LDP has a disadvantage that the data utility is lower than the central DP (CDP). Thus, this limitation should be solved to apply LDP in the real world.

In this paper, we propose a local differential privacy scheme to protect the data owner's location data in an environment where there is no trustworthy third party to perform privacy protection. The proposed local differential privacy scheme allows a data owner to set a publicly available region and apply differential privacy to the data owner's



location data within the region. For example, a certain data owner does not mind to disclose the information that he/she is located in New York. In this case, the goal of differential privacy is to ensure that the data owner's exact location cannot be distinguished from any other location within New York. We call the region that the data owner set to be publicly open as a safe region, and the differential privacy is applied only for the location within the safe region (Figure 1).

In addition, we propose an incentive mechanism that motivates the data owner to provide more accurate location data. In terms of the proposed LDP scheme with the safe region, how to set the safe region size is a major factor in the privacy protection level and data utility. Thus, the data consumer pays the incentive to motivate the data owner to set a safe region as accurate as possible to maximize their profit. We propose the two types of incentive mechanisms to determine the incentive and safe region size. One is the incentive mechanism that maximizes the data consumer's profit, and the other is to optimize the profit of both the data owner and consumer.

The contributions of this paper are as follows:

- (1) Personalized local differential privacy based on the safe region: in the proposed local differential privacy scheme, each data owner sets a safe region to reflect their own privacy sensitivity and the incentive. The safe region size is set differently for each data owner. Thus, personalized privacy protection is possible.
- (2) Adaptive grid size considering population density: we suggest an adaptive size grid configuration technique considering population density in the area to minimize the unnecessary error. By this scheme, we can improve the data utility while satisfying the privacy protection requirements.
- (3) Incentive mechanism for profit optimization: we propose an incentive mechanism that can determine the safe region size considering the profit between the data owner and the data consumer. The proposed incentive mechanism has two types: a principal-agent model that maximizes a data consumer's profit, and the Stackelberg model that negotiates the incentive to maximize a data owner and consumer's profit.

The structure of the paper is as follows. In Section 2, we describe the related works and the existing work's limitation. In Section 3, we introduce the proposed local differential privacy scheme and incentive mechanism. In Section 4, we verify the proposed method through experiments. In Section 5, we discuss the conclusions and future research studies.

## 2. Related Works

**2.1. Differential Privacy.** Differential privacy is a privacy protection mechanism that prevents private information exposure, which is proposed by Dwork [9]. Dwork defined a mathematical model to prevent information exposure, which ensures privacy protection at a specified level  $\epsilon$ . Given



FIGURE 1: The example of a safe region. In this map, users A, B, C, and D have different sizes of safe region.

two neighboring databases,  $D_1$  and  $D_2$ , which differ by only one record, a randomized function  $K$  provides  $\epsilon$ -differential privacy if all datasets with  $D_1$  and  $D_2$  differ by one element only and all O Range (K), i.e.,

$$\Pr[K(D_1) \in O] \leq \exp(\epsilon) \cdot \Pr[K(D_2) \in O], \quad \epsilon > 0. \quad (1)$$

This description of differential privacy means that specific individuals in the statistical database cannot be deduced correctly by keeping the probability of a change in query results by inserting/deleting one data to be less than  $e^\epsilon$ .

According to the definition, the value of  $\epsilon$  which is called the privacy budget affects the amount of added noise. As  $\epsilon$  decreases, the privacy protection is enhanced. Conversely, as  $\epsilon$  increases, the degree of privacy protection decreases.

The most widely used technique for inserting noise to satisfy differential privacy is the Laplace mechanism using the Laplace distribution. Let  $f(D)$  denote a function of database  $D$ . An  $\epsilon$ -differentially private Laplace noise mechanism is defined as  $L(D) = f(D) + X$ , where  $X$  is a random variable drawn from the Laplace distribution and standard deviation =  $\sqrt{2\Delta f/\epsilon}$ . The Laplace distribution is as follows:

$$\Pr(Z | (\mu, b)) = \frac{1}{2b} e^{-(|x-\mu|/b)}. \quad (2)$$

$\Delta f$  is the sensitivity of the function, which means that the maximum value of the change in the query results due to insertion/deletion of a specific individual, that is, the higher the sensitivity and the smaller  $\epsilon$  are, the greater the probability that a larger noise is inserted.

One of the main properties of differential privacy [9] is that it allows composing of queries. Suppose that the algorithms  $K_1$  and  $K_2$  satisfy  $\epsilon_1$ -DP and  $\epsilon_2$ -DP, respectively. Then,  $K_1$  and  $K_2$  also satisfy the following properties:

Sequential composition: for any database  $D$ , the algorithm that performs  $K_1(D)$  and  $K_2(D)$  satisfies  $(\epsilon_1 + \epsilon_2)$ -DP.

Parallel composition: let  $A$  and  $B$  be the partition of any database  $D$  ( $A \cup B = D, A \cap B = \emptyset$ ). Then, the algorithm that performs  $K_1(A)$  and  $K_2(B)$  satisfies the  $\max(\epsilon_1, \epsilon_2)$ -DP.

**2.2. Differentially Private Location Data.** The research for differentially private location data has mainly been studied to protect the count estimation of users for cell-based locations. The utility of these studies is evaluated by the difference between the differentially count estimation in each cell and real count estimation for range query  $Q$ .

The study of [10] applied differential privacy by dividing the entire area into hierarchical grids. In this study, they propose two spatial decomposition techniques: kd-tree, which divides the area in consideration of the density, and quad-tree, which divides the region regardless of density. The study of [11] argues that the existing differential privacy mechanism is not suitable for location data because of the problem of excessive sensitivity when considering all the points of interest. They divide the entire location data into smaller local problems using a local quad-tree with differential privacy to provide better accuracy at the same differential privacy level. Qardaji et al. [12] proposed a uniform grid method (UG) and an adaptive grid approach (AG) to determine the optimal size of the grid cell that divides the region. In the UG scheme, each cell has the same size, but in the AG scheme, the size of each cell differs depending on the data distribution. Li et al. [13] proposed a range query method that determines the optimum size for partitioning the data domain considering the data distribution and calculates the count of each region considering the query workload. Li et al. [13] have verified that the proposed method is suitable for two-dimensional data through the experiment. Chen [14] is the first study to apply differential privacy to location data in a local setting. Chen [14] has defined a safe region taxonomically where the user feels safe to disclose and provide location perturbation method, which satisfies local differential privacy.

As we have seen, the application of differential privacy to location data has mainly focused on studies in the central setting. However, existing research cannot be applied to a local setting environment where there is no trustworthy data curator to carry out differential privacy. Although the local setting has a more realistic premise than the central setting, it is important to improve the utility in the local setting because it has the disadvantage of being less useful than the central setting in terms of data utility.

In this paper, we try to improve the utility in a local setting by determining the adaptive grid size considering the population density in each area. In addition to that, we

propose an incentive mechanism that can motivate users to provide more accurate location data by paying an incentive.

**2.3. Variation of Differential Privacy.** Apple, Google, and Microsoft have introduced local differential privacy algorithms [15–17], and several studies try to apply existing CDP algorithms to local settings. The definition of local differential privacy is as follows.

*Definition 1* (local differential privacy, see [18]). A randomized algorithm  $K$  satisfies  $\epsilon$ -local differential privacy if, for any pair of values  $d$  and  $d' \in D$  and for any  $O \subseteq \text{Range}(K)$ ,

$$\Pr[K(d) \in O] \leq \exp(\epsilon) \cdot \Pr[K(d') \in O], \quad (3)$$

where the probability space is over the coin flips of  $K$ .

LDP has the advantage of not having a trusted third party that performs the DP, but it has the disadvantage of significantly reducing data utility compared to CDP. Especially, as the data domain size increases in LDP, the data utility is deteriorated because of the probability of reporting a noncorrect value by the randomization algorithm increases. For example, in the case of location data, if a country level is set as the data domain, data utility is much lower than for a city. Several techniques are proposed to avoid this problem in LDP, such as domain size reduction or fixed domain size using a hash function.

Another variation of DP is a personal DP (PDP). In general, DP applies the parameter  $\epsilon$ , which determines the level of privacy protection to all personal data. PDP is a variation of DP that each data owner can personally set  $\epsilon$  on the premise that each individual has a different privacy sensitivity. Ebadi et al. [19] defined the PDP that generalizes the definition of DP and proposed an interactive query system called ProPer to implement PDP. Jorgensen et al. [20] proposed a PDP technique that improved data utility while satisfying each user's privacy requirements using the exponential mechanism. Chen [14] proposed a personalized LDP in which the user can select the size of the safe region that each individual allows disclosing the area where his or her is located.

PDP is proposed under the realistic assumption that each individual's privacy sensitivity is different. Although PDP has the advantage of being able to meet each person's privacy requirements while providing better data utility compared to existing DP, PDP needs to consider how to make criteria to determine each user's privacy parameter. In this paper, we define the personalized LPD in which each user can set different safe regions according to each individual's privacy sensitivity and propose an incentive mechanism to motivate the user to set the smaller safe region. Our Personalized LDP definition is as follows.

*Definition 2* (personalized local differential privacy). Given the personalized privacy specification  $(\tau, \epsilon)$  of a data owner  $u$  and  $\tau$  is the data owner  $u$ 's safe region size, a randomized algorithm  $K$  satisfies  $(\tau, \epsilon)$ -personalized local differential privacy (or  $(\tau, \epsilon)$ -PLDP) for  $u$  if, for any two locations  $l$  and  $l' \in \tau$  and any  $O \subseteq \text{Range}(K)$ ,



$$\Pr[K(d) \in O] \leq \exp(\epsilon) \cdot \Pr[K(d') \in O], \quad (4)$$

where the probability space is over the coin flips of  $K$ .

**2.4. Pricing Mechanism.** Along with the study of differential privacy itself, research has studied data pricing in consideration of the privacy protection level [24–30]. Jorgensen et al. [20] proposed a pricing function considering arbitrage-free and discount-free when the buyer queries the data. Ghosh and Roth [25] proposed a compensation mechanism in which data owner is rewarded based on data accuracy when they provide data with differential privacy. In the previous research, a data pricing mechanism sets the price according to the predefined query type or proceeds auction. However, these methods have limitations in determining price only from the data consumer’s perspective. Anke et al. and Rachana et al. [26, 31] suggested a mechanism to adjust the balance between privacy and cost in the data market environment. They consider the owner’s benefit, but it is still at an early stage.

The existing pricing mechanism focuses on data pricing according to  $\epsilon$  value. In addition to the existing pricing mechanism for  $\epsilon$  value, we propose an incentive mechanism based on safe regions to satisfy the PLDP definition. We propose the two incentive mechanisms in terms of the participant’s profit: one is the principal-agent model to maximize the data consumer’s profit; the other is the Stackelberg model which optimizes both the data owner and consumer’s profit.

### 3. Differentially Private Location Data in Local Setting and Pricing Mechanism

**3.1. Overview.** As described above, the proposed local differential privacy scheme determines the adaptive grid size by considering the density information of the area and satisfies PLDP definition by applying perturbation within a personal safe region, which is set by the user. To perform the proposed scheme, we need a user’s privacy sensitivity, density information, and incentive  $incentive_{i,j}$ . Unlike CDP, user’s privacy sensitivity and density information should be collected in the LDP environment. To this end, we design the proposed scheme in two phases to collect the necessary information from the user. An overview of the entire process is shown in Figure 2.

- Step 1: the data consumer divides the entire area into a uniform size grid and then sends the grid map to each user.
- Step 2: users perturb their location using a uniform size grid map and send perturbed location data to the data consumer.
- Step 3: the data consumer aggregates perturbed location data and then divides each uniform grid area into an adaptive grid size using the aggregated perturbed data. The data consumer sends the adaptive grid map, density

information, and suggested incentive  $incentive_{i,j}$  to each user.

- Step 4: each user determines the safe region size using the adaptive grid map, density information, and  $incentive_{i,j}$  and sends the perturbed data within a safe region to the data consumer.
- Step 5: the data consumer estimates the total count estimation using the perturbed location information.

In the following sections, we describe each step in more detail. Section 3.2 describes the local differential privacy schemes, and Section 3.3 describes the proposed incentive mechanism. The notation used in this paper is as follows (Table 1).

#### 3.2. Differentially Private Location Data in a Local Setting

**3.2.1. Phase 1: Density Estimation for the Entire Area.** The first step in the proposed local differential privacy scheme is to obtain the entire area’s density information. In the central setting, it is not necessary to collect the density information because it is already known. However, in the local setting, we should collect density information to determine the adaptive grid size. We split the entire budget to  $\epsilon_1$  and  $\epsilon_2$  and use  $\epsilon_1$  to collect the entire area’s density information and  $\epsilon_2$  to perturb user’s location within the safe region.

First, we divide the entire area into a uniform grid size. When we divide the area into the grid and apply the DP to location information, we should consider two types of error. The first one is caused by noise insertion for DP, and the other is a nonuniformity error that is caused by dividing the area into the grid. If the density of all areas is uniform, the nonuniformity error is 0, but if the density is skewed, this error increases, that is, if the size of the grid increases, the nonuniformity error increases. On the contrary, the error for DP reduces as the grid size increases because of the number of the grid in which noise is inserted by DP decreases. Thus, we need to set an appropriate grid size to minimize the sum of the two types of errors. In this paper, we follow Guideline 1, which is validated by Qardaji et al. [12] to minimize the sum of errors.

Guideline 1. In order to minimize the error in uniform grid size, the grid should be partitioned into  $m_1 \times m_1$  cells, where  $m_1$  is computed as follows:

$$m_1 = \sqrt{\frac{N\epsilon_1}{c}}, \quad (5)$$

where  $N$  is the number of users in the entire area,  $\epsilon_1$  is the total privacy budget, and  $c$  is the small constant (usually  $c = 10$ ) depending on the dataset.

After the data consumer sends the grid map to the user, users send the perturbed location using a uniform size grid map to the data consumer. We use the Hadamard count-min sketch data structure for the user’s location perturbation. The count-min sketch is the probabilistic data structure [30], which is mainly used for frequency estimation in data

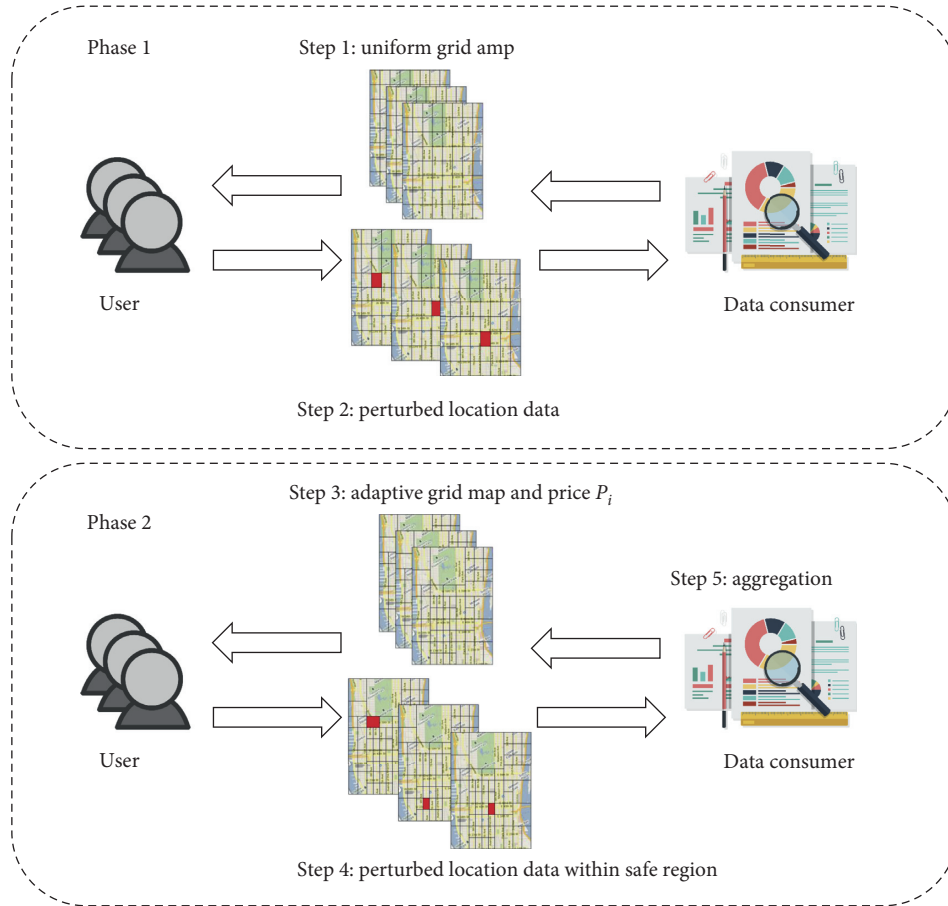


FIGURE 2: Overview of the proposed local differential privacy scheme.

TABLE 1: Key notation.

Key notations	
$C_i$	$i^{\text{th}}$ data consumer
$P_j$	$j^{\text{th}}$ user
$S_j$	$j^{\text{th}}$ user safe region
$U_{c_i}$	$i^{\text{th}}$ data consumer profit
$U_{p_j}$	$j^{\text{th}}$ user profit
$\text{incentive}_{i,j}$	Incentive by the $i^{\text{th}}$ data consumer to the $j^{\text{th}}$ user
$\text{util}_i$	$i^{\text{th}}$ data consumer's utility for $j^{\text{th}}$ user data
$\theta_j$	$j^{\text{th}}$ user privacy sensitivity
$p\_cost_j$	$j^{\text{th}}$ user privacy cost
$c\_cost_j$	$j^{\text{th}}$ user communication cost
$S_{\max}$ and $S_{\min}$	Maximum/minimum size of safe region

streaming environments where only a small fraction of elements have a high-frequency value. Our intuition is that the count-min sketch is suitable because location data is generally skewed in a specific area.

Hadamard transform is [32] a useful tool for reducing the communication cost and error. The Hadamard matrix  $H$  is defined recursively as follows:

$$H_i = \begin{bmatrix} H_{i/2} & H_{i/2} \\ H_{i/2} & -H_{i/2} \end{bmatrix}, \quad (6)$$

where  $H_1 = [1]$  and  $i$  is power of two.

Note that the columns of  $H_i$  are orthogonal and  $H_i \cdot H_i^T = i \cdot I_i$ .

Our randomizer takes as input an  $m$ -bit string represented as  $\{-(1/\sqrt{m}), (1/\sqrt{m})\}^m$ , and  $m$  could be any value that is large enough to satisfy the Johnson-Lindenstrauss Lemma (JL-Lemma).

**Theorem 1** (Johnson-Lindenstrauss lemma). *Given  $0 < \eta < 1$ , a set of  $V$  of  $m$  points in  $R^D$ , and a number  $n > 8 \ln(m)/\eta^2$ , there is a linear map  $f: R^D \rightarrow R^d$  such that*

$$(1 - \eta)u - v^2 \leq f(u) - f(v)^2 \leq (1 + \eta)u - v^2, \quad (7)$$

for all  $u, v \in V$ .

The local randomizer and count estimation algorithm are given in Algorithm 1.

This local randomizer [25] guarantees the local differential privacy. We use this local randomizer in Algorithm 2.

Algorithm 2 is based on succinct histogram protocol [25], and we describe Algorithm 2. Firstly, the server calculates the number of grid  $d$  and divides the entire area into a uniform grid size (line 1). Secondly, the server generates the  $k \times m$  sketch matrix  $M^h$  (line 5), and each user maps their location's grid to  $j$  hash function value, randomizes this hash function using local randomizer  $LR$ , and sends it to the server (lines 7-14). The server decodes the perturbed

**Input:**  $m$ -bit string  $x \in \{-(1/\sqrt{m}), (1/\sqrt{m})\}^m$ , the privacy budget  $\epsilon$ , and user's hashed location  $l_{i,j}$   
**Output:** sanitized bit  $z^j$

- (1) Generate the standard basis vector  $e_l \in \{0, 1\}^d$
- (2)  $x_l = X^T e_l$
- (3) Randomize  $j$ -bit  $x_j$  of the input  $x \in \{-(1/\sqrt{m}), (1/\sqrt{m})\}^m$
- (4)  $z^j = \begin{cases} c_\epsilon m x_l^{i,j}, & \text{with probability } (e^\epsilon / e^\epsilon + 1) \\ -c_\epsilon m x_l^{i,j}, & \text{with probability } (1/e^\epsilon + 1) \end{cases}$
- (5) where  $c_\epsilon = (e^\epsilon + 1/e^\epsilon - 1)$
- (6) **return**  $z^j$

ALGORITHM 1: Local randomizer LR.

**Input:** user's location  $l_i$ , number of user  $n$ , confidence parameter  $0 < \beta < 1$ , and user's privacy specification  $\epsilon_1$   
**Output:** user location count  $\text{Min}(M^{h_1}(l_i), \dots, M^{h_j}(l_i))$

- (1) Server calculates the number of grid  $d = \sqrt{(N\epsilon/c)}$
- (2) Server calculates  $\gamma \leftarrow \sqrt{(\log(2d/\beta)/n)}$
- (3) Server calculates  $m \leftarrow (\log(d+1)\log(2/\beta)/\gamma^2)$
- (4) Server generates a random matrix  $\phi \in \{-(1/\sqrt{m}), (1/\sqrt{m})\}^m$
- (5) Server initializes  $M^h \in \{0\}^{k \times m}$
- (6) Server initializes  $z$  and  $f$
- (7) **for** each user  $u_i$  **do**
- (8)   **for** each hash  $h_j$  **do**
- (9)     server randomly generates  $k$  from  $\{1, \dots, m\}$
- (10)    server sends  $k$ th row  $\phi_k$  to  $u_i$
- (11)     $u_i$  returns  $z_{i,j} = \text{LR}(\phi_k, h_j(l_i), \epsilon_1)$  to server
- (12)    server adds  $z_{i,j}$  to  $k$ th bit of  $M^{h_j}$
- (13)    **end for**
- (14) **end for**
- (15) **for** each hash  $h_j$  **do**
- (16)    **for** each hashed location  $h_j(l_i)$  **do**
- (17)     server sets  $M^{h_j}$ 's  $i$ th element of  $c$  to  $\langle \phi_i, z \rangle$
- (18)    **end for**
- (19) **end for**
- (20) **return**  $\text{Min}(M^{h_1}(l_i), \dots, M^{h_j}(l_i))$

ALGORITHM 2: Hadamard count-min sketch LDP algorithm.

Hadamard code, estimates the count-min sketch (lines 15–19), and returns the count-min sketch structure  $M^h$ . The server determines the user  $i^{\text{th}}$  location  $l_i$ 's count estimation as  $\text{Min}(M^{h_1}(l_i), \dots, M^{h_j}(l_i))$ .

**3.2.2. Phase 2: Count Estimation Using the Safe Region.** The data consumer estimates the density of the entire area using information gathered in phase 1 and then divides the entire area into adaptive grid sizes. We follow the adaptive grid size guideline [12].

Guideline 2. Given a cell with a noisy count of  $N^i$ , to minimize the errors, the grid should be partitioned into  $m_2 \times m_2$  cells, where  $m_2$  is computed as follows:

$$m_2 = \sqrt{\frac{N^i \epsilon_2}{c_2}}, \quad (8)$$

where  $c_2 = c/2$  and  $c$  is the same constant as in Guideline 1.

The major benefit of the adaptive grid over the existing recursive partition-based method [8] is the data utility enhancement. In the case of the existing partition-based method without considering the population density, noise is inserted into an unnecessary area where users do not exist (sparsity problem). It causes serious data utility degradation. On the contrary, in the case of an adaptive grid considering the population density, the grid size is determined according to the density of each cell. It mitigates the data utility deterioration.

In addition to that, we apply PLDP within the safe region. By using the safe region, we can reduce the data domain to improve the data utility and meet each user's realistic privacy requirements.

After the adaptive grid size determination, the data consumer distributes an adaptive grid map and the incentive  $\epsilon_{i,j}$  to each user. Each user sets a safe region based on the adaptive grid map, incentive  $\epsilon_{i,j}$ , and their own privacy sensitivity  $\theta_j$ .

**Definition 3** (safe region). The safe region is an area where each user  $j$  allows to be exposed in public. The safe region size is calculated as follows:

$$S_i = e^{(-\text{incentive}_{i,j}/\theta_j)} \times S_{\max}, \quad (9)$$

where  $S_{\max}$  is set by the data consumer.

If the proposed incentive  $\text{incentive}_{i,j}$  becomes larger, the safe region size becomes smaller. If privacy sensitivity becomes larger, the size of the safe region also becomes larger. Each user perturbs his/her location data within a safe region using an adaptive grid and sends it to the data consumer. We use  $\varepsilon_2$  for the location perturbation and modify the succinct histogram method [33] for the local environment to perturb the user's location. The data consumer aggregates the perturbed location and performs the final count estimation.

**3.3. Incentive Mechanism for Optimization.** In the proposed technique, the data utility is affected by  $\varepsilon$  value and safe region size  $S_i$ . We assume that the  $\varepsilon$  value determines the existing incentive mechanism. Thus, data consumers have the motivation to pay a reasonable incentive to encourage the user to set a safe region size as accurate as possible. We propose the two incentive models: a principle-agent model that maximizes a data consumer's profit, and the Stackelberg model to maximize a profit of both data consumer and data owner.

**3.3.1. Principal-Agent Model.** If a data consumer knows the user's privacy sensitivity, the data consumer can set an incentive to maximize his/her own profit. This incentive must be larger than the user's cost. The equation is expressed as follows:

$$\begin{aligned} & \max U_{c_i}(\text{incentive}_{i,j}), \\ & \text{such that } U_{p_j}(\text{incentive}_{i,j}) > 0. \end{aligned} \quad (10)$$

The profit of the consumer is calculated by the profit that consumer gains using the data minus the cost that the consumer pays. The consumer's profit is affected by the safe region size  $S_i$ , data utility  $\text{util}_i$ , and payment  $\text{incentive}_{i,j}$  for the data.

The safe region size is determined by each user's privacy sensitivity  $\theta_j$  and  $\text{incentive}_{i,j}$  paid by the consumer  $i$  (Figure 3).

The higher the privacy sensitivity  $\theta$ , the larger the  $S_i$ , and the higher the  $\text{incentive}_{i,j}$ , the smaller the  $S_i$ . The data consumer and user's profit function  $U(\text{incentive}_{i,j})$  is as follows:

$$U_{c_i} = \sum_j^n ((1 - S_i) \times \text{util}_i - \text{incentive}_{i,j}), \quad (11)$$

$$U_{p_j} = \text{incentive}_{i,j} - (1 - S_i) \times p\_cost_j, \quad (12)$$

where  $(1 - e^{S_i}) \times p\_cost_j$  is the user  $j$ 's privacy cost.

Since the  $\text{util}_i$  and  $\theta_j$  are constants, which are set by the consumer and user, the profit is determined by  $S_i$ , which is

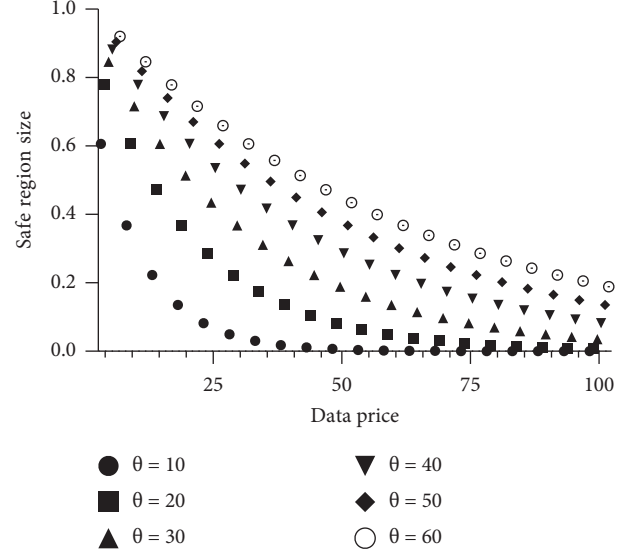


FIGURE 3: Safe region size with  $\text{incentive}_{i,j}$  and  $\theta_j$ .

affected by the  $\text{incentive}_{i,j}$  paid by the consumer. Thus, we should find a  $\text{incentive}_{i,j}$  to maximize equation (11).

The first-order derivative of the function  $U_{c_i}$  is  $(\partial/\partial \text{incentive}_{i,j})U_{c_i} = (\text{util}_i \times e^{(\text{incentive}_{i,j}/\theta_j)}/\theta_j) - 1$ . We obtain optimal  $\text{incentive}_{i,j}^*$ , where  $(\text{util}_i \times e^{(\text{incentive}_{i,j}/\theta_j)}/\theta_j) - 1 = 0$  because the second-order derivative of the function  $U_{c_i}$  is  $(\partial^2/\partial^2 \text{incentive}_{i,j}) = -(\text{util}_i \times e^{(\text{incentive}_{i,j}/\theta_j)}/\theta_j^2) < 0$ .

Then, the data consumer pays  $\text{incentive}_{i,j}^*$  for the user who is able to maximize their profits.

**3.3.2. Stackelberg Game Model.** If the data consumer does not know the user's privacy sensitivity, the principal-agent model cannot be used. In this case, we use the Stackelberg model for incentive mechanisms. The Stackelberg game [34] is a type of game theory in which one participant becomes a leader with more information than the other participants, predicting their reaction to their strategy and making decisions. The remaining participants become followers of the leader and take the action that is most profitable to himself/herself. The follower does not have information about the leader's decision, but the leader has information about the follower's decision-making process. Therefore, the leader can predict the reaction that the follower will react to the leader's decision. The leader puts his followers' responses to his choices in advance and decides his optimal strategy. The follower observes the leader's strategy and chooses his/her best strategy.

We define the incentive problem of safe region size as a Stackelberg game situation. The data consumer is acting as the leader, and the user is the follower. They try to maximize their own profit as follows:

$$\begin{aligned} & \max U_{c_i}(\text{incentive}_{i,j}), \\ & \max U_{p_j}(\text{incentive}_{i,j}). \end{aligned} \quad (13)$$



Backward induction is applied to solve the problem. First, given incentive  $i_{i,j}$ , the user determines  $S_i$  to optimize  $U_{P_j}$ . Based on the user's decision on safe region size, the data consumer decides on incentive  $i_{i,j}$  to optimize their profit  $U_{C_i}$ .

## 4. Experimental Results

*4.1. Experimental Environments.* We perform the following experiments to verify the proposed scheme:

- (1) Hadamard count-min sketch local DP performance
- (2) Impact of privacy sensitivity based on safe region size
- (3) Comparison of the principle-agent model and Stackelberg model
- (4) Comparison of the proposed PLDP and existing methods

The data used in the experiment are Yelp [35] and California datasets [36]. Yelp data is a check-in data consisting of user's location data, about 5 million data, and California data is location data of the point of interest in California, which has 85,920 data. We sampled this data in our experiments.

The parameters used in the experiments and the default values are given in Table 2.

The values in bold are the default parameter values. The size of the grid was determined by using Guidelines 1 and 2, and the ratio of  $\epsilon_1$  to epsilon  $\epsilon_2$  is 7:3 because  $\epsilon_1$  splits to the hash function which is used in sketch structure. We use the RMSE as the evaluation criteria for measuring the performance.

We use Super Micro Computer, Inc.'s SuperServer 7049P-TR (64-bit), consisting of CPU Intel Xeon Silver 4110 and 64 GB memory, and the operating system is Ubuntu 16.04.2 LTS. The proposed technique is implemented in Python 2.7.12.

*4.2. Hadamard Count-Min Sketch Local DP Performance.* The proposed PLDP scheme uses the succinct histogram method proposed in [33] using a count-min sketch and Hadamard transform. As the number of hash  $h$  and sketch vector size  $w$  become larger, the error due to collision decreases. However, if the  $w$  becomes larger, the domain size increases and data utility decreases due to the perturbation. If  $h$  increases,  $\epsilon_1$  should split by the sequential composition property. We experimented with changing the number of sample  $N$ ,  $h$ , and  $w$ .

Experimental results show that the accuracy increases when  $h$  and  $w$  increases (Figure 4). However, as the  $h$  and  $w$  increases, the accuracy enhancement ratio decreases. We find that if the epsilon value was sufficient, the accuracy enhancement ratio is sustained. This is the result of interference between the sketch structure and succinct histogram protocol.

*4.3. Impact of Privacy Sensitivity Based on Safe Region Size.* In the proposed scheme, each user has their own privacy sensitivity  $\theta_j$ , which is a factor determining the safe region size with incentive  $i_{i,j}$ .

TABLE 2: The parameter and default value.

Parameter	Value
Number of sample $N$	10,000, <b>15,000</b> , and 20,000
Epsilon value $\epsilon$	1, <b>2</b> , and 3
Number of hash $h$	2, <b>3</b> , and 4
Sketch vector size $w$	16, <b>32</b> , and 64
$\theta_j$	20, <b>40</b> , and 60
P_cost $_j$	40
util $_i$	40
Price $_{i,j}$	40

We measured the mean value of the safe region size according to the distribution of the users'  $\theta_j$  and the RMSE value when the  $price_{i,j}$  is fixed. First, we classify the users into three groups:  $(\theta=20: \theta=40: \theta=60)=(10:20:70)$ ,  $(\theta=20: \theta=40: \theta=60)=(30:40:30)$ , and  $(\theta=20: \theta=40: \theta=60)=(70:20:10)$ , that is, we classify the users into high-sensitivity group, normal sensitivity group, and low-sensitivity group.  $incentive_{i,j}$  is fixed at 40, and the other parameter is set equal to the default setting.

When  $S_{max}$  is set as the entire area, the experimental results show that safe region size is changed according to the privacy sensitivity (Figure 5). These results confirm that the group with higher privacy sensitivity set a larger safe region and the group with smaller privacy settings had a smaller safe region. Moreover, the RMSE score was changed in proportion to the safe region size.

*4.4. Comparison in the Principle-Agent Model and Stackelberg Model.* We compared the profits of data consumers and users when determining  $incentive_{i,j}$  using the proposed incentive models, the principal-agent model and Stackelberg model. We fixed the privacy sensitivity to a normal group and compared the profit and performance of both models. The consumer's total budget was limited to 100,000. As shown in the results, the principal-agent model has a higher profit for the data consumer, and the RMSE is also lower (Table 3, Figure 6). This is because the Stackelberg model basically supposes the decentralized environment, which does not have a trusted third party. However, as can be seen from the safe region size, the Stackelberg model is a more fair model for the user than the principal-agent model.

*4.5. Comparison in the Proposed PLDP and Existing Methods.* We compared the performance of the proposed PLDP and existing methods [13, 14]. We select [13] as a comparative group because it proposes a local differential privacy scheme using a safe region in the same way as the proposed technique. However, they use a uniform grid size and static tree-structure taxonomy for the safe region. The study [13] is used as a comparative group in many research studies because it shows a fine performance for differentially private location data. It [13] is not a local differential privacy scheme, but it can adapt to the local differential privacy easily. In the experiment, we set the default parameter value, but for [13], we set the average safe region size in the proposed technique. The experiment was carried out by changing the epsilon value from 1 to 3.

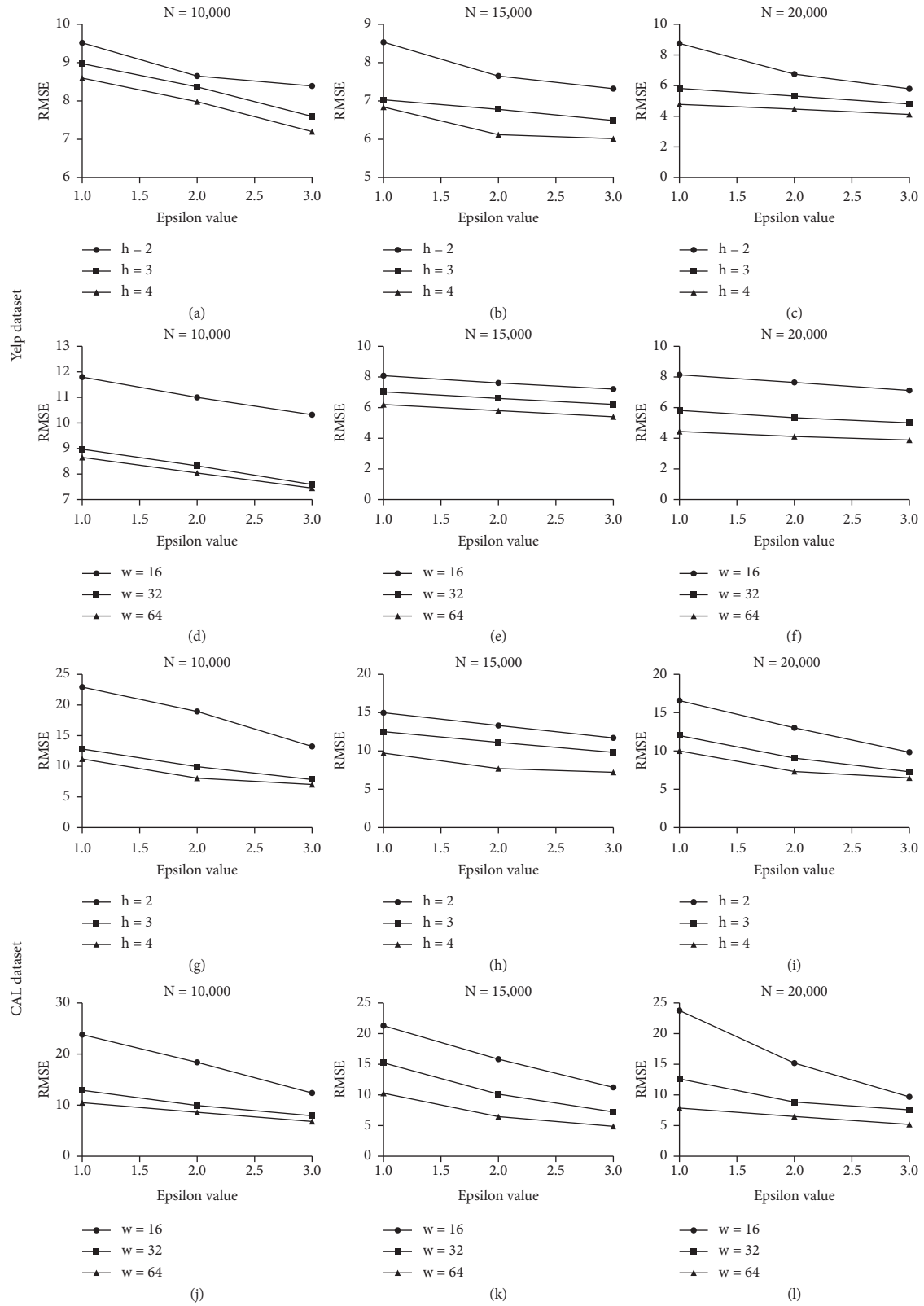


FIGURE 4: RMSE score for Sketch-Hadamard LDP for Yelp and California datasets.

The experimental result shows that the proposed technique has the lowest RMSE value (Figure 7). In the case of the proposed technique and [10], it shows higher

performance than [13] because noise is only inserted into the safe region’s grid. The proposed technique shows higher performance than [14] because the proposed technique

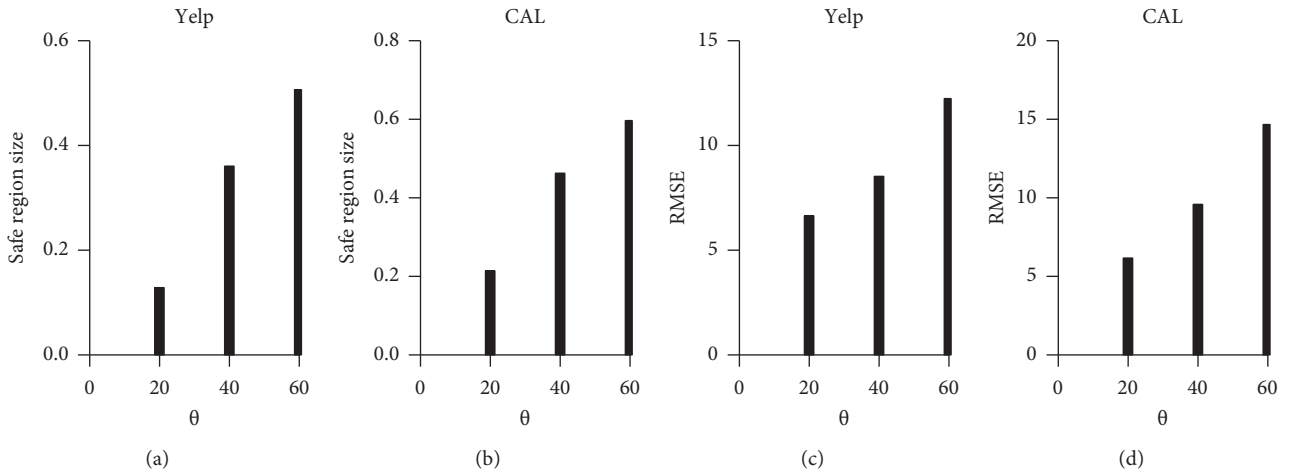


FIGURE 5: Safe regions size and RMSE score for privacy sensitivity.

TABLE 3: Parameter and default values.

	Model	Total profit	Average profit	Average safe region size	RMSE
Yelp	Principal-agent model	54,030	5.783	0.156	8.485
	Stackelberg model	39,141	4.189	0.193	10.021
CAL	Principal-agent model	39,128	4.169	0.192	9.764
	Stackelberg model	27,812	2.877	0.237	11.932

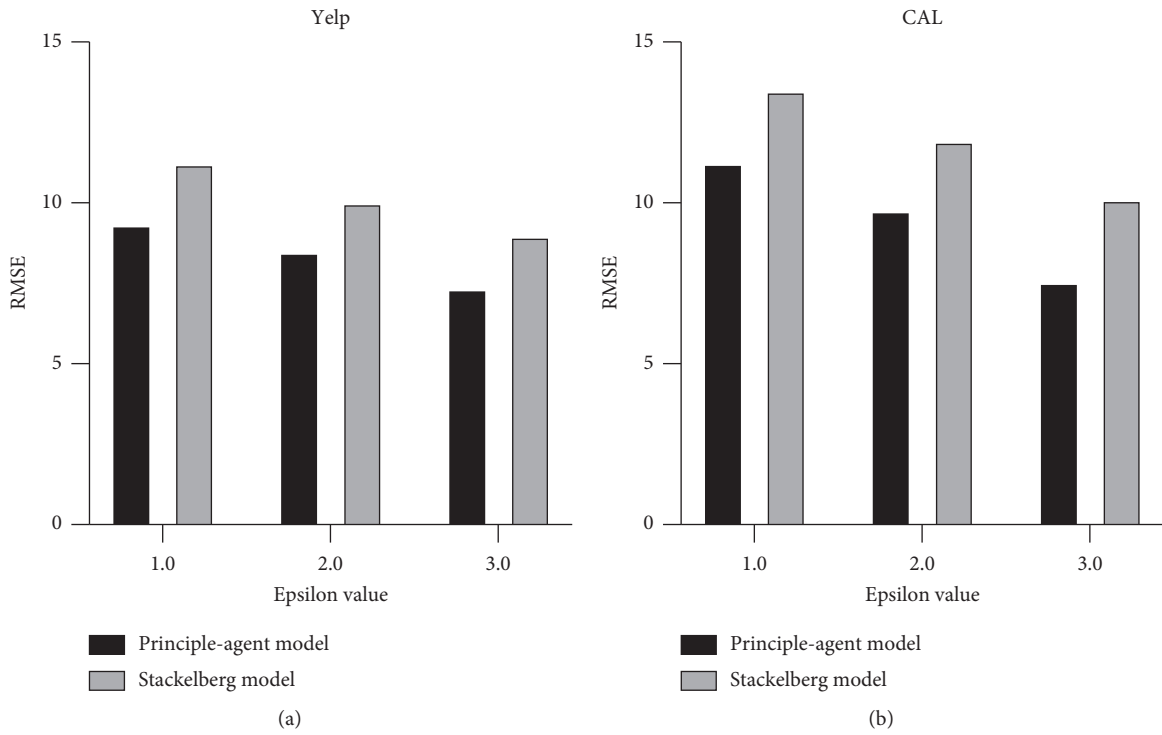


FIGURE 6: RMSE score of the principal-agent model and Stackelberg model for Yelp and California datasets.

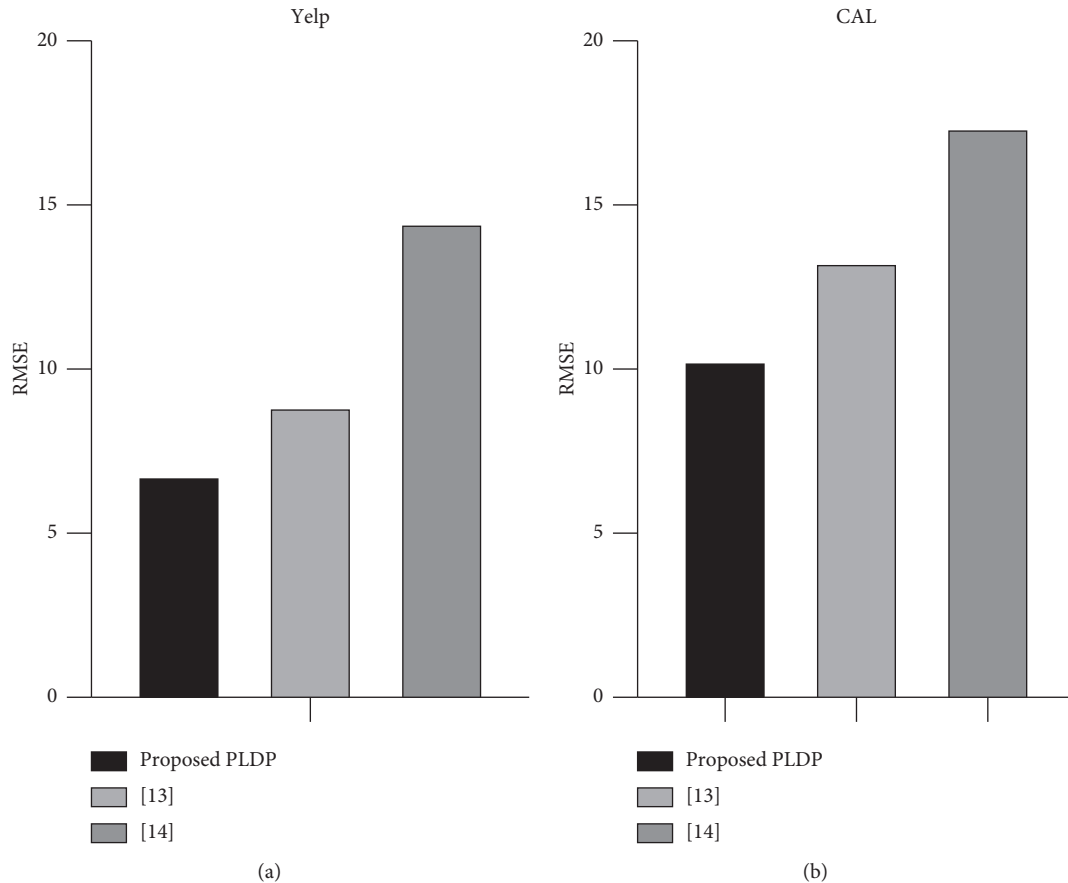


FIGURE 7: RMSE score of the proposed PLDP and existing technique [13, 14].

adjusts the grid size in consideration of the population density. In the local differential scheme, inserting noise into unnecessary grid deteriorates the data utility and the experimental result shows that the proposed technique successfully reduces unnecessary noise.

However, the proposed technique has a problem that it spends privacy budget twice to collect the population density information for grid size adaption. If we can use the publicly available data, such as [37], we can enhance the proposed technique's performance.

## 5. Conclusion

As the demand for valuable personal data increases, the privacy violation also increases. The personal location data is directly related to individual privacy. Thus, it needs to be protected more strictly. In this paper, we propose a personalized differentially private location data scheme in the local setting and an incentive mechanism in which users receive reasonable compensation for their data, while the data consumer optimizes their profit. The proposed scheme aims to satisfy both privacy protection and utility more realistically by introducing the concept of a safe region. In future work, we will study the pricing mechanism that considers epsilon values with safe region size.

## Data Availability

The data used to support the findings of this study are available from the corresponding author upon request.

## Conflicts of Interest

The authors declare that there are no conflicts of interest regarding the publication of this paper.

## Acknowledgments

This work was supported by the National Research Foundation of Korea (NRF) grant funded by the Korea government (MSIT) (no. NRF-2019R1A2C1088126).

## References

- [1] Dark Sky, <https://darksky.net/forecast/40.7127,-74.0059/us12/en>.
- [2] Curbside: <https://curbside.com/>.
- [3] W. Liu, Y. Tang, F. Yang, Y. Dou, and J. Wang, "A multi-objective decision-making approach for the optimal location of electric vehicle charging facilities," *Computers, Materials & Continua*, vol. 60, no. 2, pp. 813–834, 2019.
- [4] W. Li, Z. Chen, X. Gao, W. Liu, and J. Wang, "Multimodel framework for indoor localization under mobile edge



- computing environment,” *IEEE Internet of Things Journal*, vol. 6, no. 3, pp. 4844–4853, 2019.
- [5] C. Yin et al., “Mobile marketing recommendation method based on user location feedback,” *Human-centric Computing and Information Sciences*, vol. 9, no. 1, pp. 1–17, 2019.
  - [6] M. Liu et al., “Indoor Acoustic Localization: A Survey,” *Human-centric Computing and Information Sciences*, vol. 10, no. 1, pp. 1–24, 2020.
  - [7] J. Zhang, “Personalized product recommendation model based on user interest,” *Computer Systems Science and Engineering*, vol. 34, no. 4, pp. 231–236, 2019.
  - [8] A. Hussain et al., “Accurate location prediction of social-users using mHMM” *Intelligent Automation and Soft Computing*, vol. 25, no. 3, pp. 473–486, 2019.
  - [9] C. Dwork and A. Roth, “The algorithmic foundations of differential privacy,” *Foundations and Trends® in Theoretical Computer Science*, vol. 9, no. 3-4, pp. 211–407, 2014.
  - [10] G. Cormode et al., “Differentially private spatial decompositions,” in *Proceedings of International Conference on Data Engineering*, pp. 20–31, Arlington, VA, USA, April 2012.
  - [11] S. Ho and S. Ruan, “Differential privacy for location pattern mining,” in *Proceedings of the ACM SIGSPATIAL International Workshop on Security and Privacy in GIS and LBS*, pp. 17–24, Chicago, Illinois, November 2011.
  - [12] W. Qardaji, W. Yang, and N. Li, “Differentially private grids for geospatial data,” in *Proceedings of the International Conference on Data Engineering*, pp. 757–768, Arlington, VA, USA, April 2013.
  - [13] C. Li, M. Hay, G. Miklau, and Y. Wang, “A data- and workload-aware algorithm for range queries under differential privacy,” *Proceedings of the VLDB Endowment*, vol. 7, no. 5, pp. 341–352, 2014.
  - [14] R. Chen et al., “Private spatial data aggregation in the local setting,” in *Proceedings of the International Conference on Data Engineering*, pp. 289–300, Arlington, VA, USA, March 2016.
  - [15] Ú. Erlingsson, V. Pihur, and A. Korolova, “Rappor RaR-randomized aggregatable privacy-preserving ordinal responses,” in *Proceedings of International Conference on Computer and Communications Security*, pp. 1054–1067, Scottsdale, Arizona, USA, November 2014.
  - [16] G. Cormode et al., “Privacy at Scale: Local Differential Privacy in Practice,” in *Proceedings of the International Conference on Management of Data*, pp. 1655–1658, Houston, TX, USA, June 2018.
  - [17] T. N. Thông, X. Xiaokui, Y. Yin et al., “Collecting and analyzing data from smart device users with local differential privacy,” 2016, <https://arxiv.org/abs/1606.05053>.
  - [18] S. P. Kasiviswanathan et al., “What can we learn privately,” *SIAM Journal on Computing*, vol. 40, no. 3, pp. 7903–8826, 2011.
  - [19] H. Ebadi, D. Sands, and G. Schneider, “Differential privacy,” *ACM Sigplan Notices*, vol. 50, no. 1, pp. 69–81, 2015.
  - [20] Z. Jorgensen, T. Yu, and G. Cormode, “Conservative or liberal? Personalized differential privacy,” in *Proceedings of the International Conference on Data Engineering*, pp. 1023–1034, Arlington, VA, USA, April 2015.
  - [21] C. Yin et al., “Location recommendation privacy protection method based on location sensitivity division,” *EURASIP Journal on Wireless Communications and Networking*, vol. 2019, no. 1, pp. 1–13, 2019.
  - [22] Y. Wang, Y. Sun, S. Su et al., “Location privacy in device-dependent location-based services: challenges and solution,” *Computers, Materials & Continua*, vol. 59, no. 3, pp. 983–993, 2019.
  - [23] P. Centonze et al., “Security and privacy frameworks for access control big data systems,” *Computers, Materials & Continua*, vol. 59, no. 2, pp. 361–374, 2019.
  - [24] P. Koutris et al., “Query-based data pricing,” *Journal of the ACM (JACM)*, vol. 62, no. 5, pp. 43–86, 2015.
  - [25] A. Ghosh and A. Roth, “Selling privacy at auction,” *Games and Economic Behavior*, vol. 91, no. 1, pp. 334–346, 2015.
  - [26] H. Anke, L. B. Spector, and M. Yoshikawa, “Evidence for an acetyl-enzyme intermediate in the action of acetyl-CoA synthetase,” *Biochemical and Biophysical Research Communications*, vol. 67, no. 2, 1975.
  - [27] J. Hsu et al., “Differential privacy: an economic method for choosing epsilon,” in *Proceedings of the IEEE Computer Security Foundations Symposium*, pp. 1–29, Vienna, Austria, July 2014.
  - [28] A. Roth, “Buying private data at auction,” *ACM SIGecom Exchanges*, vol. 11, no. 1, pp. 1–8, 2012.
  - [29] L. K. Fleischer and Y. H. Lyu, “Approximately optimal auctions for selling privacy when costs are correlated with data,” in *Proceedings of the ACM Conference on Electronic Commerce*, pp. 568–585, Valencia Spain, June 2012.
  - [30] C. Aperlis and B. A. Huberman, “A market for unbiased private data: paying individuals according to their privacy attitudes,” 2012, <https://arxiv.org/abs/1205.0030>.
  - [31] N. Rachana, C. Yang, and Y. Masatoshi, “How to balance privacy and money through pricing mechanism in personal data market,” pp. 767–773, 2017, <https://arxiv.org/pdf/1705.02982.pdf>.
  - [32] G. Cormode, “Count-min sketch,” *Encyclopedia of Database Systems*, pp. 511–516, 2009.
  - [33] T. Ritter, Walshadamard transforms: a literature survey. Research Comments from Ciphers by Ritter, 1996, <http://www.ciphersbyritter.com/RES/>.
  - [34] R. Bassily and A. Smith, “Local, private, efficient protocols for succinct histograms,” in *Proceedings of the Annual ACM Symposium on Theory of Computing*, pp. 127–135, Portland, OR, USA, June 2015.
  - [35] M. Simaan and J. B. Cruz, “On the Stackelberg strategy in nonzero-sum games,” *Journal of Optimization Theory and Applications*, vol. 11, no. 5, pp. 533–555, 1973.
  - [36] Yelp, <https://www.yelp.com/dataset/challenge>.
  - [37] L. Feifei et al., “On trip planning queries in spatial databases,” in *Proceedings of the Advances in Spatial and Temporal Databases*, pp. 273–290, Brazil, South America, August 2005.

## Research Article

# User Acceptance of Internet of Vehicles Services: Empirical Findings of Partial Least Square Structural Equation Modeling (PLS-SEM) and Fuzzy Sets Qualitative Comparative Analysis (fsQCA)

Yikai Liang , Guijie Zhang , Feng Xu , and Weijie Wang 

*School of Management Science and Engineering, Shandong University of Finance and Economics, Jinan 250014, China*

Correspondence should be addressed to Yikai Liang; [yikailiang@qq.com](mailto:yikailiang@qq.com)

Received 16 October 2020; Revised 9 November 2020; Accepted 11 November 2020; Published 12 December 2020

Academic Editor: Peter Brida

Copyright © 2020 Yikai Liang et al. This is an open access article distributed under the Creative Commons Attribution License, which permits unrestricted use, distribution, and reproduction in any medium, provided the original work is properly cited.

Recently, IoV-based services and vehicles have come to the forefront as part of the growing market for the automobile industry. Since IoV-based services and vehicles were introduced, they have been expected to grow rapidly. However, contrary to optimistic expectations for future market growth, the IoV-based services and vehicles market has appeared to hit a roadblock and remains at an early market stage. Therefore, research of the determinants leading to consumers' intention to accept and purchase IoV-based services and vehicles is significant for either academics or practitioners. Drawing upon the extended unified theory of acceptance and use of technology acceptance model (UTAUT2), the perceived risk theory, and the initial trust model, we developed an integrated conceptual model and explored what and how various determinant antecedent conditions fit together on consumer intention to accept IoV-based services and vehicles. The proposed model and hypotheses were assessed by both symmetric (partial least square structural equation modeling, PLS-SEM) and asymmetric (fsQCA) approaches using online survey datasets with 362 Chinese consumers. The findings suggest that PLS-SEM and fsQCA are complementary analytical techniques providing comparable results. PLS-SEM results indicate that performance expectancy, price value, habit, and initial trust have significant effects on behavioral intention to accept IoV services. Despite other determinants, e.g., effort expectancy, social influence, facilitating conditions, hedonic motivation, and perceived risk, have no significant effect. FsQCA results reveal twelve different configurations of determinants resulting in a high level of behavioral intention to accept IoV services, and eight causal paths equifinally leading to the negation of behavioral intention to accept IoV services. These findings suggest that several conditions that were not significant in PLS-SEM are sufficient conditions when combined with other conditions. This study enriches relevant research studies on IoV-based services acceptance and provides relevant insights and marketing suggestions for incentivizing consumers to accept the IoV-based services.

## 1. Introduction

In recent years, connected autonomous vehicle (CAVs) or called intelligent connected vehicles, as the core component of the intelligent transportation system (ITS) and a node of Internet of Vehicles (IoV) system [1], have become one of the most popular research fields in network and intelligent transportation system, as well as attracted huge investments from the automotive manufacturers. Various IoV-based services and location-based services of the connected

autonomous vehicle, e.g., car navigation systems, vehicle information systems, advanced driver assistance, human-computer interaction, and car infotainment systems, play important roles in making transportation safer, cleaner, and more comfortable [1, 2]. While IoV-based services have a wide range of benefits in terms of safety, energy efficiency, environment improvement, increased mobility, and more entertainment in driving [3–10], such benefits may not be realized until IoV-based services are widely accepted and used by a critical mass of consumers [11–15]. Recent surveys

have shown that the consumers' intention to accept or purchase IoV-based services is generally low Wu et al. [3]. Therefore, it is significant to explore the determinants of consumers' intention to accept and purchase IoV-based services [16].

With ongoing technological advances in automation and connectivity, several studies have been discussed concerning IoV-based services in recent years that have concentrated on different issues [1, 17], such as the concept of IoV [18, 19], architecture (four layers including vehicle network environment sensing and control layer, network access and transport layer, coordinative computing control layer, and application layer) [20, 21], and key technologies for IoV [22, 23], as well as barriers and determinants of IoV-based services and vehicles adoption [24, 25]. Numerous studies have investigated key factors for consumers' willingness-to-pay (WTP) and the adoption of IoV-based services and vehicles from the perspectives of various innovation adoption theories [6, 26]. However, almost all of the empirical studies have been grounded in the use of the conventional symmetric-based techniques, including multiple regression model [13, 27–29], structural equation modeling (SEM) [11, 14, 15, 30, 31], and partial least square (PLS) [10, 12, 31–35], to explore the relationships between independent variables (IV) and dependent variables (DV). These conventional techniques are variable-oriented that focus on the “net effect” of IV on DV, while excluding possible asymmetric relations between variables [36], leading to the correlation and significance might vary depending on the variables the model includes. In real-life scenarios, a viable outcome often depends on combinations of several antecedents that collectively form what is referred to as an algorithm in the asymmetric method [37]. Therefore, qualitative comparative analysis (QCA), as a holistic approach, has been recommended for facilitating the analysis of complex causality and logical relations among combinations of conditions and an outcome, allowing researchers to examine multiple causal paths that lead to the same outcome [38–40].

To fill this gap, in the study, we answer the calls for the application of the holistic approach to understand the determinants' configurations on consumers' behavioral intention to accept IoV-based services. Therefore, based on the review of studies related to the acceptance of IoV-based services and vehicles, we develop an integrated theoretical model including the extended unified theory of acceptance and use of technology (UTAUT2) [41] with the constructs of perceived risk from perceived risk theory [42] and initial trust from the initial trust model [43]. These factors employed have been extensively used in innovation adoption studies and are appropriate for explaining IoV-based services' acceptance. This integrated model makes up for the inadequate explanation of the individual behavior adopted by a single model. Using online survey datasets with 362 Chinese consumers, we use both symmetric (PLS-SEM) and asymmetric (fsQCA) methods, to explore the role of the above determinants on the intention to accept IoV-based services. Our study involves some antecedents not analyzed in the literature, and it starts by analyzing the net effects of each antecedent with PLS-SEM. Moreover, to provide a more accurate understanding of the complex reality

associated with the various determinants and behavioral intention to accept IoV-based services, the configurations of causal factors are analyzed by fsQCA for explaining the complex intention that the PLS-SEM does not capture [44]. FsQCA can not only explore how the antecedent factors combine to produce multiple alternative paths that can successfully lead to this intention but also assume causal asymmetry to identify the paths that explain the negation of the intention. The findings of PLS-SEM and fsQCA provide relevant insights and marketing suggestions for incentivizing consumers to accept and purchase IoV-based services.

The study is organized as follows. Section 2 provides literature reviews for the research model. Section 3 presents our conceptual model and hypotheses. Section 4 explains the measurement and data used in the empirical analysis. Section 5 presents the results of the empirical analysis by PLS-SEM and fsQCA. The key findings, theoretical implications, managerial implications, and limitations of the present study are discussed in Section 6. Finally, Section 7 is the conclusions of this study.

## 2. Literature Review and Theoretical Basis

*2.1. The Definition and Adoption of IoV-Based Services and Vehicles.* IoV as an important part of the wisdom city is a complex integrated network system [18], which connects different people within vehicles, different vehicles, and different environment entries in cities. As an important branch of IoT in the transportation field, IoV covers a wide range of technologies and applications, including intelligent transportation, vehicular information service, modern information and communications technology, and automotive electronics. However, owing to different understandings of the connotation of IoV in various research fields, there is no uniform definition of IoV [18]. IoV is different from telematics, vehicle ad hoc networks, and intelligent transportation, in which vehicles like phones can run within the whole network and obtain various services by swarm intelligent computing with people, vehicles, and environments.

IoV-based services and vehicles introduce all sorts of different benefits such as safety, energy efficiency, environment improvement, increased mobility, and more entertainment in driving [3–5, 14]. However, there still exist several concerns about IoV-based services and vehicles, such as the relatively higher prices and maintenance costs compared with existing vehicles, performance, and safety issues when operating in complex conditions, impeding the adoption of IoV-based services and vehicles [14]. Therefore, to ensure the social acceptability of IoV-based services and vehicles, numerous studies use technology adoption theories to explore the determinants of consumers' intention to accept and purchase IoV-based services and vehicles [6, 26]. Table 1 summarizes previous studies on IoV-based services and vehicle acceptance based on a theoretical perspective of technology acceptance.

As shown in Table 1, previous studies have sought to explain the acceptance of various concepts of IoV-based services and vehicles, such as autonomous vehicles, connected vehicles, in-vehicle infotainment systems, and autonomous shuttle services. From a theoretical point of view,

TABLE 1: Related studies on IoV-based services acceptance.

References	Theory	Types of IoV-based services	Method (data collection and analysis)	Antecedent conditions (IV) and outcome (DV)	Key findings
[35]	TAM	Connected vehicles	Online survey (116 participants) and PLS-SEM	Perceived usefulness (PU), perceived ease of use (PEOU), attitude, privacy concerns, privacy risk, trust in provider, information control, social norm, and behavioral intention (BI) to use	Attitude and social norm have a significant positive effect on BI, while PU, privacy risk, and trust in provider have no effect
[10]	Social cognitive theory, TPB, prospect theory, and value perception theory	Fully autonomous vehicles	Survey (355 samples in Beijing, China) and PLS-SEM	Mass media, social media, self-efficacy, subjective norms (SN), PU, perceived risks (PR), and adoption intention to private AVs and public AVs	Mass media enhances potential users' self-efficacy of fully AVs, while social media strengthens SN; both PU and PR of AVs are perceived simultaneously via mass media, whereas PR can be significantly eliminated by social media; all constructs of self-efficacy, SN, PU, and PR are verified to drive intention to use AVs
[14]	TPB	Autonomous vehicles	Survey (526 residents in Seoul, Korea) and SEM	Attitude, SN, behavioral control, cognitive and emotive factors (comparative advantage, compatibility, complexity, and hedonic motivation), and acceptance	Individuals' mindset, subjective customs, and behavioral influence directly affect AVs acceptance; comparative advantage, compatibility, complexity, and hedonic motivation indirectly affect AVs acceptance
[45]	UTAUT2	Autonomous delivery vehicles	Online survey (501 German) and SEM	Performance expectancy (PE), effort expectancy (EE), social influence (SI), facilitating conditions (FC), hedonic motivation, price sensitivity, PR, and BI	Price sensitivity is the strongest predictor of BI, followed by PE, hedonic motivation, PR, SI, and FC, whereas no effect could be found for EE
[46]	TAM	Autonomous shuttle services	Survey (700 respondents in Taiwan) and SEM	PU, PEOU, attitude, trust, perceived enjoyment, and use intention	PU, PEOU, trust, and perceived enjoyment positively affect attitude; PU, trust, and attitude positively affect use intention
[11]	TAM and initial trust theory	Automated vehicles	Face-to-face survey (216 drivers in Shenzhen, China) and SEM	PU, PEOU, perceived safety risk, perceived privacy risk, initial trust, attitude towards using, and BI	PEOU positively affect PU; PU and perceived safety risk positively affect initial trust; PEOU and initial trust positively affect attitude; PU and attitude positively affect BI
[8]	Trust theory	Autonomous vehicles	Survey (742 Korean respondents) & PLS-SEM	Trust in technology, perceived benefit (PB), PR, general acceptance, BI, and willingness to pay.	Trust has direct and indirect effects on AV acceptance; PB is more influential than PR in affecting AV acceptance and also in mediating the trust-acceptability relationship
[47]	TAM	Autonomous vehicles	Online survey (313 Korean respondents) and PLS-SEM	Relative advantage, psychological ownership, self-efficacy, PR, PU, PEOU, and intention to use	Relative advantage positively affects PU; self-efficacy positively affects PEOU; self-efficacy, psychological ownership, PR, and PU affect intention to use autonomous vehicles



TABLE 1: Continued.

References	Theory	Types of IoV-based services	Method (data collection and analysis)	Antecedent conditions (IV) and outcome (DV)	Key findings
[48]	TAM	Autonomous electric bus	Online survey (268 passengers in Germany) and SEM	PU, PEOU, ATU, individual differences, social impacts, systems characteristics, and intention to use	Desire to exert control, SN, perceived enjoyment, PU, and PEOU positively affect ATU; trust, SN, price evaluation, and ATU positively affect intention to use
[31]	TAM and the life-oriented approach	Self-driving public bus	Online survey (268 passengers in Germany) and PLS-SEM	PU, PEOU, ATU, life choices, subjective well-being, factors of travel quality, life domains, and intention to use	Trust, price evaluation, social network, residence, family budget, PU, and ATU positively affect intention to use
[12]	TAM	Automated vehicles	Online survey (1177 participants in Europe, China, and North America) and PLS-SEM	Attitude towards environmental protection, innovativeness, perceived enjoyment, objective usability, PU, PEOU, ATU, and BI	Perceived enjoyment and objective usability positively affect both PU and PEOU; PU and PEOU positively affect ATU; ATU positively affects BI
[2]	TAM	Autonomous electric vehicles	Online survey (470 respondents in China) and SEM	Environmental concern, green PU, PEOU, and BI	Environmental concern, green PU, and PEOU positively affect BI; EC has an indirect effect on BI through mediators of green PU and PEOU
[15]	Trust and TAM	Autonomous vehicles	Online survey (369 German participants) and SEM	Trust, concern of giving up control, PU, PEOU, driving enjoyment, personal innovativeness, and the adoption intention of AVs	Trust in the technology/ concern about handing over control to a machine, PU, and personal innovativeness positively affects adoption intention, while driving enjoyment is a barrier to AVs adoption
[34]		Self-driving vehicles	Survey (1355 participants in Tianjin and Xi'an, China) and PLS-SEM	Demographic (familiarity, age, gender, education, and income) and psychological factors (PB, PR, perceived dread, and trust in SDVs)	Younger and highly educated participants with higher-income were willing to pay more; participants who had heard about SDVs reported higher WTP and higher trust and perceived higher benefits, lower risks, and lower dread; trust and PB were positive predictors of WTP, while PR and perceived dread were negative
[16]	IDT and agent-based simulation modeling	Connected autonomous vehicles	Survey (327 employees of the University of Memphis) and simulation modeling	Price reduction, mass communication (marketing), and peer-to-peer communication (word-of-mouth)	The automobile fleet will be nearly homogenous in about 2050 only if prices decrease at significant rates (15% or 20% annually); a 6-month preintroduction marketing campaign has no impact on adoption trend; CAV market share significantly alter caused by peer-to-peer communication

TABLE 1: Continued.

References	Theory	Types of IoV-based services	Method (data collection and analysis)	Antecedent conditions (IV) and outcome (DV)	Key findings
[7]	UTAUT	Autonomous car	Online survey (241 respondents in France) and SEM and multigroup analysis	PE, EE, SI, consumer innovativeness, and purchase intention	PE, EE, and SI positively affect purchase intentions; consumer innovativeness moderates the relationships between the constructs
[13]	TAM	Autonomous driving	Web-based survey (483 respondents in Greece) and multiple regression	PU, PEOU, perceived trust, SI, and BI to have AVs	PU, PEOU, perceived trust, and SI positively affect BI
[29]	UTAUT	Automated road transport systems	Survey (315 participants in Greece) and hierarchical multiple regression	PE, EE, SI, FC, hedonic motivation, and BI	PE, SI, FC, and hedonic motivation positively affect BI
[28]	UTAUT	Automated road transport systems	Survey (349 respondents from France and Switzerland) and hierarchical multiple regression	PE, EE, SI, and BI	PE, EE, and SI positively affect BI
[33]	Innovation resistance model	In-vehicle infotainment (IVI) systems	Online survey (1070 samples in Korea) and PLS-SEM	Technographics, SN, prior similar experience, PU, perceived complexity, PR, resistance, and intention to use IVI systems	PU negatively affects resistance, while perceived complexity and PR positively affect resistance (which negatively affects intention to use)
[27]	UTAUT	Self-driving vehicles	Online survey (556 residents of Austin, Texas) and an ordinal regression model	PE, EE, SI, perceived safety, anxiety, attitudes about technology, desire for control, technology use, technology acceptance, and intent to use	Intent to use self-driving vehicles are the ones who have any physical conditions that prohibit them from driving, think it would decrease accident risk, use smartphones and transportation apps, are not concerned with data privacy, think it would be fun, think it would be easy to become skilful, and believe that people whose opinions they valued would like using it
[32]	TAM and trust theory	Autonomous vehicle	Online survey (552 drivers) and PLS-SEM	System transparency, technical competence, situation management, trust, PU, PEOU, PR, external locus of control, sensation seeking, and BI	System transparency, technical competence, and situation management positively affect trust; PU, PEOU, trust, and external locus of control positively affect intention to use autonomous vehicles; PR and sensation have no impact on BI

Note: perceived usefulness, PU; perceived ease of use, PEOU; perceived benefit, PB; perceived risks, PR; performance expectancy, PE; effort expectancy, EE; social influence, SI; facilitating conditions, FC; behavioral intention, BI.

the majority of empirical studies attempt to explore the determinants of acceptance using a single theory, such as the technology acceptance model (TAM) [2, 12], the theory of planned behavior (TPB) [14], UTAUT [7, 28, 29, 45], and

innovation resistance model [33]. To provide a comprehensive understanding within the adoption decision-making of IoV-based services and vehicles [31], more and more researchers have called for integrating various theories or

additional factors depending on the certain context to improve the model's explanatory power [31, 46], such as the integration of TAM and initial trust theory [11, 15, 32, 46]. Therefore, we integrate various theories or constructs widely used and verified in different contexts for improving the model's explanatory power.

From a methodology of view, the empirical studies have been grounded mostly in the use of the conventional symmetric-based techniques, including multiple regression model [13, 27–29], SEM [11, 14, 15, 30, 31], and PLS [10, 12, 31–35], to explore the relationships between variables. However, these techniques focus on the net effect of IV on DV, while excluding possible asymmetric relations between variables [36], leading to the correlation and significance might vary depending on the variables the model includes. For example, most of the empirical previous studies of perceived ease of use, perceived risk, social influence, or facilitating conditions have produced mixed results, and its effect on technology adoption has also been inconsistent. In real-life scenarios, a viable outcome often depends on combinations of several antecedents [37]. To understand the effects of determinants on the intention to accept IoV-based services and vehicles, QCA has been recommended for facilitating the analysis of complex causality and logical relations among combinations of conditions and an outcome [38, 39]. Therefore, we also answer this call and use fsQCA to provide a more nuanced understanding of how these antecedent conditions fit together to affect consumers' intention to accept and purchase IoV-based services and vehicles.

*2.2. Unified Theory of Acceptance and Use of Technology (UTAUT).* Information technology (IT) acceptance is an enduring topic in IS research, and a variety of popular models with different sets of acceptance determinant have been developed to explain individual's acceptance and usage of innovation technology, e.g., the theory of reasoned action (TRA) [49], TAM [50], the theory of planned behavior (TPB) [51], task-technology fit (TTF), motivational model, UTAUT [41, 52], initial trust model (ITM) [43], diffusion of innovation theory (IDT) [53], and social cognitive theory. Many studies have used these traditional frameworks or added new constructs to develop models to conduct their research studies in various contexts of technologies.

Considering the choice of theoretical models for explaining user acceptance of new technology, Venkatesh et al. suggested a “need for a review and synthesis to progress toward a unified view of user acceptance” [52]. UTAUT integrating elements across the eight models (i.e., TRA, TAM, motivational model, TPB, a model combining TAM and TPB, the model of PC utilization, IDT, and social cognitive theory) explains more of the variance in user intentions to use new technology than each model [52]. UTAUT2 extends UTAUT with three variables explicitly proposed to be important in the consumer context (i.e., hedonic motivation, price value, and habit). Several studies in the IS discipline have confirmed the explanatory power of UTAUT in the acceptance and adoption studies. Therefore,

UTAUT is considered a robust and powerful model for investigating the determinants of technology adoption at the individual level, and it has generally been applied to understand the individuals' acceptance of various new IT innovations, e.g., IoT in the smart home [54] and mobile learning system [55]. UTAUT is also a commonly employed behavioral model in transport studies from a technology acceptance perspective [7, 35, 46]. Therefore, it is considered theoretically and practically useful to utilize UTAUT2 as an adequate theoretical basis for exploring the effects of factors influencing consumer's acceptance of IoV-based services and vehicles.

### 3. Conceptual Model and Hypotheses

As outlined before, UTAUT2 will be utilized as a foundation to investigate user acceptance of IoV-based services. However, to examine the specific case of IoV-based services acceptance, the model needs to be modified and extended for improving the model's explanatory power and specificity [46]. IoV services, as the emerging technology, include both two-sidedness [26], that is, the technological advantages, and the possible negative consequences of IoV-based services, which should be investigated in parallel. Hence, two perceived factors (initial trust and perceived risk) were incorporated into the original UTAUT2 to form our model because of the uncertainty of the emerging technology. The proposed model is presented in Figure 1. In the following, the constructs of the proposed model and the developed hypotheses will be presented.

*3.1. Performance Expectancy.* Performance expectancy is defined as the degree to which using technology will provide benefits to consumers in performing certain activities [41]. It is similar to the perceived usefulness of TAM and the relative advantage of IDT [53]. The effect of performance expectancy on behavior intention has been widely verified in previous studies, e.g., mobile learning [56], smart home [57], mobile health [58], and autonomous delivery vehicles [45]. According to IDT [53], users tend to accept new products or innovations if those innovations provide a unique advantage compared to existing ones. Compared with conventional vehicles, IoV-based services have functional benefits such as fewer accidents and reduced fuel consumption and emissions, as well as decreased congestion and driving time [3, 10, 48]. For example, IoV-based services can be synched with traffic signals and other vehicles by capturing the surrounding traffic conditions and environment to decrease travel time and cost [16]. IoV-based services are expected to decrease traveling time through anticipative driving, optimized routing, self-parking systems, and efficient usage of lanes [15]. More specifically, IoV-based services' integrated systems such as real-time navigation aim to provide the driver with a more comfortable and safer driving task [25]. Besides, ubiquitous connectivity allows consumers to be “always connected” or “always on,” providing them with more freedom and access to information and services, such as infotainment [33]. Extant studies have shown that



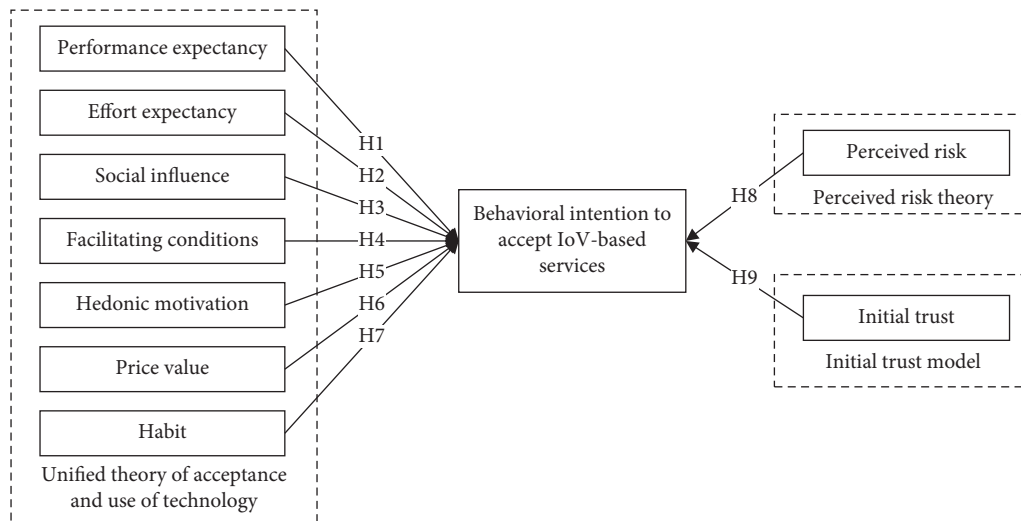


FIGURE 1: The integrated model of behavioral intention to accept IoV-based services.

technological advantages increase the satisfaction level of consumers and affect the intention of consumers [47]. In this research context, the issue is the extent to which potential consumers will find IoV-based services better than traditional vehicles. Therefore, the more performance expectancy is, the more likely consumers accept IoV-based services.

H1: performance expectancy positively affects IoV-based services' acceptance.

**3.2. Effort Expectancy.** Effort expectancy is the degree of ease associated with consumers' use of technology [41]. It quite closely with the perceived ease of use of TAM and the complexity of IDT (the degree to which an innovation is perceived as relatively difficult to understand and use) [53]. Even if potential users believe that a given system is useful, meanwhile they may believe that the system is too hard to use and that the benefits of usage are out-weighted by the effort of using the system. Essentially, if IoV-based services were viewed to be difficult to use and complexity would act as a functional barrier, it would harm acceptance [14]. Effort expectancy has also been proven to be relevant with intention in various contexts, e.g., mobile learning [56]. Unlike conventional vehicles, IoV-based services do not require the driver to monitor and take back the operational control of the vehicle even when the system becomes failure [10]. Moreover, with the effortless communication with the human-car interaction system [35], the drivers just need to issue the instructions and confirm to IoV-based services, especially when they have a special preference or instant requirement. Analogously, we pose the following hypothesis.

H2: perceived ease of use positively affects IoV-based services' acceptance.

**3.3. Social Influence.** Social influence is defined as consumers perceive that important others (e.g., family and friends) believe they should use the new technology [41, 52],

reflecting the effect of social environmental factors such as the opinions of a user's surrounding friends, relatives, and superiors on user behavior, which is similar to the subjective norm of TRA [48, 49]. Previous studies also reveal the impacts of social influence on behavioral intention in various contexts, e.g., mobile payment [59], mobile banking [60], mobile learning [56], IoT in smart home [54], wearable technology [61], and autonomous delivery vehicles [45]. As a person in society [14], an individual's decision of technology adoption is very susceptible to their social networks [31] and social norms [35, 62]. For IoV-based services, such a disruptive innovation in a burgeoning market, Talebian and Mishra [16] find that peer-to-peer communication (word-of-mouth) with a satisfied adopter from the social circles can not only convince a potential adopter that the resistances which he/she perceives are perhaps not important but also it is worthwhile to purchase IoV-based services. Besides, the use of autonomous vehicles by friends and family leads to a greater willingness to adopt the technology [63]. When friends, family, or other important ones start to use IoV-based services, consumers would be more likely to pay for an IoV-based service or vehicle [7].

H3: social influence positively affects behavioral intention to accept IoV-based services.

**3.4. Facilitating Conditions.** Facilitating conditions are defined as a user's perception of disposable resources and support when performing a behavior [41, 52], which are similar to perceived behavioral control of TPB [51]. It is significant in various technologies acceptance studies, e.g., mobile banking [60, 64] and automated public transport [29]. IoV-based service/vehicle as new technology requires users to have certain skills such as configuring and operating smart applications to connect to the wireless Internet. It is believed that users have different levels in possessing information and resources that facilitate their use of IoV-based services (e.g., personal knowledge and help-hotlines). In

general, consumers with a lower level of facilitating conditions will have lower intentions to accept or purchase IoV-based services [45].

H4: facilitating conditions positively affects behavioral intention to accept IoV-based services.

**3.5. Hedonic Motivation.** Hedonic motivation, considered as an intrinsic value, refers to the fun or pleasure derived from using a technology [41]. In IS adoption research, such hedonic motivation conceptualized as perceived enjoyment and has been found to play an important role in the acceptance and usage of various technologies, e.g., smart home [57], mobile health [58], and autonomous delivery vehicles [45]. The proposed system or technology must arouse the user's emotions and make the experience enjoyable and positive to motivate users to adopt it [57]. In the IoV context, hedonic motivation has also been found to be an important determinant of acceptance and purchase of autonomous shuttle services [29, 45, 46]. The attractiveness of new IoV-based services can be increased by the enjoyment experience provided by technology [46].

H5: hedonic motivation positively affects behavioral intention to accept IoV-based services.

**3.6. Price Value.** Price value is defined as the consumers' cognitive tradeoff between a technology's perceived benefits and its monetary costs of usage [41]. In marketing research, the perception of price/cost is usually conceptualized together with the quality to determine the perceived value of products or services, reflecting the influence of the individually perceived price-performance and personal financial aspects. A positive price value occurs if the potential consumers' perceived benefits of using technology are greater than the associated monetary costs, which has a positive impact on consumers' adoption and usage of new technology [48]. Price value is a significant determinant of behavioral intention in various contexts, e.g., smart home [54]. Price value is expected to be particularly influential on IoV-based services acceptance as IoV technologies are evaluated against their comparable non-IoV objects. Although some studies have indicated that potential consumers are generally willing to pay a higher price for autonomous vehicles than conventional ones [63], however, they need to tradeoff price value when purchasing such a disruptive product [48, 65, 66].

H6: price value positively affects behavioral intention to accept IoV-based services.

**3.7. Habit.** Habit is defined as the extent to which people tend to perform behaviors automatically as they learn how to use a new technology [41]. It usually reflects the consequences and results of prior experiences with a target technology [57]. That is when behavior is repeated, a habit is developed. Accordingly, the behavior is likely to be determined by habit strength [67]. The habit has been shown to have a direct effect on technology use, e.g., smart home [57].

Therefore, the greater the habit of consumers to use the IoV-based services, the greater will be their intentions to adopt.

H7: habit positively affects behavioral intention to accept IoV-based services.

**3.8. Perceived Risk.** Perceived risk relates to the uncertainty regarding the occurrence of adverse consequences [16, 68, 69]. It is defined as the degree to which consumers feel uncertainty and problems about the possibility of negative consequences from accepting a technology and drawing from perceived risk theory [42]. Consumers often weigh benefits and risks beliefs about technology through cognitive processes that inform their decisions to accept or reject it [34]. Numerous studies use perceived risk in analyzing consumer behavior related to innovative technology and find it is negatively related to intention to use such innovative technology as IoT [70], smart home services [68], e-government [71, 72], social commerce [73], Internet banking [74–76], mobile payment [77], particularly automated vehicles [11, 47], and autonomous delivery vehicles [45]. Dialectically, everything has two sides. Many surveys have reported that while consumers acknowledge the potential benefits of IoV-based services, they have also expressed great concerns about safety and privacy risks associated with the acceptance of IoV-based services [3, 6]. Safety risk includes the malfunctioning risk due to operating system/equipment failure/crash, virus attack, or disconnection from the Internet [16], as well as vehicle performance degradation when operating in such complex conditions as poor weather, night, limited visibility, and in areas with low Internet coverage [3]. Privacy risk originates from the possibility that travel data, behavioral data, or personal information could be transmitted to other organizations for misuse without notice or be hacked by others [11, 48]. Previous studies show that users seem to have privacy concerns when being confronted with the concept of connected vehicles because users of connected vehicular services may be concerned with the service providers' handling of data in terms of information collection, storage, and usage [35]. Such risks are considered as the most important barriers for acceptance of IoV-based services [10, 16]. Therefore, the more perceived risk consumers assess, the less consumers are willing to accept IoV-based services.

H8: perceived risk negatively affects behavioral intention to accept IoV-based services.

**3.9. Initial Trust.** Initial trust refers to the trustor's subjective knowledge and confidence of trustee without experience and knowledge [35, 43]. In technology adoption research, trust is the expectation of adopter toward the adoptee to satisfy a certain service or fulfill a certain promise. Under risky or uncertain situations, trust is treated as a vital component of a relationship [8, 78]. Numerous studies have extensively explored trust as an important determinant to affect user acceptance of various technology services, e.g., mobile banking [64, 79], e-government [71], IoT in agriculture [70],

particularly autonomous vehicles [11, 32], and autonomous shuttle [46, 48]. An individual tends to accept an innovation only if they believe that the specific attributes of this innovation will help achieve one's goals [80]. If trust is absent, even individual who tends to make adoption decision may start to defer adoption or hold a wait-and-see attitude until the market of radical innovation (IoV-based services) matures. At the early stage of the marketization of IoV-based services and vehicles, potential consumers need to shape sufficient trust that can help to increase the expectation of successful application of relevant IoV-based services, overcome perceptions of risks and uncertainties, and form a positive attitude towards it [11, 43].

H9: initial trust positively affects behavioral intention to accept IoV-based services.

## 4. Methodology

*4.1. Measurements.* A survey questionnaire was conducted to collect data for this study. Based on an extensive review of the literature, each construct and its items were adapted from validated instruments of previous studies, and wording was modified to fit the context of IoV-based services and vehicles [72], to improve content validity [50, 81]. The method of translation and back translation was used for ensuring equivalence between the source and translated versions [82]. Appropriate modifications were made based on expert reviews by two IS experts. Several postgraduate students pretested the instrument, identifying and revising ambiguous or poorly worded items to improve the clarity and understandability. The instrument was then pilot tested with 30 undergraduate students who were not included in the main survey. The results of pilot test confirmed the reliability, validity, and translational equivalence of the scales. The final items and their sources are listed in Table 2. All items were measured using a five-point Likert scale ranging from "strongly disagree" to "strongly agree."

*4.2. Data Collection.* The data were collected through an online survey by Wenjuanxing (<http://www.wenjuan.com>), a professional online questionnaire survey platform in China, from 22 to 26 June 2020. The survey targeted consumers who are using or intend to use an IoV-based service and vehicle. The survey includes a short explanation of the definition and functions of IoV-based services to help respondents understand this concept. The questionnaire was distributed randomly to actual respondents by Wenjuanxing. A total of 420 questionnaires were collected. Excluding invalid questionnaires with unusually short completion time, incomplete data, or the same options, there were 362 valid questionnaires for this study. The demographic characteristics and driving-related information of the respondents are shown in Table 3.

As seen in Table 3, the demographic data indicate that the sample was balanced regarding gender (51.38% of the respondents are male) and age (51.66% of the respondents are less than 30 years old), consisting primarily of bachelor degree and above (93.37%).

Nonresponse bias generally occurs when some of the target individuals are unwilling or unable to participate in the survey and, consequently, causes an unreliable representation of the selected sample and limit a study's external validity [84]. Following the recommendations of Urbach and Frederik [85], we took measures to address the issue of nonresponse and make sure we had a representative response rate, both before, during, and after data collection [86]. To minimize nonresponse before and during the data collection, all respondents were provided with a monetary incentive to participate in the questionnaire. Besides, following the initial invitation to participate in the questionnaire, all of the respondents were recontacted to remind them to complete the survey. After the data collection, nonresponse bias was assessed by verifying that the responses of early and late respondents were not significantly different [84, 87]. In both samples, the early and late responses had insignificant differences in the means of any demographics based on *T*-tests using SPSS. Therefore, nonresponse bias is not a major concern in this study.

Taking into consideration that all data were collected from a single source at one point in time and that all data were perceptions of key respondents, we used two approaches, i.e., Harman's one-factor test [88] and full collinearity assessment approach [89], to test the existence of common method bias (CMB), based on the guidelines of previous studies [44, 54, 90]. First, Harman's single-factor test shows that the highest variance explained by the single factor is 44.95%, which is less than the threshold value of 50%, indicating the absence of CMB in the dataset. Second, CMB is examined through a full collinearity assessment approach in PLS-SEM [89]. The variance inflation factor (VIF) values of all the latent variables are less than 4.58 (see Table 4), which is below the acceptable threshold of 5. Taken together, these results indicated that CMB was minimal in this study.

## 5. Data Analysis and Results

Data were analyzed using both the PLS-SEM method with Smart PLS 3 for validating the measurement model and structural model [81], and the fsQCA 3.0 software for exploring the set relations of the casual and outcome conditions [38]. These two methods have different focuses and rely on different principles [91]. The PLS-SEM is a variable-oriented technique that focuses on the net effect of the independent variable (IV) on the dependent variable (DV). It treats independent variables as competing to explain the variation in the dependent variables, and it relies on the principles of additive effects, linearity, and unifinality [40]. On the contrary, the fsQCA is a case-oriented technique that focuses on combinatorial effects. It assumes complex causality and focuses on asymmetric relationships between conditions (IV) and outcome (DV) [91]. FsQCA also allows for multifinality in which identical conditions can lead to different outcomes [39]. Thus, fsQCA is considered as an appropriate complementary analysis to PLS-SEM when detecting effects caused by unobserved heterogeneity [40, 92–94].

TABLE 2: Measurement scale and items.

Constructs	No.	Items	References
Perceived expectancy	PE1	Using IoV services will improve driving and travel performance	[41]
	PE2	Using IoV services will increase driving and travel effectiveness	
	PE3	Using IoV services will enhance my effectiveness while driving	
	PE4	I find IoV services are useful	
Effort expectancy	EE1	Learning how to use IoV services is easy for me	
	EE2	I would find it easy to get IoV services to do what I want to do	
	EE3	Interacting with IoV services would not require a lot of my mental effort	
Social influence	SI1	People who are important to me think that I should use IoV services	
	SI2	People who influence my behavior think that I should use IoV services	
	SI3	People whose opinions that I value prefer that I use IoV services	
Facilitating conditions	FC1	I have the resources necessary to use IoV services	
	FC2	I have the knowledge necessary to use IoV services	
	FC3	IoV services are compatible with other technologies I use	
	FC3	I can get help from others when I have difficulties using IoV services	
Hedonic motivation	HM1	Using IoV services is fun	
	HM2	Using IoV services is enjoyable	
	HM3	Using IoV services is very entertaining	
Price value	PV1	IoV service is reasonably priced	
	PV2	IoV service is a good value for the money	
	PV3	At the current price, the IoV service provides a good value	
Habit	HA1	The use of IoV services has become a habit for me	[41, 57]
	HA2	I am addicted to using IoV services	
	HA3	I must use IoV services	
Perceived risk	PR1	I'm worried about the general safety of IoV services	[8]
	PR2	I'm worried about the failure or malfunctions of IoV services which may cause accidents	
	PR3	I am concerned IoV services will collect too much personal information from me	
	PR4	I am concerned IoV services will use my personal information for other purposes without my authorization	
	PR5	I am concerned IoV services will share my personal information with other entities without my authorization	
Initial trust	TR1	IoV service is dependable	[11]
	TR2	IoV service is reliable	
	TR3	Overall, I can trust IoV services	
Behavioral intention to accept IoV services	BI1	Given the chance, I intend to use IoV services	[83]
	BI2	Given the chance, I predict that I should use IoV services in the future	
	BI3	I likely have the intention to use IoV services to conduct driving	

5.1. *PLS-SEM Analysis.* The variance-based PLS-SEM method, a symmetric approach for modeling, is widely used in various studies [90, 95]. PLS-SEM enables to estimate the complex models with many constructs, indicator variables, and structural paths without imposing distributional assumptions on the data, which is often recommended when the focus of research is prediction rather than hypothesis testing when the sample size is not large, or in the presence of noisy data [81, 95]. Following the two-step approach recommended by Zhou [79], the measurement model was used to assess reliability and validity, and the structural model was examined to test hypotheses and model fitness.

5.1.1. *Measurement Model.* A measurement model was used to assess the reliability and validity [81]. The internal consistency reliability of the scales was measured by Cronbach's alpha (CA) and composite reliability (CR) [96]. Table 4 shows that CA and CR of all constructs are more than

0.7, thus confirming the excellent reliability of scale [97]. The indicator reliability was evaluated based on the criterion that the loadings should be greater than 0.70. As shown in Table 4, the loadings (in bold) are greater than 0.708 [81], meaning that the instrument presents good indicator reliability.

Construct validity includes two fundamental aspects, i.e., convergent validity and discriminant validity [97]. Convergent validity, the extent to which the construct converges to explain the variance of its items, is determined by average variance extracted (AVE) [96]. Table 4 shows that AVE is greater than 0.5 for all of the constructs, meaning that the instrument presents good convergent validity [81].

Discriminant validity is the extent to which a construct is empirically distinct from other constructs in the structural model. The discriminant validity of the constructs is examined by using two criteria, i.e., the Fornelle-Larcker criterion and cross-loadings' criterion. Fornelle-Larcker criterion requires that the square root of AVE be higher than

TABLE 3: Demographic characteristics and driving-related information.

Variables	Items	Frequency	Percentage
Gender	Male	186	51.38
	Female	176	48.62
Age	18~25	121	33.43
	26~30	66	18.23
	31~40	131	36.19
	41~50	32	8.84
	More than 51	12	3.31
Education	High school or less	8	2.21
	Junior college	16	4.42
	Bachelor degree	135	37.29
	Master degree	117	32.32
	Ph. D. and above	86	23.76
Occupation	Senior manager	55	15.19
	Professionals	93	25.69
	Civil servant	3	0.83
	Company employee	50	13.81
	Service worker	3	0.83
	Labor	2	0.55
	Private entrepreneurs	8	2.21
	Self-employer	10	2.76
	Student	118	32.60
	Unemployed	7	1.93
	Other	13	3.59
Monthly household income (¥)	Less than 3001	22	6.08
	3001-5000	45	12.43
	5001-10,000	111	30.66
	10,001-15,000	80	22.10
	15,001-20,000	47	12.98
	20,001-30,000	34	9.39
	More than 30,000	23	6.35
Driver's license	Yes	318	87.85
	No	44	12.15
Car purchase experience	Yes	193	53.31
	No	169	46.69
Number of cars owned by the household	0	54	14.92
	1	206	56.91
	2	91	25.14
	3	8	2.21
	>3	3	0.83
IoV-based services most frequently used	Automatic parking assist	56	15.47
	Adaptive cruise control	73	20.17
	Collision avoidance system	51	14.09
	In-vehicle infotainment	81	22.38
	Human-machine interaction	168	46.41
	Intelligent navigation	109	30.11
	Unconscious pay	198	54.70
	Self-driving	9	2.49
	Other	79	21.82

the correlations between the constructs [96], and the cross-loadings' criterion requires that the factor loading must be higher than all cross loadings [98]. As seen in Tables 5 and 6, both criteria satisfy the discriminant validity of the constructs.

*5.1.2. Structural Model.* Before assessing the structural model, collinearity must be tested to make sure it does not bias the regression results [81]. The variance inflation factors

(VIF) (often used to evaluate collinearity) are between 1 and 4.1, which are less than the threshold of 5 [81]. This indicates that there is no concern about the collinearity issue. The path coefficients ( $\beta$ ), Cronbach's alpha, and  $R^2$  values were assessed through the PLS Algorithm (essentially a sequence of regressions in terms of weight vectors) and Bootstrapping (a nonparametric procedure that allows testing the statistical significance of various PLS-SEM results) with 5000 iterations of resampling [97]. The results are shown in Figure 2.



TABLE 4: CA, CR, AVE, and VIF of the constructs.

	CA	CR	AVE	VIF
PE	0.91	0.94	0.78	4.39
EE	0.96	0.97	0.92	3.92
SI	0.93	0.96	0.88	4.24
FC	0.89	0.93	0.76	4.58
HM	0.94	0.96	0.89	4.17
PV	0.93	0.96	0.88	2.76
HA	0.93	0.95	0.87	2.76
PR	0.91	0.93	0.73	1.20
TR	0.96	0.97	0.93	4.14
UI	0.94	0.96	0.89	—

Note: perceived expectancy, PE; effort expectancy, EE; social influence, SI; facilitating conditions, FC; hedonic motivation, HM; price value, PV; habit, HA; perceived risk, PR; initial trust, TR; behavioral intention of IoV-based services, BI.

TABLE 5: Loadings and cross-loadings.

	PE	EE	SI	FC	HM	PV	HA	PR	TR	BI
PE1	<b>0.92</b>	0.72	0.73	0.71	0.75	0.56	0.59	-0.26	0.68	0.69
PE2	<b>0.85</b>	0.61	0.70	0.61	0.67	0.49	0.51	-0.28	0.59	0.57
PE3	<b>0.92</b>	0.76	0.78	0.73	0.80	0.62	0.62	-0.28	0.72	0.73
PE4	<b>0.86</b>	0.73	0.67	0.67	0.70	0.46	0.50	-0.32	0.64	0.63
EE1	0.75	<b>0.96</b>	0.70	0.75	0.72	0.55	0.58	-0.31	0.62	0.67
EE2	0.77	<b>0.97</b>	0.73	0.79	0.75	0.57	0.60	-0.29	0.65	0.69
EE3	0.78	<b>0.96</b>	0.77	0.80	0.78	0.59	0.60	-0.33	0.69	0.70
SI1	0.79	0.75	<b>0.94</b>	0.75	0.80	0.60	0.59	-0.33	0.73	0.68
SI2	0.75	0.72	<b>0.95</b>	0.72	0.79	0.63	0.62	-0.36	0.70	0.68
SI3	0.75	0.69	<b>0.93</b>	0.73	0.74	0.62	0.58	-0.36	0.66	0.68
FC1	0.58	0.61	0.67	<b>0.84</b>	0.66	0.53	0.55	-0.25	0.63	0.57
FC2	0.68	0.74	0.67	<b>0.88</b>	0.70	0.53	0.54	-0.25	0.61	0.62
FC3	0.74	0.76	0.68	<b>0.90</b>	0.78	0.55	0.60	-0.25	0.67	0.68
FC4	0.67	0.72	0.71	<b>0.86</b>	0.76	0.61	0.59	-0.27	0.68	0.65
HM1	0.80	0.77	0.79	0.81	<b>0.95</b>	0.63	0.64	-0.35	0.77	0.73
HM2	0.78	0.73	0.78	0.80	<b>0.95</b>	0.61	0.62	-0.33	0.78	0.71
HM3	0.77	0.70	0.76	0.76	<b>0.93</b>	0.66	0.66	-0.33	0.86	0.76
PV1	0.54	0.55	0.61	0.60	0.61	<b>0.93</b>	0.68	-0.29	0.61	0.67
PV2	0.58	0.58	0.62	0.61	0.64	<b>0.95</b>	0.72	-0.26	0.66	0.73
PV3	0.58	0.55	0.62	0.59	0.64	<b>0.94</b>	0.72	-0.29	0.63	0.70
HA1	0.62	0.61	0.62	0.65	0.67	0.74	<b>0.95</b>	-0.29	0.65	0.76
HA2	0.51	0.50	0.53	0.53	0.56	0.64	<b>0.91</b>	-0.29	0.56	0.67
HA3	0.62	0.61	0.63	0.66	0.66	0.72	<b>0.95</b>	-0.28	0.65	0.79
PR1	-0.27	-0.26	-0.31	-0.23	-0.31	-0.17	-0.21	<b>0.88</b>	-0.21	-0.25
PR2	-0.29	-0.31	-0.33	-0.29	-0.35	-0.23	-0.23	<b>0.90</b>	-0.26	-0.27
PR3	-0.27	-0.29	-0.34	-0.24	-0.31	-0.18	-0.21	<b>0.90</b>	-0.24	-0.26
PR4	-0.29	-0.28	-0.30	-0.25	-0.29	-0.28	-0.31	<b>0.86</b>	-0.23	-0.29
PR5	-0.25	-0.24	-0.31	-0.24	-0.28	-0.40	-0.34	<b>0.75</b>	-0.27	-0.28
TR1	0.73	0.66	0.72	0.72	0.83	0.64	0.64	-0.29	<b>0.97</b>	0.75
TR2	0.70	0.62	0.68	0.70	0.80	0.64	0.62	-0.24	<b>0.96</b>	0.71
TR3	0.73	0.68	0.73	0.72	0.84	0.66	0.66	-0.30	<b>0.95</b>	0.77
BI1	0.69	0.64	0.69	0.67	0.73	0.68	0.72	-0.30	0.74	<b>0.93</b>
BI2	0.71	0.68	0.67	0.69	0.73	0.69	0.76	-0.30	0.72	<b>0.95</b>
BI3	0.71	0.70	0.69	0.70	0.75	0.74	0.77	-0.30	0.74	<b>0.96</b>

Note: the characters in bold are the indicator loadings of the constructs.

Figure 2 indicate that performance expectancy ( $\beta = 0.15$ ,  $p < 0.05$ ), price value ( $\beta = 0.153$ ,  $p < 0.01$ ), habit ( $\beta = 0.34$ ,  $p < 0.001$ ), and initial trust ( $\beta = 0.218$ ,  $p < 0.001$ ) are statistically significant to explain the intention to accept IoV-based services. Thus, hypotheses H1, H6, H7, and H9 are supported, whereas effort expectancy ( $\beta = 0.106$ ,  $p = 0.068$ ), social influence ( $\beta = -0.01$ ,  $p = 0.888$ ), facilitating conditions

( $\beta = -0.003$ ,  $p = 0.964$ ), hedonic motivation ( $\beta = 0.059$ ,  $p = 0.459$ ), and perceived risk ( $\beta = -0.008$ ,  $p = 0.771$ ) have no statistically significant effect. Thus, hypotheses H2, H3, H4, H5, and H8 are not confirmed. In sum, the model can explain the variance of 78% ( $R^2$ ) in behavioral intention to accept IoV services, indicating the model's substantial explanatory power [81].

TABLE 6: Discriminant validity of the constructs.

	PE	EE	SI	FC	HM	PV	HA	PR	TR	BI
PE	<b>0.89</b>									
EE	0.80	<b>0.96</b>								
SI	0.81	0.77	<b>0.94</b>							
FC	0.77	0.82	0.78	<b>0.87</b>						
HM	0.83	0.78	0.83	0.84	<b>0.94</b>					
PV	0.61	0.59	0.66	0.64	0.67	<b>0.94</b>				
HA	0.63	0.62	0.64	0.66	0.68	0.75	<b>0.93</b>			
PR	-0.32	-0.32	-0.37	-0.29	-0.36	-0.30	-0.31	<b>0.86</b>		
TR	0.75	0.68	0.74	0.74	0.86	0.68	0.67	-0.29	<b>0.96</b>	
BI	0.74	0.71	0.72	0.73	0.78	0.74	0.79	-0.32	0.78	<b>0.95</b>

Note: the diagonal in bold is the square root of the average variance extracted (AVE).

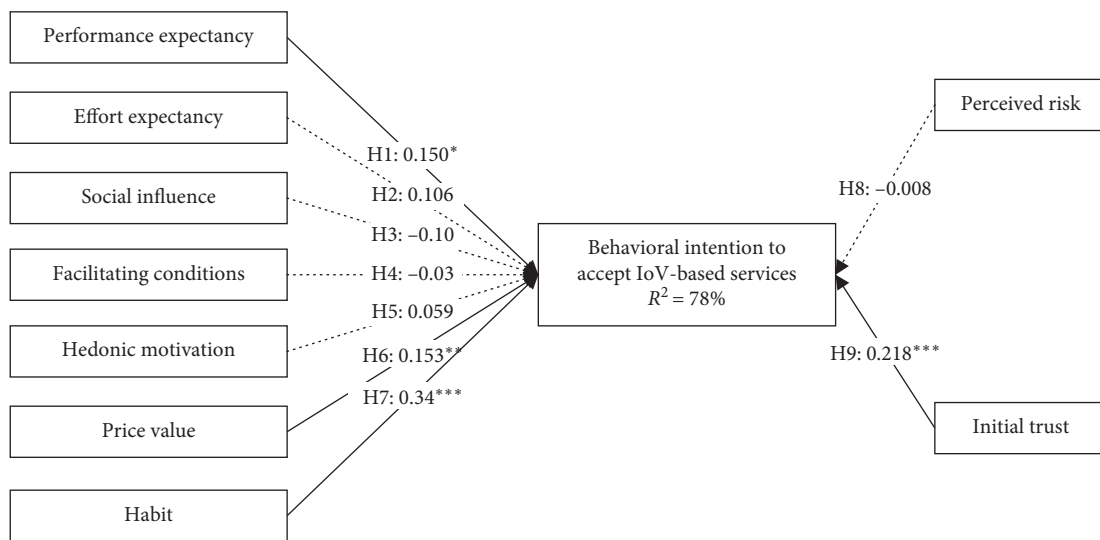


FIGURE 2: The results of structural model of IoV-based services' acceptance. Note: \*  $p < 0.05$ ; \*\*  $p < 0.01$ ; and \*\*\*  $p < 0.001$ .

5.2. Qualitative Comparative Analysis. FsQCA provides suitable methods to accommodate complex complementarities and nonlinear relationships among constructs [37]. FsQCA has attracted the attention of researchers in several fields, e.g., strategy and organization research [99, 100] and information management [94, 101]. Therefore, this study employs fsQCA for a detailed analysis of how causal conditions contribute to an outcome [39, 100]. The key stages of a fsQCA study contain model building, sampling, calibration, data analysis, reporting, and interpretation of findings [99]. Before analysis, data should be calibrated first from the original five-point Likert scale into a dataset suitable for data analysis by fsQCA.

5.2.1. Calibration. A five-point Likert scale provides information to calibrate these variables; however, the actual sample is not normally distributed [92]. Therefore, the mean of each variable was chosen as the crossover point [100], rather than the median of a five-point Likert scale [58]. Using the fsQCA 3.0 Software, calibration is automated completed and shown as Table 7.

5.2.2. Analysis of Necessary Conditions. This study begins with the analysis of necessary conditions [91, 102]. An analysis of necessary conditions determines whether any causal condition can be regarded as a necessary condition for the outcome to occur [103]. Drawing upon the recommendations [44, 58, 99, 103], a condition is necessary when its consistency score is greater than the threshold of 0.9. Table 8 presents the results of the analysis of necessary conditions considering both the presence and the absence (~) of the conditions for two outcome variables, i.e., behavioral intention to accept IoV services ("BI") and the negation of behavioral intention to accept IoV services ("~BI"). The results show that none of the conditions alone, except PE (consistency is 0.932) and EE (consistency is 0.931), is necessary conditions for the outcome "BI." Besides, none of the conditions alone is a necessary condition for the outcome "~BI," except "~HA."

5.2.3. Analysis of Sufficient Conditions for Behavioral Intention to Accept IoV Services. To explore which conditions might consistently result in the intention to accept IoV-based services, the truth table algorithm described by



TABLE 7: Full membership, full nonmembership, and a crossover point of calibration.

	Full nonmembership	Crossover point	Full membership
Perceived expectancy	1	3.9	5
Effort expectancy	1	3.9	5
Social influence	1	3.9	5
Facilitating conditions	1	3.9	5
Hedonic motivation	1	3.9	5
Price value	1	3.9	5
Habit	1	3.9	5
Perceived risk	1	2.3	5
Initial trust	1	3.9	5
Behavioral intention	1	4.1	5

TABLE 8: Analysis of necessary conditions.

Outcome	BI (behavioral intention to accept IoV services)		~BI (negation of behavioral intention to accept IoV services)	
	Consistency	Coverage	Consistency	Coverage
PE	<b>0.932</b>	0.841	0.734	0.494
~PE	0.439	0.689	0.764	0.893
EE	<b>0.931</b>	0.827	0.745	0.493
~EE	0.430	0.693	0.739	0.888
SI	0.881	0.887	0.677	0.508
~SI	0.512	0.680	0.849	0.842
FC	0.873	0.885	0.686	0.518
~FC	0.525	0.691	0.848	0.832
HM	<b>0.910</b>	0.880	0.695	0.501
~HM	0.484	0.680	0.833	0.874
PV	0.873	0.882	0.680	0.512
~PV	0.517	0.684	0.843	0.832
HA	0.835	0.941	0.621	0.521
~HA	0.576	0.671	<b>0.930</b>	0.808
PR	0.552	0.752	0.747	0.759
~PR	0.823	0.813	0.756	0.557
TR	0.893	0.893	0.693	0.516
~TR	0.516	0.693	0.856	0.857

Note: “~” indicates the absence of a condition.

[38] was used. The truth table algorithm proceeds in a two-stage analytic procedure, to empirically complete this identification of causal processes. The first step is creating a truth table with  $2^k$  ( $k$  is the number of causal conditions) rows from the fuzzy data, reflecting all possible combinations of causal conditions that lead to a specific outcome (“AI”) [58]. The second step involves specifying the causal conditions and outcomes to minimize. The number of rows is reduced in line with two principles: (1) the minimum number of cases (frequency) required for a solution to be considered and (2) the minimum consistency level of a solution [38]. In this study, we set frequency thresholds to be

5 and consistency thresholds to be 0.8 (the actual value was 0.867) to exclude less important configurations; then, the configurations selected captured 82% of the cases, which meet the recommendation that a threshold is chosen that retains at least 75–80% of the cases [99].

Based on the “Standard Analyses” procedure, the complex solution, intermediate solution, and parsimonious solution are automatically derived based on the different treatment of the remainder combinations [38], and these solutions can be distinguished based on “easy” and “difficult” counterfactuals [37]. The complex solution includes all possible configurations of conditions (i.e., includes neither easy nor difficult counterfactuals). The parsimonious solution offers vital conditions that can be either easy or difficult counterfactuals. The intermediate solution offers vital conditions based on easy counterfactuals [37]. The notion of causal conditions belonging to the core or peripheral configurations is based on these parsimonious and intermediate solutions: “core” conditions are decisive causal ingredients (those that are part of both parsimonious and intermediate solutions), and “peripheral” conditions are those that are eliminated in the parsimonious solution and thus only appear in the intermediate solution [100]. Table 9 shows the results of fsQCA providing the solution for the outcome (high-level intention to accept IoV-based services) that distinguishes between “core” and “peripheral” conditions.

The results shown in Table 9 indicate none of the isolated antecedent is a sufficient condition for the presence of “AI” and reveal seven equifinal configurations (combinations of conditions linked to the outcome) grouped by their core conditions [100]. All configurations are sufficient because all of the consistency scores resembles the notion of significance in statistical models [92, 102] and exceeds the threshold of 0.8 in the sufficiency analysis [38, 99]. Besides, each configuration’s coverage, such as an analogous measure of  $R^2$  in regression analysis [92], is greater than 0. Thus, all configurations are empirically relevant [38, 44]. According to the solution coverage value, the overall solution accounts for 86.9% of the cases associated with high intention to accept IoV-based services.

*5.2.4. Analysis of Sufficient Conditions for the Negation of Behavioral Intention to Accept IoV Services.* Contrary to most traditional techniques as SEM [104, 105] and regression model [94, 101], fsQCA focuses on causal asymmetry [38, 44, 91, 100]. FsQCA can be used to analyze separately the configurations for the presence and the absence of an outcome [99]. Therefore, to check this asymmetry, fsQCA conducts another set of analyses in which the negation of behavioral intention to accept IoV services represents the outcome and is coded as the inverse (~BI). To explore which conditions consistently lead to this outcome, the same frequency (5) and consistency (0.8, the actual value was 0.858) thresholds are set. The solution for the negation of behavioral intention to accept IoV services is shown in Table 10.

TABLE 9: Sufficient configurations for high intention to accept IoV-based services.

Causal condition	Solutions											
	1a	1b	2	3a	3b	3c	3d	4	5	6	7a	7b
Perceived expectancy	●	●	●	●	●	●	●	⊗	●	●	⊗	⊗
Effort expectancy	●	●	●	●	●	●	●	●		⊗		⊗
Social influence	•	•	•	•	•		⊗	⊗	⊗	•	⊗	⊗
Facilitating conditions	•		•	•		•	⊗	⊗	⊗	⊗	⊗	⊗
Hedonic motivation	●	●		●	●	●	●	⊗	⊗	●	⊗	⊗
Price value	⊗	⊗	•		•	•	⊗	•	⊗	⊗	⊗	⊗
Habit	⊗	⊗	•		•	•	⊗	•	⊗	⊗	⊗	⊗
Perceived risk	⊗	⊗	⊗				•	⊗	•	•	⊗	⊗
Initial trust		•	⊗	•	•	•	•	•	⊗	•	⊗	
Raw coverage	0.385	0.388	0.392	0.765	0.700	0.697	0.324	0.313	0.330	0.306	0.328	0.312
Unique coverage	0.001	0.001	0.010	0.057	0.014	0.012	0.001	0.002	0.005	0.001	0.001	0.002
Consistency	0.963	0.964	0.985	0.943	0.971	0.973	0.974	0.983	0.941	0.979	0.859	0.860
Solution consistency	0.881											
Solution coverage	0.862											

Note: black circles (“●”) indicate the presence of a condition, and circles with a cross-out (“⊗”) indicate its absence. Furthermore, large circles indicate core conditions, and small circles indicate peripheral conditions. Blank spaces indicate a “do not care” situation in which the causal condition may be either present or absent [100].

TABLE 10: Sufficient configurations for the negation of high behavioral intention to accept IoV-based services.

Causal condition	Solutions							
	1a	1b	2	3	4	5	6	7
Perceived expectancy	⊗	⊗	⊗	●	●	●	●	●
Effort expectancy	⊗		⊗	●	●	●	●	●
Social influence	⊗	⊗	⊗	⊗	●	●	●	●
Facilitating conditions	⊗	⊗	⊗	●	⊗	●	●	●
Hedonic motivation	⊗	⊗	⊗	●	●	●	●	●
Habit	⊗	⊗	⊗	●	●	⊗		●
Price value	⊗	⊗	⊗	●	●		⊗	●
Perceived risk		⊗	⊗	●	⊗			⊗
Initial trust	⊗	⊗		●	●	●	●	⊗
Raw coverage	0.586	0.494	0.468	0.424	0.468	0.506	0.554	0.468
Unique coverage	0.115	0.010	0.004	0.004	0.008	0.003	0.017	0.002
Consistency	0.967	0.966	0.963	0.902	0.870	0.843	0.826	0.892
Solution consistency	0.794							
Solution coverage	0.809							

As shown in Table 10, seven identified solutions comply with the recommended consistency and unique coverage thresholds [38]. The overall solution coverage indicates that causal conditions account for 84.4% of cases in the solution.

## 6. Discussion

**6.1. Key Findings.** This study aims to show how the analysis of net and combinatory effects of specific antecedent variables can improve the understanding of behavioral intention to accept IoV services [91].

The PLS-SEM results show that performance expectancy ( $\beta = 0.150$ ) has a significantly positive effect on consumers’ behavioral intentions. The analysis of necessary conditions of fsQCA also confirms that performance expectancy (consistency = 0.932) is a necessary condition for high behavioral intention. Moreover, PE is indeed core conditions in nine of the twelve configurations for behavioral intention, reinforcing the findings of PLS-SEM. The relevance of

performance expectancy is consistent with the previous studies that highlight the importance of the users’ expectancy of performance to achieve the behavioral intention, e.g., autonomous car [7] and autonomous delivery vehicles [45].

Such smart technology usage should be simple and obvious, surprisingly, effort expectancy, as an important functional characteristic of technology, has no significant effect on the behavioral intention from PLS-SEM results. This result is in line with previous research on the acceptance of emerging technologies as smart home [57] and autonomous delivery vehicles [45], but contradicts results from some studies on the adoption of autonomous car [7]. Nevertheless, the results from fsQCA confirm that effort expectancy (consistency = 0.931) is a necessary condition of consumers’ behavioral intention. Moreover, it is indeed core conditions in eight of the twelve configurations for behavioral intention, complementing the findings PLS-SEM failed to detect. In such circumstances, IoV-based services and vehicles are not well understood by the users, and they did not

have sufficient information and they were not familiar with the technology behind the concept. The level of information provided could reduce the perceived complexity, as the less the technology is perceived as complex, the more likely it is that the innovation will be adopted [57].

Different from the significant effect of SI and FC in previous studies [29, 45], PLS-SEM results show that neither SI nor FC has a significant “net effect” on behavioral intention to accept IoV, which is aligned with previous studies that find a nonsignificant direct effect of SI on behavioral intention [55, 57], and nonsignificant direct effect of FC on behavioral intention [54, 76]. Nevertheless, in the fsQCA result, SI is present as a peripheral condition in six of the twelve configurations for BI and is absent as a core condition in four of the eight configurations for the negation of behavioral intention to accept IoV-based services, suggesting the relevance of SI on AI. The result is consistent with numerous studies in IoT [106], Internet banking [75, 76], e-government [71], autonomous vehicle [4, 7, 13], and automated public transport [28]. Besides, the presence of FC is a peripheral condition in four of the twelve configurations for behavioral intention to accept IoV-based services and the absence of FC is a core condition in four of the eight configurations for the negation of behavioral intention to accept IoV-based services, showing the existence of causal asymmetry in a complex context. The result confirms results from previous research carried out on technology acceptance such as mobile banking [60, 64] and automated public transport [29]. Overall, the absence of SI and FC as core condition in four solutions for the negation of behavioral intention to accept IoV-based services, especially in solution 3 and solution 4 (the absence of SI or FC, even if all else conditions are present, will determine the outcome the absence of BI), indicates that the lower SI and FC about potential consumers, the lower the acceptance of IoV-based services. The results show that IoV-based service/vehicle is a new technology not yet widely adopted and the intention to purchase an innovation is stronger when the innovation is already used by others. Once the concept becomes part of daily life, the impact of SI could be higher.

The PLS-SEM results show that hedonic motivation (HM) does not significantly impact behavioral intention (BI) to use IoV-based services. Nevertheless, fsQCA results indicate that HM is present as a core condition in seven of the twelve configurations for BI and is absent as a peripheral condition in three of the eight configurations for the negation of BI to accept IoV-based services, suggesting the low-level significance of HM on BI. The finding is contrary to previous studies on the acceptance of autonomous delivery vehicles [45], automated road transport systems [29, 46], social networking service [107], wearable technology [61], and mobile health [58], while it is aligned with some studies such as smart home acceptance [57] and consumer e-loyalty [108]. In summary, IoV services are perceived by connected autonomous vehicle consumers as more of an intelligent utilitarian solution rather than a hedonic one.

Price value (PV) ( $\beta = 0.153$ ) is found to be a significant determinant of behavioral intention (BI) in SEM-PLS results, which is in line with previous research on the

acceptance of emerging technologies, e.g., autonomous delivery vehicles [45], autonomous electric bus [31, 48], Internet of things [54], and electric vehicles [65]. This means that consumers consider the benefits of IoV-based services against the monetary value. Furthermore, fsQCA results indicate the absence of PV, as a core condition in four of the eight configurations for the negation of BI to accept IoV-based services, suggesting the low price-performance of consumers' perception on IoV-based services is the barrier of accepting IoV-based services. There is a price premium on IoV-based services compare with the conventional vehicle. Consumers who believe that the price of IoV-based service is justified by the potential benefits have a stronger behavioral intention to adopt. Talebian and Mishra suggest that the automobile will be nearly homogenous in about 2050 only if prices decrease at significant rates (15% or 20% annually) [16].

The PLS-SEM results show habit has the strongest effect ( $\beta = 0.34$ ) on behavioral intention, as confirmed in previous studies on the acceptance of emerging technologies, e.g., smart home [57]. Besides, the fsQCA results also confirm that the negation of habit ( $\sim$ HA) is a necessary condition (consistency = 0.930) for the negation of behavioral intention ( $\sim$ BI), and the absence of habit is indeed a core condition in four of the eight configurations for behavioral intention, indicating the lower the habit to use IoV-based services, the less likely it is to accept IoV-based services. Therefore, for the emerging and not widely used technologies, the lack of habit may be the biggest obstacle to technology adoption.

Despite perceived risk has been frequently cited as one major concern in accepting IoV-based services in several studies [3], in this study, PLS-SEM has failed to identify its significant net effect on behavioral intention to accept IoV-based services. This result is aligned with the previous studies, e.g., social commerce [73], e-government [72], autonomous vehicle [32, 34], and connected vehicle [35]. Interestingly, fsQCA results show that the absence of perceived risk is indeed a core condition in six of the twelve configurations for behavioral intention, which corroborates previous studies that observe a negative effect of perceived risk on the adoption of innovative technologies, e.g., mobile payment [59, 77, 109], Internet banking [74–76], IoT in agriculture [70], social media purchase [110], electric vehicles [111, 112], and autonomous vehicle [8, 10, 45, 47]. Previous empirical findings are rather mixed, resulting in the argument that perceived risk cannot be seen as a steady predictor of IoV-based services acceptance [8, 45]. FsQCA results show that perceived risk has been proven as a core condition (an important determinant) in six configurations, indicating the lower the risk perception by potential users, the higher the acceptance of IoV-based services.

It is found from PLS-SEM that the role of initial trust ( $\beta = 0.41$ ) is much stronger in influencing behavioral intention to accept IoV-based services than other perceptual factors. Although “the presence of initial trust” is just a peripheral condition of configuration for behavioral intention, however, “the absence of initial trust” is indeed a core condition in two of the seven configurations for the

negation of behavioral intention (i.e., the presence of BI), suggesting that the lack of initial trust in IoV-based services will also reduce the acceptance intention. The significance of initial trust in shaping behavioral intention corroborates previous studies, e.g., mobile banking [79, 113], cloud technology [114], e-government [72], autonomous vehicles [8, 15, 32, 34], and autonomous shuttle/bus [31, 46, 48]. This finding suggests that trust, as “a tool for the reduction of cognitive complexity,” can help to simplify and facilitate the decision-making process, especially in situations with risks and uncertainty [11, 115]. Therefore, insufficient trust has been thought to be one of the major psychological barriers to the wide adoption of IoV-based services [15, 34].

In summary, results from PLS-SEM reveal that higher levels of performance expectancy, price value, habit, and initial trust increase behavioral intention. Moreover, results from fsQCA which is used as a supplementary analysis technique [93] and reinforces the symmetric findings of PLS-SEM, as well as offer additional novel interesting, and more nuanced insights that indicate a combination of the conditions needs to be taken into account to explain the outcome of behavioral intention. Five configurations for “BI” and seven configurations for “~BI” are identified. This synergetic effect could not be captured by PLS-SEM since it examines the condition in isolation from the other conditions [44, 92].

**6.2. Theoretical Implications.** This study has two key theoretical contributions. Firstly, this study takes an integrated approach towards technology acceptance in the context of the IoV-based services, which complements and extends technology acceptance studies. As different theories emphasize the different insights regarding technology acceptance, most researchers have called for a holistic and comprehensive approach that integrates more than one single theoretical perspective for understanding the acceptance of innovative technologies [31, 46, 64, 116], to make full use of the advantages of different models, and make up the deficiency of the one-sidedness from a single model. Therefore, to provide broad coverage of factors for IoV-based services acceptance, this study answers this call by developing an integrated model incorporating UTAUT, perceived risk theory, and initial trust model. The net effect analysis of this integrated model shows an explained variance ( $R^2$ ) of 78% for behavioral intention to accept IoV services, indicating a moderate explanatory power.

Secondly, this study contributes to the IoV-based services’ acceptance literature at the methodological level. Existing studies on the topic generally rely on multiple regression models, SEM, and PLS methodology and view consumer’s intention to accept IoV-based services primarily as the outcome of several isolated antecedents. Besides the PLS-SEM, the study uses the fsQCA to investigate which configurations of determinants lead to the intention to accept IoV-based services and which ones lead to the negation of intention to accept IoV-based services. To the best of our knowledge, this study is the first to use this type of analysis to explore the intention to accept IoV-based

services. This study demonstrates that the fsQCA offers much in terms of understanding how various determinants explain the acceptance of IoV-based services, more so than the PLS-SEM. Besides, this study by fsQCA also answers the call for the application of this technique to complex behavior research, since it can offer new insights into understanding the IoV-based services acceptance phenomena [44, 94]. Therefore, the value of this study lies in the effort to describe combinatorial complexities assuming asymmetrical relationships between variables, rather than symmetrical net effects that PLS-SEM estimates [105].

**6.3. Managerial Implications.** From a practical point of view, this study’s findings provide several managerial implications for automobile manufacturers, marketers, and policymakers. Based on our findings of PLS-SEM and fsQCA, they should focus on different configurations of antecedents that give rise to an outcome, rather than the impact of these antecedents isolation from each other.

First, as suggested by our findings of PLS-SEM and fsQCA, both the utilitarian benefits (i.e., performance expectancy, and effort expectancy) and hedonic benefits are favored by potential users. Hence, automobile manufacturers and marketers should focus more on the development and the marketing communication activities of IoV-based services on the utilitarian benefits and hedonic benefits compared to conventional vehicles. Moreover, lower perceived risk is also found to contribute to IoV-based services acceptance to a large extent. Besides, if potential risks are not well understood thoughtfully, they could slow IoV-based services adoption rates to socially suboptimal levels. Therefore, marketers should take perceived risk reduction into consideration when promoting IoV-based services in society. Most importantly, high quality and low price, the best cost effective. Price is the most stimulating and sensitive factor influencing consumers’ purchasing behavior. Sell IoV-based services at a premium decreased consumers’ willingness to pay, hence, manufacturers and sellers should give consumers discounts and cut prices to more reasonable levels.

Second, habit and initial trust is a major construct for explaining the adoption of IoV-based services, with the first and second-largest effect, respectively, and meanwhile, the lack of habit and initial trust is likely to lead to the lower intention to accept IoV-based services. As IoV-based services are in its initial stage, manufacturers, marketers, and policymakers should be more concerned about the measures to increase the individuals’ habit and initial trust toward this innovative technology. Therefore, consumers’ habit formation and trust building become an urgent mission for these stakeholders [8]. For instance, exhibitions and user experience activities of IoV-based technologies and services should be held to help consumers observe and directly experience IoV-based services, such experiences and knowledge are conducive to the formation of habit and trust toward IoV-based services [80] and are critical ingredients for widespread and rapid technology diffusion [53].



Finally, the lower level of social influence and facilitating conditions also lead to a lower level of behavioral intention to accept IoV services. When the individuals' knowledge levels about a specific technology are low or the technology is still in its initial stages, and public communication significantly influences societal acceptance [8]. For the acceptance of IoV-based services, it is of particular relevance to what the social environment (i.e., family, friends, and acquaintances) thinks, what the media reports, and what opinion experts reflect [16]. Hence, marketers might use social influence when promoting IoV-based services during the market introduction stage.

**6.4. Limitations and Future Directions.** Our study has several limitations that could be addressed in the future. First, we did not take into account other factors that might affect consumers' intention to accept or purchase IoV-based services. Our model based on UTAUT2, perceived risk theory, and initial trust theory only considers some important factors, but it is far from reaching a comprehensive explanation. In the future, the extent to which consumers' purchase intentions are affected can be explored based on other consumer behavior and technology adoption theories that match the characteristics of IoV-based services. Second, this study uses data collected through a purposive sample in a single country, China, which implies that our findings reflect only the situation in this nation, and may affect the generalization of our findings due to differences in the cultural environment and political system of countries. Therefore, a future study may consider a comparative study across different countries, e.g., the U.S. of North America, Germany of Europe, Japan, South Korea, and India of the Asian-Pacific region, and Brazil of South America.

## 7. Conclusions

IoV-based services, as radical innovations for changing transportation fundamentally, introduce all sorts of different benefits such as safety, energy efficiency, environment improvement, increased mobility, and more entertainment in driving [3–5, 9, 14]. IoV-based services are not widely accepted by consumers without understanding IoV-based services diffusion. Thus, investigation of the determinants leading to consumers' intention to accept and purchase IoV-based services is significant for both academics and practitioners. This study identifies the determinants of behavioral intention to accept IoV services by using an integrated model that combines UTAUT, perceived risk theory, and initial trust theory. This study uses both symmetric (PLS-SEM) and asymmetric (fsQCA) methods to explore the role of determinants in consumers' intention to accept and purchase IoV-based services. Specifically, the net effects of each antecedent factor on intention are analyzed by conventional correlational techniques (PLS-SEM). The direct effects of performance expectancy, price value, habit, and initial trust on intention are found to be significant. Despite the determinants (e.g., effort expectancy, social influence, facilitating conditions, hedonic motivation, and perceived

risk) are found to be nonsignificant effects on intention, however, it cannot be said they are not important to intention to accept IoV-based services, due to the existence of causal complexity. For the high levels of causal complexity, fsQCA provides a more nuanced understanding of how these antecedent conditions fit together to affect consumers' intention to accept and purchase IoV-based services. The results from fsQCA provide twelve different configurations to achieve high levels of behavioral intention to accept IoV services and eight causal paths equifinally to lead to the negation of behavioral intention to accept IoV services. The findings provide relevant insights and marketing suggestions for incentivizing consumers to accept IoV-based services.

## Data Availability

The data used to support the findings of this study are available from the corresponding author upon request.

## Conflicts of Interest

The authors declare that there are no conflicts of interest regarding the publication of this paper.

## Acknowledgments

This research was funded by the National Social Science Fund of China (20FGLB070), Shandong Provincial Natural Science Foundation of China (ZR2019BG004), Shandong Provincial Humanities and Social Sciences Research Program for University of China (J18RA047), and National Natural Science Foundation of China (72072103).

## References

- [1] S. E. Shladover, "Connected and automated vehicle systems: introduction and overview," *Journal of Intelligent Transportation Systems*, vol. 22, no. 3, pp. 190–200, 2018.
- [2] J. Wu, H. Liao, J.-W. Wang, and T. Chen, "The role of environmental concern in the public acceptance of autonomous electric vehicles: a survey from China," *Transportation Research Part F: Traffic Psychology and Behaviour*, vol. 60, pp. 37–46, 2019.
- [3] J. Wu, H. Liao, and J.-W. Wang, "Analysis of consumer attitudes towards autonomous, connected, and electric vehicles: a survey in China," *Research in Transportation Economics*, vol. 80, Article ID 100828, 2020.
- [4] N. Adnan, S. Md Nordin, M. A. Bin Bahrudin, and M. Ali, "How trust can drive forward the user acceptance to the technology? In-vehicle technology for autonomous vehicle," *Transportation Research Part A: Policy and Practice*, vol. 118, pp. 819–836, 2018.
- [5] P. Bansal and K. M. Kockelman, "Forecasting Americans' long-term adoption of connected and autonomous vehicle technologies," *Transportation Research Part A: Policy and Practice*, vol. 95, pp. 49–63, 2017.
- [6] F. Becker and K. W. Axhausen, "Literature review on surveys investigating the acceptance of automated vehicles," *Transportation*, vol. 44, no. 6, pp. 1293–1306, 2017.
- [7] T. Leicht, A. Chtourou, and K. Ben Youssef, "Consumer innovativeness and intentioned autonomous car adoption,"

- The Journal of High Technology Management Research*, vol. 29, no. 1, pp. 1–11, 2018.
- [8] H. Liu, R. Yang, L. Wang, and P. Liu, “Evaluating initial public acceptance of highly and fully autonomous vehicles,” *International Journal of Human-Computer Interaction*, vol. 35, no. 11, pp. 919–931, 2019.
- [9] M.-K. Kim, J.-H. Park, J. Oh, W.-S. Lee, and D. Chung, “Identifying and prioritizing the benefits and concerns of connected and autonomous vehicles: a comparison of individual and expert perceptions,” *Research in Transportation Business & Management*, vol. 32, Article ID 100438, 2019.
- [10] G. Zhu, Y. Chen, and J. Zheng, “Modelling the acceptance of fully autonomous vehicles: a media-based perception and adoption model,” *Transportation Research Part F: Traffic Psychology and Behaviour*, vol. 73, pp. 80–91, 2020.
- [11] T. Zhang, D. Tao, X. Qu, X. Zhang, R. Lin, and W. Zhang, “The roles of initial trust and perceived risk in public’s acceptance of automated vehicles,” *Transportation Research Part C: Emerging Technologies*, vol. 98, pp. 207–220, 2019.
- [12] J. M. Müller, “Comparing technology acceptance for autonomous vehicles, battery electric vehicles, and car sharing—a study across Europe, China, and North America,” *Sustainability*, vol. 11, no. 16, Article ID 4333, 2019.
- [13] I. Panagiotopoulos and G. Dimitrakopoulos, “An empirical investigation on consumers’ intentions towards autonomous driving,” *Transportation Research Part C: Emerging Technologies*, vol. 95, pp. 773–784, 2018.
- [14] K. F. Yuen, G. Chua, X. Wang, F. Ma, and K. X. Li, “Understanding public acceptance of autonomous vehicles using the theory of planned behaviour,” *International Journal of Environmental Research and Public Health*, vol. 17, no. 12, Article ID 4419, 2020.
- [15] S. M. Hegner, A. D. Beldad, and G. J. Brunswick, “In automatic we trust: investigating the impact of trust, control, personality characteristics, and extrinsic and intrinsic motivations on the acceptance of autonomous vehicles,” *International Journal of Human-Computer Interaction*, vol. 35, no. 19, pp. 1769–1780, 2019.
- [16] A. Talebian and S. Mishra, “Predicting the adoption of connected autonomous vehicles: a new approach based on the theory of diffusion of innovations,” *Transportation Research Part C: Emerging Technologies*, vol. 95, pp. 363–380, 2018.
- [17] T. H. Rashidi, A. Najmi, A. Haider, C. Wang, and F. Hosseinzadeh, “What we know and do not know about connected and autonomous vehicles,” *Transportmetrica A: Transport Science*, vol. 16, no. 3, pp. 987–1029, 2020.
- [18] F. Yang, J. Li, T. Lei, and S. Wang, “Architecture and key technologies for internet of vehicles: a survey,” *Journal of Communications and Information Networks*, vol. 2, no. 2, pp. 1–17, 2017.
- [19] K. M. Alam, M. Saini, and A. E. Saddik, “Toward social internet of vehicles: concept, architecture, and applications,” *IEEE Access*, vol. 3, pp. 343–357, 2015.
- [20] J. Contreras-Castillo, S. Zeadally, and J. A. Guerrero-Ibañez, “Internet of vehicles: architecture, protocols, and security,” *IEEE Internet of Things Journal*, vol. 5, no. 5, pp. 3701–3709, 2018.
- [21] O. Kaiwartya, A. H. Abdullah, Y. Cao et al., “Internet of vehicles: motivation, layered architecture, network model, challenges, and future aspects,” *IEEE Access*, vol. 4, pp. 5356–5373, 2016.
- [22] J. Cheng, J. Cheng, M. Zhou, F. Liu, S. Gao, and C. Liu, “Routing in internet of vehicles: a review,” *IEEE Transactions on Intelligent Transportation Systems*, vol. 16, no. 5, pp. 2339–2352, 2015.
- [23] M. Chen, Y. Tian, G. Fortino, J. Zhang, and I. Humar, “Cognitive internet of vehicles,” *Computer Communications*, vol. 120, pp. 58–70, 2018.
- [24] A. Shariff, J.-F. Bonnefon, and I. Rahwan, “Psychological roadblocks to the adoption of self-driving vehicles,” *Nature Human Behaviour*, vol. 1, no. 10, pp. 694–696, 2017.
- [25] M. Guériau, R. Billot, N.-E. El Faouzi, J. Monteil, F. Armetta, and S. Hassas, “How to assess the benefits of connected vehicles? a simulation framework for the design of cooperative traffic management strategies,” *Transportation Research Part C: Emerging Technologies*, vol. 67, pp. 266–279, 2016.
- [26] P. Jing, G. Xu, Y. Chen, Y. Shi, and F. Zhan, “The determinants behind the acceptance of autonomous vehicles: a systematic review,” *Sustainability*, vol. 12, no. 5, Article ID 1719, 2020.
- [27] J. Zmud, I. N. Sener, and J. Wagner, “Self-driving vehicles: determinants of adoption and conditions of usage,” *Transportation Research Record: Journal of the Transportation Research Board*, vol. 2565, no. 1, pp. 57–64, 2016.
- [28] R. Madigan, T. Louw, M. Dziennus et al., “Acceptance of automated road transport systems (ARTS): an adaptation of the UTAUT model,” *Transportation Research Procedia*, vol. 14, pp. 2217–2226, 2016.
- [29] R. Madigan, T. Louw, M. Wilbrink, A. Schieben, and N. Merat, “What influences the decision to use automated public transport? using UTAUT to understand public acceptance of automated road transport systems,” *Transportation Research Part F: Traffic Psychology and Behaviour*, vol. 50, pp. 55–64, 2017.
- [30] S. Deb, L. Strawderman, D. W. Carruth, J. DuBien, B. Smith, and T. M. Garrison, “Development and validation of a questionnaire to assess pedestrian receptivity toward fully autonomous vehicles,” *Transportation Research Part C: Emerging Technologies*, vol. 84, pp. 178–195, 2017.
- [31] B. Herrenkind, I. Nastjuk, A. B. Brendel, S. Trang, and L. M. Kolbe, “Young people’s travel behavior—using the life-oriented approach to understand the acceptance of autonomous driving,” *Transportation Research Part D: Transport and Environment*, vol. 74, pp. 214–233, 2019.
- [32] J. K. Choi and Y. G. Ji, “Investigating the importance of trust on adopting an autonomous vehicle,” *International Journal of Human-Computer Interaction*, vol. 31, no. 10, pp. 692–702, 2015.
- [33] J. Kim, S. Kim, and C. Nam, “User resistance to acceptance of In-Vehicle Infotainment (IVI) systems,” *Telecommunications Policy*, vol. 40, no. 9, pp. 919–930, 2016.
- [34] P. Liu, Q. Guo, F. Ren, L. Wang, and Z. Xu, “Willingness to pay for self-driving vehicles: influences of demographic and psychological factors,” *Transportation Research Part C: Emerging Technologies*, vol. 100, pp. 306–317, 2019.
- [35] J. Walter and B. Abendroth, “On the role of informational privacy in connected vehicles: a privacy-aware acceptance modelling approach for connected vehicular services,” *Teleatics and Informatics*, vol. 49, Article ID 101361, 2020.
- [36] J. Chaparro-Peláez, Á. F. Agudo-Peregrina, and F. J. Pascual-Miguel, “Conjoint analysis of drivers and inhibitors of e-commerce adoption,” *Journal of Business Research*, vol. 69, no. 4, pp. 1277–1282, 2016.
- [37] B. Kaya, A. M. Abubakar, E. Behraves, H. Yildiz, and I. S. Mert, “Antecedents of innovative performance: findings



- from PLS-SEM and fuzzy sets (fsQCA),” *Journal of Business Research*, vol. 114, pp. 278–289, 2020.
- [38] C. C. Ragin, *Redesigning Social Inquiry: Fuzzy Sets and Beyond*, University of Chicago Press, Chicago, IL, USA, 2008.
- [39] B. Rihoux and C. C. Ragin, *Configurational Comparative Methods: Qualitative Comparative Analysis (QCA) and Related Techniques*, Sage Publications, Thousand Oaks, CA, USA, 2009.
- [40] A. G. Woodside, “Moving beyond multiple regression analysis to algorithms: calling for adoption of a paradigm shift from symmetric to asymmetric thinking in data analysis and crafting theory,” *Journal of Business Research*, vol. 66, no. 4, pp. 463–472, 2013.
- [41] V. Venkatesh, J. Y. L. Thong, and X. Xu, “Consumer acceptance and use of information technology: extending the unified theory of acceptance and use of technology,” *MIS Quarterly*, vol. 36, no. 1, pp. 157–178, 2012.
- [42] J. W. Taylor, “The role of risk in consumer behavior,” *Journal of Marketing*, vol. 38, no. 2, pp. 54–60, 1974.
- [43] D. H. McKnight, V. Choudhury, and C. Kacmar, “Developing and validating trust measures for e-Commerce: an integrative typology,” *Information Systems Research*, vol. 13, no. 3, pp. 334–359, 2002.
- [44] S. F. Jahanmir, G. M. Silva, P. J. Gomes, and H. M. Gonçalves, “Determinants of users’ continuance intention toward digital innovations: are late adopters different?” *Journal of Business Research*, vol. 115, pp. 225–233, 2020.
- [45] S. Kapsler and M. Abdelrahman, “Acceptance of autonomous delivery vehicles for last-mile delivery in Germany-extending UTAUT2 with risk perceptions,” *Transportation Research Part C: Emerging Technologies*, vol. 111, pp. 210–225, 2020.
- [46] C.-F. Chen, “Factors affecting the decision to use autonomous shuttle services: evidence from a scooter-dominant urban context,” *Transportation Research Part F: Traffic Psychology and Behaviour*, vol. 67, pp. 195–204, 2019.
- [47] J. Lee, D. Lee, Y. Park, S. Lee, and T. Ha, “Autonomous vehicles can be shared, but a feeling of ownership is important: examination of the influential factors for intention to use autonomous vehicles,” *Transportation Research Part C: Emerging Technologies*, vol. 107, pp. 411–422, 2019.
- [48] B. Herrenkind, A. B. Brendel, I. Nastjuk, M. Greve, and L. M. Kolbe, “Investigating end-user acceptance of autonomous electric buses to accelerate diffusion,” *Transportation Research Part D: Transport and Environment*, vol. 74, pp. 255–276, 2019.
- [49] M. Fishbein and I. Ajzen, *Belief, Attitude, Intention, and Behavior: An Introduction to Theory and Research*, Addison-Wesley Publishing Company, Boston, MA, USA, 1975.
- [50] F. D. Davis, “Perceived usefulness, perceived ease of use, and user acceptance of information technology,” *MIS Quarterly*, vol. 13, no. 3, pp. 319–340, 1989.
- [51] I. Ajzen, “The theory of planned behavior,” *Organizational Behavior and Human Decision Processes*, vol. 50, no. 2, pp. 179–211, 1991.
- [52] V. Venkatesh, M. G. Morris, G. B. Davis, and F. D. Davis, “User acceptance of information technology: toward a unified view,” *MIS Quarterly*, vol. 27, no. 3, pp. 425–478, 2003.
- [53] E. M. Rogers, *Diffusion of Innovations*, Simon & Schuster, New York, NY, USA, 4th edition, 2020.
- [54] M. Q. Aldossari and A. Sidorova, “Consumer acceptance of Internet of things (IoT): smart home context,” *Journal of Computer Information Systems*, vol. 60, no. 6, pp. 507–517, 2020.
- [55] M. A. Almaiah, M. M. Alamri, and W. Al-Rahmi, “Applying the UTAUT model to explain the students’ acceptance of Mobile learning system in higher education,” *IEEE Access*, vol. 7, pp. 174673–174686, 2019.
- [56] M. Shorfuzzaman and M. Alhussein, “Modeling learners’ readiness to adopt mobile learning: a perspective from a GCC higher education institution,” *Mobile Information Systems*, vol. 2016, Article ID 6982824, , 2016.
- [57] P. Baudier, C. Ammi, and M. Deboeuf-Rouchon, “Smart home: highly-educated students’ acceptance,” *Technological Forecasting and Social Change*, vol. 153, Article ID 119355, 2020.
- [58] P. Duarte and J. C. Pinho, “A mixed methods UTAUT2-based approach to assess mobile health adoption,” *Journal of Business Research*, vol. 102, pp. 140–150, 2019.
- [59] Q. Cao and X. Niu, “Integrating context-awareness and UTAUT to explain Alipay user adoption,” *International Journal of Industrial Ergonomics*, vol. 69, pp. 9–13, 2019.
- [60] T. Zhou, Y. Lu, and B. Wang, “Integrating TTF and UTAUT to explain mobile banking user adoption,” *Computers in Human Behavior*, vol. 26, no. 4, pp. 760–767, 2010.
- [61] Y. Gao, H. Li, and Y. Luo, “An empirical study of wearable technology acceptance in healthcare,” *Industrial Management & Data Systems*, vol. 115, no. 9, pp. 1704–1723, 2015.
- [62] F. Liao, E. Molin, and B. van Wee, “Consumer preferences for electric vehicles: a literature review,” *Transport Reviews*, vol. 37, no. 3, pp. 252–275, 2017.
- [63] P. Bansal, K. M. Kockelman, and A. Singh, “Assessing public opinions of and interest in new vehicle technologies: an Austin perspective,” *Transportation Research Part C: Emerging Technologies*, vol. 67, pp. 1–14, 2016.
- [64] T. Oliveira, M. Faria, M. A. Thomas, and A. Popovič, “Extending the understanding of mobile banking adoption: when UTAUT meets TTF and ITM,” *International Journal of Information Management*, vol. 34, no. 5, pp. 689–703, 2014.
- [65] K. Degirmenci and M. H. Breitter, “Consumer purchase intentions for electric vehicles: is green more important than price and range?” *Transportation Research Part D: Transport and Environment*, vol. 51, pp. 250–260, 2017.
- [66] G. Cecere, N. Corrocher, and M. Guerzoni, “Price or performance? a probabilistic choice analysis of the intention to buy electric vehicles in European countries,” *Energy Policy*, vol. 118, pp. 19–32, 2018.
- [67] N. Adnan, S. Md Nordin, M. Hadi Amini, and N. Langove, “What make consumer sign up to PHEVs? predicting Malaysian consumer behavior in adoption of PHEVs,” *Transportation Research Part A: Policy and Practice*, vol. 113, pp. 259–278, 2018.
- [68] A. Hong, C. Nam, and S. Kim, “What will be the possible barriers to consumers’ adoption of smart home services?” *Telecommunications Policy*, vol. 44, no. 2, Article ID 101867, 2020.
- [69] Y. Liang, G. Qi, K. Wei, and J. Chen, “Exploring the determinant and influence mechanism of e-Government cloud adoption in government agencies in China,” *Government Information Quarterly*, vol. 34, no. 3, pp. 481–495, 2017.
- [70] P. Jayashankar, S. Nilakanta, W. J. Johnston, P. Gill, and R. Burres, “IoT adoption in agriculture: the role of trust, perceived value and risk,” *Journal of Business & Industrial Marketing*, vol. 33, no. 6, pp. 804–821, 2018.
- [71] Q. Xie, W. Song, X. Peng, and M. Shabbir, “Predictors for e-government adoption: integrating TAM, TPB, trust and perceived risk,” *The Electronic Library*, vol. 35, no. 1, pp. 2–20, 2017.

- [72] F. Bélanger and L. Carter, "Trust and risk in e-government adoption," *The Journal of Strategic Information Systems*, vol. 17, no. 2, pp. 165–176, 2008.
- [73] S. T. Biucky, N. Abdolvand, and S. Rajae Harandi, "The effects of perceived risk on social commerce adoption based on the tam model," *International Journal of Electronic Commerce Studies*, vol. 8, no. 2, pp. 173–196, 2017.
- [74] M.-C. Lee, "Factors influencing the adoption of internet banking: an integration of TAM and TPB with perceived risk and perceived benefit," *Electronic Commerce Research and Applications*, vol. 8, no. 3, pp. 130–141, 2009.
- [75] A. Kesharwani and S. Singh Bisht, "The impact of trust and perceived risk on internet banking adoption in India," *International Journal of Bank Marketing*, vol. 30, no. 4, pp. 303–322, 2012.
- [76] C. Martins, T. Oliveira, and A. Popovič, "Understanding the Internet banking adoption: a unified theory of acceptance and use of technology and perceived risk application," *International Journal of Information Management*, vol. 34, no. 1, pp. 1–13, 2014.
- [77] R. Thakur and M. Srivastava, "Adoption readiness, personal innovativeness, perceived risk and usage intention across customer groups for mobile payment services in India," *Internet Research*, vol. 24, no. 3, pp. 369–392, 2014.
- [78] R. P. Q. Falcao, J. B. Ferreira, and M. Carrazedo Marques da Costa Filho, "The influence of ubiquitous connectivity, trust, personality and generational effects on mobile tourism purchases," *Information Technology & Tourism*, vol. 21, no. 4, pp. 483–514, 2019.
- [79] T. Zhou, "An empirical examination of initial trust in mobile banking," *Internet Research*, vol. 21, no. 5, pp. 527–540, 2011.
- [80] D. H. Mcknight, M. Carter, J. B. Thatcher, and P. F. Clay, "Trust in a specific technology," *ACM Transactions on Management Information Systems*, vol. 2, no. 2, pp. 1–25, 2011.
- [81] J. F. Hair, J. J. Risher, M. Sarstedt, and C. M. Ringle, "When to use and how to report the results of PLS-SEM," *European Business Review*, vol. 31, no. 1, pp. 2–24, 2019.
- [82] R. W. Brislin, "Back-translation for cross-cultural research," *Journal of Cross-Cultural Psychology*, vol. 1, no. 3, pp. 185–216, 1970.
- [83] P. A. Pavlou, "Consumer acceptance of electronic commerce: integrating trust and risk with the technology acceptance model," *International Journal of Electronic Commerce*, vol. 7, no. 3, pp. 101–134, 2003.
- [84] J. S. Armstrong and T. S. Overton, "Estimating nonresponse bias in mail surveys," *Journal of Marketing Research*, vol. 14, no. 3, pp. 396–402, 1977.
- [85] N. Urbach and A. Frederik, "Structural equation modeling in information systems research using partial least squares," *Journal of Information Technology Theory and Application*, vol. 11, no. 2, pp. 5–40, 2010.
- [86] P. Mikalef, M. Boura, G. Lekakos, and J. Krogstie, "The role of information governance in big data analytics driven innovation," *Information & Management*, vol. 57, no. 7, Article ID 103361, 2020.
- [87] Y. Zhang, J. Sun, Z. Yang, and Y. Wang, "What makes people actually embrace or shun mobile payment: a cross-culture study," *Mobile Information Systems*, vol. 2018, Article ID 7497545, 13 pages, 2018.
- [88] P. M. Podsakoff, S. B. MacKenzie, and N. P. Podsakoff, "Sources of method bias in social science research and recommendations on how to control it," *Annual Review of Psychology*, vol. 63, no. 1, pp. 539–569, 2012.
- [89] N. Kock, "Common method bias in PLS-SEM," *International Journal of e-Collaboration*, vol. 11, no. 4, pp. 1–10, 2015.
- [90] Y. Liang, G. Qi, X. Zhang, and G. Li, "The effects of e-Government cloud assimilation on public value creation: an empirical study of China," *Government Information Quarterly*, vol. 36, no. 4, Article ID 101397, 2019.
- [91] C. Afonso, G. M. Silva, H. M. Gonçalves, and M. Duarte, "The role of motivations and involvement in wine tourists' intention to return: SEM and fsQCA findings," *Journal of Business Research*, vol. 89, pp. 313–321, 2018.
- [92] P. Mikalef and A. Pateli, "Information technology-enabled dynamic capabilities and their indirect effect on competitive performance: findings from PLS-SEM and fsQCA," *Journal of Business Research*, vol. 70, pp. 1–16, 2017.
- [93] M. A. Stanko, "Toward a theory of remixing in online innovation communities," *Information Systems Research*, vol. 27, no. 4, pp. 773–791, 2016.
- [94] Y. Liu, J. Mezei, V. Kostakos, and H. Li, "Applying configurational analysis to IS behavioural research: a methodological alternative for modelling combinatorial complexities," *Information Systems Journal*, vol. 27, no. 1, pp. 59–89, 2017.
- [95] C. M. Ringle, M. Sarstedt, and D. W. Straub, "Editor's comments: a critical look at the use of PLS-SEM in MIS quarterly," *Management Information Systems Quarterly*, vol. 36, no. 1, 2012.
- [96] C. Fornell and D. F. Larcker, "Evaluating structural equation models with unobservable variables and measurement Error," *Journal of Marketing Research*, vol. 18, no. 1, pp. 39–50, 1981.
- [97] J. F. Hair, C. M. Ringle, and M. Sarstedt, "PLS-SEM: indeed a silver bullet," *Journal of Marketing Theory and Practice*, vol. 19, no. 2, pp. 139–152, 2011.
- [98] W. W. Chin, "The partial least squares approach to structural equation modeling," *Modern Methods for Business Research*, vol. 295, no. 2, pp. 295–336, 1998.
- [99] T. Greckhamer, S. Furnari, P. C. Fiss, and R. V. Aguilera, "Studying configurations with qualitative comparative analysis: best practices in strategy and organization research," *Strategic Organization*, vol. 16, no. 4, pp. 482–495, 2018.
- [100] P. C. Fiss, "Building better causal theories: a fuzzy set approach to typologies in organization research," *Academy of Management Journal*, vol. 54, no. 2, pp. 393–420, 2011.
- [101] I. O. Pappas, S. Papavlasopoulou, P. Mikalef, and M. N. Giannakos, "Identifying the combinations of motivations and emotions for creating satisfied users in SNSs: an fsQCA approach," *International Journal of Information Management*, vol. 53, Article ID 102128, 2020.
- [102] C. Q. Schneider and C. Wagemann, "Standards of good practice in qualitative comparative analysis (QCA) and fuzzy-sets," *Comparative Sociology*, vol. 9, no. 3, pp. 397–418, 2010.
- [103] N. Del Sarto, D. A. Isabelle, and A. Di Minin, "The role of accelerators in firm survival: an fsQCA analysis of Italian startups," *Technovation*, vol. 90-91, Article ID 102102, 2020.
- [104] A. Urueña and A. Hidalgo, "Successful loyalty in e-complaints: FsQCA and structural equation modeling analyses," *Journal of Business Research*, vol. 69, no. 4, pp. 1384–1389, 2016.
- [105] T.-H. Jiang, S.-L. Chen, and J. K. C. Chen, "Examining the role of behavioral intention on multimedia teaching materials using FSQCA," *Journal of Business Research*, vol. 69, no. 6, pp. 2252–2258, 2016.

- [106] L. Gao and X. Bai, "A unified perspective on the factors influencing consumer acceptance of internet of things technology," *Asia Pacific Journal of Marketing and Logistics*, vol. 26, no. 2, pp. 211–231, 2014.
- [107] S. Choi, "The flipside of ubiquitous connectivity enabled by smartphone-based social networking service: social presence and privacy concern," *Computers in Human Behavior*, vol. 65, pp. 325–333, 2016.
- [108] J. Fang, Y. Shao, and C. Wen, "Transactional quality, relational quality, and consumer e-loyalty: evidence from SEM and fsQCA," *International Journal of Information Management*, vol. 36, no. 6, pp. 1205–1217, 2016.
- [109] J. Li, J. Wang, S. Wang, and Y. Zhou, "Mobile payment with Alipay: an application of extended technology acceptance model," *IEEE Access*, vol. 7, pp. 50380–50387, 2019.
- [110] D. D. Gunawan and K.-H. Huarng, "Viral effects of social network and media on consumers' purchase intention," *Journal of Business Research*, vol. 68, no. 11, pp. 2237–2241, 2015.
- [111] S. Wang, J. Wang, J. Li, J. Wang, and L. Liang, "Policy implications for promoting the adoption of electric vehicles: do consumer's knowledge, perceived risk and financial incentive policy matter?" *Transportation Research Part A: Policy and Practice*, vol. 117, pp. 58–69, 2018.
- [112] L. Qian and J. Yin, "Linking Chinese cultural values and the adoption of electric vehicles: the mediating role of ethical evaluation," *Transportation Research Part D: Transport and Environment*, vol. 56, pp. 175–188, 2017.
- [113] T. Zhou, "Examining mobile banking user adoption from the perspectives of trust and flow experience," *Information Technology and Management*, vol. 13, no. 1, pp. 27–37, 2012.
- [114] S. M. Ho, M. Ocasio-Velázquez, and C. Booth, "Trust or consequences? causal effects of perceived risk and subjective norms on cloud technology adoption," *Computers & Security*, vol. 70, pp. 581–595, 2017.
- [115] D. J. Kim, D. L. Ferrin, and H. R. Rao, "A trust-based consumer decision-making model in electronic commerce: the role of trust, perceived risk, and their antecedents," *Decision Support Systems*, vol. 44, no. 2, pp. 544–564, 2008.
- [116] R. Martins, T. Oliveira, and M. A. Thomas, "An empirical analysis to assess the determinants of SaaS diffusion in firms," *Computers in Human Behavior*, vol. 62, pp. 19–33, 2016.

## Research Article

# A Smart System for Sitting Posture Detection Based on Force Sensors and Mobile Application

Slavomir Matuska , Martin Paralic, and Robert Hudec

*Department of Multimedia and Information-Communication Technologies,  
Faculty of Electrical Engineering and Information Technology, University of Zilina, 01008 Zilina, Slovakia*

Correspondence should be addressed to Slavomir Matuska; [slavomir.matuska@feit.uniza.sk](mailto:slavomir.matuska@feit.uniza.sk)

Received 5 October 2020; Revised 2 November 2020; Accepted 5 November 2020; Published 19 November 2020

Academic Editor: Ondrej Krejcar

Copyright © 2020 Slavomir Matuska et al. This is an open access article distributed under the Creative Commons Attribution License, which permits unrestricted use, distribution, and reproduction in any medium, provided the original work is properly cited.

The employees' health and well-being are an actual topic in our fast-moving world. Employers lose money when their employees suffer from different health problems and cannot work. The major problem is the spinal pain caused by the poor sitting posture on the office chair. This paper deals with the proposal and realization of the system for the detection of incorrect sitting positions. The smart chair has six flexible force sensors. The Internet of Things (IoT) node based on Arduino connects these sensors into the system. The system detects wrong seating positions and notifies the users. In advance, we develop a mobile application to receive those notifications. The user gets feedback about sitting posture and additional statistical data. We defined simple rules for processing the sensor data for recognizing wrong sitting postures. The data from smart chairs are collected by a private cloud solution from QNAP and are stored in the MongoDB database. We used the Node-RED application for the whole logic implementation.

## 1. Introduction

The development of informatization currently brings new health risks. People move much less and work more often on the computer. Long-term sitting harms the spine and causes chronic problems that need long-time therapy [1]. Diseased people have a significant impact on office productivity. Our motivation is to help people pay attention to their health and proper sitting in addition to work. Adopting the correct sitting position is essential for maintaining good posture and a healthy back and spine. Sitting with a straight back and shoulders not only will improve a person's physical health but also can make them feel more confident. Good posture means that the parts of a person's body are correctly aligned and supported by the right amount of muscle tension.

Haynes [2], in his study, looked at the effect of sitting position on typing speed and overall well-being in people with chronic back pain. He used a unique positional wheelchair system with the possibility of position fixation and tested the efficiency of office work at varying in 6

different writing positions. The presented results showed that sitting posture has a definite impact on typing speed and user comfort.

There are several ways to monitor people's postures. Tlili [3] made an overview of systems on sitting posture monitoring. According to the principle of how to obtain this information, the systems can be divided into three main categories based on the following:

- Computer image processing
- Wearable clothing with sensors
- Measuring the load distribution on some form of substrate

Sathyanarayana [4] conducted a general review on the topic of patient monitoring based on image processing and made an overview of the algorithms used and the area of intentions that the individual systems addressed. He pointed out the limits of such systems, especially with regard to the patient's distance from the camera. Obdržálek [5] used a

Microsoft Kinect camera to recognize human activity and rehabilitation. His research focuses on monitoring elderly humans. He modeled 6 different exercises and consequent positions, of which 4 of them were in sitting poses. He used the properties of Kinect to skeletonize the figure from the stereo image. Using a video system, Kuo [6] monitored the correct posture of the head against the body and spine in the sitting position. Placing the reflective markers on the human body around the head, neck, and spine simplified video signal analysis. The markers detection provides data for further estimates of the angles of curvature of the spine in the neck and cervical spine.

Systems using wearable sensors or intelligent clothing have several advantages over image-based systems. They are usually easily portable and independent of the angle of view like camera systems. The sensor either is part of the clothing or can be easily attached to the clothing. Other types of sensors can even be placed directly on human skin. Ailneni [7] used a wearable posture correction sensor to improve posture while sitting. The sensor detects postures and gives the user feedback in the form of vibrations. He claims that he can improve the posture of a man working in the office in about 25 days. The sensors are located on the head and the neck; the system reacts to incorrect head-neck position by light vibrations. Bismas [8] proposed the 3 systems for monitoring health and wellness through wearable and ambient sensors. The system is focusing on the activity monitoring of older people with incipient dementia. He designed a comprehensive sensor system that collects data from several sources located not only on the wearables but also around the living area. Analyzed data from the sensors can manage processes, for example, automatic help calling.

Otoda [9] designed the Census sensory chair, which can classify 18 types of sitting positions. The chair has 8 accelerometers. The author states an 80% success rate of sitting position classification. Zemp et al. [10] used several sensors. They equipped an ordinary office chair with their custom module for motion detection. The module consists of an accelerometer, gyroscope, and magnetometer. Comparison to [9], they placed this module on the back of the chair and placed several pressure sensors on the backrest. These sensors respond by changing the resistance depending on the pressure. It is interesting in this work that they tried to analyze the measured data with various pattern recognition algorithms. They compared the following algorithms: Support Vector Machine (SVM), Multinomial Regression (MNR), Boosting, Neural Networks (NN), Radial Basis NN, Random Forest (RF), and their various configurations. The combination of 3 methods, Boosting, NN, and RF, has reached in this experiment the best results. Huang [11] developed a piezoresistive sensor matrix with a thickness of 0.255 mm, which can monitor the way of sitting by a noninvasive method. The sensor field consists of two layers of polyester film.

The next section will deal with the concept of the whole system and how to implement it in the office room. The consequent section deals with the description of the microcontroller hardware solution implemented in the chair. In Arduino Software section, we describe the concept

of the application solution of the microcontroller and its communication with the server. We will also focus on the server side based on the QIoT Suite cloud solution. QIoT features MQTT gateways, Node-RED application, and MongoDB database. In this section, we will describe the carried out experiments and explain the algorithm for the detection of sitting posture correctness. The last part of the system is a client application. It is a smartphone application for communication with a smart chair. It provides a fundamental interaction with the smart chair. We describe here the concept of the communication protocol between the client and the server.

## 2. System Concept Proposal

In our system proposal, we were focusing on creating a practical smart system for sitting posture detection in the office. Our primary goal is to design a system, which could be easy to implement in any office space where the person does not have to use the same chair every day. Figure 1 illustrates the proposal of the system concept. The overall system consists of a variable number of chairs, the cloud server, and client stations, smartphones. Each chair has an electronic device based on the Arduino microcontroller, external battery power source, and six flexible force sensors. The network-attached storage from QNAP holds the cloud solution. It features the Message Queuing Telemetry Transport (MQTT) broker for communication, Node-RED for the logic, and Mongo database for data storage.

The daily routine for the people working in our smart office should be as follows:

The person chooses a free chair in the office and sits down. The Arduino hardware will wake up from sleep at this point and connect to the cloud.

The person turns on the mobile application and logs in to the chair. Each smart chair has an identification number to login. The information about the sitting posture with additional data is displayed in the smartphone application.

After finishing the work, the person logs out from the chair. Finally, you can view the daily report.

The following sections describe the individual parts of the system in more detail.

## 3. Smart Chair Hardware Design

To make a smart chair capable of measuring the pressure of the sitting person, it was necessary to embed the force sensor into the regular office chair. The six single-zone force-sensing resistors FSR402 are used to measure the force. The resistance of the sensors decreases with increasing force. Measured resistance changes from tens of kOhm to hundreds of ohms. The sensor does not need calibration before or between the measurements. The seat is equipped with 4 sensors and the backrest with 2 sensors. The appropriate sensor positions are found empirically. The sensors are under the lining, so they are not visible to the user. We use the NodeMCU microcontroller based on the Arduino board



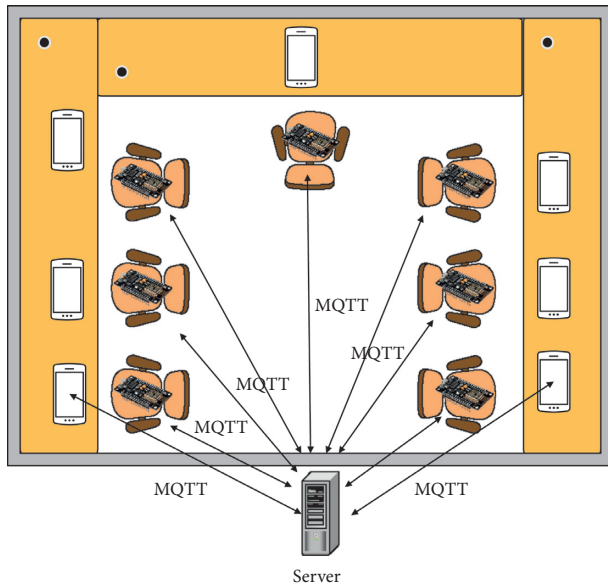


FIGURE 1: The system concept proposal.

to collect data from sensors. The communication via WiFi with the server is provided by the module ESP8266. The main advantage of this board is that it can be directly connected to the WiFi and processes the data from sensors at the same time from one source code. The board supports up to 16 general-purpose input-output pins. Only one pin can work as the analog input. Figure 2 represents the hardware schematic of NodeMCU.

The voltage divider with a 22 kOhm resistor measures the FSR 402 resistance. Since there is only one analog input available, we have to solve the fast switching between the sensors during the measurements. We achieved this by selecting a particular sensor with digital output from NodeMcu. The output pins from D0 to D5 were selecting the appropriate sensor.

**3.1. Arduino Software.** Figure 3 shows the NodeMCU flowchart diagram. The start begins with the definition of variables and their initialization. The most important variables are the WiFi network name (SSID), WiFi password, cloud server IP address, and MQTT credentials. Then the general input/output pins, serial, and WiFi communication are initializing. The first thing that the program does is connecting to the WiFi network. If the initial login fails, the system waits for 5 seconds and then retries the operation until the successful login.

The next step is building a connection with the NodeMCU. It connects to the MQTT broker using predefined credentials. The MQTT protocol communication is provided by an external library Adafruit MQTT Library ESP8266. To build the MQTT connection, we require the client instance of the class `Adafruit_MQTT_Client`. This client connects to the MQTT broker. We have to create an additional object for receiving the responses from the broker. The instance of the class `Adafruit_MQTT_Subscribe` provides such an interface. For sending data, we need an

instance of a class `Adafruit_MQTT_Publish`. The consequence loop checks if the MQTT connection is still live. If the connection is active, the pointer to the object from class `Adafruit_MQTT_Subscribe` is created for fetching the new data on the subscribed channel. The channel identifier for reading commands is as follows: `"qiot/things/Matuska/chairs/ch" + String(CHAIR_ID) + "/sendingEnabled"`, where `CHAIR_ID` is the smart chair identification number. On the cloud side, the MQTT broker sends the chair command using this channel. When the user connects to the smart chair using a smartphone application, the start command is issued on this channel and the NodeMCU starts the measurement and sends the data. After the user logs out, the stop command is issued from the broker. Because there is only one analog input, the resistance measurement is done in these steps:

Set up the DX as output and toggle it to the high value.

Read the analog value from pin A0.

Calculate the force value from measured resistance. The calculated force represents the pressure, and its value is in the range between 0 and 15.

Toggle to a low value and set DX as an input pin.

These steps are looping per each sensor. Afterward, the string in JavaScript Object Notation (JSON) format is prepared and published to the broker using `Adafruit_MQTT_Publish` object. The data are published every 1 second. If there are no active measurements incoming in time, we need to send a periodical ping command to keep the connection with MQTT alive. Without this ping, a link would break down after some time if no communication took place.

#### 4. Cloud Solution and QIoT

The central unit of our smart system is the NAS from QNAP [12]. This unit runs all programs and cloud services that provide connectivity, chairs management, data storage, and data evaluation. There are two primary services:

QIoT Suite.

MongoDB [13].

The QIoT Suite is an application, which could be installed directly from the application center on NAS. QIoT Suite integrates different services, which are necessary to provide a complex solution in the IoT world, into one application. It includes the MQTT broker [14], Node-RED, and Freeboard and supports multiple protocols and dashboards.

MongoDB is a popular, general-purpose, document-based, distributed database, which is common in a cloud solution and IoT world. All data are stored in MongoDB for further evaluation. Figure 4 shows the flowchart of the system functionalities.

The smartphone application also uses the MQTT protocol to communicate with the QIoT Suite server. The communication is processed via the Node-RED application. Both sides are using the MQTT communication protocol to exchange messages with the QIoT. NodeMCU sends the



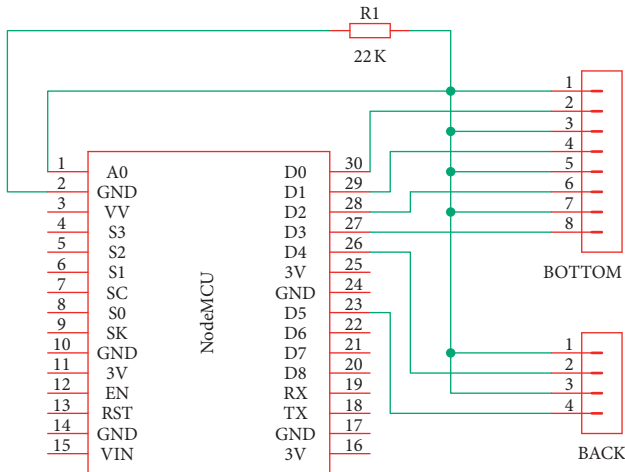


FIGURE 2: Hardware schematic with NodeMCU.

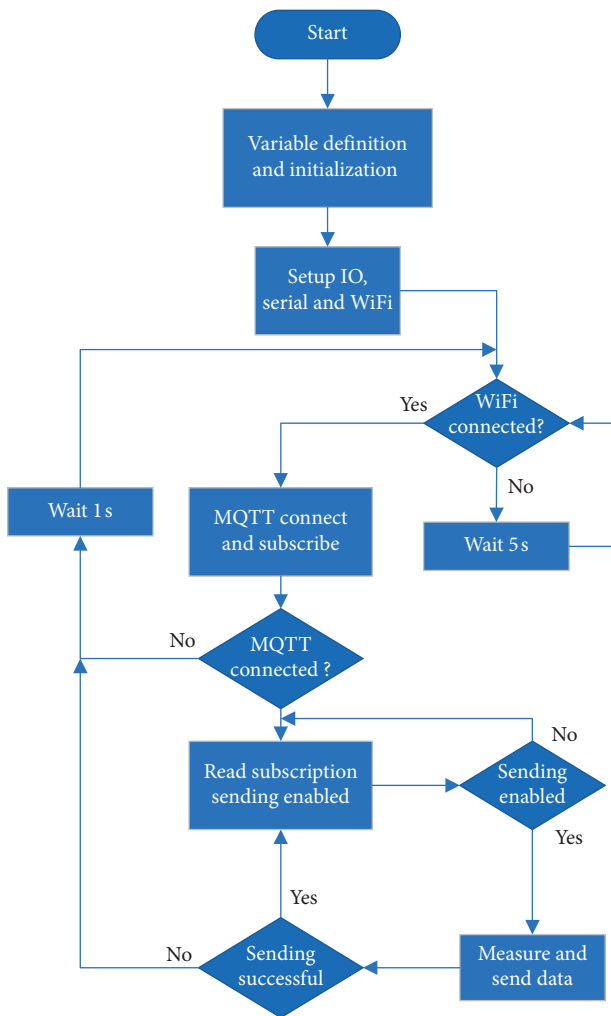


FIGURE 3: NodeMcu source code flowchart.

measured data to the cloud. Data are processed via Node-RED, stored into MongoDB, and then sent to the mobile application. More details and communication descriptions of the mobile application will be in Mobile Application section.

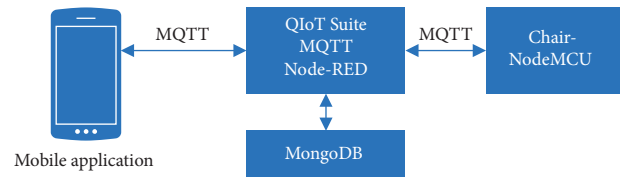


FIGURE 4: The system communication chain.

**4.1. QIoT Suite Lite.** QIoT Suite Lite is a complete and practical IoT private cloud platform for building and managing IoT applications. QIoT Suite leverages popular tools like Node-RED and Freebord to create an IoT environment easily and helps in efficient IoT development cases. It supports multiple protocols such as MQTT, Hypertext Transfer Protocol (HTTP), and Constrained Application Protocol (CoAp). It allows us to simply create multiple dashboards and quickly connect them with multiple sensors. QIoT Suite also supports MQTT's and HTTP's security layers on the protocol for secure network connections. The suite was designed to shorten the IoT application design lifecycle and its deployment. By default, the suite provides a quick setup wizard to assist in creating IoT applications. It is also possible to use prepared codes of Python or Node.js on starting kits such as Arduino Yun, Raspberry Pi, Intel Edison, or MTK LinkIt Smart 7688. For using other kits or use a custom source code database, it is necessary to create custom Thing. The QIoT home screen is shown in Figure 5.

The left side of the screen provides a link to other pages. The mainframe of the screen provides links to IoT applications, Things and Things types, and their total number. The quick setup wizard is also accessible from the main screen. It is possible to create IoT applications using a quick setup wizard or custom step by step. The custom IoT application requires at the beginning only identification name. The core application is complete after the confirmation. The details of our smart IoT system application for sitting posture detection are shown in Figure 6.

There are three tabs on this screen, providing links to application dashboard, rule engine, and Things. Figure 6 shows the table with the active Things for this application. There are two different types of Things in our application:

General Thing type for mobile applications

The chair types

The general type is only one in the system where the mobile application uses this credential to log in to the MQTT broker. The second type is for the chairs. Each chair in the system needs to have a unique record in Things. In the QIoT Suite, each Thing has its topic on the MQTT broker created automatically with the Thing creation. The topic looks like "qiot/things/Matuska/chairDuino1," where chairDuino1 is the Thing name. The Representational State Transfer (REST) application programming interface (API) is also available for each Thing to fetch the data using the HTTP protocol. Each Thing can define one or more "resources." These resources could be sensors, peripheral, switch, or another data channel/state that needs to be transmitted or received. Adding a resource means creating the data channel ID

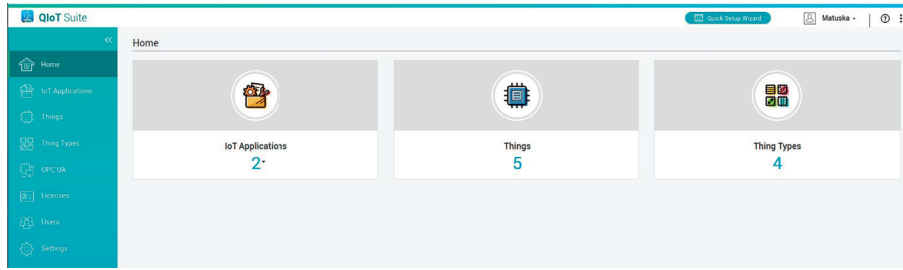


FIGURE 5: The QIoT home screen.

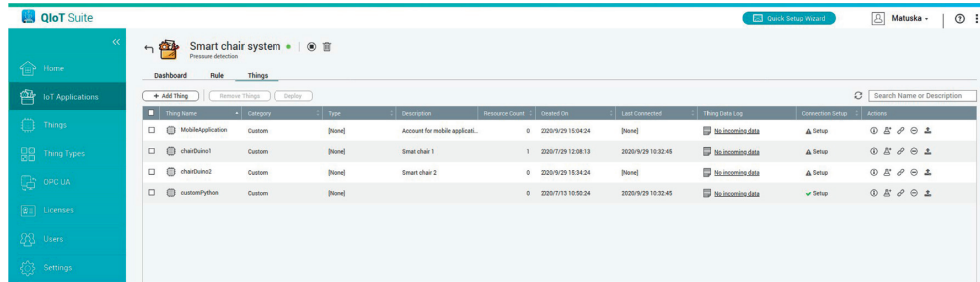


FIGURE 6: The details of the IoT application.

(MQTT → topic, HTTP, and CoAP → URL) to connect with QIoT Suite Lite. Using QIoT Graphical User Interface (GUI), it is possible to generate JSON configuration file different connection types (MQTT, HTTP, or CoAP) for particular Thing. This file can be used with prepared codes to accelerate and simplify the Thing deployment. The example of this file is shown as follows:

```
{
  "username": "generated_username",
  "myqnapcloudHost": "Not Available",
  "clientId": "chairDuino1_1601447263",
  "host": [
    "IP address"
  ],
  "password": "generated_password",
  "port": MQTT_port,
  "resources": [
    {
      "description": "",
      "datatype": "String",
      "resourceid": "pressureData",
      "topic": "qiot/things/Matuska/chairDuino1/pressureData",
      "resourcename": "Tlakove senzory",
      "resourcetypename": "Custom Sensor(String)",
      "unit": "bar"
    }
  ]
}
```

The main advantage of the resources is that they could be implemented in a few steps as a dashboard gadget and are automatically stored in the MongoDB database if this database is configured. The resource can be imported to the dashboard using the rule engine QBroker. There are two methods to use QBroker:

- Importing data from the resource
- Importing data from the rule engine

After a few steps, the resource value will appear on the dashboard. The dashboard supports different kinds of widgets, such as text, gauge, sparkline, pointer, indicator, action widget, or QIoT historic chart. The third tab is the rule engine based on Node-RED and features a flow editor to simplify IoT development. There are four customized QIoT nodes:

- QDashboard: it provides a live data API endpoint
- QBroker (in): it receives Thing data
- QBroker (out): it transmits Thing data
- QHistoricData: it retrieves the maximum, minimum, and average values stored in the database for defined resources

4.2. Node-RED Application. The Node-RED application implements the logic part of the smart system for sitting posture detection on the private cloud platform. Such an application is usually splitting into the program Flows. There are two main flows in our solution:

- The flow for pressure data processing
- The flow for chairs and mobile application management

Figure 7 shows the schematic design of flow for chairs and mobile application management.

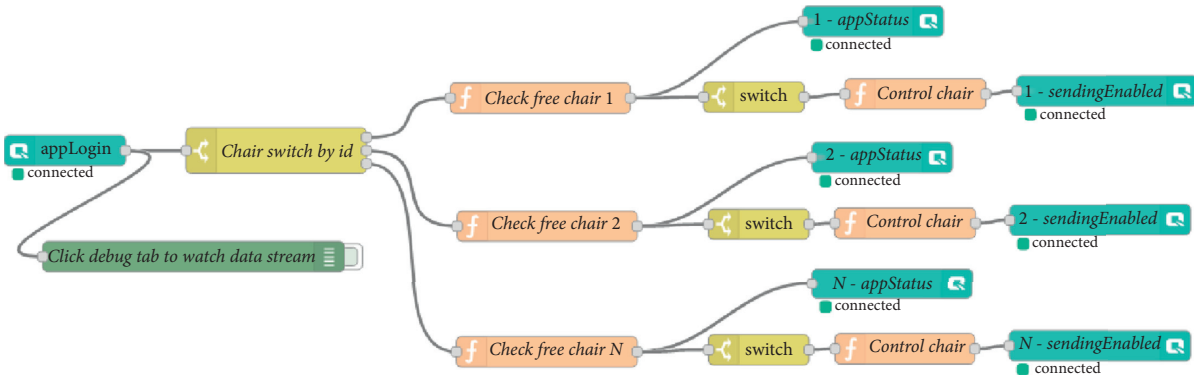


FIGURE 7: Node-RED flow for chairs and mobile application management.

The flow starts with the QBroker in node. This input node listens on the topic “appLogin.” The purpose of this flow is to manage chairs and mobile applications and there is only one common input node for all applications and applications in this flow. All data coming through the QBroker node have to be in JSON format. The example of the expected JSON response data is as follows:

```
{
  "chairId": 1,
  "query": "login"
}
```

The chairId specifies the identification number of the chair. The tag “query” represents the performed action. The action could be “login” or “logout” action to the chair. The message is routed in the switch node depending on the chair identification number “chairId.” Then the system checks if the selected chair is unoccupied. The function for checking the chair state adds an attribute to the message about the operation success. The message with the response is then sent to the mobile application via the QBroker out node on the topic “chairs/ch1/appStatus.” The message is also router via another switch, which evaluates if the added attribute is true or false. If the added attribute is true, the command message is sent to the chair using the topic “chairs/ch1/sendingEnabled.” The sent message contains a command to start or stop sending the pressure data. There are two QBroker out nodes for each chair. If there is a request for adding a new chair to the system, it is necessary to copy the whole block for the chair and change the topic name according to the chair identification number. This could be done easily with a few steps. Figure 8 shows the flow for pressure data processing.

The flow starts with the QBroker in the node. This input node listens on the topic “chairPressureData.” The purpose of this flow is to collect, evaluate, and propagate the chair pressure data. There is only one common input node for all chairs in this flow. Only chairs publish the data on this topic. The example of sending data by “publish” command is as follows:

```
{
  "chairId": 1,
```

```
  "data": [ "6.04", "6.21", "7.80", "6.75", "2.21",
            "1.35" ]
}
```

The next node “Sum pressure data” sums the pressure data and adds the message timestamp in Unix format. The message is routed in the switch node based on the chair identification. The next node “Chair ID statistic” is the most important in the system. In this node, the function implements the whole logic for bad sitting posture detection. The QBroker out is implemented for each chair with the topic “chairs/ch1/appData,” where ch1 is chair identification number. The WebSocket node is also implemented with URL “/ws/ch1/appData.” The same message is sent via MQTT QBroker and WebSocket. Websocket is implemented because we expect further communication with the client application. The sent message structure is as follows:

```
{
  "chairId": 1,
  "data": [ "5.63", "5.70", "5.61", "5.51", "2.64", "5.71" ],
  "sum": 30.80,
  "actual_time": 1601455127,
  "avg": 5.612500000000001,
  "deviation": 0.00461875,
  "chdata": {
    "actual_sitting_state": "green",
    "avg_deviation": 0.007027499999999825,
    "avg_back_deviation": 2.7907049999999999,
    "chair_id": 1,
    "actual_sitting_time": 45,
    "back_data_present": 1,
    "long_sitting": 0,
    "duration": 1358,
    "start_time": 1601453768.362,
    "sitting_history": [
      { "timestamp": 1601455120.569, "sitting_status":
1},
```

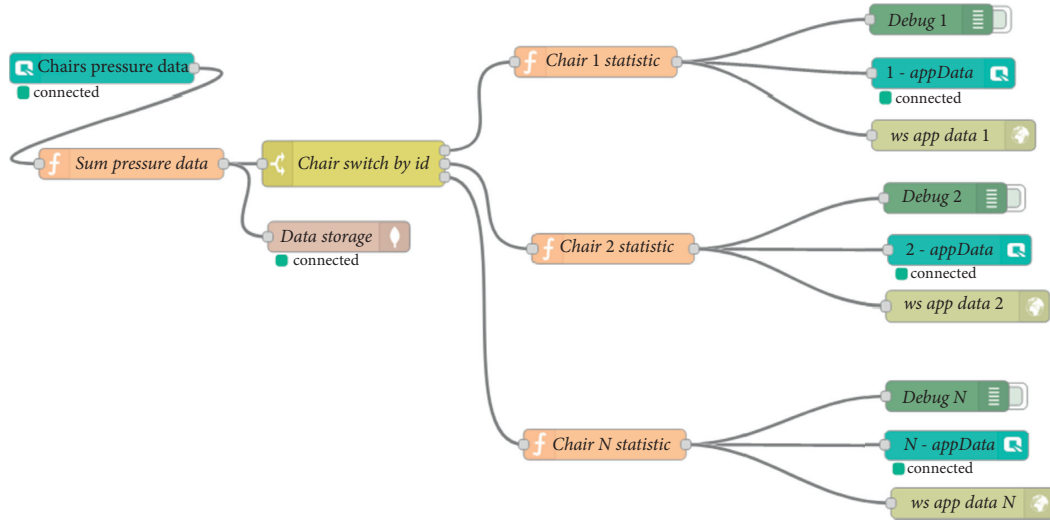


FIGURE 8: Node-RED flow for pressure data processing.

```

    { "timestamp":1601456131.239, "sitting_status":
0},
    { "timestamp":1601456822.133, "sitting_status":
1}],
    "actual_sitting_status":1
}
}

```

Here, “chairId” is the chair identification number, “data” contains the pressure values from sensors, “sum” is the sum of the pressure values, and “actual\_time” is the message timestamp. The “avg” stands for actual average and “deviation” is the actual standard deviation of values from four bottom sensors. JSON object “chdata” contains information about sitting posture for the mobile application. Attributes meaning is explained in Table 1.

The function starts with variable initialization. If this function is executed for the first time after the user was logged in, the object “chdata” is created with initial values. The object contains all necessary variables for statistical computations and information about sitting posture propagated to the mobile application. The function accumulates the pressure data from the chair. The function starts to recalculate statistics as soon as it collects data in the last 10 measurements. The last 10 measurements are used to detect a seated person. The longer time is suppressing the false detection of a state change of sitting or standing. For the computation of the standard deviation, only the last 5 measurements are used. Deviations are calculated separately for back sensors and separately for seat sensors. These deviations are the primary features of the incorrect seating position detection algorithm.

For the sitting poses’ detection by the proposed method, it was necessary to determine empirically 3 threshold values of deviation. These threshold deviations are computed from the sensors in the seating area. In the seating part, we use Orange Deviation Threshold ODT=3.0, Red Deviation Threshold RDT=6.8, and Orange Conditional Deviation

Threshold OCDT = 0.8. A summary of the rules is given in Table 2.

Based on our previous work [15] and the findings presented in [16, 17], we defined 9 different sitting postures for further examination. Figure 10 shows the defined sitting postures.

The sitting position number 1 is considered as a correct sitting posture. The positions 2–5 represent the orange state, and 6–9 are the red state. To find out the threshold values, we carried out experiments to measure the standard deviation for each posture. Twelve test subjects participated in this experiment.

For each subject, we recorded 10 measurements for each posture. Then we calculated the average standard deviation for each pose. The next step was the average calculation for each posture. Afterward, we determined the 3 threshold values based on the collected data. Table 3 contains all obtained and calculated data.

When new data arrives, unnecessary data is released using the first in-first out method (FIFO). If at least one amount exceeds the threshold in a series of 10 measurements, it is considered as continuous seating. The mechanism for detecting the presence of a seated person seeks to eliminate false detections of leaving the chair. The feature to compute is the sum of pressures from each sensor. If this  $\sum(S_i) < 1$  for 10 consecutive measurements, leaving the chair is detected. Thus, short standing up or reaching for the object will not be considered as leaving the chair. The system cumulatively calculates the continuous sitting time and, after exceeding the time threshold, which is currently set to 1 hour, sends the flag for long sessions and changes the status to red.

## 5. Mobile Application

The smartphone application serves as client access to the smart chair measurements. In the first step, the user must connect to the MQTT server. The user should fill the

TABLE 1: Description of chair data attributes.

Attribute	Explanation	Type/states
actual_sitting_state	Information about sitting posture.	String {green, orange, red}
avg_deviation	Average standard deviation from the last five measurements for four bottom sensors.	Float
avg_back_deviation	Average standard deviation from the last five measurements for two back sensors.	Float
actual_sitting_time	Current uninterrupted sitting on the chair in seconds.	Integer
back_data_present	It indicates if there are present valid data from back sensors.	Integer {0, 1}
long_sitting	It indicates long uninterrupted sitting on the chair.	Integer {0, 1}
Duration	The elapsed time in second from the login.	Integer
start_time	Login time.	Unix timestamp
sitting_history	History of the sitting states with the Unix timestamp, when the changes occurred.	Array of objects
actual_sitting_status	It indicates if there is somebody sitting in the chair.	Integer {0, 1}

Object "chdata" is added to the message in the node "Chair 1 statistic." Figure 9 describes the function node flowchart.

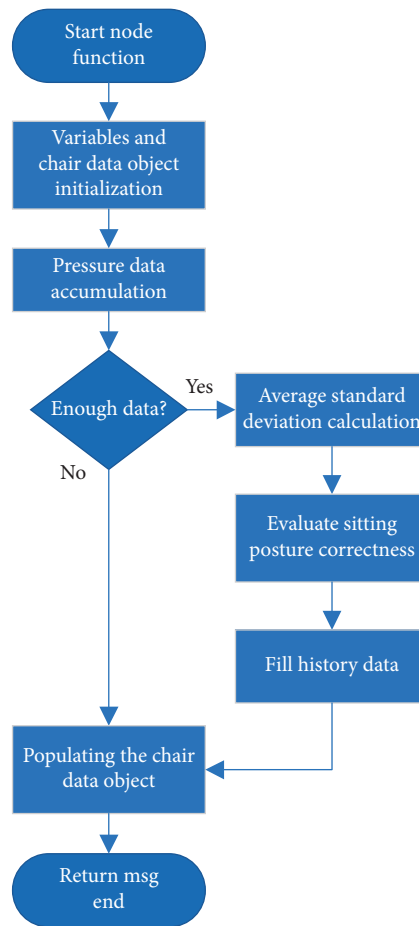


FIGURE 9: Sitting posture evaluation flowchart.

TABLE 2: Rules for the incorrect seating detection algorithm.

Sitting state	Rules
Green	avg_deviation < ODT && back data presented
Orange	(avg_deviation > ODT && avg_deviation < RDT) or (avg_deviation > ODDT && avg_deviation < ODT && back data NOT presented)
Red	(avg_deviation > RDT) or (avg_deviation > ODT && back data NOT presented)





FIGURE 10: Tested sitting posture [15].

TABLE 3: Average standard deviation for each sitting posture.

Posture subject	1	2	3	4	5	6	7	8	9
1	0.06	1.2	1.15	7.2	6.2	12.3	13.31	11.03	10.45
2	0.2	0.4	0.24	3.62	2.27	14.03	12.92	12.43	12.3
3	0.05	0.6	4.53	1.83	1.3	9.06	8.29	11.83	12.72
4	0.14	0.76	1.78	0.79	2.12	4.02	11.23	0.65	1.53
5	0.19	0.54	8.42	1.74	1.27	8.9	9.4	10.84	11.87
6	0.06	0.23	0.32	1.56	3.13	8.46	4.81	1.76	2.5
7	0.24	0.57	4.15	0.95	1.73	9.37	1.49	4.96	7.01
8	0.37	1.99	9.95	15.93	11.65	11.15	7.96	8.99	9.61
9	0.3	0.87	0.64	10.48	6.41	13.02	9.53	9.52	11.08
10	0.28	0.86	13.52	4.72	2.3	13.6	1.87	12.39	13.14
11	1.27	1.2	0.18	4.25	0.96	9.84	0.8	5.93	0.75
12	0.03	0.98	0.21	1.84	1.83	1.12	0.77	2.04	2.55
Average	0.266	0.850	3.758	4.576	3.431	9.573	6.865	7.698	7.959
STDEV	0.335	0.467	4.534	4.586	3.152	3.840	4.729	4.421	4.820

connection form with the server address, communication port, user login, password, and chair identification number. The login activity is shown in Figure 11 with filled connection data.

The data from multiple chairs are stored on one server. The successful connection to the MQTT server is followed by automatic login to the selected chair. If the smart chair is occupying another person or chair is inactive at the time, in such a case application is connected to the MQTT server but

has no connection to the chair. Figure 11(b) is displaying the state when the MQTT link is open, but the chair is still not accessible. The current active client must release the chair to make further connections. The client application allows only one active connection per chair. If login to smart chair is successful, the full chair image appears with its measured parameters. The current sitting position is represented by the colors. Additional sound alerts signalize poor sitting postures. The color representation is as follows:

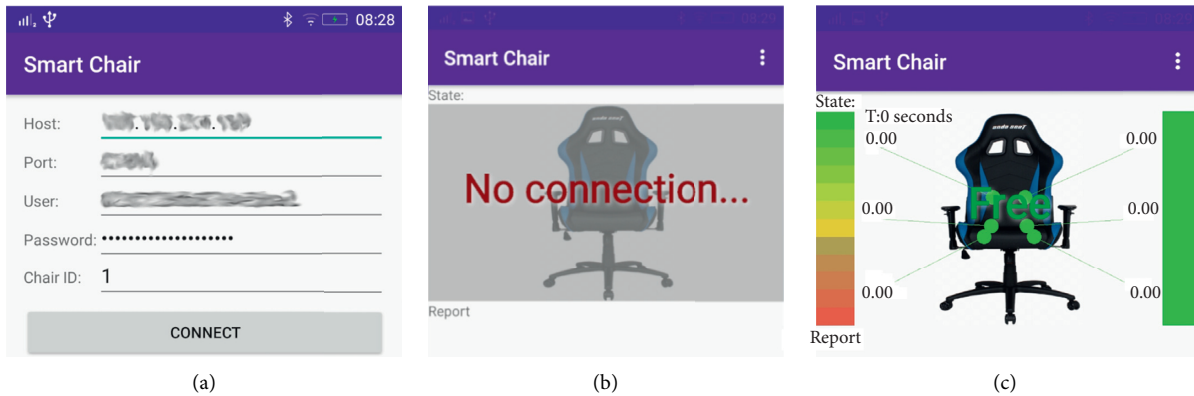


FIGURE 11: The connection to the MQTT server and login to the chair: (a) Login activity, (b) succeed connection to MQTT server, and (c) succeed logging to chair.

Green: the client is sitting in the correct position with an evenly distributed load. The unoccupied smart chair is also green, with an additional title “Free,” as shown in Figure 11(c).

Orange: the participant is sitting, but his weight is not distributing evenly.

Red: the participant is sitting in an unhealthy sitting position. This position is signaling an excessive load on one side. This condition may also occur when the client sits continuously for more than an hour.

The first color scale panel to the left of the chair represents the measuring range, in Figure 12, where the green color is the lowest pressure, and the red is the highest pressure. The second single color panel to the right of the chair picture represents the basic sitting state {green, orange, or red}. The circles represent sensor positions, and their color depends on the pressure, following the color palette. In the middle is a symbolic representation of a chair. The numbers (no units) are pressure measurements that express the intensity of the load. The color of individual points is adjusting according to the current load. Figure 12(a) represents an evenly distributed body weight on the pressure sensors following the orange state. After transferring the scale to one side of the chair, the system detects the incorrect position of Figure 12(b), seating condition (condition orange). In the orange state, the application plays a short quiet tone (“elevator tone”). It unobtrusively alerts the user to the wrong sitting position. In case when the user load distribution is extreme, the state changes to the red state. The red state is signaling by an annoying audio signal (alert tone). The user has the option to turn the application of or move his body to a healthy sitting position to stop the annoying alarm. The bottom of the screen reports different events. The report can hold a history of sitting states, variety events, logging and connection issues, and debug information.

Figure 13 shows the schematics of the mobile application and its communication with the MQTT server. The design of modules for communication with the MQTT server is considered to be a reusable code for further applications. The

login activity is the first screen that the user can see. He passes the login data to the MqttChair communication module. This module uses the MQTT communication protocol services with the help of the “eclipse/paho.mqtt.android” library. The inputs to the module are the login data to connect the server and the necessary user and chair identification. First, it ensures the establishment of a connection with the MQTT server. The entire communication takes place asynchronously since it is event-controlled. After successfully connecting to the server, it subscribes to the subscription, whether the chair is available SUBSCRIBE\_LOGIN. Subsequently, a request to join the PUBLISH\_LOGIN chair is published. Availability LOGIN\_ACK returns information about whether the smart chair is occupied by another participant. If the smart chair is unoccupied, the module MqttChair subscribes to collecting chair data using SUBSCRIBE\_DATA. The new data is received via the call-back function.

The communication ends when the user requests a logout action, or the connection is unexpectedly broken. The standard way is to send the message PUBLISH\_LOGOUT and consequently disconnect from the MQTT server. The response to logout action is an acknowledgment of LOGOUT\_ACK. The communication with the server is user terminated by sending a message DISCONNECT and subsequently confirmed by DISCONNECT\_ACK. The MQTT module provides an interface with two listener call-back functions. The first function onReport() returns a message designed to monitor traffic and generate events. The second function onDataReceived() provides data received from the smart chair. To transfer chair data internally, the ChairData object is used. The most user interaction is performed by the Monitor Activity. This activity represents the main GUI for the user, sends commands to the MqttChair module, and receives data and messages using MqttChair listeners. It provides basic functionality for user login and logout actions. The Monitor Activity is also holder place for the ChairView widget. The ChairView widget is a module for displaying smart chair data. The input is the instance of the ChairData object. The document-view

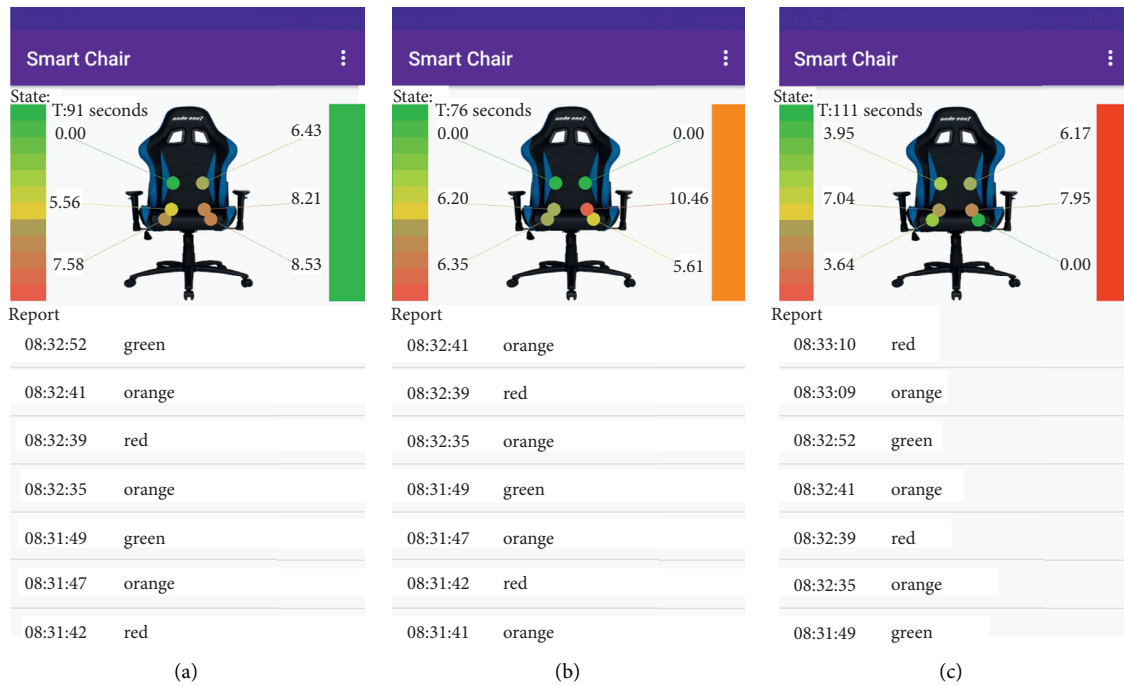


FIGURE 12: The examples of sitting states: (a) green (standard sitting), (b) orange (bad sitting), and (c) red (heavy load for the backbone).

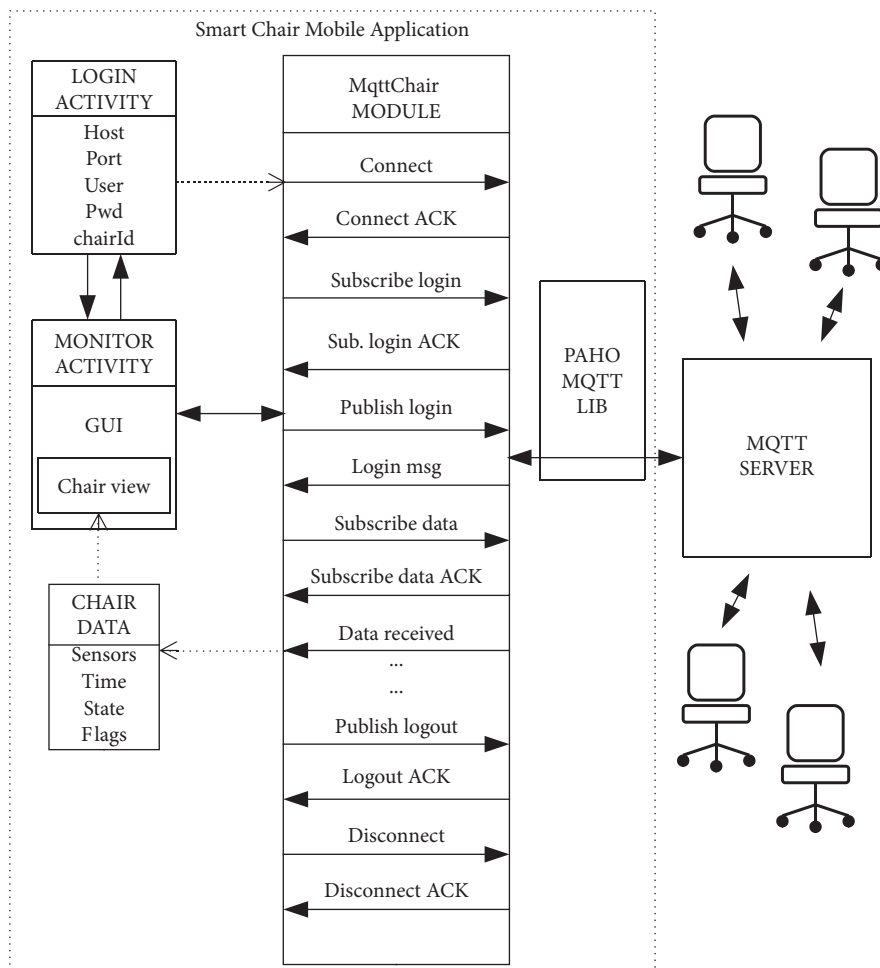


FIGURE 13: The communication between the mobile application and MQTT server.

architecture system is used, where the document is represented by the ChairData object, and the view is displayed by the ChairView module.

## 6. Discussion

The most crucial part of our proposed smart chair is the hardware uptime without the need for a recharge. During the testing, we used the external power bank with a capacity of 4000 mAh as the power source. With this external source, our hardware can run up to 48 h of active measurement. For most of the day, the chair is not occupied and the NodeMCU could enter the sleep mode and wake up only when someone is sitting on the chair. This will theoretically improve uptime up to 12 days and thus can be used in a real application. The other issue is implementing the force sensors into the chair. This process is rather difficult and the implementation itself takes some time. On the other hand, if we want to produce the smart chair in numbers, it will be necessary to create a more automated way. Software deployment on the server side is easy and straightforward and while it can run on as cheap hardware as Raspberry Pi, it is also cost-effective. Overall, the proposed system is easy to implement.

The user receives the notifications about the sitting posture correctness on the mobile application on Android. For Apple users, it is necessary to develop an application for iOS or use the multiplatform framework to write one application for both platforms with a common codebase. Using the information from the application users can adjust their sitting customs and improve their health and well-being easily.

## 7. Conclusions

This paper presents a smart IoT system for sitting posture detection based on force sensors and mobile applications. Six flexible force sensors, two on the backrest and four on the bottom seat, were embedded in the office chair. NodeMCU board was used to measure the sensor's resistance and sends the data to the cloud using the MQTT protocol. The data are stored and evaluated on the cloud using Node-RED and MongoDB. The user can see the information about sitting posture correctness and other pieces of detailed information in the mobile application. Our goal was to create simple rules to detect correct sitting posture in the term of minimal computation power requirements. We defined 9 sitting postures and carried out experiments on 12 people to identify the rules. The standard deviation from the bottom seat sensors shows a strong dependence on sitting postures. The calculation of the standard deviation is not hard for computing power. Based on our observation, we divided the sitting posture correctness into three groups, namely, green, orange, and red, and defined the three threshold values. We used these threshold values for the evaluation of the sitting posture into one of the three groups. The system also calculates the time of sitting without a break and informs the user in the case of long-term continuous sitting. We deploy our solution on the network-attached storage from QNAP. But because of the evaluation algorithm simplicity, it is

possible to run our smart system on cheap hardware such as Raspberry Pi with only minimal changes. The QIoT specific gateway must replace it with a regular MQTT gateway. It is also necessary to install services like Mosquitto MQTT broker, standalone Node-RED application, and optional MongoDB manually on Raspberry Pi.

## Data Availability

The source codes are available upon request to the corresponding author.

## Conflicts of Interest

The authors declare that they have no conflicts of interest.

## Acknowledgments

This work was supported by the European Union's Horizon 2020 Research and Innovation Program under the Marie Skłodowska-Curie Grant agreement no. 734331 and by the project "Competence Centre for Research and Development in the Field of Diagnostics and Therapy of Oncological Diseases," ITMS: 26220220153, cofunded from EU Sources and the European Regional Development Fund.

## References

- [1] Vos, "GBD 2015 Disease and Injury Incidence and Prevalence Collaborators, "Global, Regional, and National Incident, Prevalence, and Years Lived with Disability for 310 Diseases and Injuries, 1990-2015: A Systematic Analysis for the Global Burden of Disease Study 2015," *The Lancet*, vol. 388, no. 10053, pp. 1545-1602, 2016.
- [2] H. Scott and K. Williams, "Impact of seating posture on user comfort and typing performance for people with chronic low back pain," *International Journal of Industrial Ergonomics*, vol. 38, no. Issue 1, pp. 35-46, 2008.
- [3] F. Tlili, R. Haddad, Y. Ouakrim, R. Bouallegue, and N. Mezghani, "A Survey on Sitting Posture Monitoring Systems," in *Proceedings of the 2018 9th International Symposium On Signal, Image, Video And Communications (ISIVC)*, pp. 185-190, Rabat, Morocco, November 2018.
- [4] S. SathyanarayanaR. K. Satzoda et al., "Vision-based patient monitoring: a comprehensive review of algorithms and technologies," *Journal of Ambient Intelligence and Humanized Computing*, vol. 9, no. 2, pp. 225-251, 2018.
- [5] Š. Sathyanarayana et al., "Accuracy and Robustness of Kinect Pose Estimation in the Context of Coaching of Elderly Population," in *Proceedings of the 2012 Annual International Conference Of the IEEE Engineering In Medicine and Biology Society*, pp. 1188-1193, San Diego, CA, USA, August 2012.
- [6] Y.-L. Kuo, E. A. Tully, and M. P. Galea, "Video analysis of sagittal spinal posture in healthy young and older adults," *Journal of Manipulative and Physiological Therapeutics*, vol. 32, no. 3, pp. 210-215, 2009.
- [7] R. C. Ailneni, K. R. Syamala, Kartheek, I.-S. Kim, and J. Hwang, "Influence of the wearable posture correction sensor on head and neck posture: Sitting and standing workstations," *Work*, vol. 62, pp. 27-35, 2019.
- [8] J. Biswas, A. Tolstikov, M. Jayachandran et al., "Health and wellness monitoring through wearable and ambient sensors: exemplars from home-based care of elderly with mild

- dementia,” *annals of telecommunications - annales des télécommunications*, vol. 65, no. 9-10, pp. 505–521, 2010.
- [9] Y. Otoda, “Census: Continuous Posture Sensing Chair for Office Workers,” in *Proceedings of the, 2018 IEEE International Conference on Consumer Electronics (ICCE)*, pp. 1-2, Hindawi Publishing Corporation, Las Vegas, NV, USA, 2018.
  - [10] R. Zemp, W. R. Taylor, S. Lorenzetti et al., “Seat pan and backrest pressure distribution while sitting in office chairs,” *Applied Ergonomics*, vol. 53, pp. 1–9, Article ID 5978489, 2016.
  - [11] M. Huang, I. Gibson, and R. Yang, “Smart Chair for Monitoring of Sitting Behavior,” *DesTech Conference Proceedings The International Conference on Design and Technology*, vol. 2017, no. 1, pp. 274–280, 2017.
  - [12] N. Rushton, *QNAP NAS Setup Guide*, Kindle Edition, Portland, Oregon, 2020.
  - [13] S. Bradshaw, E. Brazil, and K. Chodorow, *MongoDB: Definitive Guide 3e: Powerful and Scalable Data Storage*, O’Reily, CA, USA, 2019.
  - [14] G. C. Hillar, *MQTT Essentials A Lightweight IoT Protocol*, Packt Publishing, Birmingham, UK, 2017.
  - [15] A. A. Ishaku, “Flexible force sensors embedded in office chair for monitoring of sitting postures,” in *Proceedings of the IEEE International Conference on Flexible and Printable Sensors and Systems (FLEPS)*, pp. 1–3, Glasgow, UK, 2019.
  - [16] S. Ma, W. Cho, C. Quan, and S. Lee, “A Sitting Posture Recognition System Based on 3 axis Accelerometer,” in *Proceedings of the 2016 IEEE Conference on Computational Intelligence in Bioinformatics and Computational Biology (CIBCB)*, pp. 1–3, Chiang Mai, Thailand, 2016.
  - [17] H. Cho, H.-J. Choi, Ch.-E. Lee, and Ch.-W. Sir, “Sitting posture prediction and correction system using arduino-based chair and deep learning model,” in *Proceeding of the IEEE 12th Conference on Service-Oriented Computing and Applications (SOCA)*, pp. 98–102, Kaohsiung, Taiwan, November 2019.



## Research Article

# Research and Development of Palmprint Authentication System Based on Android Smartphones

Xinman Zhang <sup>1</sup>, Kunlei Jing <sup>1</sup> and Guokun Song <sup>2</sup>

<sup>1</sup>School of Automation Science and Engineering, Faculty of Electronic and Information Engineering, MOE Key Lab for Intelligent Networks and Network Security, Xi'an Jiaotong University, Xi'an, Shaanxi 710049, China

<sup>2</sup>Sichuan Gas Turbine Research Institute of AVIC, No. 6 Xinjun Road, Xindu District, Chengdu, Sichuan, China

Correspondence should be addressed to Xinman Zhang; zhangxinman@mail.xjtu.edu.cn

Received 27 June 2020; Revised 8 August 2020; Accepted 23 October 2020; Published 16 November 2020

Academic Editor: Peter Brida

Copyright © 2020 Xinman Zhang et al. This is an open access article distributed under the Creative Commons Attribution License, which permits unrestricted use, distribution, and reproduction in any medium, provided the original work is properly cited.

The security problems of online transactions by smartphones reveal extreme demand for reliable identity authentication systems. With a lower risk of forgery, richer texture, and more comfortable acquisition mode, compared with face, fingerprint, and iris, palmprint is rarely adopted for identity authentication. In this paper, we develop an effective and full-function palmprint authentication system regarding the application on an Android smartphone, which bridges the algorithmic study and application of palmprint authentication. In more detail, an overall system framework is designed with complete functions, including palmprint acquisition, key points location, ROI segmentation, feature extraction, and feature coding. Basically, we develop a palmprint authentication system having user-friendly interfaces and good compatibility with the Android smartphone. Particularly, on the one hand, to guarantee the effectiveness and efficiency of the system, we exploit the practical Log-Gabor filter for feature extraction and discuss the impact of filtering direction, downsampling ratio, and discriminative feature coding to propose an improved algorithm. On the other hand, after exploring the hardware components of the smartphone and the technical development of the Android system, we provide an open technology to extend the biometric methods to real-world applications. On the public PolyU databases, simulation results suggest that the improved algorithm outperforms the original one with a promising accuracy of 100% and a good speed of 0.041 seconds. In real-world authentication, the developed system achieves an accuracy of 98.40% and a speed of 0.051 seconds. All the results verify the accuracy and timeliness of the developed system.

## 1. Introduction

Mobile Internet technologies have brought humans a new lifestyle. The emergence of smartphones has better accelerated people's daily life with popular social networks such as online transactions [1]. However, frequent online transactions by smartphones often bring security problems. Specifically, to facilitate the payment, the "mobile wallet" should be linked with a cash card. Then, phenomena like Internet fraud and network "phishing" begin to spread extensively, which leads consumers to be still distrustful of the reliability of mobile payment. Moreover, when people trade online, they have to set different complex passwords on various occasions, which may be forgettable. These facts indicate that mobile payment still demands for reliable mechanisms extremely [2]. Over the

last years, fingerprint authentication has drawn significant attention. However, fingerprint can be easily damaged due to physical work and is not informative enough for identity authentication. For iris authentication, users have to suffer from an uncomfortable acquisition mode.

Recently, many researchers focus on face biometrics. Nevertheless, face information is always exposed to the environment and can be easily stolen for identity forgery. As for hand geometry biometric, its physical uniqueness needs further discussion [1]. All in all, with the advantages of abundant textures, comfortable acquisition mode, and lower risk of forgery, palmprint is more acceptable to users in some situations, compared with the other biometrics [1].

The earliest palmprint authentication system was developed on an embedded device by Zhang and Shu team in

1999. They acquired palmprint by scanning the printed palmprint templates [3]. The offline operating mode renders the system not only time-consuming but also unacceptable to users. To make improvement, in 2003, they utilized CCD to acquire images and set pegs to restrain the palm position. However, the improved equipment is immovable for its large size and still unacceptable for its contacting acquisition mode [4]. In 2010, Zhang et al.'s team further developed a new palmprint device with a smaller size compared with the previous ones, but this device remains to suffer from the contact-based acquisition mode [5]. In 2015, Aykut and Ekinci developed a contactless palmprint authentication system that obtained good usage experience whereas it is inconvenient for mobile applications. In summary, the existing palmprint authentication systems are still not mature enough for general application and deserve in-depth research. Table 1 presents a total comparison among the abovementioned systems.

From Table 1, the contact-based palmprint authentication systems are unacceptable for the uncomfortable acquisition mode, while the contactless systems are not robust to the real disturbance [7]. Besides, the widely adopted feature extractor, Log-Gabor filter, in these systems has a high computation cost, which can greatly reduce the timeliness of the system [8]. Furthermore, the adopted Quadrant coding is unsuitable to make full play of the discrimination of the extracted features [9]. In current years, the Android operation system-based smartphones have occupied 76% of the smartphone market in the world. So, it is meaningful to further study an efficient contactless palmprint authentication system with the application on the Android smartphone.

According to the aforementioned analysis, we design an overall system framework with complete functions for palmprint authentication. Specifically, a vital acquisition scheme is established to ensure the image quality in the contactless acquisition process. Some improvements are introduced to the Log-Gabor filter and the original coding method to reduce the computational complexity and enhance the discriminability of the coding results. On the basis, a system with user-friendly interfaces and good compatibility is developed for the application on the Android smartphone.

Most systems only focus on the palmprint authentication method. Actually, as the primary work, it is crucial to establish an acquisition scheme. Thus, the image quality and accurate ROI segmentation can be ensured for more reliable identity authentication. Besides, the authentication algorithm is the core issue of our system. Considering the practicality and effectiveness, the Log-Gabor filter is the most suitable one for our system. However, to guarantee the timeliness of our system, we should consider reducing the computational complexity of the Log-Gabor filter. Moreover, a proper coding method should be exploited to enhance the discriminability of the extracted features, which helps the system distinguish one class from the others more easily. Finally, all the procedures should be programmed into modules and linked to the well-designed functional interfaces to

facilitate the operation. Depending on the above motivations, the overall system framework proposed in this paper is displayed in Figure 1. Table 2 lists all the involved evaluation parameters and their definitions in advance. The main contributions of our work are summarized as follows:

- (i) A palmprint acquisition scheme is proposed against the potential disturbances such as the variation of palm posture and illumination. Then, we present a complete set of procedures for palmprint ROI extraction, such as key points location, palmprint angle correction, and the final ROI segmentation.
- (ii) To guarantee the efficiency of the system and obtain more discriminative feature coding results, we discuss the impact of filtering direction and downsampling to the performance of Log-Gabor filter and improve the original coding scheme [10, 11].
- (iii) A palmprint authentication framework with complete functions is designed. We explore and show the details of developing the corresponding system with user-friendly interfaces and good compatibility with Android smartphones.
- (iv) Our work provides an open technology to extend the palmprint authentication algorithms to real-world applications, which bridges the algorithmic studies and applications of biometrics.



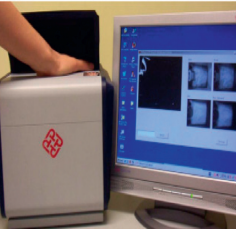
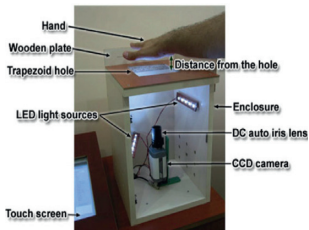
The rest of the paper is organized as follows: Section 2 defines an acquisition scheme and provides a method for palmprint ROI extraction. Section 3 describes the improvements for palmprint authentication. Section 4 introduces the hardware components of the smartphone and the software realization of the palmprint authentication system. Section 5 performs experimental verifications. Section 6 concludes this paper.

## 2. Palmprint Acquisition and ROI Extraction

*2.1. Acquisition Scheme.* In our system, ROI segmentation is finished according to three key points among fingers. However, palm gesture and the position of the palm can affect the key point locating [12, 13]. Taking some cases into consideration. The palm deformation often produces visual textures. The large gaps among fingers can lead to imprecise locating results. A long distance between palm and camera can lead the acquired image to have too much background. All of these potential disturbances will bring difficulties for key points locating. So, it is necessary to define an acquisition scheme.

Considering the aforementioned potential disturbances, the acquisition scheme in this paper is determined as follows: five fingers extended and the other four fingers close to each other except for the thumb. A red line and a center point are marked on the interface to conduct the position of the finger root and palm center.

TABLE 1: Comprehensive comparisons among some typical palmprint authentication systems.

Team/company	Products	Acquisition approach	Performance online/offline	Advantages	Disadvantages
HKPU, in 1999 [3]		Contact-based	Offline	(i) Robust to disturbance	(i) Poor usage experience (ii) Poor portability (iii) Poor timeliness
HKPU, in 2003 [4]		Contact-based	Online	(i) Robust to disturbance (ii) Good timeliness	(i) Poor usage experience (ii) Poor portability
HKPU, in 2010 [5]		Contact-based	Online	(i) Robust to disturbance (ii) Good timeliness	(i) Poor usage experience (ii) Poor portability
Karadeniz Technical University, in 2015 [6]		Contactless	Online	(i) Good usage experience (ii) Good timeliness	(i) Not robust to disturbance (ii) Poor portability

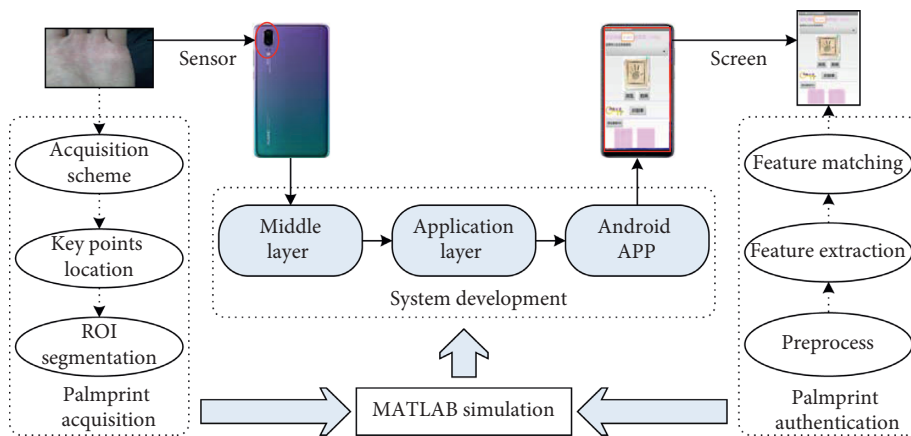


FIGURE 1: The designed framework of the palmprint authentication system.

TABLE 2: Parameter definitions.

Parameter	Definition
$FP$ (false positive)	The number of imposter acceptances
$TN$ (true negative)	The number of imposter rejections
$FN$ (false negative)	The number of legitimate rejections
$TP$ (true positive)	The number of legitimate acceptances
$AA$ (authentication accuracy)	$AA = (TP + TN)/(TP + FP + TN + FN)$
$FAR$ (false acceptance rate)	$FAR = FP/(TN + FP)$
$FRR$ (false rejection rate)	$FRR = FN/(TP + FN)$
$EER$ (equal error rate)	Equates to the point at which the FAR and FRR cross
$D_1$	Interval length of the intraclass hamming distance distribution
$D_2$	Interval length of the interclass hamming distance distribution
$Dis$	The distance from the upper bound of $D_1$ to the lower bound of $D_2$
$L_1$	$Dis/D_1$
$L_2$	$Dis/D_2$

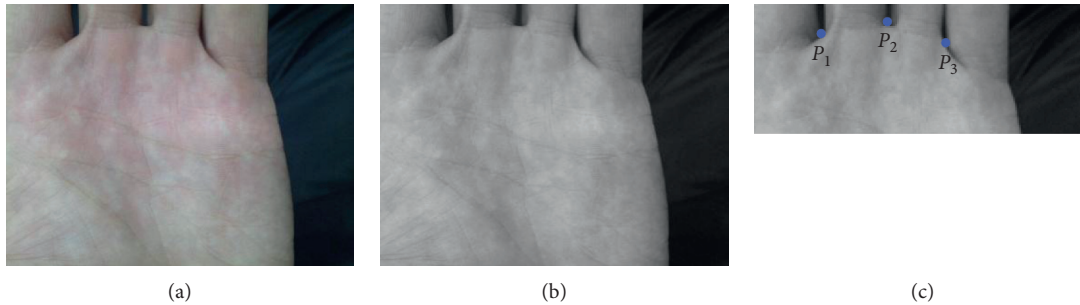


FIGURE 2: Palmprint images. (a) Original palmprint image. (b) Gray palmprint image. (c) Reserved subimage.

## 2.2. Key Point Location

**2.2.1. Image Graying.** The original palmprint image ( $540 \times 600$ ) shown in Figure 2(a) is converted into a gray image shown in Figure 2(b). To cut down the searching range, the upper portion ( $270 \times 600$ ) of the gray image is reserved, shown in Figure 2(c).

In the reserved subimage, the gaps between fingers root are deemed as the key points and denoted as  $P_1$ ,  $P_2$ , and  $P_3$ , respectively, as shown in Figure 2(c).

**2.2.2. Columns of Key Points.** The average gray value versus the column of the reserved subimage can be calculated by

$$\begin{cases} F_y(i, j) = \frac{(F(i, j+1) - F(i, j-1))}{2}, \\ F_x(i, j) = \frac{(F(i+1, j) - F(i-1, j))}{2}, \end{cases} \quad (1)$$

where  $F_y$  and  $F_x$  denote the gradient versus column and row, respectively.  $(i, j)$  denotes the pixel coordinate. The three local minima are shown in Figure 3, which correspond to the column indexes of the three key points.

**2.2.3. Rows of Key Points.** The three subimages ( $100 \times 20$ ) containing three key points are, respectively, cropped from Figure 4(a) shown in Figure 4(b). For each subimage, the row index of the key point can also be obtained according to formula (1). The average gradient value versus the rows of the first subimage is shown in Figure 5. The  $X$ -coordinate of the maximal value corresponds to the row index of the key point.

**2.3. ROI Segmentation.** The acquired images often contain redundant information such as fingers and background. Palmprint ROI refers to the palm center that contains three flexor lines [14, 15]. Here, we segment ROI according to the above located key points.

Since the size of a smartphone screen is generally different from the size of a palmprint image and there exists rotation between them, it is necessary to correct the scale and angle of the palmprint image before ROI segmentation.

**2.3.1. Scale Correction.** The key point lying in the original image with a size of  $w \times h$  is denoted as  $P_i(x_i, y_i)$  ( $i = 1, 2, 3$ ). The corresponding position in the smartphone interface with a size of  $w' \times h'$  is denoted as  $P'_i(x'_i, y'_i)$  ( $i = 1, 2, 3$ ). Then, the transformation can be defined as

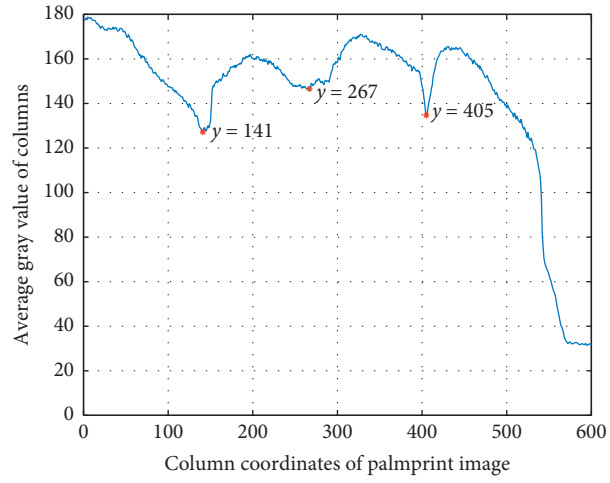


FIGURE 3: Average gray value versus the columns.

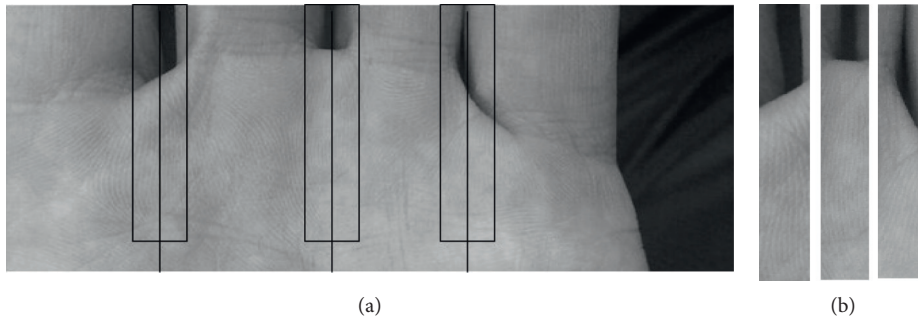


FIGURE 4: Subimages containing the three key points. (a) Marked subimages. (b) Cropped subimages.

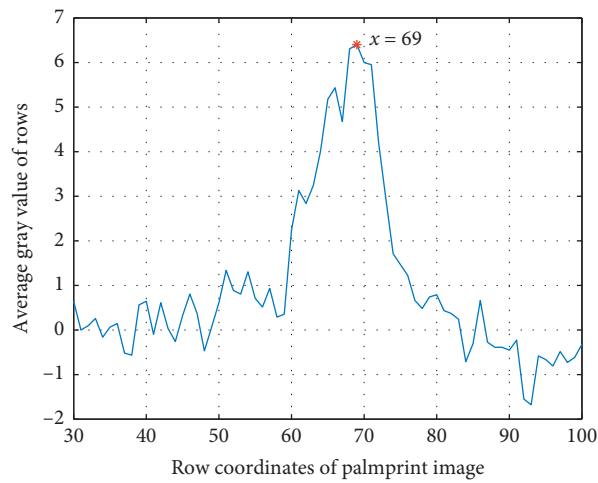


FIGURE 5: Average gray value versus the rows.

$$\begin{cases} x'_i = x_i \times \left(\frac{w'}{w}\right), \\ y'_i = y_i \times \left(\frac{h'}{h}\right). \end{cases} \quad (2)$$



2.3.2. *Rotation Correction.* The purpose of the rotation is to place  $P_1$  and  $P_3$  on a horizontal line to facilitate ROI segmentation. The calculation of the rotation angle is shown as follows:

$$a = \arctan\left(\frac{(y'_3 - y'_1)}{(x'_3 - x'_1)}\right), \quad (3)$$

where  $(x'_1, y'_1)$  and  $(x'_3, y'_3)$  are the coordinates of  $P'_1$  and  $P'_3$ , respectively. The corresponding coordinates after rotation are denoted as  $P''_i(x''_i, y''_i)$  ( $i = 1, 2, 3$ ). We define the rotation transformation as follows:

$$\begin{cases} x''_i = \left[ \left( x'_i - \frac{w'}{2} \right) \times \cos\left(\frac{a}{180} \times \pi\right) + \left( y'_i - \frac{h'}{2} \right) \times \sin\left(\frac{a}{180} \times \pi\right) + \frac{w'}{2} \right] \\ y''_i = \left[ -1 \times \left( x'_i - \frac{w'}{2} \right) \times \sin\left(\frac{a}{180} \times \pi\right) + \left( y'_i - \frac{h'}{2} \right) \times \cos\left(\frac{a}{180} \times \pi\right) + \frac{h'}{2} \right], \end{cases} \quad (4)$$

where  $\lceil \cdot \rceil$  reserves the integer value, while the line  $P''_1P''_3$  is set as the  $x$ -axis, and its vertical line is set as the  $y$ -axis. Then, the coordinate system is established in the palmprint image. The length of  $P''_1P''_3$  is denoted as  $d$ . Moving it down alongside the  $y$ -axis by  $d/3$ , a square is built up with the side length of  $d$ , as shown in Figure 6(a). To obtain a standard ROI, we scale the segmented square to a size of  $128 \times 128$ , shown in Figure 6(b).

### 3. Palmprint Authentication

In experiments, we find that image preprocessing has a little effect on ROI segmentation results. To shorten the running time of the system, we perform image preprocessing after ROI segmentation.

#### 3.1. Image Preprocessing

3.1.1. *Gray Enhancement.* The pixel value of the original ROI image is denoted as  $F_{old}(i, j)$ , and the pixel value after the

preprocessing is denoted as  $F_{new}(i, j)$ . The gray enhancement is defined as [16]

$$F_{new}(i, j) = \begin{cases} low\_out, & F_{old}(i, j) < low\_in, \\ high\_out, & F_{old}(i, j) > low\_high, \\ CLog(1 + F_{old}(i, j)), & \text{else.} \end{cases} \quad (5)$$

where  $low\_in, high\_in, low\_out$ , and  $high\_out$  are four given constants, according to which the original pixel value between  $[low\_in, high\_in]$  is then transformed between  $[low\_out, high\_out]$ .

3.1.2. *Gray Normalization.* To balance the uneven illumination, we normalize the gray image by the following formulas [17]:

$$F_{new}(i, j) = \begin{cases} M_o + \sqrt{\frac{VAR_o(F_{old}(i, j) - M(F))^2}{VAR(F)}}, & F_{old}(i, j) > M(F), \\ M_o - \sqrt{\frac{VAR_o(F_{old}(i, j) - M(F))^2}{VAR(F)}}, & \text{else,} \end{cases} \quad (6)$$

where  $M(F)$  and  $VAR(F)$  signify the mean function and the variance function, respectively. The preprocessed ROI images are shown in Figure 7(c), from which we observe that the three flexor lines and the surrounding details are more obvious and abundant.

3.2. *Discussion on Log-Gabor Filter.* The three principal lines in palmprint are not sufficient to signify the uniqueness of individuals. So, the feeble wrinkles around them should be amplified to provide more valuable information. What is more, direction information in palmprint should be

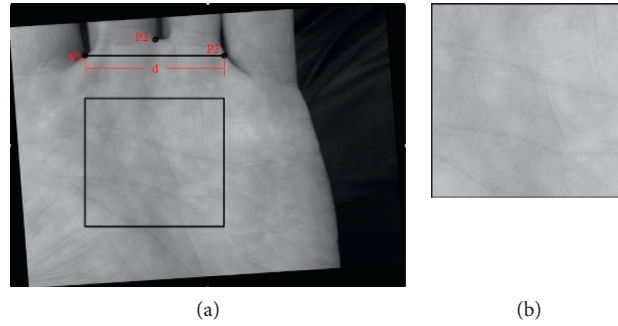


FIGURE 6: Palmprint ROI segmentation. (a) Marked ROI. (b) Segmented ROI.

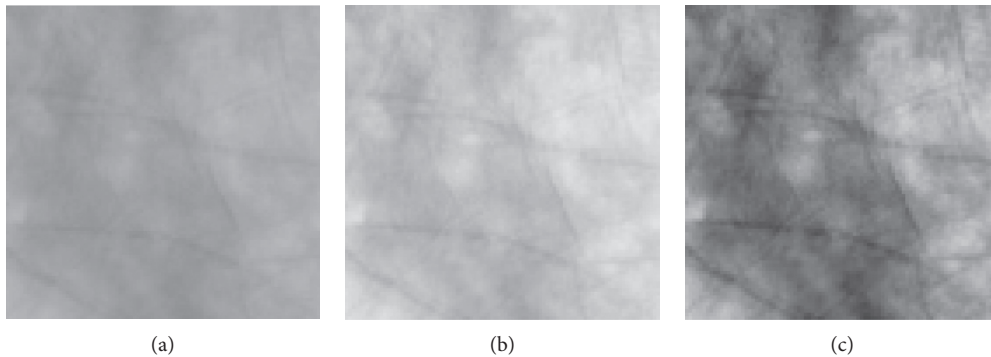


FIGURE 7: ROI image preprocessing. (a) Segmented ROI image. (b) Gray enhancement. (c) Gray normalization.

characterized. The Log-Gabor filter is capable of supporting us to extract such a kind of features. By setting various factors and filtering directions, we can obtain more representative abundant features through the Log-Gabor filter [18, 19]. Feature coding is the other important process, in which a more discriminative feature coding method helps to further improve the performance of the system.

Note feature extraction corresponding multiple factors and directions can result in a large computation. To guarantee the timeliness and the effectiveness of our system, we will take the discussion on the original Log-Gabor filter and feature coding method (we call the original algorithm in the later content).

**3.2.1. Log-Gabor Filter.** The transfer function of the Log-Gabor filter in the linear frequency domain is defined as [20]

$$G(f) = \exp\left(\frac{-(\log(f/f_0))^2}{2(\log(\sigma/f_0))^2}\right), \quad (7)$$

where  $f_0$  and  $\sigma$  denote the central frequency domain and the bandwidth, respectively. To maintain the shape of the filter, the ratio  $\sigma/f_0$  is usually fixed [21]. The output of the Log-Gabor filter is related to the filtering direction. Here, we set  $\theta = [0^\circ, 45^\circ, 90^\circ, 135^\circ]$  to discuss the influence of filtering direction to feature extraction results. The scale wavelength is set as 3, and the ratio is fixed by  $\sigma/f_0 = 0.6$ . The filtered results are shown in Figure 8. When  $\theta = 0^\circ$ , textures in all directions are

well characterized except for the horizontal textures. When  $\theta = 45^\circ$ , textures in direction  $135^\circ$  is mostly represented. When  $\theta = 90^\circ$ , the horizontal textures are the clearest. When  $\theta = 135^\circ$ , textures in direction  $45^\circ$  are clearly represented. Thus, we conclude that the extracted textures are more representative when the filtered direction is perpendicular to texture.

**3.2.2. Feature Extraction and Coding.** Since the distribution of palmprint textures is complex, we set  $\theta = [0^\circ, 45^\circ, 90^\circ, 135^\circ]$  to cover the most directions. In addition, five scale factors, say  $\sigma = [3, 4.5, 6.75, 45.5]$ , are chosen in each direction to extract more abundant information, with  $\sigma/f_0 = 0.6$ . Then, a feature matrix with the dimension of  $4 \times 5 \times 128 \times 128 = 327680$  is obtained by the original algorithm, which leads to a computation disaster [7]. To this end, we bring some improvements to the Log-Gabor filter.

In detail, the ROI image and extracted features will be downsampled to get rid of the redundant information while reducing the computational time. To obtain distinguishable coding results for the final identity matching, we adopt the Gray code to replace Quadrant code to enhance the discriminability of features. The specifics are shown as follows:

Step 1: ROI image ( $128 \times 128$ ) is downsampled to the size of  $64 \times 64$ . The pixel value before and after filtering is denoted as  $i(x, y)$  and  $I(x, y)$ , respectively.  $G_m(x, y)$  ( $m = 1, 2, 3, 4$ ) denotes the Log-Gabor filter

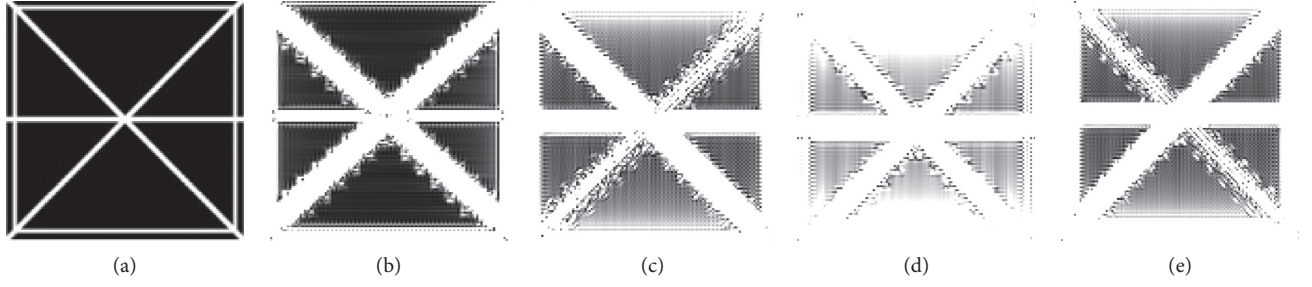


FIGURE 8: Filtering results in different directions: (a) Test image. (b) Direction  $0^\circ$ . (c) Direction  $45^\circ$ . (d) Direction  $90^\circ$ . (e) Direction  $135^\circ$ .

with different filtering directions. The filtering process (feature extraction) is formulated as follows:

$$I_m(x, y) = i(x, y) \times G_m(x, y). \quad (8)$$

Step 2: the features are downsampled with a ratio of 1 : 2 to obtain a feature matrix with a dimension of

$4 \times 32 \times 32$ . Let  $I_m(x, y)$  and  $I'_m(x, y)$  denote the pixel value before and after the feature downsampling. The feature downsampling can be performed by the following formula:

$$I'_m(x, y) = I_m(x-1, y-1) + x[I_m(x+1, y-1) - I_m(x-1, y+1)] + y[I_m(x-1, y+1) - I_m(x-1, y-1)] + xy[I_m(x+1, y+1) + I_m(x-1, y-1)] - xy[I_m(x+1, y-1) + I_m(x-1, y+1)]. \quad (9)$$

Step 3: according to the real part and imaginary part of the features, Quadrants coding achieves two kinds of coding results, while Gray coding achieves four kinds of coding results. Hence, Gray coding is conducive to enhance the discriminability of features. Denoting the coding result as  $Code I'_m = [Code I'_m R, Code I'_m I]$ , then Gray coding can be defined as follows:

$$Code I'_m R = \begin{cases} 1, & \text{Re}[I'_m(x, y)] \geq 0, \\ 0, & \text{Re}[I'_m(x, y)] < 0, \end{cases} \quad (10)$$

$$Code I'_m I = \begin{cases} 1, & \text{Im}[I'_m(x, y)] \geq 0, \\ 0, & \text{Im}[I'_m(x, y)] < 0. \end{cases}$$

All the above steps are repeated regarding five scales to obtain a matrix with a dimension of  $4 \times 5 \times 32 \times 32 \times 2 = 40960$ . The flow chart of the improved algorithm is shown in Figure 9.

**3.2.3. Feature Matching.** Hamming distance is exploited for feature matching to judge whom the acquired palmprint image belongs to. By the bitwise XOR operation on two feature vectors, the rate of the number “1” is defined as Hamming distance. If the samples come from the same user, the Hamming distance can be small enough. Otherwise, the Hamming distance can be large. The calculation of Hamming distance is defined as

$$HD = \frac{\sum_{i=1}^N P(i) \otimes Q(i)}{N}, \quad (11)$$

where  $P(i)$  and  $Q(i)$  denote the  $i$ th elements in two vectors and  $N$  denotes the vector dimension. Theoretically, when  $P$  and  $Q$  are exactly the same,  $HD = 0$ . Otherwise,  $HD = 1$ . There exist no palmprint images that are totally the same or different in practice, so generally  $HD \in (0, 1)$ . The final authentication is achieved by comparing the Hamming distance with the predetermined matching threshold.

## 4. System Development

### 4.1. Structure of the Hardware and Software

**4.1.1. Hardware.** In recent years, Android smartphones have occupied a large market share in the world. Among the most mainstream models in 2018, HUAWEI P20 is the most popular one that carries a host processor HiSilicon Kirin 970, 6 GB RAM, 128 GB ROM, and a 6.1-inch touchscreen with a resolution ratio of  $2240 \times 1080$ . Its operating system is Android 8.1. Among these, the camera and GPU are the key components. Four mainstream brands released in the same period with HUAWEI P20 are listed in Table 3 [22].

For the CMOS camera, the larger the camera numbers and the pixel size, the more information can be captured. The smaller the aperture size, the more light could be passed to enhance the image. What is more, G72MP12 is more powerful than Adreno540 and 418 for image processing. After the synthetic comparison, HUAWEI P20 is chosen as the platform of our system. The main hardware structure of HUAWEI P20 is shown in Figure 10.

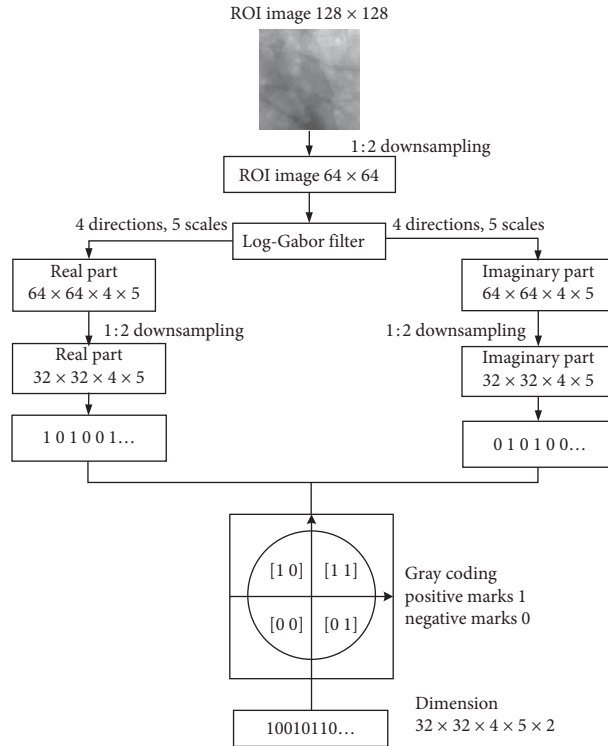


FIGURE 9: The flow diagram of the improved algorithm.

TABLE 3: Camera and GPU comparison of four mainstream Android smartphone brands.

Manufactures	Numbers	Camera			GPU
		Megapixel	Pixel size ( $\mu\text{m}$ )	Aperture size	
MOTOROLA X	1	21	1.1	F2.0	Adreno418
SAMSUNG S8+	1	12	1.4	F1.7	Adreno540
HTC U11+	1	12	1.4	F1.7	Adreno540
HUAWEI P20	2	20 + 8	1.55	F1.8	Mali-G72MP12

4.1.2. *Software.* According to the designed framework in Figure 1, the system development can be finished through three steps: middle layer development, application layer development, and Android APK generation [23]. The entire development structure is displayed in Figure 11. The details are described as follows:

- (i) Underlying layer development: in the QT environment, we first develop executable files to call the hardware of the smartphone to finish each procedure in the designed framework. Procedures, like palmprint acquisition, ROI segmentation, feature extraction, feature coding, and feature matching, are all separately programmed into executable functional files by C++ language.
- (ii) Application layer development: using Android SDK, we develop interfaces to call the executable functional files. Through user-friendly interfaces, the user can operate the system in real time. The development in this stage is finished in Eclipse Java EE environment.

- (iii) Android APK generation: we use NDK to compile the functional files developed in the underlying layer. The compiled files are packaged with the JNI standard to facilitate the callback from the application layer. Then, dynamic link libraries are generated and packaged into an APK to install on the smartphone.

4.2. *System Function Design.* Activity is the functional unit in the application layer. Since an activity occupies a certain part of memory, to save the resource, we integrate the interrelated functions into one activity. It is also convenient for us to debug the code and maintain the software. Our APK is composed of four activities: main activity (main interface), database activity (database interface), authentication activity (authentication interface), and acquisition activity (acquisition interface).

4.2.1. *Main Activity.* The main activity provides entrances for the other activities. Additionally, the initialization and

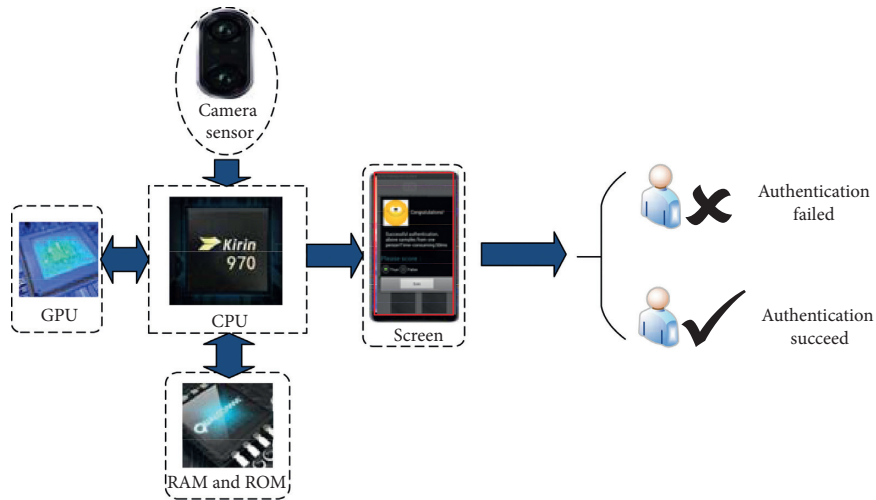


FIGURE 10: The hardware structure of HUAWEI P20.

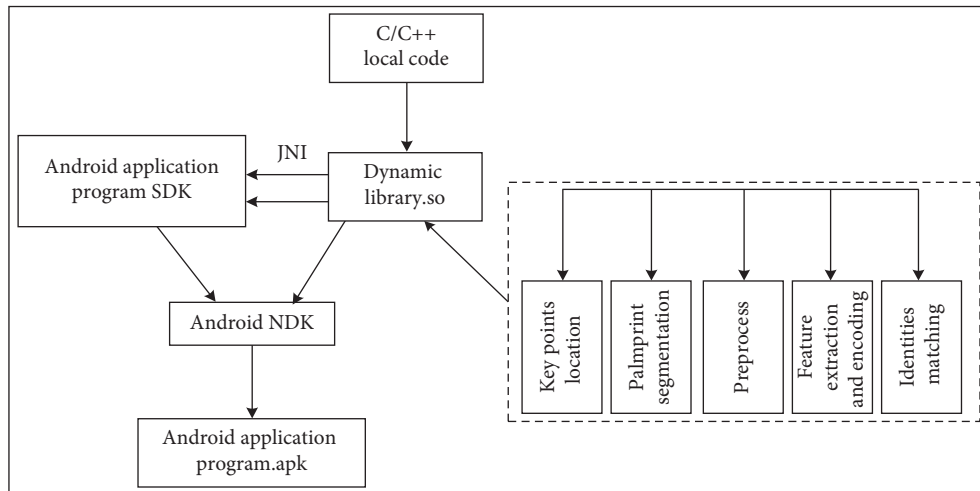


FIGURE 11: The entire structure of software development.

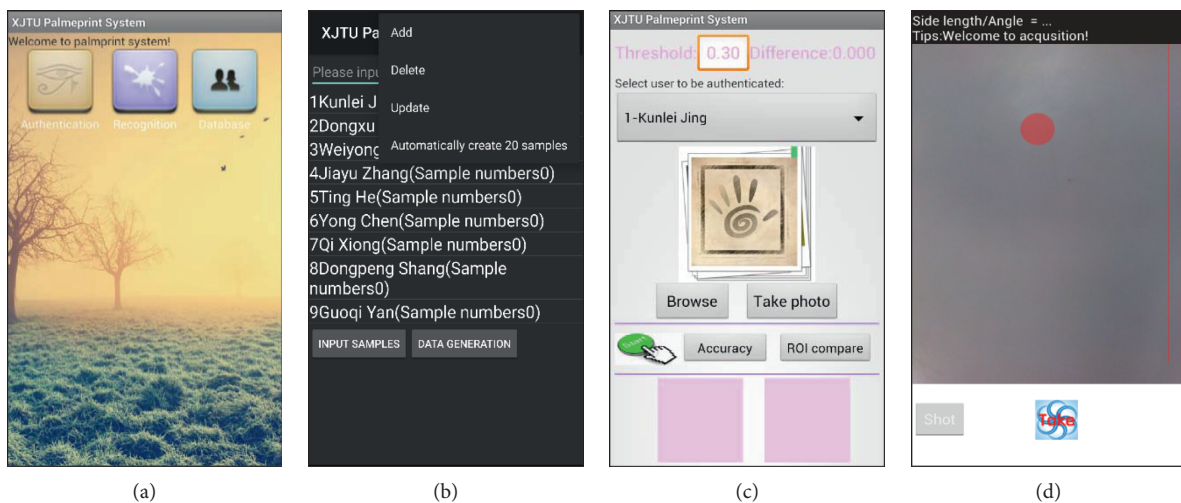


FIGURE 12: The developed four interfaces: (a) Main interface. (b) Database interface. (c) Authentication interface. (d) Acquisition interface.



storage of the database are finished in this activity. The developed main interface is shown in Figure 12(a).

**4.2.2. Database Activity.** Users finish identity registration in this activity. They can append their identity information by clicking “Add” button and input their palmprint images for the later authentication (5 samples are necessary) by clicking “INPUT SAMPLES” button. Features extraction is finished by clicking “DATA GENERATION” button. Meanwhile, we design “Delete” and “Update” buttons to facilitate database management. The database interface is shown in Figure 12(b).

**4.2.3. Authentication Activity.** Identity authentication is achieved in this activity. After choosing the identity to be confirmed in the identity list, users can click the “Browse” button or “Take photo” button to select the test sample. When clicking the “Start” button, the system will display authentication result, elapsed time, and encourage users to evaluate the authentication result. Users can examine the correct authentication number and the accuracy by clicking the “Accuracy” button. Also, they can click the “ROI Compare” button to check the difference between two segmented ROI images. The authentication interface is shown in Figure 12(c).

**4.2.4. Acquisition Activity.** When users enter the real-time acquisition, the rear camera is driven to work. Two modes, “long press” and “click,” are designed for the “Take” button. When it is long pressed (about 2 seconds), the located key points and ROI are displayed on the screen. Tips for distance and angle adjustment are given on the top to guide the acquisition. Users can click the “Take” button (about 0.5 seconds) to finish the final acquisition. The developed acquisition interface is shown in Figure 12(d), where the red line and point are set to conduct the palm position.

## 5. Results and Discussion

### 5.1. Verification of the Improved Algorithm

**5.1.1. Statistical Analysis.** The blue spectrum samples in the PolyU multispectral palmprint database containing 6000 samples from 500 volunteers are chosen to verify the improved algorithm [18]. 12 samples of each volunteer are divided into two equal parts. The first part is regarded as the training samples, while the second part is used for the test.

Each volunteer is tested 6 times, and the total intraclass test times reach 3000. For interclass verification, test samples of each volunteer are, respectively, utilized to match each training sample of a selected volunteer. The minimum Hamming distance is deemed as the final matching result. If it is less than the threshold, they are regarded as the same class. Otherwise, they are regarded as different ones [24].

In our simulation, the intraclass Hamming distances distribute in interval [0.1317, 0.2265], while the interclass

Hamming distances distribute in interval [0.3118, 0.5271]. The distribution density curves are shown in Figure 13.

Based on the above discussion, *AA*, *FRR*, and *FAR* are brought to evaluate the improved algorithm. We set the threshold  $th \in [0.10, 0.55]$ , and the step length is 0.01. The *FAR* and *FRR* threshold curves are drawn in Figure 14. It can be seen that the *FAR* and *FRR* curves have no intersection, which means *EER* is 0. Note Figure 14 is more intuitive for us to find the optimum threshold interval, compared with the *ROC* curve [20].

A comprehensive comparison between the improved algorithm and the original one is listed in Table 4. The evaluation items include the intraclass and interclass Hamming distance, indicator *L*, feature dimension, and the authentication time. For Hamming distance and indicator *L*, compared with the original algorithm, the improved algorithm presents more obvious separation between the intraclass and interclass Hamming distance distributions, which greatly reduce the *ERR*. In addition, we find that the feature dimension is reduced by 6.25%. This guarantees the efficiency of our system.

**5.1.2. Comparison with the Other Biometrics.** Apart from palmprint, there are some other biometrics that can be used for identity authentication. This subsection carries out a comparison among the proposed system and some other biometrics-based methods. We particularly consider the new emerging biometrics, *EEG* [25] and *ECG* [26–28]. The comparison results are shown in Table 5.

The collected data in Table 5 indicates that the methods based on the new biometrics all achieved promising accuracy. Recent years have witnessed the great application value of the *EEG* and *ECG* biometrics based on the brain wave and heartbeat pattern [25, 26]. Meanwhile, the good performance presented in [25–28] also manifests the great potential of the deep neural networks to learn valuable pattern information in the complicated biometric signals. All of these facts motivate us to further study identity authentication using the new biometrics by deep neural networks.

**5.1.3. Complexity Analysis.** As is introduced in Subsections 3.2.2 and 3.2.3, given an ROI image  $y \in \mathbb{R}^{N \times M}$ , the entire authentication procedure includes three stages, that is, feature extraction, feature coding, and feature matching [29, 30]. The first stage involves image downsampling and Log-Gabor filtering. The computational complexity of image downsampling is  $N \times M$ . After that, the image size becomes  $(N/2) \times (M/2)$ . According to formula (8), the filtering process should be repeated along 4 filtering directions, respectively, with 5 different scale factors [31, 32]. Hence, its computational complexity is  $4 \times 5 \times (N/2) \times (M/2)$ . So, the operation complexity of the feature extraction stage is  $N \times M + 5 \times N \times M$ . The feature coding stage involves feature downsampling and coding. Formula (9) indicates that the computational complexity of feature downsampling is  $(N/2) \times (M/2)$ . Then, the feature dimension becomes  $(N/4) \times (M/4)$ . From formula (10), we know the coding process

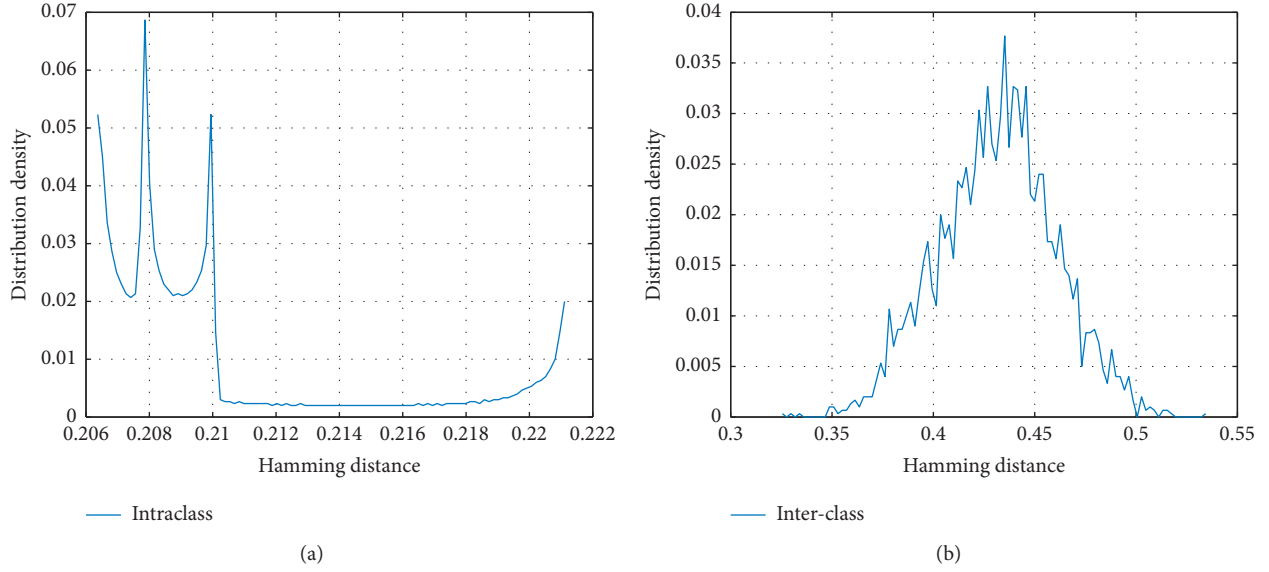


FIGURE 13: Distribution density curves of the Hamming distance. (a) Intra-class. (b) Inter-class.

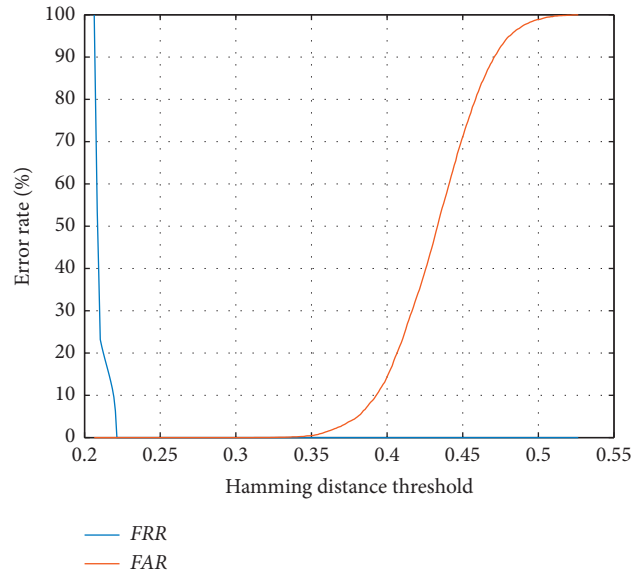


FIGURE 14: Threshold curve of FAR and FRR.

TABLE 4: A comprehensive comparison of the algorithms.

Algorithm	Intra-class	Inter-class	Indicator $L$	Dimension	Authentication time (s)
Original	0.1441–0.1501	0.1721–0.2681	3.6667, 0.2292	327680	0.2607
Improved	0.2054–0.2214	0.3254–0.5344	6.5000, 0.4976	40960	0.0278

has a complexity of  $2 \times (N/4) \times (M/4)$ . Thus, the feature coding stage has an operation complexity of  $N \times M/4 + N \times M/8$ . Finally, formula (11) indicates the operation complexity of the feature matching stage is  $2 \times (N/4) \times (M/4)$ . In summary, the total operation complexity of the entire authentication procedure is  $(N \times M + 5 \times N \times M) + (N \times M/4 + N \times M/8) + N \times M/8 = 13NM/2$ .

## 5.2. Verification of the Developed System

**5.2.1. Test of Palmprint Acquisition.** To demonstrate the effectiveness of the defined acquisition scheme, we acquire the palmprint samples during a random period in one day and randomly rotate the palm within a finite angle range [33]. The palmprint acquisition interface is shown in Figure 15.

TABLE 5: Comparison with some other biometrics.

Literature	Biometrics	Running time (s)	AA (%)	FAR (%)	FRR (%)
[25]	EEG	—	100.00	—	—
[26]	ECG	0.082	99.27	0.81	0.54
[28]	ECG	—	99.2	—	0.60
[27]	ECG + fingerprint	0.126	99.74	0.30	0.20
This paper	Palmprint	0.051	100	0.00	0.00

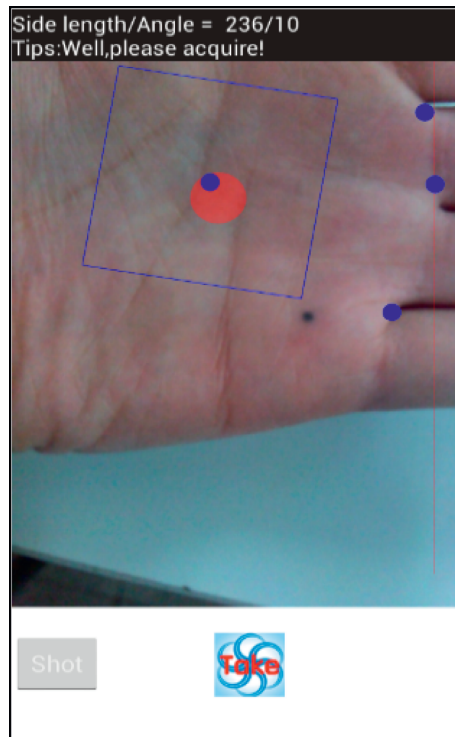


FIGURE 15: Palmprint acquisition.

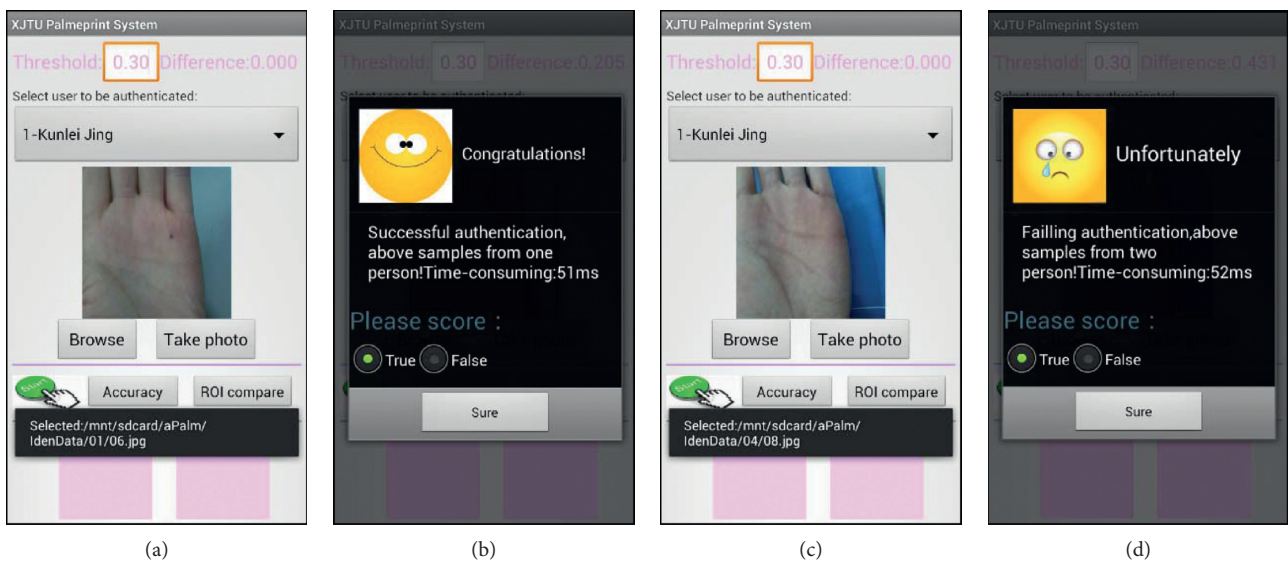


FIGURE 16: Palmprint authentication interfaces 1. (a) The acquired sample. (b) Intra-class authentication. (c) Sample selected in database. (d) Interclasses authentication.

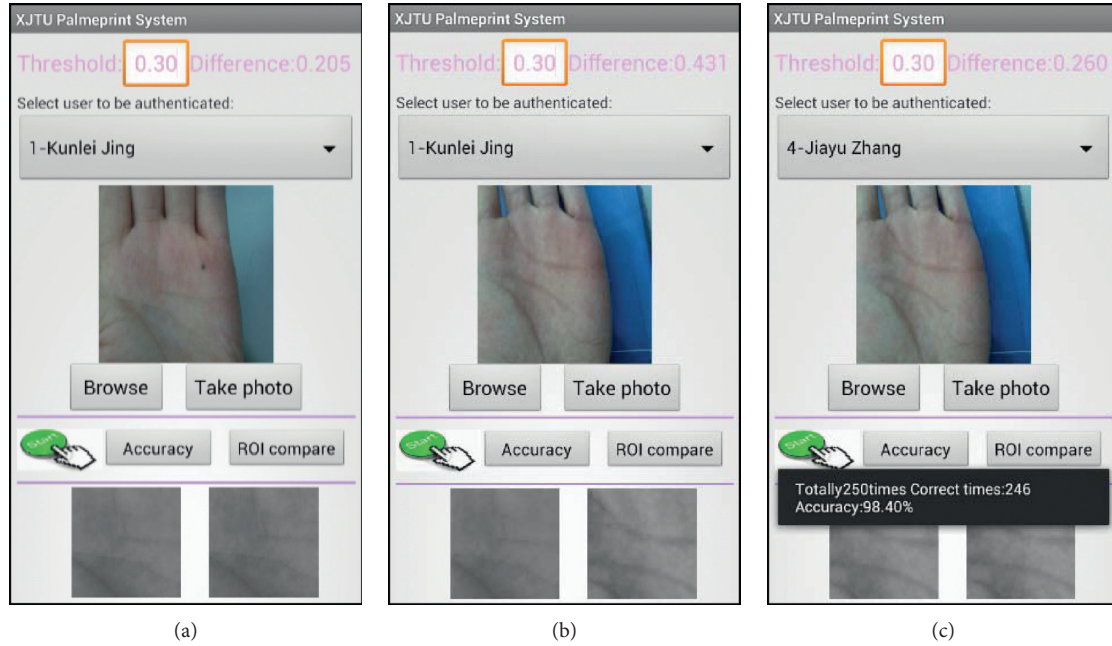


FIGURE 17: Palmprint authentication interfaces 2. (a) Intra-class ROI comparison. (b) Inter-classes ROI comparison. (c) Authentication accuracy.

TABLE 6: Comprehensive comparison on different platforms.

Environment	Samples	AA (%)	FAR (%)	FRR (%)	EER (%)	Authentication time (s)
MATLAB	6000	100	0	0	0	0.028
Smartphone	500	98.40	1.60	0	—	0.051

Under the constraint of the acquisition scheme, most potential disturbances are suppressed. Meanwhile, with the conduction of the set marks, palm appears on the screen with a proper scale. After long pressing the “Take” button (about 2 seconds), key points locating and ROI segmentation are all finished. The side length and rotation angle of ROI are calculated and displayed on the top to suggest users to make the final acquisition.

**5.2.2. Test of Palmprint Authentication.** We recruited 500 samples acquired from 50 volunteers in the real world to verify the effectiveness of the developed system. At the beginning, each volunteer was required to register identity with 5 training samples. Then, they are required to implement 5 times intra-class real-time authentication and 5 times inter-class real-time authentication, respectively. Since the palmprint database is established in real application [34], the variations of palm posture, background, and illumination commonly exist in the samples. Here, we set the threshold as 0.30. Specifically, after selecting the identity to be confirmed from the identity list, users can click the “Take photo” button to finish real-time acquisition for the test or click the “Browse” button to choose a previously acquired sample for the test. The system will display the storage path of the

selected sample. The intra-class and inter-class authentication operations are shown in Figures 16(a)–16(d), respectively.

Users can click the “Start” button to trigger authentication. Then, the system will display authentication result and running time and encourage the user to make an evaluation. Additionally, we can check ROI of the test sample and training sample by clicking the “ROI compare” button. We can also view the total authentication times, correct authentication number, and authentication accuracy, by click the “Accuracy” button, as shown in Figure 17(c).

After a 250-time test, we find that the authentication accuracy of the developed system is close to that in MATLAB simulation. Due to the unavoidable disturbances in the acquired sample, the authentication accuracy in real-time acquisition is reduced to 98.40%. Note the authentication in MATLAB simulation takes about 0.0278 seconds for average, while it is 0.051 seconds on the smartphone. All the test results on MATLAB and smartphone are listed in Table 6.

Meanwhile, we find that if the acquisition process follows the defined constraint scheme, we can obtain more promising accuracy. Otherwise, the accuracy will be impacted. This indicates the importance of the established acquisition scheme. We also find that when the light intensity changes within a limited degree, the authentication accuracy can be



nearly not reduced, which demonstrates that our system shows robustness to some extent.

## 6. Conclusion

In recent years, there emerges an extreme demand for reliable identity authentication system for secure mobile transactions. This paper presents an effective and efficient palmprint authentication framework towards the application on the Android smartphone. It contains all the required functions during palmprint authentication, including palmprint acquisition, ROI segmentation, feature extraction, and the final identity authentication. More importantly, our method provides an open technology to extend the palmprint authentication algorithms to real-world applications by exploring the development of a user-friendly palmprint authentication system based on the Android smartphone, which well bridges the algorithmic study and the real-world application of palmprint authentication.

This paper presents our exploratory work of propelling the application of palmprint authentication on the mobile smart terminals. Considering the timeliness of the system, we choose the practical and effective Log-Gabor filter for feature extraction. However, when the palmprint is subjected to corruption or occlusion, the Log-Gabor filter is unable to extract robust features anymore. In the next stage, we will manage to enhance the robustness of our system concerning more complicated application scenarios. Furthermore, we will also consider achieving identity authentication using the new emerging EEG and ECG biometrics with the powerful deep neural networks.

## Data Availability

The adopted public PolyU multispectral palmprint database was downloaded from <http://www.comp.polyu.edu.hk/~biometrics/MultispectralPalmprint/MSP.html>.

## Disclosure

This paper is an extended version of an earlier conference paper: Research of Palmprint Authentication Arithmetic Based on Smartphone, in proceedings of the 2018 VII International Conference on Network, Communication and Computing, Taipei City, Taiwan, Dec. 14–16, 2018

## Conflicts of Interest

The authors declare no conflicts of interest.

## Acknowledgments

This work was supported in part by the National Natural Science Foundation under Grant 61673316 and in part by the project commissioned by the Sichuan Gas Turbine Research Institute of AVIC.

## References

- [1] L. Fei, G. Lu, W. Jia, S. Teng, and D. Zhang, "Feature extraction methods for palmprint recognition: a survey and evaluation," *IEEE Transactions on Systems, Man, and Cybernetics: Systems*, vol. 49, no. 2, pp. 346–363, 2019.
- [2] S. Zhao and B. Zhang, "Learning salient and discriminative descriptor for palmprint feature extraction and identification," *IEEE Transactions on Neural Networks and Learning Systems*, 2020.
- [3] D. Zhang and W. Shu, "Two novel characteristics in palmprint verification: datum point invariance and line feature matching," *Pattern Recognition*, vol. 32, no. 4, pp. 691–702, 1999.
- [4] W. K. Kong, D. Zhang, and W. Li, "Palmprint feature extraction using 2-D Gabor filters," *Pattern Recognition*, vol. 36, no. 10, pp. 2339–2347, 2003.
- [5] D. Zhang, Z. Guo, G. Lu, L. Zhang, and W. Zuo, "An online system of multispectral palmprint verification," *IEEE Transactions on Instrumentation and Measurement*, vol. 59, no. 2, pp. 480–490, 2010.
- [6] M. Aykut and M. Ekinci, "Developing a contactless palmprint authentication system by introducing a novel ROI extraction method," *Image and Vision Computing*, vol. 40, pp. 65–74, 2015.
- [7] X. Pan and Q. Ran, "Palmprint recognition using Gabor-based local invariant features," *Neurocomputing*, vol. 72, no. 7–9, pp. 2040–2045, 2009.
- [8] S. Fisher, F. Sroubek, L. Perrinet, R. Redondo, and G. Cristobal, "Self-invertible 2D log-gabor wavelets," *International Journal of Computer Vision*, vol. 75, no. 2, pp. 231–246, 2007.
- [9] P. Patil, S. Kolhe, and R. Patil, "The comparison of Iris recognition using principal component analysis, Log gabor and gabor wavelets," *International Journal of Computer Applications*, vol. 43, no. 1, pp. 29–33, 2012.
- [10] J. Tao, W. Jiang, Z. Gao, S. Chen, and C. Wang, "Palmprint recognition based on 2DPCA," in *Proceedings of the 9th Pacific Rim International Workshop on Multi-Agents*, pp. 455–462, Wuhan, China, August 2006.
- [11] M. Miura, S. Sakai, S. Aoyama, J. Ishii, K. Ito, and T. Aoki, "High-accuracy image matching using phase-only correlation and its application," in *Proceedings of the 51th Annual Conference Of Society Instrument And Control Engineers Of Japan*, pp. 307–312, Akita, Japan, August 2012.
- [12] M. Franzgrote, C. Borg, B. Ries et al., "Palmprint verification on mobile phones using accelerated competitive code," in *Proceedings of the 2011 International Conference On Hand-Based Biometrics*, pp. 124–129, Hong Kong, China, November 2011.
- [13] Y. Lee, N. Kim, H. Lim, H. Jo, and H. Lee, "Online banking authentication system using mobile-OTP with QR-code," in *Proceedings Of the 5th International Conference On Computer Sciences And Convergence Information Technology*, pp. 617–716, Seoul, South Korea, December 2010.
- [14] D.-J. Kim, K.-W. Chung, and K.-S. Hong, "Person authentication using face, teeth and voice modalities for mobile device security," *IEEE Transactions on Consumer Electronics*, vol. 56, no. 4, pp. 2678–2685, 2010.
- [15] M. Choras and R. Kozik, "Contactless palmprint and knuckle biometrics for mobile devices," *Pattern Analysis and Applications*, vol. 15, pp. 73–85, 2012.
- [16] Y. Hao, Z. Sun, T. Tan, and C. Ren, "Multispectral palm image fusion for accurate contact-free palmprint recognition," in



- Proceedings Of the 15th IEEE International Conference On Image Processing*, pp. 281–284, San Diego, CA, USA, October 2008.
- [17] C. Li, F. Liu, and Y. Zhang, “A principal palm-line extraction method for palmprint images based on diversity and contrast,” in *Proceedings Of the 3rd IEEE International Conference On Image And Signal Processing*, pp. 1772–1777, Yantai, China, October 2010.
- [18] F. Yue, W. Zuo, D. Zhang, and B. Li, “Fast palmprint identification with multiple templates per subject,” *Pattern Recognition Letters*, vol. 32, no. 8, pp. 1108–1118, 2011.
- [19] X. Zhang, K. Jing, G. Yan, X. Xu, and W. Gong, “Research of palmprint authentication arithmetic based on smartphone,” in *Proceedings of the International Conference On Network Communication And Computing.*, pp. 242–246, Taipei, Taiwan, December 2018.
- [20] W. Wang, J. Li, F. Huang, and H. Feng, “Design and implementation of Log-Gabor filter in fingerprint image enhancement,” *Pattern Recognition Letters*, vol. 29, no. 3, pp. 301–308, 2008.
- [21] X. Gao, F. Sattar, and R. Venkateswarlu, “Multiscale corner detection of gray level images based on log-gabor wavelet transform,” *Transactions on Circuits and Systems for Video Technology*, vol. 17, no. 7, pp. 868–875, 2007.
- [22] <https://www.phonearena.com/phones/>, 2018.
- [23] S. K. Kwok, J. S. L. Ting, A. H. C. Tsang, W. B. Lee, and B. C. F. Cheung, “Design and development of a mobile EPC-RFID-based self-validation system (MESS) for product authentication,” *Computers in Industry*, vol. 61, no. 7, pp. 624–635, 2010.
- [24] Z. Guo, W. Zuo, L. Zhang, and D. Zhang, “A unified distance measurement for orientation coding in palmprint verification,” *Neurocomputing*, vol. 73, no. 944–950, pp. 2359–2362, 2010.
- [25] M. Miao, W. Hu, H. Yin, and K. Zhang, “Spatial-frequency feature learning and classification of motor imagery EEG based on deep convolution neural network,” *Computational and Mathematical Methods in Medicine*, vol. 2020, Article ID 1981728, 13 pages, 2020.
- [26] M. Hammad, P. Plawiak, K. Wang, and U. R. Acharya, “ResNet-Attention model for human authentication using ECG signals,” *Expert Systems*, no. e12547, 2020.
- [27] M. Hammad, Y. Liu, and K. Wang, “Multimodal biometric authentication systems using convolution neural network based on different level fusion of ECG and fingerprint,” *IEEE Access*, vol. 7, pp. 26527–26542, 2019.
- [28] M. Hammad, S. Zhang, and K. Wang, “A novel two-dimensional ECG feature extraction and classification algorithm based on convolution neural network for human authentication,” *Future Generation Computer Systems*, vol. 101, pp. 180–196, 2019.
- [29] T. Fawcett, “An introduction to ROC analysis,” *Pattern Recognition Letters*, vol. 27, no. 8, pp. 861–874, 2006.
- [30] G. Michael, T. Connie, and A. Teoh, “Touch-less palm print biometrics: novel design and implementation,” *Image and Vision Computing*, vol. 26, no. 12, pp. 1551–1560, 2008.
- [31] J. Chen, Y.-S. Moon, M.-F. Wong, and G. Su, “Palmprint authentication using a symbolic representation of images,” *Image and Vision Computing*, vol. 28, no. 3, pp. 343–351, 2010.
- [32] A. Meraoumia, S. Chitroub, and A. Bouridane, “Palmprint and Finger-Knuckle-Print for efficient person recognition based on Log-Gabor filter response,” *Analog Integrated Circuits and Signal Processing*, vol. 69, no. 1, pp. 17–27, 2011.
- [33] W. Li, D. Zhang, and Z. Xu, “Palmprint identification by Fourier transform,” *International Journal of Pattern Recognition and Artificial Intelligence*, vol. 16, no. 4, pp. 417–432, 2002.
- [34] A. Kong, D. Zhang, and M. Kamel, “Palmprint identification using feature-level fusion,” *Pattern Recognition*, vol. 39, no. 3, pp. 478–487, 2006.

## Research Article

# A Method to Diagnose, Improve, and Evaluate Children's Learning Using Wearable Devices Such as Mobile Devices in the IoT Environment

Mohammad Moradi  and Kheirollah Rahsepar Fard

*Computer Engineering and Information Technology, University of Qom, Qom, Iran*

Correspondence should be addressed to Mohammad Moradi; [mohammad.moradi@alumni.ut.ac.ir](mailto:mohammad.moradi@alumni.ut.ac.ir)

Received 16 August 2020; Revised 30 September 2020; Accepted 21 October 2020; Published 30 October 2020

Academic Editor: Ondrej Krejcar

Copyright © 2020 Mohammad Moradi and Kheirollah Rahsepar Fard. This is an open access article distributed under the Creative Commons Attribution License, which permits unrestricted use, distribution, and reproduction in any medium, provided the original work is properly cited.

Every day we see an increasing tendency to use technology in education. In recent years, the impact of technology on the education process has received much attention. One of the important effects of technology is that it increases children's motivation and self-confidence and increases group collaboration. The purpose of this paper is to transform the traditional classroom into a modern classroom in order to increase the ease and efficiency of the teaching process. The method includes phases of diagnosis and improvement. In the diagnose phase, the classroom is equipped with modern items such as Internet of Things (IoT) and game-based learning. In the improvement phase, the field method is used to extract and weight the effective criteria in improving the educational status. The proposed method has been tested on two English language kindergartens. The children tested were in the age group of 8 to 10 years. In the implementation of the proposed educational method in the first English language kindergarten, the average improvement of education and learning of children has almost doubled, which has been maintained by doubling the number of children tested in the implementation of the proposed educational method in the second English language kindergarten. As a result, the proposed educational method can increase the learning performance of children.

## 1. Introduction

Childhood is one of the influential periods in human life. Childhood has a great impact on adulthood. During this time, the foundation of a healthy and prosperous life can be laid and many future problems can be prevented. Therefore, attention to children is essential [1–5]. Education is one of the basic principles of life. In the world, a person cannot be found not owing his or her basic and sophisticated performance to learning. Education is a set of decisions and actions that are taken to achieve specific goals [6, 7]. The importance of childhood education is in two aspects: one is the children's effectiveness and the other the profound effects of learning during this period. There is a relationship between intellectual growth and initial experiences of children. Benjamin Bloom believes that about 50% of the growth of intelligence is from birth to age 4, about 30%

between ages 4 and 8, and the remaining 20% between 8 and 17 years of age, which shows to pay special attention to childhood [8]. Therefore, addressing the issue of the child, especially the aspect of child education, is very necessary.

We live in a modern world of technology where technology directly or indirectly affects the daily life of every person. Research has shown that technology can enhance children's learning [9, 10]. There are several reasons for using technology in teaching and learning [11]:

- (1) One of the main reasons is that learners are interested in using technology and feel comfortable with these devices. They are more interested in using technology to learn.
- (2) The technology employs four components of learning: active participation, teamwork, frequent feedback, and interaction with real-world experts.

- (3) Provides learners with professional opportunities.
- (4) Technology has made it easier for teachers. They can specify course materials, submit automated online quizzes, and save time. Class management is easier and more efficient.
- (5) Technology provides an opportunity beyond the classroom. Learners can use the resources available on the Internet.
- (6) This technology helps learners do their homework using online systems. They can browse lesson videos and view other related resources.
- (7) This helps save resources and money. Technology can make teachers more efficient.

The purpose of this study is to transform the traditional classroom into a modern classroom in order to increase the ease and efficiency of the teaching process and thus improve children's learning performance. To this end, the classroom is equipped with IoT and game-based learning. These types of classes are implemented as an element of the IoT in the learning process instead of traditional learning. The method involves three phases of diagnosis, improvement, and evaluation. The questions of this research include the following:

- (1) Can using IoT in game-based learning increase children's motivation and learning rate?
- (2) Is it possible to extract and analyze children's communication and education network using IoT in game-based learning?
- (3) Do IoT and game-based learning scenarios increase cooperation and communication between children in the learning process?
- (4) Can the criteria presented based on each child's situation lead to an improvement in the learning process?

In the continuation of this paper, the items used in the proposed educational method, including IoT, selective dissemination of information (SDI), multiple attribute decision-making (MADM) such as interpretive structural modeling (ISM) and analytical hierarchy process (AHP), complex networks, centrality measures, and game-based learning, are briefly explained. In the next section, related works and their challenges are described. Then, the proposed educational method of training will be discussed with three phases of diagnosis, improvement, and evaluation. Then, the proposed method of teaching children is implemented and tested on a number of children, and the results are presented. Finally, the conclusions are explained.

## 2. Theoretical Framework

In this section, the items used in the proposed educational method, including IoT, SDI, MADM, complex networks, centrality measures, and game-based learning, are briefly described.

*2.1. IoT.* IoT is one of the new technologies that can help in information gathering and management. It was the term coined by Ashton in 1999. In IoT, other entities besides humans can connect to the Internet. Entities and objects will be able to automatically communicate and exchange needed data [12]. With IoT, all objects are interconnected that can be controlled and managed with the help of apps [13]. In fact, IoT is a new concept in the world of technology and communications that, as a modern technology, enables the transmission of data over communication networks for anything [14–16]. IoT has many applications in various fields and sciences, including education, smart city, smart farming, transportation, health, and energy [17–19]. In this study, objects are items such as educational cards and smartphones that children use to create connections between objects based on the communication and education they have. Figure 1 shows an example of the use of IoT in this study on the subject of child education. According to Figure 1, the objects are educational cards, smartphones, and laptops. During the educational game, children scan the educational cards using a smartphone, and the information from the educational game is sent to the laptop. According to the information obtained, the educator manages the children in order to improve their educational status.

Another example is the study of de la Guía. He has introduced a game in the study of e-books for children in the IoT environment. Puppet characters have been used to motivate children to read the book. Objects are smartphones and puppet characters. By bringing his/her favorite character closer to the smartphone, in each part of the story of the book, the child can determine the continuation of the story with his/her favorite character. As shown in Figure 2, fictional characters can be defined on objects such as toys (with an NFC chip) or other NFC cards such as a subway card.

As another example, Figure 3 shows a child interacting with an owl robot in the IoT environment to enhance language skills. The objects used are owl robots and shapes (prints or three-dimensional objects). The child hears the name of the shape as he/she approaches it to the owl robot. This helps the child to learn language skills.

*2.2. Game-Based Learning.* The game is an activity that the child does willingly. The reason for this is it arises from inner tendencies. When done, it makes the child happy. Here are some important features to consider:

- (i) The game is innate.
- (ii) The game depends on the needs, talents, and abilities of the player.
- (iii) Playing is a physical, mental, and verbal activity with imagination, thinking, and imitation.
- (iv) The game is fun and entertaining.

According to these characteristics, play is not only a matter of wasting excess energy, wasting time, and preventing congestion but also has many important effects on the well-being of children and the development of children's thinking, imagination, accuracy, and creativity [22].



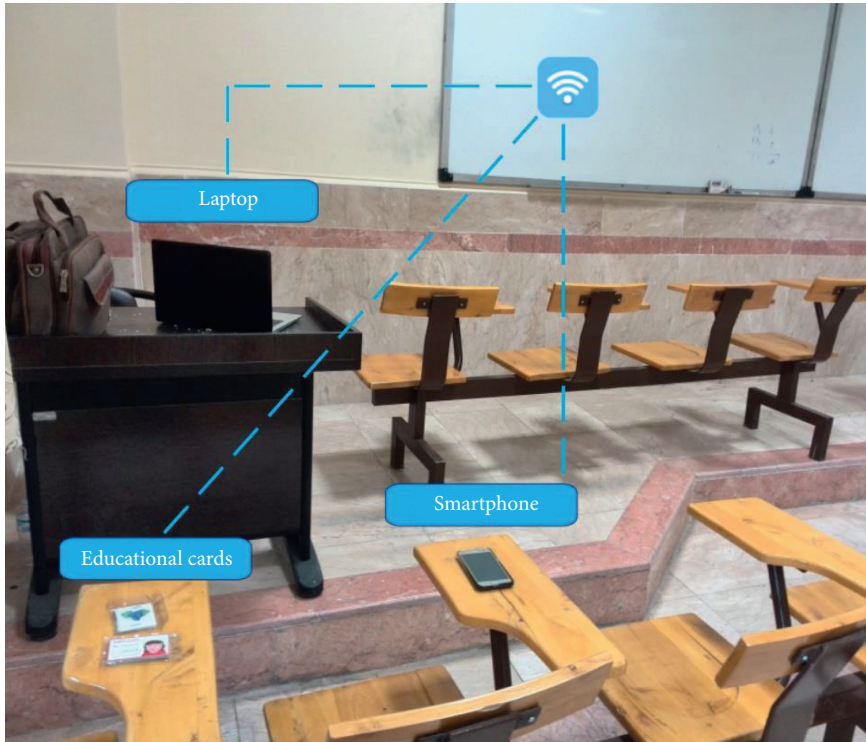


FIGURE 1: An example of the use of IoT in this study on child education.

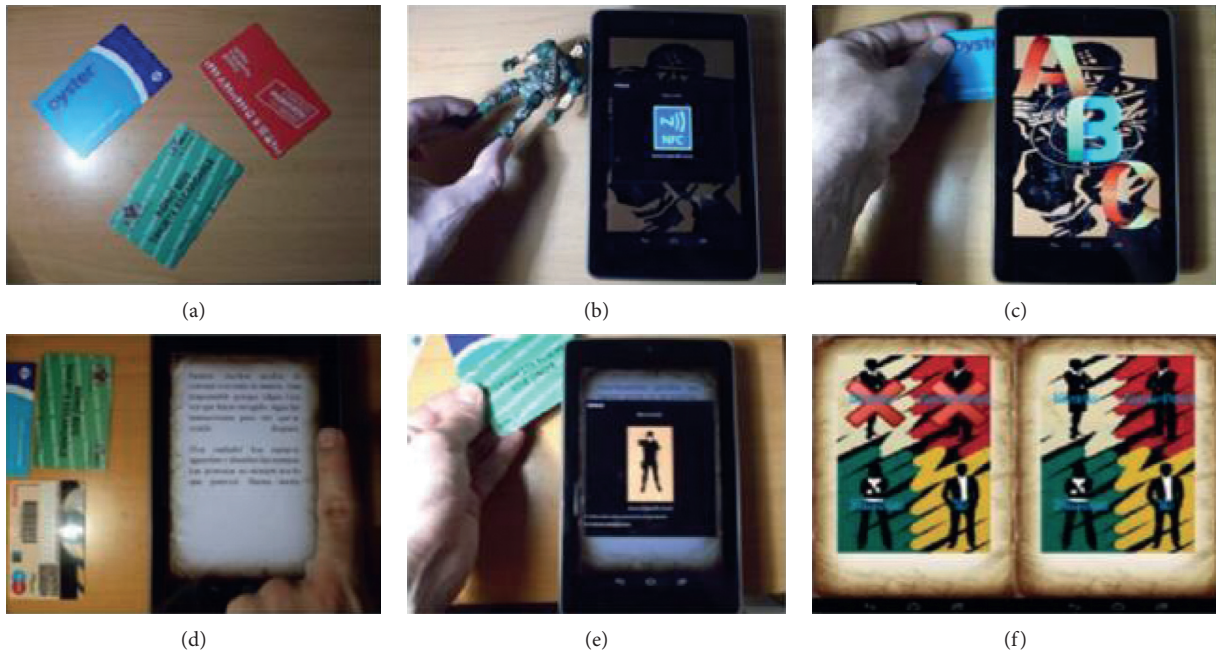


FIGURE 2: An example of presenting a game in the study of e-books for children in the IoT environment [20].

One of the most popular teaching methods is game-based learning. Game-based training is an educational game that uses game elements to learn a specific skill or reach a specific output [23]. Educational games are suggested to increase motivation and thereby improve learning processes [24]. The motivational psychology involved in

game-based learning allows students to engage with educational materials in a playful and dynamic way. Game-based learning is not just creating games for students to play, it is designing learning activities that can incrementally introduce concepts and guide users towards an end goal [25].



FIGURE 3: An example of a child interacting with an owl robot to enhance language skills in the IoT environment [21].

**2.3. SDI.** SDI is a form of presenting and transmitting information, using the search, and sending information required by each user individually, regularly, and continuously [26]. Users identify topics of interest, and new information related to each user's interest is sent separately. The field of new information is usually characterized by words and terms. This is usually done regularly and at specified intervals. In general, the purpose of SDI is to provide, organize, select, and disseminate information to individuals and organizations on a regular basis according to their predetermined needs. The SDI system always keeps a person informed of new developments in his or her field. The SDI system is an information service and an information item, but it is not like a newspaper or magazine to provide everyone with the same information and equality. The list of information for each individual is distinct and personalized. Whatever is sent to anyone depends on their interests and needs. Understanding the interests and needs of users and providing relevant, up-to-date, and timely information to meet their needs are the requirements of information dissemination [27]. O'Neil provides two main reasons for addressing information services [28]:

- (1) Increasing information: information is growing exponentially, and users' time to search for their needs and interests is very limited. The information service solves this problem.
- (2) Increasing specialization in all disciplines of knowledge leads to information on a subject being available from multiple sources. Information in a source may also be sporadic. The information service helps to capture and aggregate them into a single form.

SDI input is keywords. In this study and in the discussion of education, the key words are the educational status of children.

**2.4. MADM.** MADM techniques are widely used in many different fields. The reason for this is the ability and capability of these methods to model real issues and make them

simple and understandable for most users. In making these decisions, several criteria may be used instead of one. MADM has a variety of decision-making techniques [29]. In this study, attributes are effective criteria in improving the learning and educational status of children.

**2.4.1. AHP.** One of the most efficient decision-making techniques is the AHP first introduced by Thomas L. Saaty in 1980. This technique was proposed for modeling the decision process, based on pairwise comparisons, allowing managers to examine different scenarios. AHP can be applied to a variety of industrial, commercial, financial, and political applications, and so on [29]. AHP has also been used in education. Anggrainingsih, for example, uses AHP to determine the success factor of e-learning in higher education based on the user's perspective [30]. Effective criteria in improving children's educational and learning status are weighed through AHP to identify criteria with higher priority.

**2.4.2. ISM.** ISM analyzes the relationship between the criteria at several different levels. ISM is able to determine the relationship between criteria that are individually or in-group interdependent. The ISM technique steps are identifying the variables related to the problem, filling out the questionnaire and forming the structural self-interaction matrix (SSIM), forming the primary reachability matrix, forming the final reachability matrix, surface segmentation, modeling, penetration power analysis, and the degree of dependency [29]. The ISM technique is used to identify which criteria in the education process can be effective in improving other criteria.

**2.5. Complex Networks and Centrality Measures.** A complex network is a set of entities (nodes) that are interconnected. Complex network analysis is one of the most useful items in examining the relationships between entities [31]. Centrality measures are one of the most important metrics in analyzing complex networks. Centrality is the descriptive characteristic of actors or groups of actors with multiple structural and parametric determinants for understanding and analyzing their roles in complex networks [32]. Centrality measures are often used to identify powerful, influential, or important actors [33]. The most widely accepted definition of centrality was introduced by Freeman in the late 1970s. Because of their location, they have better access to information and a better opportunity to spread information. In general, centrality is a concept used for network analysis and has different types. Depending on the purpose and definition of the problem, one or more centrality is used. The greater the centrality of an entity, the higher the rank, the more the communication, and the more favorable the position. The centrality measures of different networks are based on several indicators, the most important of which are degree centrality, closeness centrality, betweenness centrality, page rank centrality, and so on. Studying the structure of networks can help you make better decisions. In this study,



complex networks and centrality measures have been used to identify each child's educational status and which children can be effective in improving the process of educating other children.

**2.5.1. Degree Centrality.** The degree centrality measure is one of the network metrics or indicators that is useful in analyzing the network structure and positions of entities (nodes) in the network. The degree centrality refers to the number of connections a node has in a network [34]. This measure is related to the position of the nodes in a network and is the number of direct relationships a node has to the network. The degree centrality for each node in the network is measured by counting the number of connections that a node has in the network. In a network graph in this study, nodes are children and links are relationships between children, and degree centrality is calculated by counting the number of connections each child has with other children. The node with the highest degree is the central node in the degree centrality measure [35]. Actors who have a higher centrality have more opportunities and positions than other actors. The absolute degree centrality of the node  $v_i$  is obtained by the following formula [36]:

$$c_D(i) = \text{degree of vertex } i. \quad (1)$$

The relative degree centrality of node  $v_i$  can be calculated by the following formula:

$$C_D(i) = \frac{c_D(i)}{n-1}, \quad (2)$$

where  $n-1$  is the largest possible degree of a network with  $n$  nodes.

**2.5.2. Closeness Centrality.** In some cases, those nodes may be of interest, located close to the other nodes of the network. These nodes disseminate information in fewer steps on the network. This type of centrality is called closeness centrality. The closeness centrality of node  $v_i$  can be calculated by the following formula [36]:

$$C_i = \frac{n}{\sum_j d_{ij}}, \quad (3)$$

where  $n$  is the number of network nodes and  $d_{ij}$  is the shortest distance between node  $v_i$  and node  $v_j$ .

### 3. Related Works

In this section, research and related works done in the use of modern technologies to enhance the child's learning (by increasing the motivation of the child to learn and increase the ease of learning of the child) are discussed. The purpose of this section is to examine the research conducted on the use of technology in the educational process in order to identify the scientific gap that exists in this field.

Abdi and Cavus have created an affordable, sustainable, and safe educational toy for prekindergarten children between the ages of 4 and 5 for teaching English language as a

second language in developing countries. This toy is made with Raspberry Pi and uses RFID technology [37].

Higgins et al. explore the impact of digital technologies on children's learning. The purpose of this study is to provide some evidence on the impact of digital technologies on academic achievement. The purpose of this study is to identify the future investment implications of using digital technology for learning in schools [38].

Safar et al. discuss the effectiveness of using augmented reality applications as a teaching and learning item when instructing kindergarten children the English alphabet in the State of Kuwait. The study concludes with relevant proposals and recommendations regarding the implementation of AR technology in education [39].

Sadiq et al. created an educational application that can be run on a mobile phone based on the principles of user interface design using voice recognition engines to convert text into speech, which will help children learn English language [40].

Uzelac et al. have extracted the parameters that influence students' focus during lectures using IoT. The main purpose is to identify the parameters that significantly influence the students' focus of lectures. Several parameters have been measured in a real classroom environment using inexpensive smart devices. The study is based on data collected from 14 lectures attended by 197 students. After the experiments, 5 parameters that had significant effect were finally extracted [41].

Manches et al. have designed three questions about IoT and children. Research shows how digitizing objects such as toys can influence children's attitudes and behavior and thus educate children and affect children's daily activities [42].

Zhamanov et al. combine IoT with gaming. They state that it is difficult today to motivate students with traditional ways. In this article, the authors examine the classroom equipped with modern items such as IoT and gaming. They implement these types of classes as an element of IoT for the learning process rather than traditional learning. The authors compare the IoT-equipped classroom with the traditional methods. The results show that the modern classroom method is better than the traditional classroom with a difference of approximately 20% increase in average attendance, laboratory work, tests, midterm exams, and final exams [43].

Spyrou et al. use IoT in the game. A learning goal is set, and the way to achieve it is divided into several tasks, called learning atoms, that are realized as serious games. The user impact status is constantly monitored by devices such as cameras and microphones. A learning goal, for example, counting, is considered. The learning goal is broken down into several learning atoms. For example, in the learning objective of counting, it is divided into learning atoms larger or smaller in numbers, and so on. Then, a learning game is designed for each of the learning atoms. The level of the game is commensurate with the level of learning and user status [44].

Tangworakitthaworn et al. deal with the game-based learning system for plant monitoring based on IoT technology. A new approach, synchronization between the three

main components of real plant care, game-based learning, and IoT technology, is discussed. A game-based learning system has been introduced, and empirical investigations of satisfaction with the use of suggested games in practical use have been reported. The innovation of this proposed game is that players must complete the level of play by taking care of the actual plant. There are three key components, namely, game-based learning, plant monitoring, and IoT technology, that work together to achieve game results [45].

de la Guía et al. present an e-book for children. Doll characters have been used to increase children's motivation to read books. By approaching each of their favorite characters in each part of the story, the children can determine the continuation of the story with their favorite character [20].

Li et al. examine the use of games to teach serious subjects such as math to 7- to 8-year-old children. In this study, an exploratory experiment is reported to examine how the various interaction techniques (digital screen-touch interaction vs. real-world tangible interaction) and the different feedback mechanisms in mathematics education for children are affected. Results show that diegetic feedback led to the game being considered significantly more enjoyable, as well as inducing greater feelings of competence and autonomy; screen-touch interaction versus tangible interaction did not change motivation directly nor did find interaction effects between the presentation and interaction modes. After analyzing the results, recommendations for increasing the motivation of serious games for children are suggested [46].

de la Guía et al. explore the impact of using IoT to help teachers strengthen social and classroom interactions. IoT-based systems have been developed to improve motivation, collaboration, and learning in schools. The system is made up of three main components: the home screen (user interface), which shows training tasks, activity, feedback, results, and so on; the wearable device; and the smart object commonly used by NFC sensors. Also, in order to work with the system for teaching English language, according to a word that appeared on the home screen, students would have to search for the relevant object right around the classroom and place it near the wearable device to select it. However, it is difficult for the teacher to control the classroom. To improve the use of this system, new functions and data for teachers have been provided to a web application. The teacher can interact with the system and students through a platform (smartphone, tablet, and laptop). Based on student behavior, the teacher can immediately send a message to control, increase participation and motivation, and encourage cooperation among students. 40 students aged 9–12 years, and 5 teachers participated in the study. The study was conducted in two Spanish classrooms. The results were very positive. 100% of students responded positively to messages sent by teachers [47].

López-Faican and Jaen evaluate the use of mobile-based multiplayer games for primary school children. A game scenario that can be used to improve communication skills and emotional intelligence in children is evaluated. In this research, two applications of this type of games are considered: (1) competition against the common game; (2) game using mobile technology that creates a geographical scenario

with unlimited physical space. The results show that both modes of play create positive emotions such as enthusiasm, pleasure, and curiosity in children. In addition, it has been observed that joint play has a greater impact on emotional affection, social interaction, and interest. In addition, it was observed that the quality of communication in the participatory mode is good in terms of various factors such as maintaining mutual understanding, dialogue management, information collection, reaching consensus, time management, and interaction. In this study, several methods have been proposed in the design of game time management, competitive and participatory modes, dynamic 3D content, and active learning [26]. The table in Appendix summarizes the relevant research based on the researchers' names, year of publication, brief description, and results.

In the following, the challenges of related works as well as proposed solutions to the challenges are presented as the output of this research:

- (i) Boring educational methods have been used in most related works to educate the child. In childhood, the most important interests of children are games, which the child does with a tendency and lack of boredom. The proposed educational method is to use games (which are appealing to children) to teach them.
- (ii) In related works, effective criteria for children's education have not been extracted, and the education of children has been taken into account regardless of the criteria that affect them which was not the expected performance. In the proposed educational method, it is attempted to extract and measure the criteria influencing children's education and the importance of each criterion through MADM techniques.
- (iii) Individual education is usually used in related works and children's pedagogy, and using other children to motivate and learn from each other is not intended, which is the case in the proposed educational method.
- (iv) In related works, the child communication network and the issue of networking (learning by using influential children in the network or the so-called charismatic to increase motivation) and the level of education of other children have not been addressed. In the proposed educational method, this issue will be addressed by using complex networks and centrality measures.
- (v) Given the high volume of information and the difficulty in selecting the right information, the necessary solutions and communication with parents and child caregivers are not considered. This has been considered using SDI in the proposed method.

#### 4. Research Methodology

Today, it is difficult to motivate students with traditional methods. The purpose of this paper is to transform the

traditional classroom into a modern classroom in order to increase the ease and efficiency of the teaching process and thus improve children's learning performance. The method includes phases of diagnosis and improvement. In the diagnose phase, the classroom is equipped with modern items such as IoT and game-based learning. These types of classes are implemented as an element of the IoT in the learning process instead of traditional learning. In the improvement phase, the field method is used to extract and weight the effective criteria in improving the educational status. The techniques used are AHP and ISM. The data collection tool in this phase is a questionnaire from experts. The proposed method has been tested on two English language kindergartens. The number of participants in the first English language kindergarten is 3 children, and the number of participants in the second English language kindergarten is 6 children. The children tested were in the age group of 8 to 10 years.

## 5. Proposed Educational Method

In this section, the proposed educational method, which includes three phases of child status diagnosis, improvement, and evaluation, is described. In order to increase the attractiveness of the educational process for children, an educational game is provided. The IoT has been used to extract communication networks and training from educational games. Centrality measures have been used to analyze networks and identify children's educational status in the phase of recognizing the proposed educational method. In the phase of improving the educational situation of children, MADM techniques have been used. SDI has been used to inform about the child's status, provide solutions, and communicate with the child's parents.

*5.1. Proposed Educational Game.* In this section, the steps of the proposed game in the IoT environment are presented. The steps of the proposed game are as follows:

- (1) The division of educational materials into  $n$  sections (where  $n$  is the number of children).
- (2) The allocation of each educational section for a child.
- (3) The division of each of the  $n$  sections into  $m$  components to make it easier for the child to learn.
- (4) Teaching the assigned section of each child to him/her by the instructor.
- (5) Two types of cards are provided for each child with the following details:
  - (a) Identification card: this card contains the child's details such as the child's name. Behind the cards, there is the NFC tag or the child's own QR code.
  - (b) Educational card: the child-assigned section, divided into  $m$  components, is written on educational cards with pictures (to enhance visual style). There are  $m$  different cards of this type. For example, in English language teaching, educational materials can be animal vocabulary. These words are divided into  $n$  sections where  $n$  is the number of children. In the example mentioned, the sections can be aquatic animals, insects, and so on. Then, each section is divided into  $m$  components. For example, the insect section is divided into the words "ant" and "bee," which are written on the educational cards along with the image. Behind the cards, there is the NFC tag or the child's own QR code.
- (6) Children are asked to come together and teach educational cards in accordance with the following rules:
  - (a) When child  $i$  refers to child  $j$ , child  $i$  gives the child identification card to child  $j$  and child  $j$  after scanning the NFC tag or QR code (by NFC reader or QR code reader that can be an NFC-equipped smart bracelet or smartphone reader or QR code) returns it to child  $i$ .
  - (b) Then, child  $i$  teaches the educational cards to child  $j$ .
  - (c) If teaching is successful, child  $i$  will give that card to child  $j$  and child  $j$  will return it to child  $i$  after scanning the NFC tag or QR code.
- (7) After a specified time, the game ends.
- (8) After the game is over, the educational materials and cards listed on each child's training list are tested to determine if the child has learned them correctly. If a child has not been successful, that educational card will be removed from the list of successful trainings.
- (9) Children receive scores based on the number of successful training taught to other children and the number of training that has been successfully learned.

Figure 4 shows how to divide educational materials into sections and components and assign them to children (steps 1 to 5 of suggested play).

Through the sixth step of the game, a multilayer network is formed. One layer is the children's communication network with each other and the other is the children's education network with each other. The nodes in both layers are children. The links in the communication network represent the communication of the children, and in the education network, the children teach each other. The rules for forming networks are as follows:

- (i) Whenever child  $i$  refers to child  $j$  for teaching, a directed link from child  $i$  to child  $j$  is drawn on the communication network. Children's references to each other can be detected by scanning the NFC tag or QR code on each child's identification card.
- (ii) Whenever child  $i$  successfully teaches child  $j$ , a directional link from child  $i$  to the child trained, i.e., child  $j$ , is drawn to the education network.
- (iii) When a child learns several trainings from another child or teaches several trainings to another child,

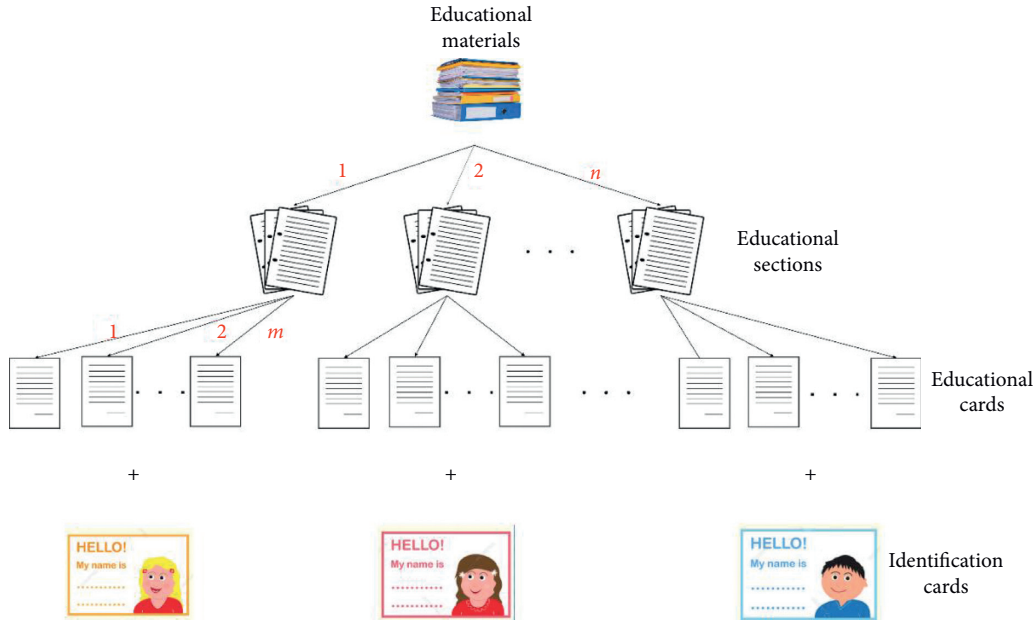


FIGURE 4: Dividing educational materials into educational sections and cards.

the education network link will receive weight on the number of trainings.

- (iv) Children are free to choose who to teach or from whom to learn.

Figure 5 shows an example of the layers of the communication and education networks from the proposed training game. The nodes in both networks are children, and the education network links are a subset of the communication network links.

**5.2. The Technical Part of IoT in the Proposed Method.** As mentioned in the previous section, two types of introduction cards and training cards have been prepared for the educational game. To implement the IoT system, the cards are equipped with the NFC or QR code. Smart bracelets or smartphones equipped with an NFC reader or QR reader code are used for scanning. Figure 6 shows the technical components of the IoT system for extracting the communication network and the education network from the educational game.

As shown in Figure 6, NFC or QR code and wearable devices for scanning them are the main components of the IoT system used in the proposed game. Near-field communication (NFC) is a set of standards in portable devices that allows you to establish peer-to-peer radio communication, which results in the exchange of data by putting them together or pasting them together. NFC is a means of transmitting data over radio waves. From this point of view, it is similar to WiFi and Bluetooth, but it is much faster than Bluetooth and connects two devices by creating an electrical circuit. The NFC data exchange frequency is 13.566 MHz. NFC has evolved from radio frequency identification (RFID) and is compatible with most high-frequency RFID-related standards. However, NFC is designed to be used only at close range to prevent RFID from being turned on remotely.

Quick response code (QR) is a square code. Unlike NFC, QR codes do not have any electrical components or do not require special hardware technology. QR codes are the only type of black and white code printed on paper that can be scanned and decrypted using wearable devices such as smartphones.

Wearable devices can be defined as a technology that uses devices that can be placed on the human body. Wearable technologies can be in the form of a smart bracelet, watch, shoes, shirt, hat, necklace, glasses, and more. These smart devices have sensors that collect raw data and can analyze the collected data.

**5.3. The Diagnostic Phase of the Child's Status.** In this section, the status of children is diagnosed based on the analysis of the communication network and education network from the educational game. Complex network analysis and centrality measures are used to identify important network nodes (which are children) and to divide children into different categories. The following labels can be considered based on the analysis of the communication network:

- (i) High input communications: these nodes which have a high input degree of the communication network are actually children who have been referred to by a large number of educators. Other children have a great deal of interest in communicating with these children. These children are called charismatic.
- (ii) Low input communications: nodes that have a low input degree centrality in the communication network. In fact, there are very few children who go to train them. These children may be malicious or lack good social interaction and may not be interested in other children.



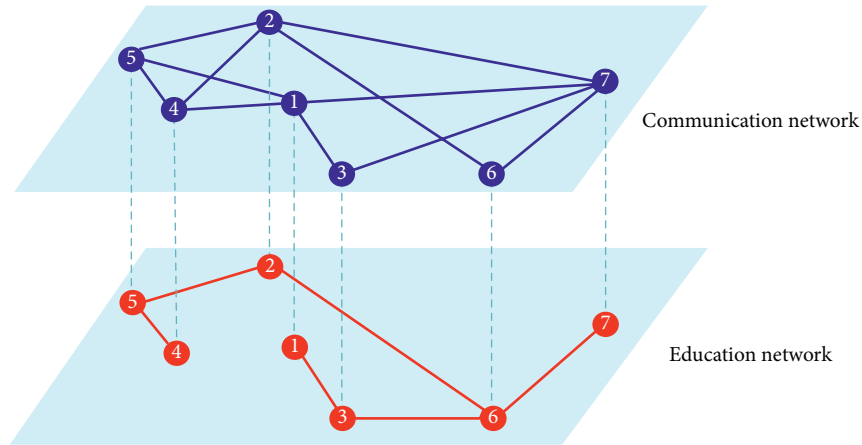


FIGURE 5: An example of a multilayer network consisting of the proposed training game.

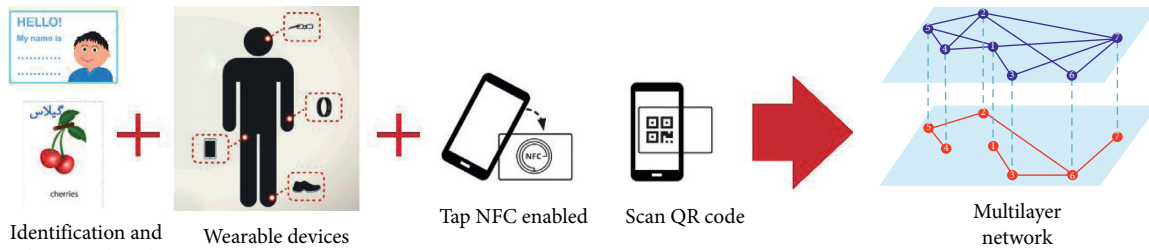


FIGURE 6: Technical components of the IoT system for extracting the communication network and the education network from the educational game.

- (iii) High output communications: nodes that have a high output degree centrality in the communications network. In fact, children who have gone to many children for teaching. These children communicate well with almost all children.
- (iv) Low output communications: nodes that have a low output degree centrality in the communications network. In fact, children who have trouble communicating with other children.

The following labels can also be considered based on the education network analysis:

- (i) High teaching: nodes that have a high output degree centrality in the education network. In fact, children who have been able to teach many children successfully. These children have a great ability to educate and consider the criteria of education.
- (ii) Low teaching: nodes with low output degree centrality in the education network. In fact, children who have failed to teach other children well. Two states are possible for this case. Children had low output communication and therefore no teaching or the children had no low output communication but were not successful in teaching. This can be diagnosed by examining other categories in which the child is placed.
- (iii) High learning: nodes that have a high input degree centrality. In fact, children who have been able to successfully learn from other children.

- (iv) Low learning: nodes that have low input degree centrality. There are two possible cases for this. Children had low input communication in the communication network and consequently low learning occurred or the children had no low input communication but were not successful in learning.

Categories can be defined based on the combination of labels (both labels on the same network and labels on two different networks). Here are some of the most important categories:

- (1) High output communications, high teaching: these children have both referred to many children for teaching and have been successful in their teaching.
- (2) High output communication, low teaching: these children although have referred to many children for teaching have not been successful in teaching.
- (3) High input communications, high learning: many of the children have referred to teach them and they have been successful in the learning process.
- (4) High input communications, low learning: although many have referred to teach these children, they have had low learning. This shows that regardless of the educator and the type of education the learning of these children is low. For example, they may have low focus and accuracy.



- (5) Low output communications, high input communications: although many have come to teach these children, they have found it difficult to communicate with other children to teach their educational cards.
- (6) Low output communications, low input communications: these children have had difficulty communicating with other children whether for teaching or learning.
- (7) High output communications, high input communications: these children have been successful in social interaction and communication.
- (8) High output communications, low input communications: these children had no difficulty in communicating with other children for education, but other children were reluctant to communicate and educate.
- (9) High teaching, high learning: these children have been successful in both teaching and learning.
- (10) High teaching, low learning: these children were good educators but not good learners.
- (11) Low teaching, high learning: these children were not good educators, but they were good learners.
- (12) Low teaching, low learning: these children have been neither successful in teaching nor learning.
- (13) Low output communications, low teaching: these children have had difficulty in communicating with other children for teaching, so they have failed in teaching.
- (14) Low input communications, low learning: because few children have come to teach these children, little has been learned.

Each child can be into one or more categories, which can be used to determine the final status of the child based on the categories of the child. For example, in the category of “low teaching, low learning,” these children may have difficulty in communicating and therefore no education. If these children are also in the category of “low output communication, low input communication,” this is true. Also, considering other centrality such as closeness centrality in the communication network, we can diagnose children who are able to teach and disseminate information and educational materials on the network more quickly and give them educational sections that must be taught quickly.

*5.4. Improvement Phase.* This section outlines the strategies needed to improve the child education process. In the following, the solutions are expressed according to labels and categories.

*5.4.1. Categories including “High Teaching”.* If we want to teach a particular educational section to most children, it is best to give it to these children. Because these children interact with many children and are successful in teaching.

*5.4.2. Categories including “High Input Communications”.* These children are charismatic because many tend to go to them. Therefore, it is important to consider which other categories these children fall into. If they were in the category of “low output communication” or “low teaching,” communication and teaching of these children should be strengthened in order to educate a wide range of children. How to improve teaching is described in detail in Section 5.4.4.

*5.4.3. Categories including “Low Output Communications” or “Low Input Communications”.* These children’s communication skills need to be strengthened so they can learn or teach educational materials.

*5.4.4. Categories including “Low Teaching”.* This section deals with the improvement of children in the categories including “low teaching.” The following can also be applied to the early process of instructor-to-child teaching (teaching of the educational section allocated to the child by the instructor). By studying articles, books, and queries from experts, child teaching criteria were extracted. Criteria of the child teaching process are as follows:

- (1) Morality and respect
- (2) Providing motivation and interest for learning
- (3) Mastering the subject of teaching
- (4) Patience
- (5) Ability to transfer essential content
- (6) Appearance decoration
- (7) Using modern teaching tools and methods
- (8) General knowledge of educational materials
- (9) Assessment based on educational purpose
- (10) Learner participation
- (11) Learner satisfaction from the teacher
- (12) The form and structure of the educational content
- (13) Being objective
- (14) In-game training
- (15) Discipline

Then, a questionnaire was designed to find the effective criteria, and experts were asked to determine the importance of each of the criterion in the child teaching process. In designing the questionnaire, linguistic variables were used which were converted into five-scale Likert. It should be noted that Cronbach’s alpha coefficient for the questionnaires of the importance of child teaching criteria was 0.788 which confirms its reliability. According to the experts’ opinion, the criteria above the weighted average were selected as the effective criteria as shown in Figure 7.

Next, we used the ISM technique to investigate which criteria may underlie other criteria and to investigate the influence and dependence. Figure 8 shows the levels of effectiveness criteria extracted in the child teaching process based on the ISM technique.

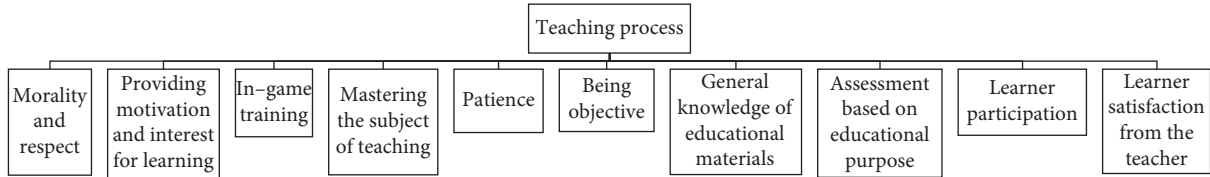


FIGURE 7: Hierarchical chart of effective criteria in the child teaching process.

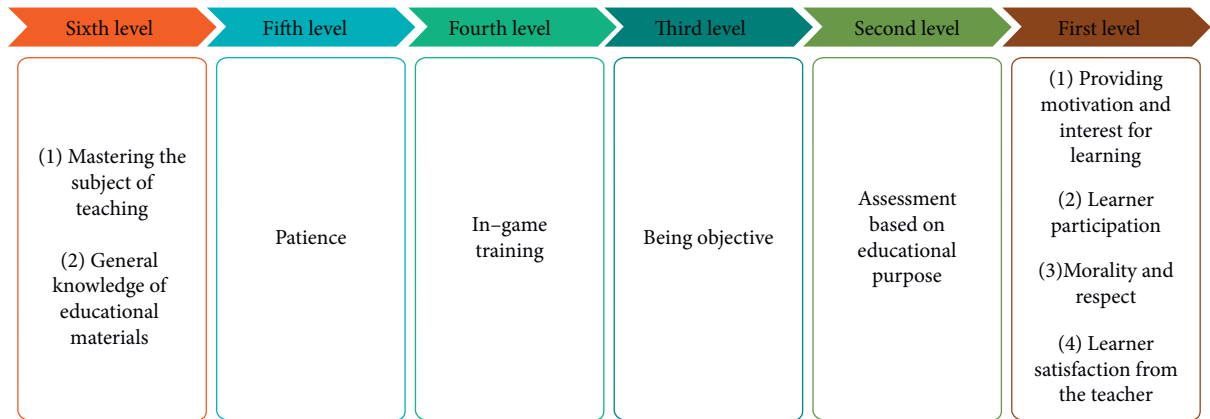


FIGURE 8: Levels of effective criteria extracted in the child teaching process based on the ISM technique.

Figure 9 shows the MICMAC diagram of effective criteria of the child teaching process in the ISM model based on the degree of dependency and influence.

The AHP technique was used to weight the effective indicators extracted in the child teaching process. Table 1 and Figure 10 show the weight and priority of the criteria. It should be noted that the inconsistency rate was 0.02301 which confirms the reliability of the AHP questionnaires because it is less than 0.1.

As it can be seen from Table 1 and Figure 10, “in-game training” has been ranked first for the child teaching process. The next rankings are “providing motivation and interest for learning,” “mastering the subject of teaching,” “morality and respect,” “being objective,” “learner participation,” “general knowledge of educational materials,” “learner satisfaction from the teacher,” “patience,” and “assessment based on educational purpose.”

5.4.5. *Categories including “Low Learning”.* This section deals with the improvement of children in the categories including “low learning.” The following can also be applied to the early process of instructor-to-child education. By studying articles, books, and queries from experts, child learning criteria were extracted. Criteria of a child’s learning process include the following:

- (1) Preparation and health of body and mind
- (2) Purpose and motivation
- (3) Past experiences
- (4) Learning environment

- (a) Acoustic and thermal relaxation, use of nature, open spaces, and so on.
- (b) Class arrangement (color and light)
- (6) Practice
- (7) Attention and focus
- (8) Discipline
- (9) Pay attention to learning style
- (10) Intelligence
  - (a) Hormones
  - (b) Nutrition
- (11) Bonus and rewards
- (12) Parental participation
- (13) Organization of contents
- (14) Find the main theme of each topic

Then, a questionnaire was designed to find effective criteria, and experts were asked to determine the importance of each criterion in the child’s learning process. In designing the questionnaire, linguistic variables were used which were converted into five-scale Likert. It should be noted that Cronbach’s alpha coefficient for the questionnaires of the importance of child learning criteria was 0.724 which confirms its reliability. According to the experts’ opinion, the criteria above the weighted average were selected as the effective criteria as shown in Figure 11.

Next, we used the ISM technique to investigate which criteria may underlie other criteria and to investigate the degree of influence and dependence. Figure 12 shows the

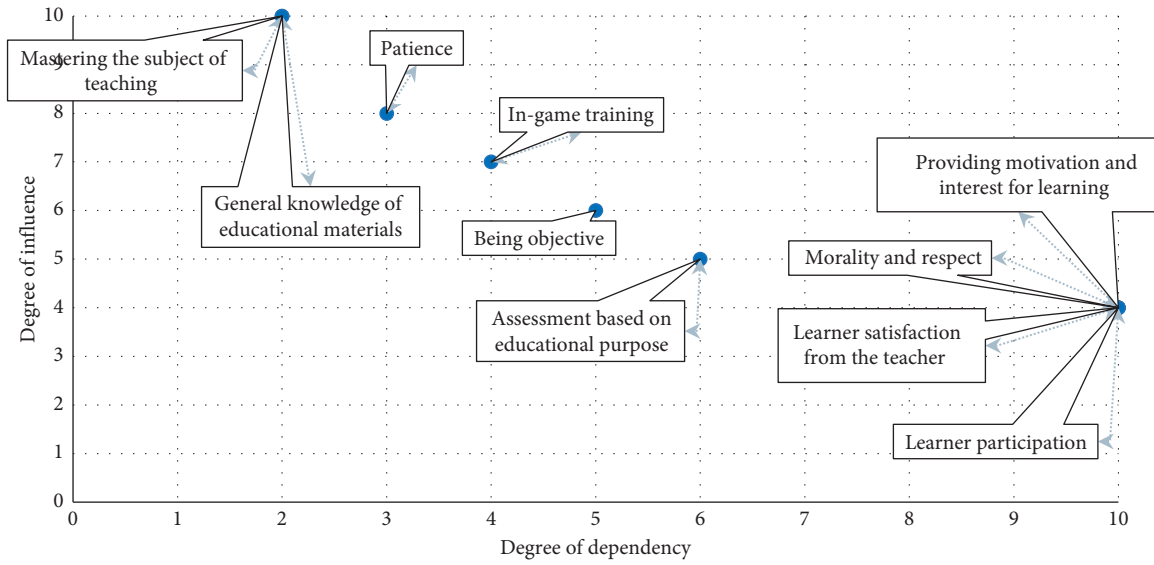


FIGURE 9: MICMAC diagram of effective criteria of the child teaching process in the ISM model.

TABLE 1: Weight and priority of effective criteria extracted in child teaching process based on the AHP technique.

Priority	Criterion name	Criterion weight
1	In-game training	0/18439
2	Providing motivation and interest for learning	0/13472
3	Mastering the subject of teaching	0/12615
4	Morality and respect	0/09784
5	Being objective	0/08697
6	Learner participation	0/08481
7	General knowledge of educational materials	0/08183
8	Learner satisfaction from the teacher	0/07968
9	Patience	0/0732
10	Assessment based on educational purpose	0/0504

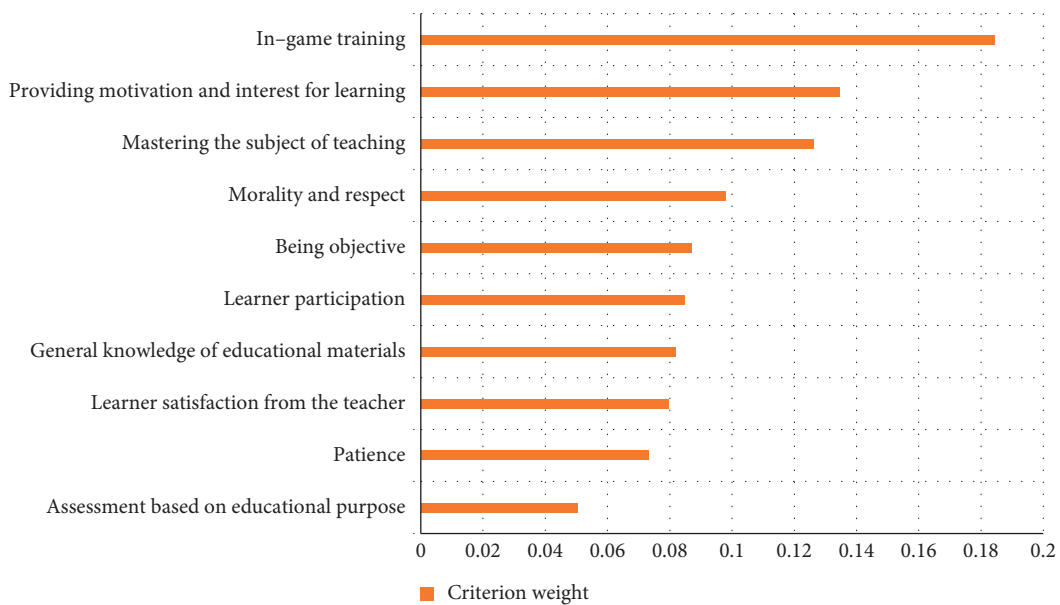


FIGURE 10: Weight chart of the effective criteria extracted in the child teaching process based on the AHP technique.

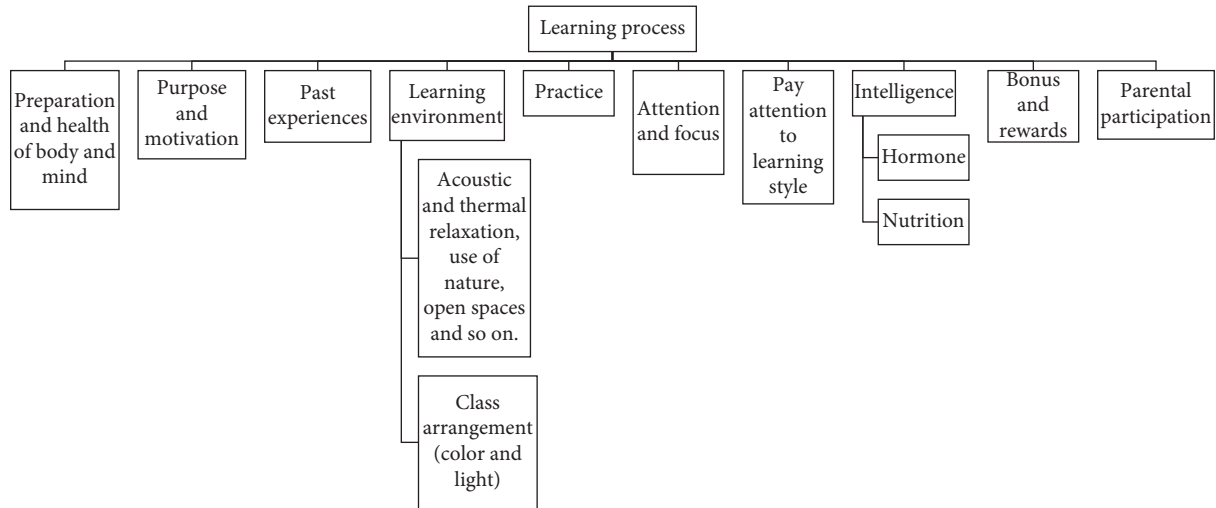


FIGURE 11: Hierarchical chart of effective criteria in the child's learning process.

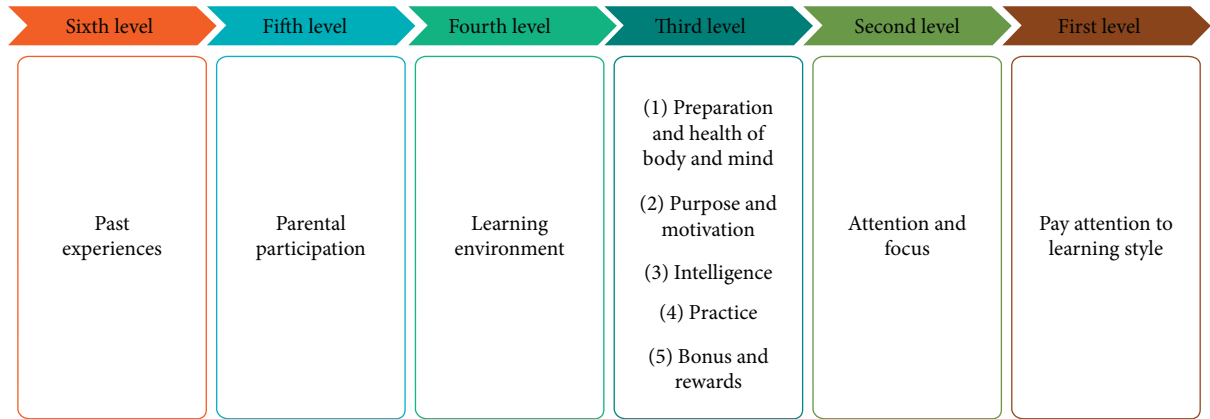


FIGURE 12: Levels of effective criteria extracted in the child learning process based on the ISM technique.

levels of effectiveness criteria extracted in the child learning process based on the ISM technique.

Figure 13 shows the MICMAC diagram of the effective criteria of the child's learning process in the ISM model based on the degree of dependency and influence.

The AHP technique was used to weight the effective criteria extracted in the child's learning process. Table 2 and Figure 14 show the weight and priority of the criteria. It should be noted that the inconsistency rate was 0.0229 which confirms the reliability of the AHP questionnaires because it is less than 0.1.

As it can be seen from Table 2 and Figure 14, for the child's learning process, the "purpose and motivation" has been ranked first. The next rankings are "practice," "preparation and health of body and mind," "attention and focus," "intelligence," "parental participation," "learning environment," "pay attention to learning styles," "past experiences," and "bonus and rewards." Also, based on the "learning environment" criterion, the subcriterion "acoustic and thermal relaxation, use of nature, open spaces, and so on" with a weight of 0.564 ranked first, and the subcriterion

"class arrangement (color and light)" with a weight of 0.436 ranks second.

5.4.6. *Children with High Closeness Centrality in the Communication Network.* These children are able to teach and disseminate information and educational materials more quickly on the network, so that materials that must be taught quickly can be allocated to them for teaching.

5.4.7. *Using SDI System.* One of the things that can help improve the education process for children is the use of SDI. In the SDI system, required documents and content are entered as keywords, and the system notifies the user of the matching documents using keywords and matching functions. Therefore, depending on what labels the child receives and in which category, the keywords to improve the child's educational performance can be selected and entered into the SDI system. In addition to the guidelines outlined in this study to improve the child's educational process, articles, books, etc., related to the child labels and category, will be

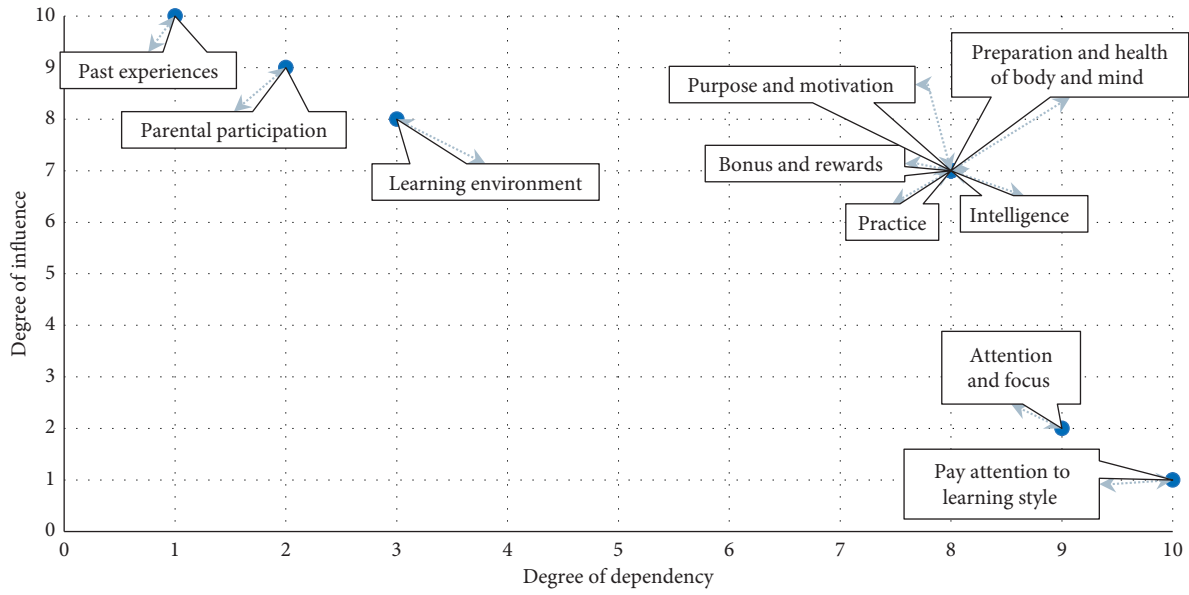


FIGURE 13: MICMAC diagram of effective criteria of the child's learning process in the ISM model.

TABLE 2: Weight and priority of effective criteria extracted in the child learning process based on the AHP technique.

Priority	Criterion name	Criterion weight
1	Purpose and motivation	0/22504
2	Practice	0/11879
3	Preparation and health of body and mind	0/10942
4	Attention and focus	0/10274
5	Intelligence	0/08824
6	Parental participation	0/08151
7	Learning environment	0/07514
8	Pay attention to learning style	0/07282
9	Past experiences	0/07093
10	Bonus and rewards	0/05537

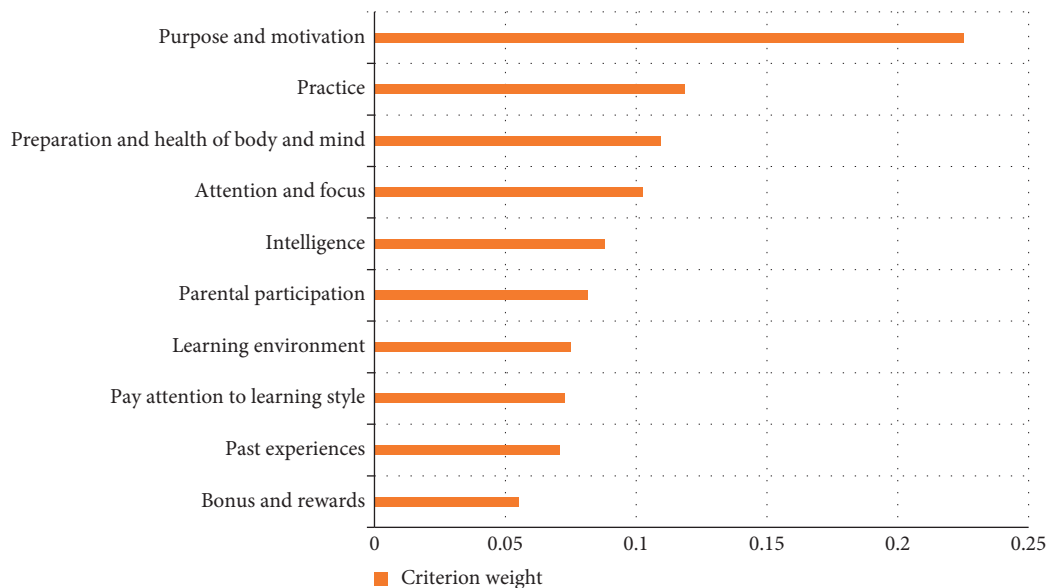


FIGURE 14: Weight diagram of effective criteria extracted in the child learning process based on the AHP technique.



sent to the caregiver. Keywords can be entered into the SDI system in two ways:

- (1) Manually: in this case, educators alert the child's status to his/her parents, and they select the keywords and enter them into the SDI system according to the child's status.
- (2) Automatically using IoT: in this case, the objects are interconnected and do not require human intervention. This way the labels and categories where the child is placed are converted into keywords and sent to the SDI system. The SDI system also sends matching documents to child caregivers after matching keywords with documents.

*5.4.8. Parents and Their Impact on Children's Education and Performance.* As stated in the proposed educational method and previous sections, the diagnostic status of each child and the most up-to-date strategies and content are sent to the child's parents. Also, in order to communicate properly, parents should pay attention to the following points:

- (1) Parents should have a friendly relationship with their children so that they can implement the proposed solutions with high efficiency.
- (2) In order to improve the status of their child, parents should keep the family environment away from any conflicts and tensions.
- (3) Parents should interact with mentors while using the solutions provided and use their advice.
- (4) Parents should be careful not to go to extremes in applying the proposed solutions. The child's activities during the week should be divided and given a specific time for fun, watching TV, and doing homework.
- (5) Parents should try to reduce children's fear of failing to do what is suggested.
- (6) In the modern world, parents are involved in many different things, and they may not have enough time to raise their children. It is important to note that parents should not only pay attention to the duration but also to the quality. Parents can make the most of their time despite their small presence. That is, the quality of communication is important.

*5.5. Evaluation Phase.* In this section, the methods of evaluating children's educational progress after the proposed educational method and strategies are discussed. For evaluation, the game is repeated, and the multilayer networks of communication and education are extracted. Two local and general measures can then be used to measure children's educational progress as described below.

*5.5.1. Local Measures.* These measures are used to evaluate the educational progress of each child separately. Suggested measures are as follows:

- (1) Comparison of the input degree of each node (child) from the initial communication network with the input degree of that node from the secondary communication network.
- (2) Comparison of the output degree of each node (child) from the initial communication network with the output degree of that node from the secondary communication network.
- (3) Comparison of the input degree of each node (child) from the initial education network with the input degree of that node from the secondary education network.
- (4) Comparison of the output degree of each node (child) from the initial education network with the output degree of that node from the secondary education network.
- (5) Comparison of the distance of input degrees of each node (child) from the initial communication network with the complete communication network.
- (6) Comparison of the distance of output degrees of each node (child) from the initial communication network with the complete communication network.
- (7) Comparison of the distance of input degrees of each node (child) from the initial education network with the complete education network.
- (8) Comparison of the distance of output degrees of each node (child) from the initial education network with the complete education network.

*5.5.2. General Measures.* This measure is used to evaluate the level of educational improvement of all children. Suggested measures are as follows:

- (1) Comparison of the average degrees of the initial communication network with the average degrees of the secondary communication network.
- (2) Comparison of the average degrees of the initial education network with the average degrees of the secondary education network.
- (3) Comparison of the distance between the average degrees of the initial communication network with the average degrees of the complete network.
- (4) Comparison of the distance between the average degrees of the initial education network with the average degrees of the complete network.

*5.6. Diagram of the Proposed Educational Method.* In Figure 15, the diagram of the proposed method is plotted. Rectangles are inputs and outputs, and processes are written in front of them.

## **6. Implementation and Testing of the Proposed Educational Method**

This section tests the proposed educational method in two English language kindergartens. The number of children

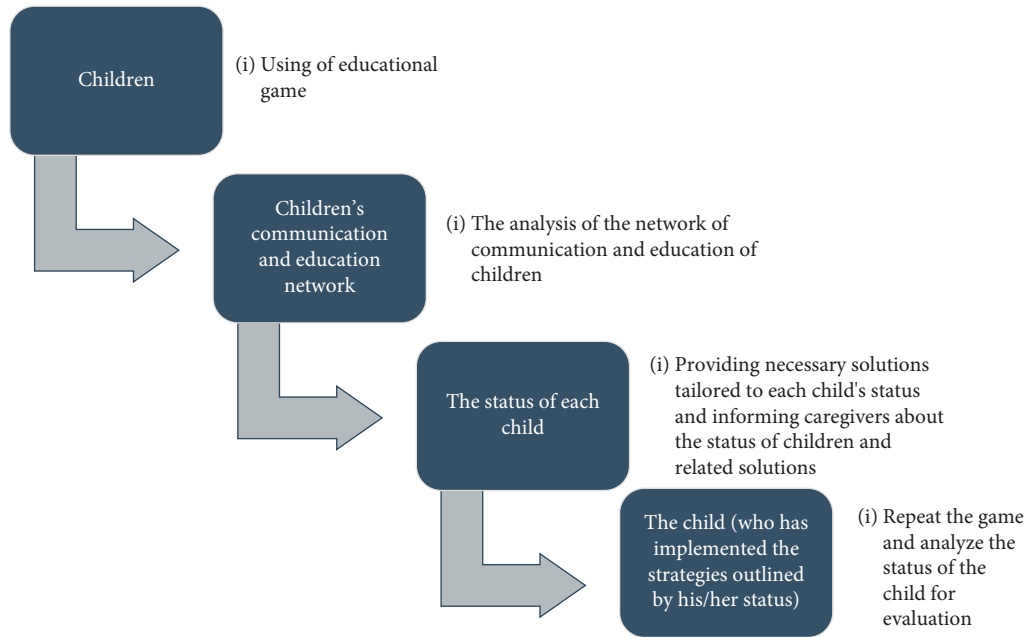


FIGURE 15: Diagram of the proposed educational method.

tested in the first English language kindergarten was 3 ( $n = 3$ ), and the number of children tested in the second English language kindergarten was 6 ( $n = 6$ ). In total, the proposed educational method has been tested on 9 children. According to reference [48], this number has been approved. Also, all necessary permissions have been obtained from parents and the responsible person of the kindergarten. The children ranged in age from 8 to 10 years. In consultation with the instructor, two topics were new to the selected children for the experiment. Topics were planets and fruits.

According to the game-based learning, the educational game was designed. The educational game was such that each child was taught an English word by the instructor and assigned to the child ( $m = 1$ ). The children had to refer to each other and teach their English word to other children. Children received points based on words they had successfully taught or learned. Also, in order to identify the children's communication network, another card was considered as an identification card. Figure 16 shows the identification and educational cards.

IoT was used to extract the communication and education networks. The identification and educational cards were equipped with a QR code for each child. Each child scanned the QR code of the identification card when referring to other children to teach English words. Also, if he was able to successfully teach his word to another child, he would scan the QR code of that child's educational card. Figure 17 shows an example of a QR code scan of the cards.

Figure 18 shows part of the educational play between children in the first and second English language kindergartens.

From scanning QR codes and identification and educational cards, communication and education networks were formed. Figure 19 shows an example of a system output

matrix related to the network resulting from the educational game.

Complex networks and centrality measures were used to analyze the communication and education networks from the educational game. The child's status was determined based on the number of communications each child had with the other children and the number of words the child was able to teach successfully.

MADM techniques including ISM and AHP which were mentioned in the proposed educational method were used to provide solutions based on the status of each child. At the end, the educational game was performed again after presenting the solutions. The communication and education networks obtained from the first and second experiments were compared in order to evaluate the improvement of the children's educational status.

## 7. Results

In this section, the improvements of the proposed educational method are discussed. Figure 20(a) shows the communication network from the results of the first experiment, and Figure 20(b) shows the education network from the results of the first experiment in the first English language kindergarten.

Because the number of nodes in the communication network is 3, each node can have a maximum of 2 input links and 2 output links. According to the proposed educational method, nodes with less than half of the total number of input and output links are designated as low-communication children for teaching and learning. According to Figure 20(a), a child with low communication was not identified. In the education network, nodes that have at least half the maximum number of input links can be identified as weak learners. According to Figure 20(b), child 1 is identified as a weak



FIGURE 16: Identification and educational cards for testing.

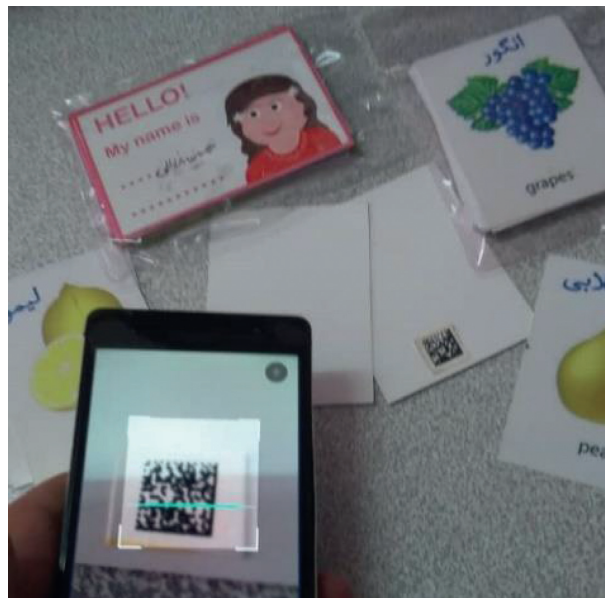


FIGURE 17: Example of scanning QR codes of cards.

learner (due to the number of input links less than 1). Also, in the education network, nodes with less than half the maximum possible number of output links are designated as a weak educator. According to Figure 20(b), child 2 was identified as a weak educator (due to the number of output links less than 1).

After analyzing the communication network and the education network obtained from the first experiment and using the solutions, the second experiment was performed with the second topic. Figure 21(a) shows the communication network from the results of the second experiment, and Figure 21(b) shows the education network from the results of the second experiment in the first English language kindergarten.

Table 3 compares the performance of each child and their evaluation (according to the local and general

evaluation measures expressed in the previous sections) based on the results of the first and second experiments.

Figure 22 shows the child performance diagrams in the education network from the first and second experiments in the first English language kindergarten.

As can be seen in Figure 22, child learning rate 1 and child teaching rate 2 increased in the second experiment compared to the first experiment.

The proposed educational method was also tested on another English language kindergarten with 6 children. Figure 23(a) shows the communication network from the results of the first experiment, and Figure 23(b) shows the education network from the results of the first experiment.

Then, these networks are analyzed, and the solutions described are discussed. For example, according to Figure 23(a), child 1 had low communication with other



FIGURE 18: Part of the educational game between children in the first and second English language kindergartens.

	1	2	3	4	5	6	7	8	9	10
1	0	0	0	0	0	0	0			
2	0	0	1	1	0	0				
3	0	1	0	1	1	1				
4	1	1	1	0	1	1				
5	1	0	0	1	0	1				
6	0	1	1	1	1	0				
7										
8										
9										
10										
11										
12										
13										
14										
15										
16										
17										
18										
19										
20										
21										

FIGURE 19: An example of a network output matrix from the educational game.

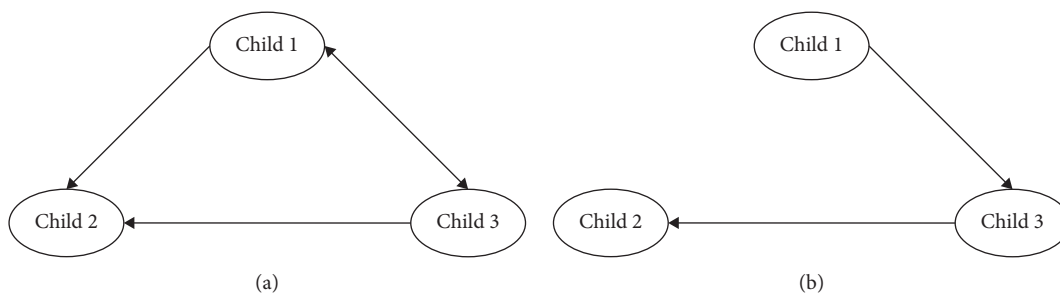


FIGURE 20: (a) Communication network from experiment 1; (b) education network from experiment 1.

children (he did not go to teach other children and only two children referred him for teaching) resulting in low education for this child. This child was placed in the category of low input and output communication and tried to improve his communication skills. Child 4 has referred to all children to teach, and all children except child 1 have turned to him to

teach. This child was placed in the high input and output communication category and was identified as a charismatic child. But this child, according to Figure 23(b), has not been very successful in the teaching and learning process, despite having high referrals. Therefore, due to the charisma of this child, it was tried to reinforce his teaching and learning skills



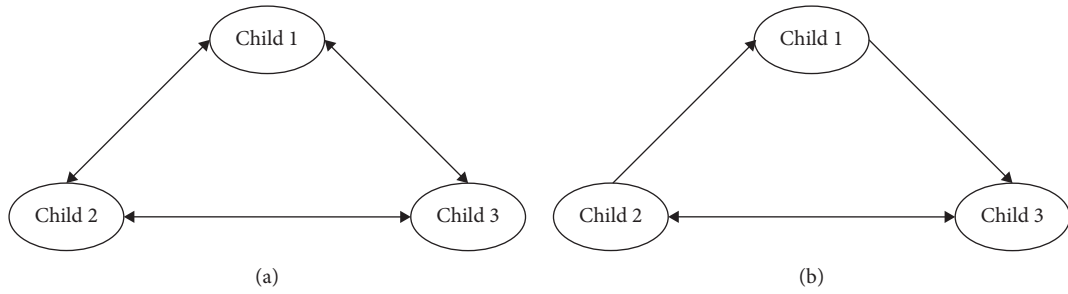


FIGURE 21: (a) Communication network from experiment 2; (b) education network from experiment 2.

TABLE 3: Children’s performance in the first and second experiments in the first English language kindergarten using local and general measures.

Experiment number	Type of measure	Child	Number of words learned	Number of words taught
Experiment 1	Local measure	Child 1	0	1
		Child 2	1	0
		Child 3	1	1
	General measure	Average for all children	0.66	0.66
Experiment 2	Local measure	Child 1	1	1
		Child 2	1	2
		Child 3	2	1
	General measure	Average for all children	1.33	1.33

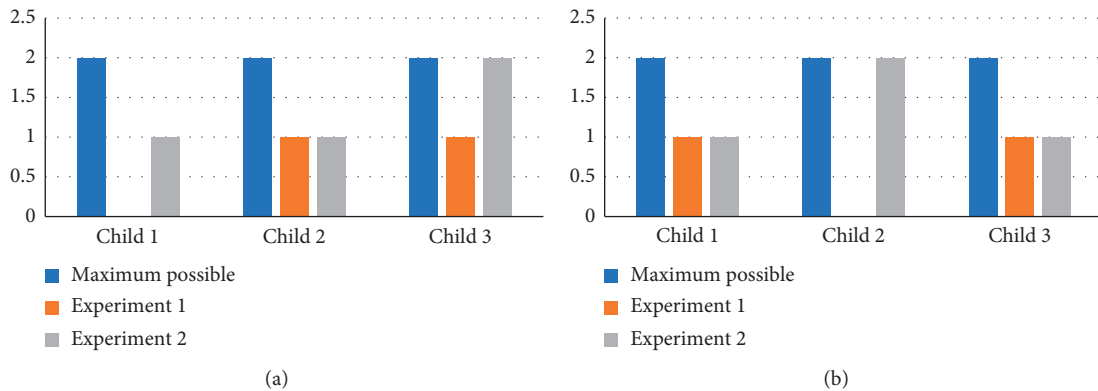


FIGURE 22: Child performance diagrams in the education network from experiments 1 and 2 in the first English language kindergarten. (a) Number of words learned. (b) Number of words taught.

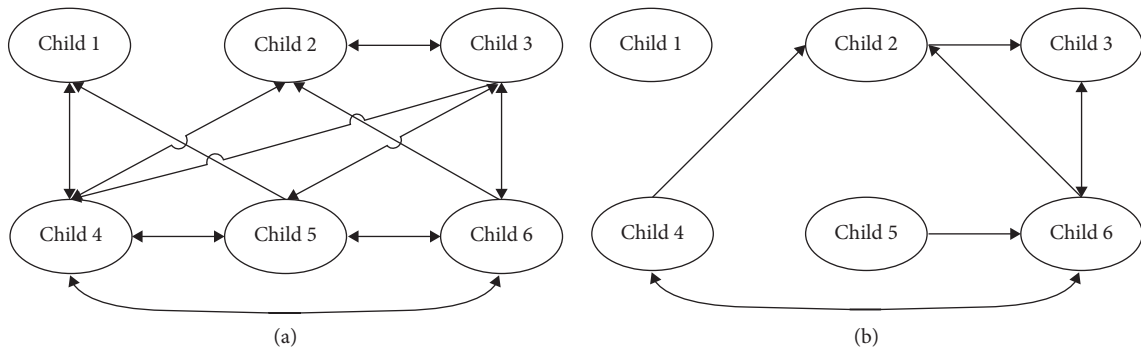


FIGURE 23: (a) Communication network derived from the first experiment; (b) education network derived from the first experiment.



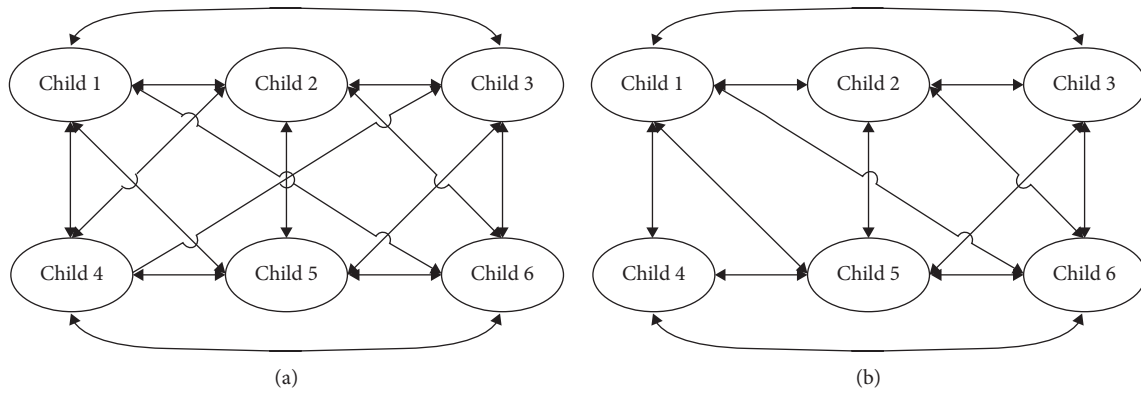


FIGURE 24: (a) Communication network derived from the second experiment; (b) education network derived from the second experiment.

TABLE 4: Evaluation of children's performance in experiments 1 and 2 in the second English language kindergarten using local and general measures.

Experiment number	Type of measure	Child	Number of input communications	Number of output communications	Number of words learned	Number of words taught
Experiment 1	Local measure	Child 1	2	0	0	0
		Child 2	3	2	2	1
		Child 3	3	4	2	1
		Child 4	4	5	1	2
		Child 5	3	3	0	1
		Child 6	3	4	3	3
	General measure	Average for all children	3	3	1.33	1.33
Experiment 2	Local measure	Child 1	5	5	2	5
		Child 2	5	5	4	1
		Child 3	5	5	4	1
		Child 4	5	5	2	3
		Child 5	5	5	2	4
		Child 6	5	5	3	3
	General measure	Average for all children	5	5	2.83	2.83

so that his referrals to others and those referring to him could be effective in teaching more vocabulary. Also, according to Figure 23(b), child 6 had better learning. We tried to identify the criteria that helped him in the learning process and reinforce it in other children.

After analyzing the communication and education networks obtained from the first experiment and applying the strategies, the second experiment was conducted with the second subject. Figure 24(a) shows the communication network from the results of the second experiment, and Figure 24(b) shows the education network from the results of the second experiment.

Table 4 compares the performance of each child and their evaluation based on the results of the first and second experiments.

Figure 25 shows the results of the child performance diagrams in the communication and education networks obtained from the first and second experiments.

As can be seen from Table 4 and Figure 25, we can observe a good improvement of children in the teaching and

learning process. Also, as can be seen in Table 3, in the implementation of the proposed educational method in the first English language kindergarten, the rate of improvement of education and learning of children according to the general measure has almost doubled (from 0.66 to 1.33), which is proportional to the doubling of the number of children tested in the implementation of the proposed educational method in the second English language kindergarten, which has also been maintained (from 1.33 to 2.83), which can be seen in Table 4. Therefore, we can expect the compatibility of the results of the proposed educational method for different populations. Table 5 shows the percentage of children's learning in the first and second experiments in the first and second English language kindergartens.

Other advantages of the proposed educational method include the following:

- (1) Games are attractive for children, so using games to teach children can be very effective and useful. It is difficult for the teacher to control the children,

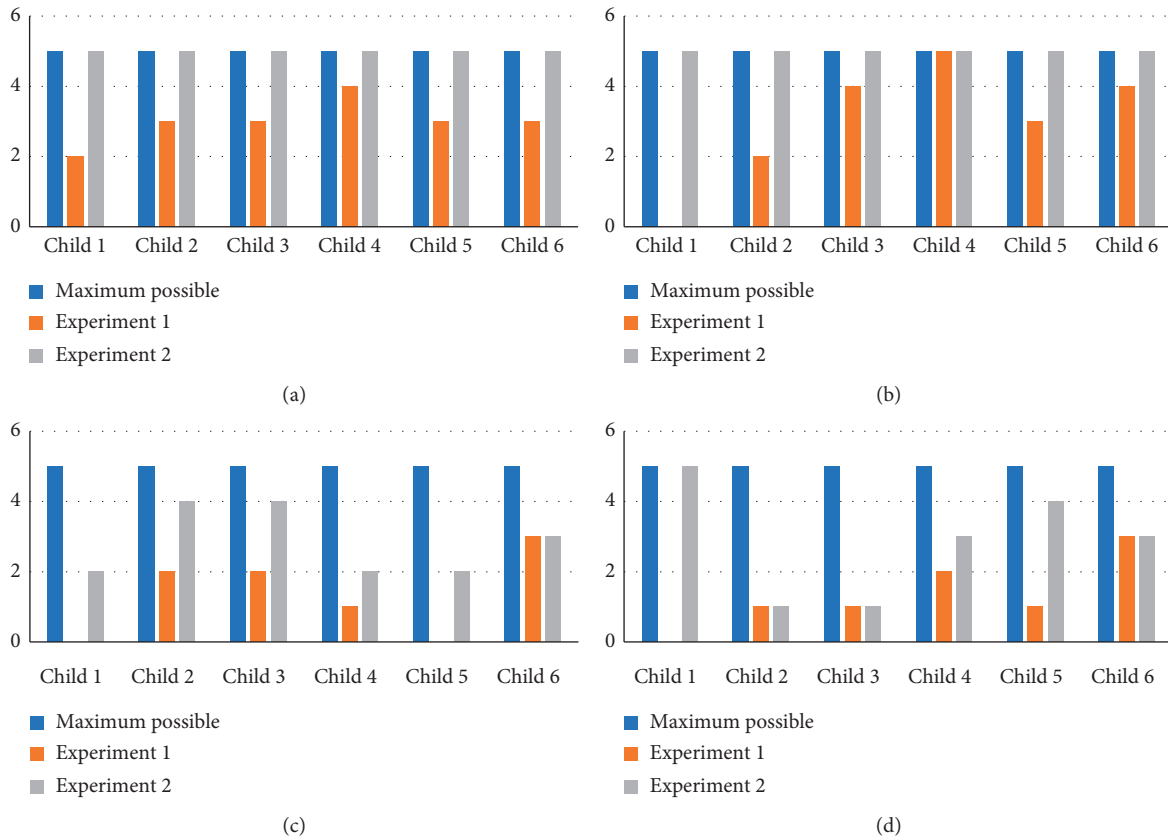


FIGURE 25: Child performance diagrams in the communication and education networks from experiments 1 and 2 in the second English language kindergarten. (a) Number of input communications. (b) Number of output communications. (c) Number of words learned. (d) Number of words taught.

TABLE 5: Percentage of children’s learning in the first and second experiments in the first and second English language kindergartens.

Study	Experiment number	Vocabulary gains (%)
Proposed method, English language kindergarten 1	Experiment 1	33
	Experiment 2	66.5
Proposed method, English language kindergarten 2	Experiment 1	26.6
	Experiment 2	56.6

TABLE 6: Related work summaries based on researchers’ name, year of publication, brief description, and results.

Name of researchers	Year of publication	Brief description	Results
López-Faican	2020	This study evaluates the use of mobile-based multiplayer games for primary school children. In this research, two applications of this type of games are considered: (1) competition against the common game; (2) game using mobile technology that creates a geographical scenario with unlimited physical space.	The results show that both modes of play create positive emotions such as enthusiasm, pleasure, and curiosity in children. It has been observed that joint play has a greater impact on emotional affection, social interaction, and interest. In addition, it was observed that the quality of communication in the participatory mode is good in terms of various factors such as maintaining mutual understanding, dialogue management, information collection, reaching consensus, time management, and interaction.

TABLE 6: Continued.

Name of researchers	Year of publication	Brief description	Results
Abdi	2019	This study examines the creation of an affordable, sustainable, and safe educational toy for prekindergarten children between the ages of 4 and 5 for teaching English language as a second language in developing countries.	The findings of this study show that the developed toy can be suitable for use as an educational toy for prekindergarten children to teach English language as a second language.
Sadiq	2019	Creating an educational application that can be run on a mobile phone based on the principles of user interface design using voice recognition engines to convert text to speech, which will help children learn English language.	The opinions of a group of children showed that they were happy to use the developed application. Furthermore, it can be said that the mobile application achieved its aims in teaching English as a foreign language and that the application is suitable as an educational item. Results show that diegetic feedback led to the game being considered significantly more enjoyable, as well as inducing greater feelings of competence and autonomy; screen-touch interaction versus tangible interaction did not change motivation directly nor did find interaction effects between the presentation and interaction modes.
Li	2019	In this paper, an exploratory experiment is reported to examine the impact of different interaction techniques and different feedback mechanisms in mathematics education for children.	The modern classroom method is better than the traditional classroom with a difference of approximately 20% increase in average attendance, lab work, tests, midterm exams, and final exams.
Zhamanov	2018	The study looked at the combination of IoT and gaming and examined a classroom equipped with modern items such as IoT and gaming.	
Spyrou	2018	In this research, the use of IoT in the game is discussed. A learning goal is set, and the path to that goal is divided into several tasks called learning atoms, which are designed for each game.	Increasing learning motivation
Tangworakitthaworn	2018	In this research, a game-based learning system for plant monitoring based on IoT technology has been designed.	Increasing the motivation to learn and care for plants
de la Guía	2018	It discusses the impact of using IoT to help teachers strengthen social interactions and classroom interactions.	It enables teachers to gain a deeper insight into their classroom. The teacher can interact with the system and students in real time. Based on student behavior, the teacher can immediately send a message to control, increase participation and motivation, and encourage cooperation among students.
Safar	2016	This experimental research study scrutinized the effectiveness of using augmented reality applications as a teaching and learning item when instructing kindergarten children in the English alphabet in the State of Kuwait.	Very strong linear correlation between children's interaction with English alphabet lesson and their scores in the English alphabet test of children using these applications.
Uzelac	2015	The parameters that affect the students' focus during the lecture are extracted using IoT.	After the experiments, 5 parameters that had a significant effect on students' concentration were finally extracted.
Manches	2015	Three questions have been designed about the IoT and children. This study examines these questions according to the IoT.	Digitizing everyday objects, such as toys, can influence children's attitudes, behavior, and thus educate children and affect children's daily activities.
de la Guía	2014	An e-book for children is presented. Doll characters have been used to increase children's motivation to read books.	Increasing the motivation to read books
Higgins	2012	First, an overview of extensive research on the impact of technology on learning to determine the rationale for the value of this information is provided. The next section examines evidence from research analysis of the impact of digital technology. The other part looks at the process of using digital technology and learning in the UK and the international world to provide more context for the necessary recommendations.	(i) Technology sharing (in pairs or small groups) is usually more effective than individual use. (ii) Technology can be used as a centralized intervention to improve learning. (iii) Technology should be used as a supplement to conventional education rather than as a substitute.

especially in games, due to their high mobility. Using the IoT technology discussed in the proposed educational method, it is possible to extract the communication network and the education network from the educational game automatically and without the need for teacher control.

- (2) In traditional methods, the network of communication and education of children is not extracted and analyzed. In the proposed educational method, using the knowledge of complex networks and centrality measures, different status of children has been identified in order to strengthen their learning process. More importantly, this analysis can be done in real time while extracting networks through IoT technology, which can help the teacher identify the status of children in the shortest possible time, especially in high-node networks.
- (3) In traditional methods, identifying the most up-to-date content and strategies to improve a child's diagnosed status is either not done or will take a long time. In the proposed educational method, using SDI, the teacher and parents will get the most up-to-date information and strategies to improve their child's diagnosed status in the shortest possible time. Also, in the proposed method, using SDI, it is possible to choose how to access this information (using social networks, e-mail, and mobile phone), the number of contents and documents, the author of the content, the time of publishing the content, etc., for parents and teachers which will increase the ease and efficiency that did not exist in traditional methods.
- (4) In the proposed educational method, all steps from identifying the children's status, providing solutions and evaluation, are done automatically and in the shortest possible time, which will increase ease, accuracy, and efficiency, which was not possible with traditional methods.

## 8. Discussion

The results showed that the proposed educational method can improve children's communication in the educational process. By improving communication, children can help each other in the learning process. This is child-to-child education. In traditional methods, there is only instructor-to-child education, and child-to-child education is not considered. The data obtained in this study showed that the proposed method has improved the education process by considering child-to-child education. Also, according to the research questions and the results of Tables 3 and 4, the proposed solutions using MADM techniques have been able to improve the educational status of children. In the proposed method, the condition of each child is diagnosed separately, and solutions are provided in accordance with the condition of each child, which is not considered in traditional methods. Also, according to the results of Table 5, the proposed educational method has been able to double the rate of children's learning, which is maintained by

doubling the number of children tested. According to the purpose of the research, in the proposed educational method, the art and creativity of combining games that are attractive to children with technologies such as IoT were used to increase children's motivation and participation in the learning process and thus improve the learning process. The results confirmed the realization of this goal.

## 9. Conclusion

This paper presents a method for educating children. The proposed educational method utilized technologies and items such as SDI, complex networks and centrality measures, MADM, and games in the IoT environment. Each of these items was explained first. Then, the proposed educational method was expressed in three phases of diagnosis, improvement, and evaluation. In related works, only one of the phases is usually considered, but in the proposed educational method, all three phases are considered. In the proposed educational method, IoT was used to extract the children's communication network and education. These networks were then analyzed using centrality measures, and the children were categorized into different categories that reported their status. MADM techniques were used to provide solutions for some categories. The child's learning styles were also addressed in providing strategies. In the evaluation phase, local and general measures were defined for evaluation. The proposed educational method was tested in 2 experiments and on a total of 9 children. The results showed that the proposed educational method was able to improve children's learning. The most important reasons for this are the combination of technology in educational games in order to extract the network of communication and education of children using IoT technology, provide the best solutions using SDI, etc., and in general, to automate the steps from identifying each child's educational status to providing the most up-to-date strategies related to each child's diagnosed status.

In this study, the educational game was designed so that each child should teach the other children. It was not considered to divide the children into groups and that each group would teach the children of the other group. This restriction did not allow the use of other network measures such as betweenness centrality and page rank centrality. Considering group games and using other measures of centrality in the analysis of the resulting networks can be considered as future work.

## Appendix

- (1) Table of related works based on researchers' names, year of publication, brief description, and results (Table 6).
- (2) The data for this paper are available at the following link:  
[https://www.4shared.com/zip/VQm8\\_xWRiq/Data.html](https://www.4shared.com/zip/VQm8_xWRiq/Data.html).

## Data Availability

The data for this paper are available at the following link: [https://www.4shared.com/zip/VQm8\\_xWRiq/Data.html](https://www.4shared.com/zip/VQm8_xWRiq/Data.html).

## Conflicts of Interest

The authors declare that there are no conflicts of interest regarding the publication of this manuscript.

## References

- [1] S. Agnihotri, "The importance of early childhood education for a sustainable society: a sociological analysis," *Journal of Bank Management & Financial Strategies*, vol. 2, no. 3, pp. 26–32, 2019.
- [2] M. T. Merrick, K. A. Ports, D. C. Ford, T. O. Afifi, E. T. Gershoff, and A. Grogan-Kaylor, "Unpacking the impact of adverse childhood experiences on adult mental health," *Child Abuse & Neglect*, vol. 69, pp. 10–19, 2017.
- [3] P. N. Stearns, *Childhood in World History*, Routledge, Abingdon, UK, 2016.
- [4] C. Magnusson and M. Nermo, "From childhood to young adulthood: the importance of self-esteem during childhood for occupational achievements among young men and women," *Journal of Youth Studies*, vol. 21, no. 10, pp. 1392–1410, 2018.
- [5] A. Bell, R. Chetty, X. Jaravel, N. Petkova, and J. Van Reenen, "Who becomes an inventor in America? The importance of exposure to innovation," *The Quarterly Journal of Economics*, vol. 134, no. 2, pp. 647–713, 2018.
- [6] K. Sylva, E. Melhuish, P. Sammons, I. Siraj-Blatchford, and B. Taggart, *Early Childhood Matters: Evidence from the Effective Pre-School and Primary Education Project*, Routledge, Abingdon, UK, 2010.
- [7] E. L. Essa, *Introduction to Early Childhood Education*, Cengage Learning, Boston, MA, USA, 2012.
- [8] B. S. Bloom, *Stability and Change in Human Characteristics*, Wiley, Hoboken, NJ, USA, 1964.
- [9] K. W. M. Siu and M. S. Lam, "Early childhood technology education: a sociocultural perspective," *Early Childhood Education Journal*, vol. 32, no. 6, pp. 353–358, 2005.
- [10] N. A. Jennings, S. D. Hooker, and D. L. Linebarger, "Educational television as mediated literacy environments for preschoolers," *Learning, Media and Technology*, vol. 34, no. 3, pp. 229–242, 2009.
- [11] S. M. Fisch and R. T. Truglio, *G is for Growing: Thirty Years of Research on Children and Sesame Street*, Routledge, Abingdon, UK, 2014.
- [12] D. Evans, "The internet of things: how the next evolution of the internet is changing everything," 2011, [http://www.cisco.com/web/about/ac79/docs/innov/IoT\\_IBSG\\_0411FINAL.pdf](http://www.cisco.com/web/about/ac79/docs/innov/IoT_IBSG_0411FINAL.pdf).
- [13] K. Ashton, "That "internet of things" thing," *RFID Journal*, vol. 22, 1999.
- [14] G. C. Fox, S. Kamburugamuve, and R. D. Hartman, "Architecture and measured characteristics of a cloud-based internet of things," in *Proceedings of the 2012 International Conference on Collaboration Technologies and Systems (CTS)*, IEEE, Denver, CO, USA, 2012.
- [15] M. Chui, M. Löffler, and R. Roberts, "The internet of things," *McKinsey Quarterly*, vol. 2, pp. 1–9, 2010.
- [16] J. Ritz and Z. Knaack, "Internet of things," *Technology & Engineering Teacher*, vol. 76, no. 6, 2017.
- [17] T. T. Mulani and S. V. Pingle, "Internet of things," *International Research Journal of Multidisciplinary Studies*, vol. 2, no. 3, 2016.
- [18] M. Keerthana and S. Ashika Parveen, "Internet of things," *International Journal of Advanced Research Methodology in Engineering and Technology*, vol. 1, no. 2, 2017.
- [19] J. Lin, W. Yu, N. Zhang, X. Yang, H. Zhang, and W. Zhao, "A survey on internet of things: architecture, enabling technologies, security and privacy, and applications," *IEEE Internet of Things Journal*, vol. 4, no. 5, pp. 1125–1142, 2017.
- [20] E. de la Guía, M. D. Lozano, V. M. Penichet, and R. Nieto, "NFCBOOK: GameBook digital based on tangible user interfaces," in *Proceedings of the 15th International Conference on Human Computer Interaction*, Munich, Germany, September 2014.
- [21] I. Soute and H. Nijmeijer, "An owl in the classroom: development of an interactive storytelling application for preschoolers," in *Proceedings of the 2014 Conference on Interaction Design and Children*, Aarhus, Denmark, 2014.
- [22] C. D. Clark, "Therapeutic advantages of play," *Play and Development: Evolutionary, Sociocultural, and Functional Perspectives*, pp. 275–293, Taylor & Francis, Abingdon, UK, 2007.
- [23] J. Huizenga, W. Admiraal, S. Akkerman, and G. T. Dam, "Mobile game-based learning in secondary education: engagement, motivation and learning in a mobile city game," *Journal of Computer Assisted Learning*, vol. 25, no. 4, pp. 332–344, 2009.
- [24] K. D. Stiller and S. Schworm, "Game-based learning of the structure and functioning of body cells in a foreign language: effects on motivation, cognitive load, and performance," *Frontiers in Education*, vol. 4, p. 18, 2019.
- [25] A. Pho and A. Dinscore, *Game-Based Learning. Tips and Trends*, American Library Association, Chicago, IL, USA, 2015.
- [26] L. López-Faicán and J. Jaen, "Emofindar: evaluation of a mobile multiplayer augmented reality game for primary school children," *Computers & Education*, vol. 149, Article ID 103814, 2020.
- [27] S. Trench, "Dissemination of information," *Handbook of Special Librarianship and Information Work*, Aslib, London, UK, 1997.
- [28] E. k. O'Neil, "Selective dissemination of information in the dynamic web environment," Master thesis, University of Virginia: Faculty of the School of Engineering and Applied Science, Charlottesville, VA, USA, 2001.
- [29] J. J. Huang and K. Yoon, *Multiple Attribute Decision Making: Methods and Applications*, Chapman and Hall/CRC, London, UK, 2011.
- [30] R. Anggrainingsih, M. Z. Umam, and H. Setiadi, "Determining e-learning success factor in higher education based on user perspective using fuzzy AHP," in *Proceedings of the 2nd International Conference on Engineering and Technology for Sustainable Development*, vol. 154, p. 03011, Yogyakarta, Indonesia, 2018.
- [31] R. V. Donner, M. Lindner, L. Tupikina, and N. Molkenhain, "Characterizing flows by complex network methods," in *A Mathematical Modeling Approach from Nonlinear Dynamics to Complex Systems*, pp. 197–226, Springer, Cham, Switzerland, 2019.
- [32] M. E. J. Newman, "The structure of scientific collaboration networks," *Proceedings of the National Academy of Sciences*, vol. 98, no. 2, pp. 404–409, 2001.
- [33] P. J. Carrington, J. Scott, and S. Wasserman, *Models and Methods in Social Network Analysis*, Cambridge University Press, Cambridge, UK, 2005.



- [34] L. Freeman, "Centrality in social networks: conceptual clarification," *Social Networks*, vol. 1, pp. 215–239, 1979.
- [35] B. Cheng, *Using social network analyses to investigate potential bias in editorial peer review in core journals of comparative/international education*, Ph.D. dissertation, Brigham Young University, Provo, Utah, 2006.
- [36] E. Estrada, *The Structure of Complex Networks: Theory and Applications*, Oxford University Press, Oxford, UK, 2012.
- [37] A. S. Abdi and N. Cavus, "Developing an electronic device to teach English as a foreign language: educational toy for pre-kindergarten children," *International Journal of Emerging Technologies in Learning (ijET)*, vol. 14, no. 22, pp. 29–44, 2019.
- [38] S. Higgins, Z. Xiao, and M. Katsipataki, *The Impact of Digital Technology on Learning: A Summary for the Education Endowment Foundation*, Education Endowment Foundation and Durham University, Durham, UK, 2012.
- [39] A. H. Safar, A. A. Al-Jafar, and Z. H. Al-Yousefi, "The effectiveness of using augmented reality apps in teaching the English alphabet to kindergarten children: a case study in the state of Kuwait," *EURASIA Journal of Mathematics, Science and Technology Education*, vol. 13, no. 2, pp. 417–440, 2016.
- [40] R. B. Sadiq, N. Cavus, and D. Ibrahim, "Mobile application based on CCI standards to help children learn English as a foreign language," *Interactive Learning Environments*, vol. 27, pp. 1–16, 2019.
- [41] A. Uzelac, N. Gligoric, and S. Krco, "A comprehensive study of parameters in physical environment that impact students' focus during lecture using internet of things," *Computers in Human Behavior*, vol. 53, pp. 427–434, 2015.
- [42] A. Manches, P. Duncan, L. Plowman, and S. Sabeti, "Three questions about the internet of things and children," *Tech-Trends*, vol. 59, no. 1, pp. 76–83, 2015.
- [43] A. Zhamanov, Z. Seong-MooYoo, Z. Sakhiyeva, and M. Zhaparov, "Implementation and evaluation of flipped classroom as IoT element into learning process of computer network education," *International Journal of Information and Communication Technology Education*, vol. 14, no. 2, pp. 30–47, 2018.
- [44] E. Spyrou, N. Vretos, A. Pomazanskyi, S. Asteriadis, and H. C. Leligou, "Exploiting IoT technologies for personalized learning," in *Proceedings of the 2018 Conference on Computational Intelligence and Games (CIG)*, Maastricht, Netherlands, August 2018.
- [45] P. Tangworakitthaworn, V. Tengchaisri, K. Rungsuptaweekoon, and T. Samakit, "A game-based learning system for plant monitoring based on IoT technology," in *Proceedings of the 15th International Joint Conference on Computer Science and Software Engineering (JCSSE)*, Nakhon Pathom, Thailand, July 2018.
- [46] J. Li, E. D. van der Spek, J. Hu, and L. Feijs, "Turning your book into a game: improving motivation through tangible interaction and diegetic feedback in an AR mathematics game for children," in *Proceedings of the Annual Symposium on Computer-Human Interaction in Play*, pp. 73–85, Barcelona, Spain, 2019.
- [47] E. de la Guía, V. López, T. Olivares, and L. Orozco, *Using Internet of Things to Support Teachers to Enhance Social and Classroom Interactions*, Albacete Research Institute of Informatics (I3A), Albacete, Spain, 2018.
- [48] M. Brysbaert, "How many participants do we have to include in properly powered experiments? A tutorial of power analysis with reference tables," *Journal of Cognition*, vol. 2, no. 1, 2019.

## Research Article

# A Smart Parking System Based on Mini PC Platform and Mobile Application for Parking Space Detection

Vladimir Sobeslav  and Josef Horalek 

*Department of Information Technologies, Faculty of Informatics and Management, University of Hradec Kralove, Rokitanskeho 62, Hradec Kralove 500 01, Czech Republic*

Correspondence should be addressed to Vladimir Sobeslav; [vladimir.sobeslav@uhk.cz](mailto:vladimir.sobeslav@uhk.cz)

Received 24 June 2020; Revised 25 September 2020; Accepted 9 October 2020; Published 26 October 2020

Academic Editor: Peter Brida

Copyright © 2020 Vladimir Sobeslav and Josef Horalek. This is an open access article distributed under the Creative Commons Attribution License, which permits unrestricted use, distribution, and reproduction in any medium, provided the original work is properly cited.

Car parking is a major problem in urban areas in developed and also in developing countries. The growing number of vehicles creates a problem with parking spaces mainly in the city center and the surrounding streets. The local authorities have to react with regulations, and the current situation is unpleasant for many citizens. Therefore, the aim of this article is to propose a complex outdoor smart parking lot system based on the mini PC platform with the pilot implementation, which would provide a solution for the aforementioned problem. Current outdoor car park management is dependent on human personnel keeping track of the available parking lots or a sensor-based system that monitors the availability of each car. The proposed solution utilizes a modern IoT approach and technologies such as mini PC platform, sensors, and IQRF. When compared to a specialized and expensive system, it is a solution that is cost-effective and has the potential in its expansion and integration with other IoT services.

## 1. Introduction

The number of vehicles is constantly increasing, not only in the Czech Republic but also in other countries. According to the data from Central Auto-moto Club of the Czech Republic, more than 5.5 million cars are registered here, which means that their number has increased 2.4 times since 1989. With the increasing number of the vehicles, the problems with the parking also arise. First and foremost, these problems become prevalent during sport and cultural events, as well as in the proximity of administrative buildings or banks. Parking in the towns and cities during the traffic peak times also poses a significant problem. A lack of knowledge of current number of parking spaces can lead the drivers to fully occupied parking lots, which consequently leads to having to move to another location, along with searching for a spot on another parking lot. Therefore, not only do the drivers waste their time, but also fuel, and it all causes the deterioration of the traffic situation and negatively affects the environment.

The aim of this article is to propose a complex smart parking lot system based on the mini PC platform, along

with its pilot implementation, which would provide a solution for the aforementioned problem. The solution aims to use the newest principles in the IoT area, mesh networks, and tools offered by the Android OS as for the whole solution to be affordable and quickly deployable.

The proposed solution contains a complete design and realization based on the mini PC platform, IQRF technology, including use of the DPA protocol. As a gateway, UpBoard with DK-EVAL-04A communication module has been used. Before the solution itself, an in-depth analysis of the currently used solutions and approaches has been performed. The findings of this analysis are provided below.

## 2. Related Works

Firstly, an analysis of the approach to the smart parking solution must be performed. The article IoT-Based Smart Parking System [1] is a prominent input in this area, which is similarly to [2] and describes the architecture of a smart parking system based on the IoT (Internet of Things) technology. In [1], sensors placed on the parking spaces detect the proximity of the vehicle and send these data to

cloud using mini PC (Raspberry Pi) deployed on the parking lot. The authors describe the use of Raspberry Pi GPIO pins, to which 26 sensors can be connected. The number can be increased even further using a suitable multiplexor. This solution utilizes an IBM MQTT server, to which the Raspberry sends data from the sensors via MQTT messages. The user communicates with the system via a mobile app written in Apache Cordova, which communicates with the server with messages in the JSON format. The user can use the mobile app to see the number of the free spots on the parking lot, make a reservation of a parking space, and pay the parking fee. In [2], besides the general architecture, the authors focus on using Elliptic Curve Cryptography (ECC) as an attractive alternative to the conventional public key cryptography such as RSA. Interesting algorithms employed in the contemporary smart parking systems are presented in [3]. Finally, an overall overview of the approaches and solutions is provided by [4].

Another topic covered by this article is the optimization of the logic and IoT approaches used to find and navigate to the parking space itself. Tsai et al.[5] describe the use of a mobile app and Internet of Things (IoT) technology in the parking system: the process of finding a parking lot, parking space reservation, and indoor navigation inside the parking lot. Another topic is finding the suitable algorithm to calculate the priority for recommending a specific parking lot based on the distance of the driver from the parking lot, number of free parking spaces, and the parking fee, with the preferences being set up by the user. After selecting the parking lot, the driver has an opportunity to book the parking space via the app. For the calculation of the distance from the parking lot and the navigation, the app uses GPS coordinates acquired from the Google API. Detection of the presence of the vehicle on the parking space is realized via an ultrasound sensor and transferred to the server via a WiFi module. The described solution is designated mainly for indoor parking lots, with the indoor navigation provided by iBeacon Bluetooth transmitters. The presence of the driver on the parking lot is detected by an RFID chip. The matter of parking specifically on the side of the roads is discussed in [6]. It describes the detection of the roadside parking spaces using sensors placed on the vehicle on the passenger's side. These sensors are placed on public transport vehicles, taxis, or sometimes on the vehicles of the volunteers who frequently pass through the marked measured areas.

The system uses an ultrasound detector to detect the parked vehicles and empty spots along the road in conjunction with the GPS system, and by using Map Matching (which compares the detected spots with the map), a map of available parking spaces is continuously generated and is distributed to the users via the mobile app or a website. According to the performed measuring, to map the same number of the parking spaces, mobile sensors are more efficient than sensors placed directly on the parking spaces. The success rate of the detection was between 76 and 94 percent, depending on the accuracy of the GPS system.

In the hereby presented complex solution, IQRF networks are utilized. Their communication system is discussed

in [7] and the spread of the networks' usage is discussed in [8, 9].

### 3. The Proposed System Architecture

The aim of the proposed parking system is a complex and economic system for detection of free parking spaces on an outdoor parking lot, which is based on the mini PC platform. The system partially handles the problems with undisciplined drivers who would use the parking lot without the respective authorization. This is provided by using the automatic gate system at the parking lot entrance. Because of the budget requirements, the variant where the parked vehicles would be detected via ultrasound or infra-sensors has been abandoned, and therefore, the proposed solution discusses the variant using magnetometric sensors connected to a mesh network. In regular intervals, the mini PC checks whether the individual parking spaces are occupied and stores the data in a real-time database. The driver is then informed via the mobile app for Android, and so they have current information about the numbers of available parking spaces on the selected parking lot. The availability can be checked either manually or automatically using the Geofencing service. The user is also able to book a parking space for 60 minutes. If they do not arrive at the parking lot during this time, the reservation is automatically canceled.

The proposed solution enables opening the parking lot gate directly from the mobile app by adding an entry into the real-time database. After the entry is added, the mini PC performs the corresponding steps. To check the presence of the driver (their smartphone, to be precise) on the parking lot, the mobile app compares the GPS coordinates before registering the vehicle as present on the parking lot. If the distance between the smartphone and the parking lot is higher than a given limit, the access is denied. Thanks to this solution, there is no necessity for use of an RFID chip, and to make use of the parking lot, a smartphone with the installed app and connection to the Internet should suffice. The identification of the smartphone is performed using a unique 64-bit number, ANDROID ID. The general model of the proposed solution is depicted in Figure 1.

*3.1. Functional Diagram of the Proposed Solution.* The mobile app monitors the entry in the database with the number of empty spots. On every change, the state of the notification icon on the app's main screen is changed. After tapping this icon, the current occupancy of the individual parking spaces is loaded from the database, and it is displayed on the smartphone screen. By tapping on the respective icon on the main screen, navigation to the parking lot is started. Using Google API, the application starts navigation on Google Maps. More detailed information is described in Section 5. To enable the automatic notifications about parking lots in proximity and the number of available parking spaces, the application uses Geofencing service, which is described in Section 5.2.

The following diagrams describe two main functions:

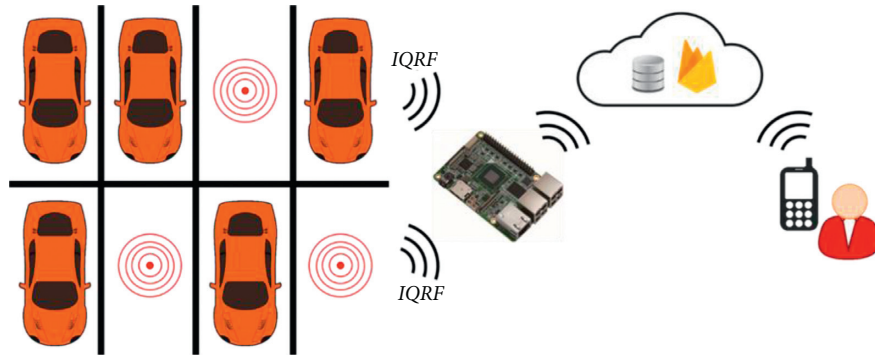


FIGURE 1: General system structure design.

Displaying the available spots at the parking lot and their current occupancy (Figure 2)

Turning on the automatic notification about available parking lot (Figure 3)

The following diagram (Figure 4) describes the logical steps required for opening the parking lot gate. First, the application checks the database of the parked vehicles to determine whether the vehicle is entering or leaving the parking lot.

When entering the parking lot, it is also checked whether there are available spots or if the driver who is sending a request to open the gate has a reservation saved in the database. If everything is in order, the distance from the parking lot is checked to prevent an unintentional or deliberate gate closure at higher distance from the parking lot. If any condition is not met, the driver receives information about the parking lot unavailability. Otherwise, the gate opens, and the arriving vehicle is added to the parking lot's database. At the same time, the driver's reservation validity is checked and deleted from the database if invalid. When leaving the parking lot, the system opens the exit gate and deletes the record of the vehicle from the parking lot's database.

The realization of the reservation process is depicted in Figure 5. During an attempt at making a reservation, the system first checks whether the vehicle is not currently located at the parking lot and that its ID does not have a reservation created already. Then, the available spots are checked. If all the conditions are met, a reservation entry is made in the parking lot's database. Otherwise, the app informs the driver that the reservation cannot be made. Duration of the reservation is limited to 60 minutes. For this reason, in 1-minute intervals, the mini PC on the parking lot checks the database if any reservation has exceeded this limit. If this occurs, the entry is deleted from the database.

On the general communication schema (Figure 6), you can see that the common storage for the whole system is a Firebase database. The communication between the database and the mini PC is procured via TCP/IP protocol. The communication between the database and the mobile app uses mobile network data transfers and the communication between the mini PC and the individual sensors is procured by the IQRF technology described in Chapter 3.

#### 4. IQRF Communication Platform

From the principle of the intelligent parking system proposal, it is necessary for the system itself to be able to detect whether the respective physical spot is occupied or not, and it must also be connected to the suitable network so it can communicate with the central mini PC. For this purpose, IQRF technology has been chosen [10].

IQRF is a platform suitable for wireless data transfer, which utilizes wireless data transfer, using the frequencies of 868 MHz and 433 MHz for the communication. The IQRF platform makes use of special transceivers that reciprocally interchange the data. The IQRF transceivers are known to have a very low consumption rate (12.3 mA during communication and 380 nA in sleep mode), and thanks to the supported MESH topology, communication at relatively long distance is possible. These parameters appear to be an ideal solution for the IoT technologies. The wireless IQRF network uses the IQMEST protocol [11, 12], which uses the principle that in any given area, and there are always at least two IQRF transceivers within the transmission reach. The maximum distance between two communicating transceivers is around 500 meters in space without obstacles. The transceivers transmit in synchronization, so they do not interrupt each other during the transmission. The communication is governed by a coordinator, which sends the data, transceivers in the reach receive the data, during their time-slot send the data further, and this way the data gradually spread through the whole network. Thanks to this principle, the whole network is very reliable and has a high success rate of the data transmission. Because of the duplicate paths between individual transceivers, the data reach their destination even if multiple communication paths are disrupted at the same time. The principle is depicted in Figure 7, where the coordinator C sends the data for the transceiver N2. The communication paths that are interrupted, e.g., by signal disruption, are represented by the red crosses. The data reach their destination, as the green arrows suggest, via the transceivers N1, N3, and N4.

*4.1. DPA Protocol.* Every transceiver has a hardware profile (HWP). Assigning a HWP to the transceivers enables their control via messages with DPA (direct peripheral access) protocol [13]. Because of this protocol, it is possible to build

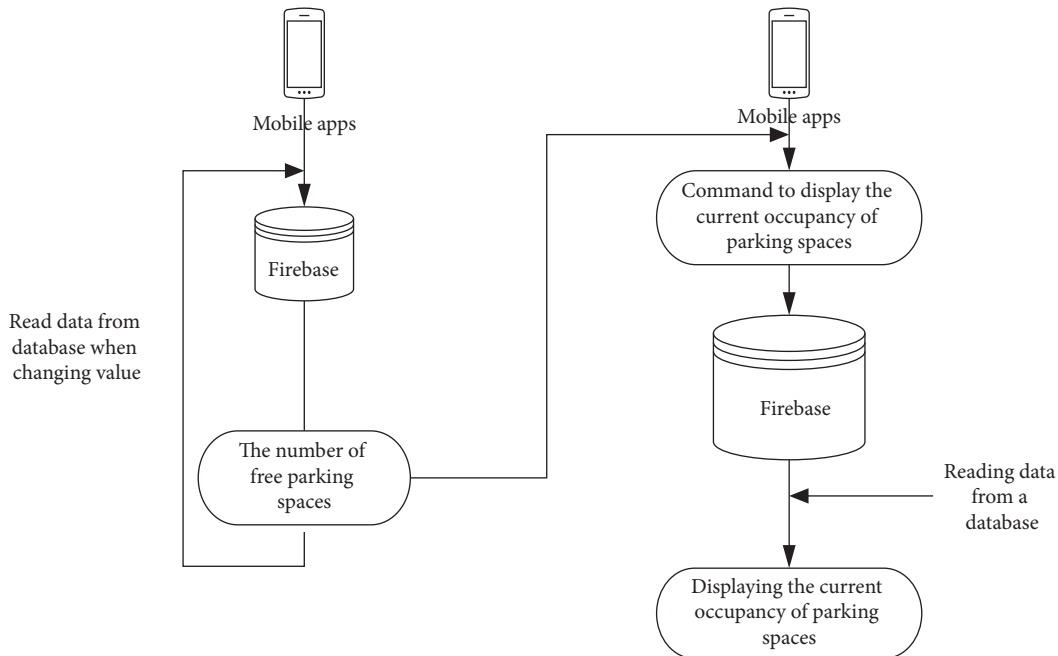


FIGURE 2: Functional diagram to show the number of available parking spaces and their current occupancy.

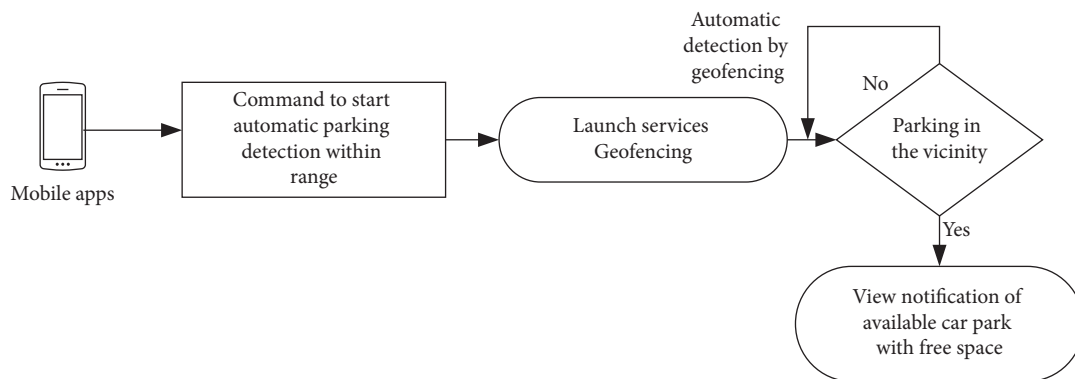


FIGURE 3: Functional diagram to trigger the automatic notification of available car parking.

a network comprised of up to 240 transceivers, and the transceivers can be controlled by sending the data in the specific format (Table 1).

NADR (node address) has the address 0x00 for the coordinator and 0x01–0xEF for the other transceivers and PNUM (peripheral number) 0x03 EEPROM, 0x08 SPI, 0x0C UART, etc. PCMD (peripheral command) is designated only by the type of the used periphery; HWPID (hardware profile ID) uniquely determines the functionality of the periphery device. If 0xFFFF number is used, the command is executed on any HW profile. PDATA (peripheral data) is an optional 56-byte field for additional command parameters.

**4.2. Custom DPA Handler.** For creating the own logic of the transceiver, custom DPA handler is used, i.e., it uses code written in C, which can be used to define custom user periphery and set up its behavior during received a DPA command with this periphery's ID and the ID of the

respective command. Using the DPA handler, it is also possible to expand the set of the HW groups described above, and thus it enables the filtering of control message for the groups of peripheries of the respective type.

**4.3. FRC.** Fast response command (FRC) is a special coordinator DPA periphery, which enables sending a command that can be processed by all the transceivers in the network. The moment the transceiver processes the command, it stores the response on the specific position in the message and it passes through the whole network along with the data and collects the responses of individual transceivers. If we need to get the same information from all the transceivers, which is, in our case, the input from a detector about the presence of a vehicle on a parking space, the use of FRC is very practical as it is not necessary to send individually to every transceiver, but sending one command is enough. This positively affects not only the amount of the



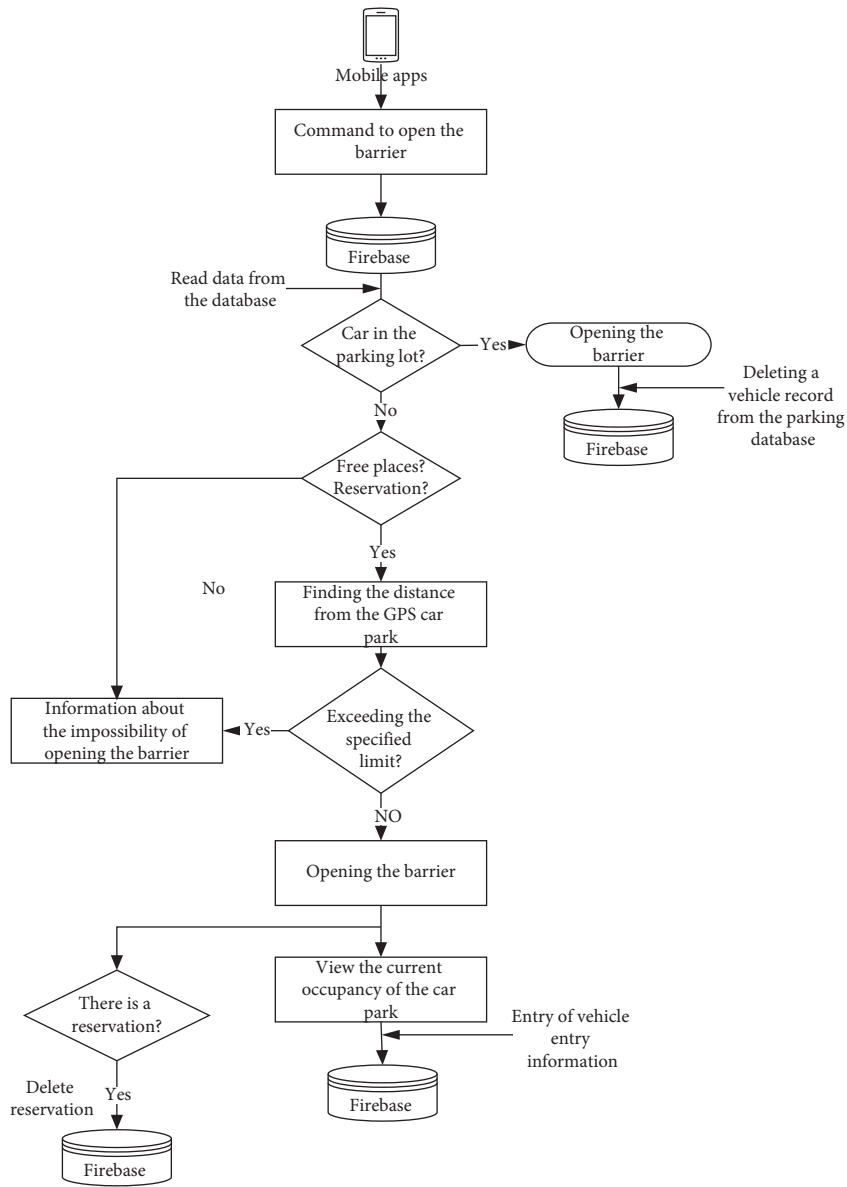


FIGURE 4: Functional diagram of the entry and exit gate control.

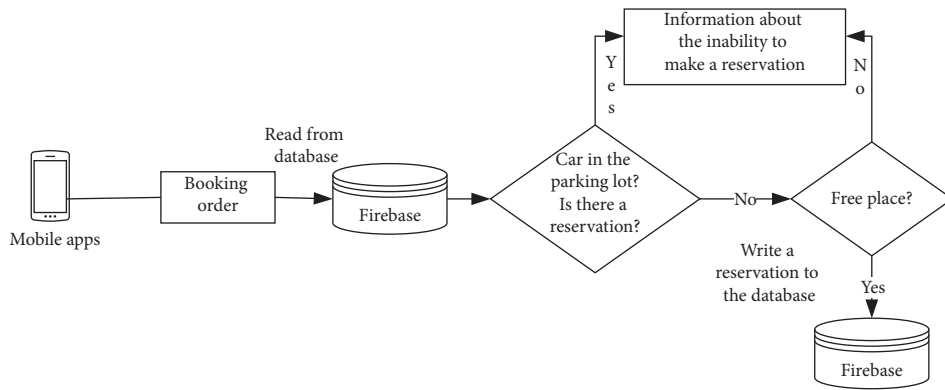


FIGURE 5: Functional diagram for making a reservation.

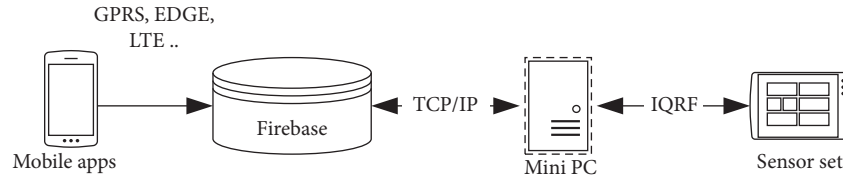


FIGURE 6: Functional diagram to communication.

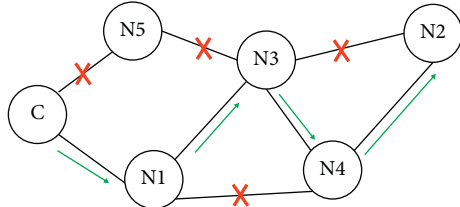


FIGURE 7: Principle of IQRF communication between coordinator C and N2 transceiver.

transferred data but also time needed to get a response. The FRC command is sent via the DPA protocol (Table 2).

User data item is not required by all the FRC commands, and if not used, it must be replaced by a 2-byte value of 00.00. SEND command can be replaced by the SEND selective (0x02) command, which makes it possible to send the command only to the chosen transceivers, which are defined in the data field between ID and user data entries.

The selected transceivers can be specified through 30-byte binary information. In IQRF network, there can be the maximum of 240 transceivers, which corresponds to 30 bytes, i.e., 240 bits. If the respective bit has a value of 1, the command will be sent to the corresponding transceiver. Otherwise (the value of 0), the transceiver will not be included into processing of the command.

For the initial configuration of the transceivers and for the creation of the IQRF network, it is necessary to use CK-USB-04K programmer and IQRF IDE development interface. It is also necessary to get hardware profiles for the coordinator and the individual nodes.

Into the newly created project, the author must add the HW profiles and the DPA custom handler for FRC command for detecting the state of the sensors on the parking spaces. The HW profiles belong to plug-ins section and the DPA custom handler to source section. Considering the fact that the inserted DPA handler is in the format of the source file written in C, this file must be compiled to \* hex format so it can be uploaded to the transceiver. After inserting the first transceiver into the programmer and connecting it to a USB port of a PC, in the “Project” window in the “TR Configuration” section, the configuration settings for the inserted transceiver can be opened. For all the communicating transceivers, it is necessary to set the same communication channel (typically 52) in the “OS” tab. Next, in the “HWP” section, the option to process the FRC commands for the coordinator and use of custom DPA handler for every node must be enabled. In the “Security” tab, a password and communication encryption can be set up (Figure 8).

After programming all the transceivers and inserting them into the DK-EVAL-04A testing modules or alternatively by connecting custom modules that would need to be adjusted according to the transceiver connection schema (Figure 9), for the transceiver to be powered by the right voltage and have accessible RESET and bonding buttons, by connecting the coordinator into the CK-USB-04K programmer, an IQRF network can be created.

If a red LED is blinking after connecting the power source, it means that no previous bonding is stored in the memory. Otherwise, it is necessary to manually unbind by pressing the reset and the user buttons on the testing module and then releasing the reset button. After a green LED blinks, the user button must be released at once. For erasing the data about bonding from the coordinator, IQMESH Network Manager, which is a part of the IQRF IDE program, must be used. To do so, press the “Clear All Bonds” button. Afterwards, by pressing the “Bond” button, the coordinator start searching for a new node, and in the frame of ten seconds, the bonding must be confirmed by pressing the user button on the respective testing module. By repeating this procedure, all the nodes must be bonded with the coordinator. At the time of the bonding, all the nodes must be in the communication reach of the coordinator. After the bonding is finished and the respective nodes are placed on their final positions, by clicking the “Discovery” button in IQMESH Network Manager, the IQMESH network topology is created. It can be viewed in the “MapView” tab (Figure 10).

**4.4. IQRF Gateway.** The created IQRF network requires a gateway for transmitting the data to the database/cloud via the Internet. For the purposes of the best compatibility and technical support, a one-board computer UpBoard has been used as it, in comparison to Raspberry Pi, offers a micro-processor with better performance in Intel Atom, as well as higher memory capacity, and does not require an OS to be installed on an external memory card, which can pose potential problems in conjunction with the mechanical connector. UpBoard is also used in Intel® RealSense™ Robotic Development Kit and has the following characteristics:

- Intel® Atom™ x5-Z8350 SoC
- Onboard DDR3L Memory up to 4 GB
- Onboard eMMC Storage up to 64 GB
- Gigabit LAN × 1, USB 2.0 × 4, USB 3.0 × 1, HDMI × 1
- 5V DC-in
- 40 pin GPIO × 1
- DSI/eDP × 1
- MIPI-CSI × 1

TABLE 1: DPA packet structure.

NADR (node address)	PNUM (peripheral number)	PCMD (peripheral command)	HWPID (hardware profile ID)	PDATA (peripheral data)
[2B]	[1B]	[1B]	[2B]	[0-56B]

TABLE 2: FRC (SEND) command structure.

NADR (node address)	PNUM (peripheral number)	PCMD (peripheral command)	HWPID (hardware profile ID)	PDATA (peripheral data)	
0x00	0x0D	0x00	0xFFFF	ID	User data
Coordinator	FRC	SEND	All groups	Command ID	Data for FRC processing

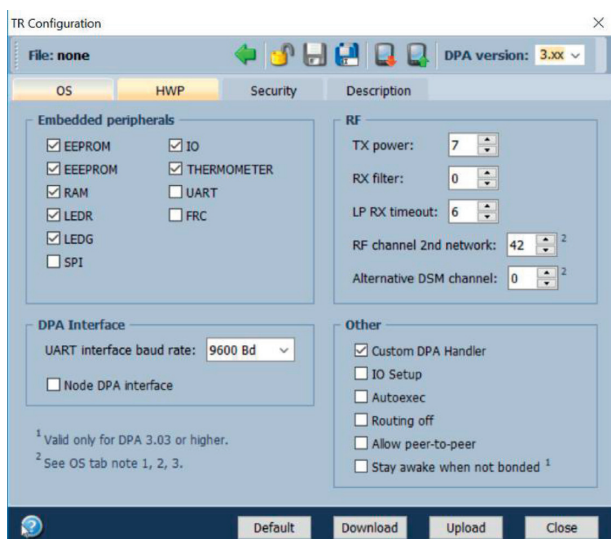


FIGURE 8: Example of HWP setting for “NOD” transceiver.

Considering the availability of the technical support, Ubinux OS has been chosen for the smart parking system. The chosen mini PC serves for controlling the IQRF network and for conjoining the whole app via the Internet and the database. For those reasons, the IQRF coordinator had to be connected using an available reduction with UpBoard’s GPIO pins, and corresponding utilities for the communication with the IQRF network and the database had to be installed as well. For interchanging the information between the UpBoard and the IQRF network, an MQTT Broker has been used. For the administration, we have chosen a web app for IQRF Daemon and NodeRED environment that will serve for programming the IQRF network maintenance. For the IQRF gateway we have used the following software setup. As an MQTT broker, we have decided to use the mosquito and mosquito-clients packages. Furthermore, the dirnmgr server was used for certificate management. The IQRF Gateway Daemon package was used as an open-source IQRF gateway solution which is being widely used in this area, and it is supported also by Raspberry, Belagone, traditional PC and others. Node.js open-source server platform was used for code execution;

for programming of IQRF network jobs, a database management, a NodeRED, was utilized.

**4.5. Android Geofencing.** The last component used in the presented solution is the Android Geofencing service, which serves to alert the driver about the availability of a parking lot within the mobile application. This service uses the capabilities of the mobile phone to determine its current location using GPS, the availability of known WIFI networks, and the distance from the mobile operator’s BTS based on the signal strength of the mobile network. To use the service, firstly, it is needed to enter the latitude and longitude of a specific place (parking lot) and the radius of the circle centered in this coordinate. The circle created in this way is called geofence, and then it serves for detecting notifications or other actions such as turning on Bluetooth and turning off the phone’s ringtone. The notification can be set for a situation when the phone enters a defined circle (we use this notification in the presented solution), or if it leaves the circle or stays in it for a certain period of time. Each Android user can have up to 100 geofences (circles) registered in all applications on their phone. If the phone is located at the intersection of several geofences, it can perform actions separately for each of them, or a notification of the availability of multiple geofences (parking lots) and the distance to the center of each can be sent and calculated from the difference of two GPS coordinates (phone and geofence).

## 5. Implementation of Key System Functions

In Section 5.1, the solutions described above, including the used IQRF network and NodeRED and the main component of the Android app are documented in detail.

**5.1. Vehicle Detection.** Vehicle detection is realized via MPU-9250 magnetometric sensor, which is connected via I2C bus with an Arduino Mini microprocessor unit (Figure 11).

For the communication with the sensor, MPU9250\_asukiaaa.h has been used as it enables a simple maintenance of the magnetometric sensor. After the initial establishment, the measured values are stored for a reference and then

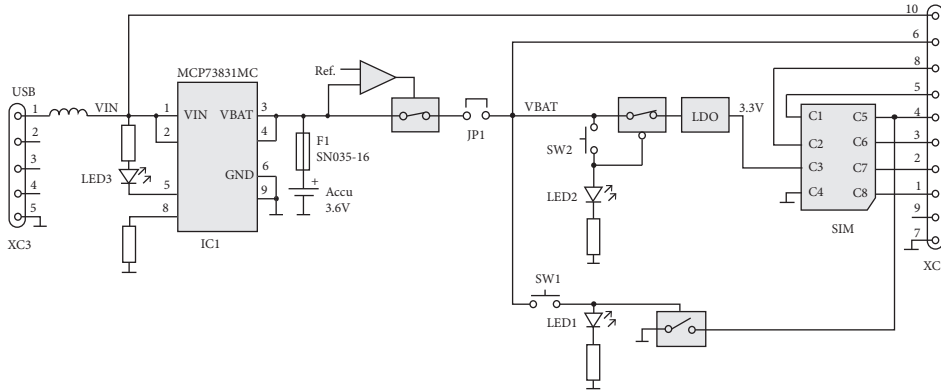


FIGURE 9: DK-EVAL-04A test module connection.



FIGURE 10: Example of network topology in IQMESH Network Manager.

compared with the currently measures values in the 500-millisecond intervals (during the initialization, the parking space must be empty). The measured values are transferred to the serial port for the purpose of checking the functionality of the sensor and checking the measured values. See the following code for the main program enabling the communication with the magnetometric sensor:

```
void loop() {
  if(start){delay(5000);}
  mySensor.magUpdate();
  mX = mySensor.magX();
  mY = mySensor.magY();
  mZ = mySensor.magZ();
  if(start){initSensor(); start = false;}
  Serial.println("magX: " + String(mX));
  Serial.println("magY: " + String(mY));
  Serial.println("magZ: " + String(mZ));
  testSensor();
  Serial.println(""); // Add an empty line
  delay(500);
}
```

If a metal object (a vehicle) is detected in the proximity and the values in any of the axes exceed the given limit, the digital output signals the presence of a vehicle. After every

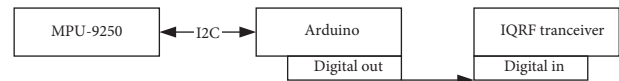


FIGURE 11: Block diagram of vehicle detector.

vehicle detection and its subsequent departure from the parking space, new rest values are saved as referential in order to reduce the amount of unprompted or erroneous detections caused by long-term changes of the magnetic field intensity. The implementation of the vehicle detection through the change of the magnetic field is described below.

```
void testSensor(){
  deltaMx = abs(normalMx-mX);
  deltaMy = abs(normalMy-mY);
  deltaMz = abs(normalMz-mZ);
  Serial.println("deltaMx: " + String(deltaMx));
  Serial.println("deltaMy: " + String(deltaMy));
  Serial.println("deltaMz: " + String(deltaMz));
  if(deltaMx > 7 || deltaMy > 7 || deltaMz > 7){
    Serial.println("Car is present");
    digitalWrite(13, HIGH);
    detect = true;
  }
  else
  {Serial.println("Car is not present");
  digitalWrite(13, LOW);
  if(detect){start = true; detect = false;}
  }
}
```

The digital output of the Arduino module is connected to the IQRF transceiver, which provides the connection of the individual sensors into the IQMESH network.

5.2. *Car Parking with NodeRED.* As it has been already mentioned, the database communicates not only on the

mobile app but also the mini PC via NodeRED. For greater clarity, individual program flows are split into individual IQRF\_Request tabs. The commands are sent to the IQRF network, IQRF\_Response processes the responses from the IQRF network, Firebase communicates with the Firebase database, Gate operates the entrance and exit gate, and Reservations maintains the user reservations.

5.3. *IQRF\_Request*. The program flow IQRF\_Request (Figure 12) uses program nodes on the lines 2 through 5, which send the requests to open or close the entrance or exit gate. The requests come from other tabs via the connections (grey arrows at the beginning of the lines).

Individual requests are realized via custom functions written in JavaScript. That is the DPA command for the IQRF network (code: create a request for an IQRF network). Because of the physical absence of a gate, for the tuning purposes of the app, the commands were simulated by turn on or off a red LED on the IQRF coordinator (entry gate) and a green LED (exit gate). In practice, the LED would be replaced by a digital output that would send the command to the gate.

```
var data = {
  type: "raw",
  request: {
    nadr: "0x0000",
    pnum: "0x06",
    pcmd: "0x01",
    hwpid: "0xFFFF",
    pdata: "",
  },
  timeout: 1000
}
msg.payload = data;
return msg;
```

5.4. *Gate*. For the communication itself and its procurement, the gate is a key component of the whole architecture. The gate process flow is split into two parts. The first part controls the entry gate, and the other controls the exit gate (Figure 13).

The first flow begins with the Gate node, which is, in fact, a listener that watches the Gate item in the database. It follows with the switch on the value of 1 (opens the gate) and continues with the second path to the GateEntranceOpen node. The next node is a time delay for the vehicle to pass (sensors for the detection of a vehicle in the gate space are its part) and then the flow continues with the link to GateEntranceClose and sets the value of the gate item in the database to 0. In that case, the switch ensures that the gate does not open again after the value in the database is changed when the value of 0 is added, and so it takes the path 1, to which no other program node is connected. After opening the entry gate, the ID of the smartphone that asked

for the gate to open is stored in reservationID item. This ID is then compared to the records in reservations, and if a valid reservation is found, it is deleted. After the time delay, the reservationID item is reset by ResetReservID.

The second flow starts with the GateID node, which continuously checks the database for changes in the gateID item. Into this item, the mobile app saves the ID of the smartphone registered on the parking lot (it has a record in carInPark) and sends a request to open the exit gate. The program continues with the link to IQRF\_Request, where it opens the exit gate via the GateExitOpen node. After a time delay for the vehicle to pass through, the gate is closed again via the link to GateExitClose. The flow continues with loading the CarInPark items from the database and converts them to the JSON format. These data are passed to the FirebaseConvert function (code: finding and passing the item ID for deletion), which, from the smartphone ID stored in GlobalContext, searches for a record in the database and deletes the record via the DeleteValue node. The last step of the program is the gateID item reset.

5.5. *Reservations*. In the case of this flow, a division into two parts has been done too (Figure 14). Every minute, the first part checks the reservation length, and in case of exceeding the time limit, the reservation is removed. The other part checks the reservations of the drivers entering the parking lot, and if such an entry exists, it is deleted.

Every minute, the inject node loads the reservations from the database and converts them to JSON. The data are passed by the FirebaseConvert (code: check out booking timeout) function, which checks the length of every reservation and in case of exceeding the time limit and passes the respective reservation for deletion. If a reservation that should be deleted is found, the switch continues with the second path. Otherwise, it continues with the first path, where the program ends.

```
var response = msg.payload;
var data = "";
var nic = 1;

var data1 = response.split("{}").toString();
var l = data1.length;
for(i=0;i<l;i++){
  var s = data1.substring(i, i + 1);
  if(s == "\\"){}
  else if(s == "{}"){}
  else if(s == "{}"){}
  else {data = data + s;}
}
var allmsg = data.split(",");
l = allmsg.length;
for(i=1;i<l;i++){
  var data1 = allmsg[i].split(":");
  var fh = parseInt(data1[4]);
```



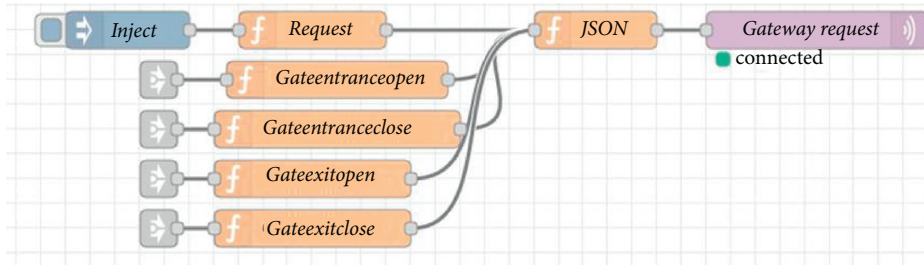


FIGURE 12: Program flow IQRF\_Request.

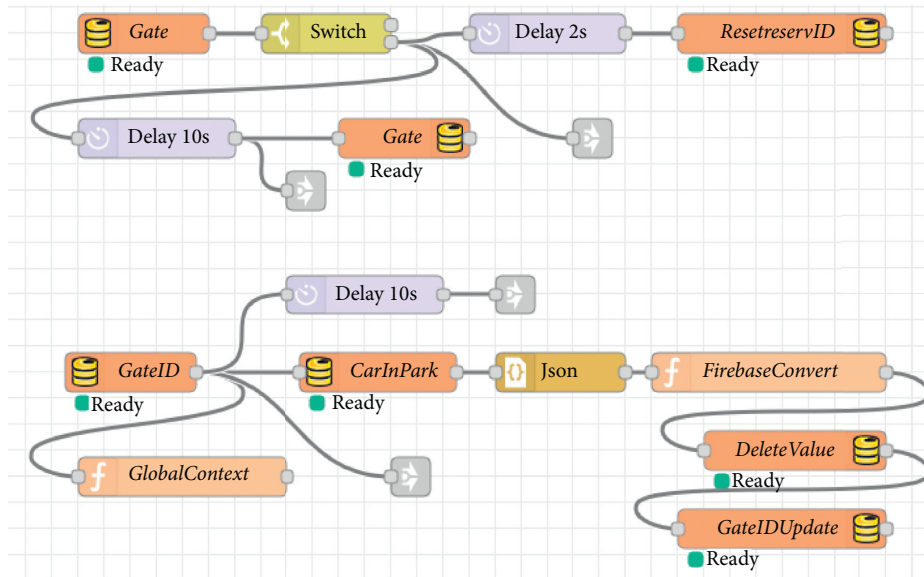


FIGURE 13: Program flow gate.

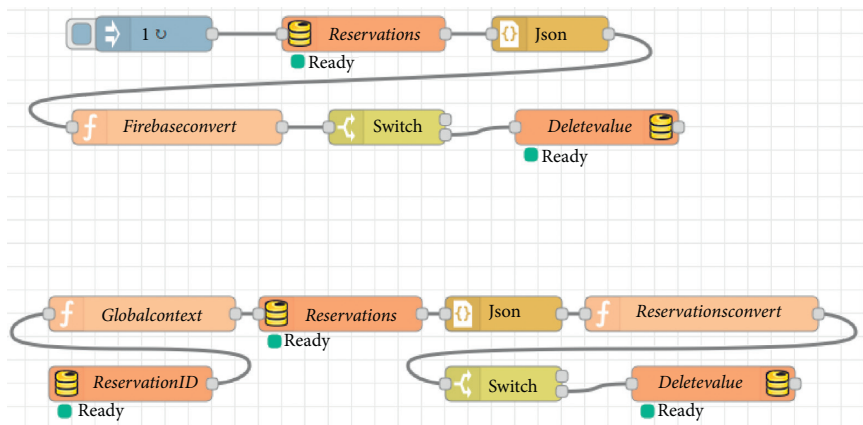


FIGURE 14: Parking reservation management.

```

var fm = parseInt(data1[5]);
var date = new Date();
var h = date.getHours()+1;
var m = date.getMinutes();
var delta = (h * 60 + m)-(fh*60+fm);
if(delta > 60){

```

```

var cesta = "parkings/parking1/reservations/
-" + data1[0];
node.send({childpath:cesta});
}
else{
node.send({payload:nic});

```

```

    }
}
return;

```

As mentioned previously, when the entrance barrier is opened, the phone ID is written to the reservationID entry. The change of its state is monitored by the ResourceID node, which begins the second part of this flow. The phone ID is stored in a global variable, and all reservations are read from the database, converted to JSON format and passed to the ReservationConvert (code: delete driver's reservation for parking) function, which compares the records in the database with the stored phone ID. When a match is found, the entry is deleted. The switch performs the same function as in the previous case.

```

var response = msg.payload;
var reservationID = global.get("reservationID");
var data = "";
var data1 = response.split("{}").toString();
var l = data1.length;
for(i=0;i<l;i++){
    var s = data1.substring(i, i + 1);
    if(s == "\\"){
    }
    else if(s == "{}"){
    }
    else if(s == "{"){
    }
    else {data = data + s;}
}
var allmsg = data.split(",");
var al = allmsg.length;
for(i=1;i<al;i++){
    var data3 = allmsg[i].split(",");
    var androidID = data3[1].substring(10, data3[1].length);
    var path = "parkings/parking1/reservations/" +
    data3[2].substring(3, data3[2].length);
    if(androidID == reservationID){
        node.send({childpath:path});
    }
    else {node.send({payload:1});}
}
return;

```

**5.6. Smartphone Application.** For the purposes of the testing and validating, an Android app has been developed. This app enables control of all the functions on the screen, so the controls are user-friendly and simple. The functions are started by tapping simple icons, so the driver is not forced to read through the context menus while driving. The overview of all the functions and meaning of the individual icons is represented by the image.

**5.7. Automatic Detection of a Nearby Parking Lot.** As described in chapter 4.5, the automatic detection of a nearby

parking lot is procured via geofencing service. For this purpose, the Constants class is used. It contains the parameters such as creating a geofence (GPS coordinates and radius). Using a hash map, several geofences can be created simply by adding a name and coordinates via another command.

```

LANDMARKS.put(. . . . .); (code: set geofence
parameters).
public class Constants {
    public static final float GEOFENCE_RADIUS_
    IN_METERS = 1000;
    public static final HashMap < String,
    LatLng > LANDMARKS = new HashMap < String,
    LatLng > ();
    static {
        // Parking 1
        LANDMARKS.put("Parking 1", new LatLng
        (50.420860, 16.185796));
    }
}

```

By calling the populateGeofenceList() method in MainActivity, custom geofence is created (code: creating geofence).

```

public void populateGeofenceList() {
    for (Map.Entry < String, LatLng > entry: Constants.LANDMARKS.entrySet()) {
        mGeofenceList.add(new Geofence.Builder()
            .setRequestId(entry.getKey())
            .setCircularRegion(
                entry.getValue().latitude,
                entry.getValue().longitude,
                Constants.GEOFENCE_RADIUS_IN_
                METERS
            )
            .setExpirationDuration(Geofence.
                NEVER_EXPIRE)
            .setTransitionTypes(Geofence.GEOFENCE_
                TRANSITION_ENTER)
            .build());
    }
}

```

The GeofenceTransitionsIntentService class subsequently creates a notification channel that it uses to inform the driver with a notification about available parking lot upon entering inside the created geofence (Figure 15).

**5.8. Navigation to the Parking Lot.** To run the navigation, the app uses Google API and Google Maps for Android, which enables running a map in the following modes:

Display the map on a given place with given zoom level

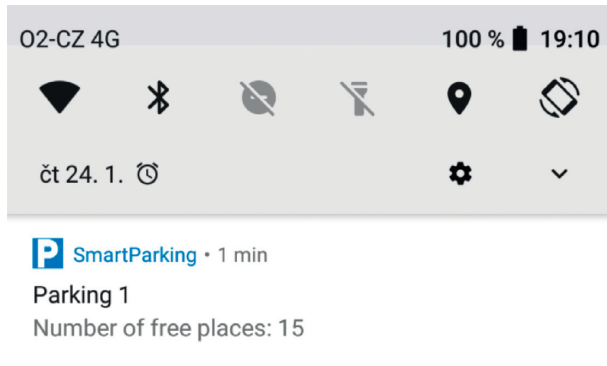


FIGURE 15: Notification after entering geofence.

Searching for a place and displaying it on the map

Navigation with the selected means of transport (car, bicycle, and walking)

Displaying the panorama view in Google Street View service

To run the map, it is first necessary to create an “Intent” object and specify the mode in which the map will be opened. Intent contains a special string (URI), which accurately specifies the requested action. After creating the Intent, the activity gets started by the `startActivity()` method. As you can see in the following code (code: create Intent and run Map Activity), Intent is created via URI, which defines the type of the action as navigation to a set GPS coordinate. Subsequently, the Intent is injected with a packet to secure that is processed by Google Maps.

```
public void startNavigationButtonHandler(View view)
{
    Uri gmmIntentUri = Uri.parse("google.navigation:q=50.475367,16.179489");
    Intent mapIntent = new Intent(Intent.ACTION_VIEW, gmmIntentUri);
    mapIntent.setPackage("com.google.android.apps.maps");
    startActivity(mapIntent);
}
```

**5.9. Information about the Parking Lot Occupancy.** The information about number of available and occupied parking space is saved by NodeRED into the Firebase database, and in the Android app, the instance of the database is created: `FirebaseDatabase database = FirebaseDatabase.getInstance()`, along with the references for its individual items: `DatabaseReference myRef... = database.getReference("parkings/parking1/.....")`. This is followed by the listener performing the corresponding actions every time a value changes in any of the values it is monitoring.

```
public void readFreePlaces(){
    myRefFplaces.addValueEventListener(new ValueEventListener() {
```

```
@Override
public void onDataChange(@NonNull DataSnapshot dataSnapshot) {
    places = dataSnapshot.getValue().toString();
    int pl = Integer.parseInt(places);
    int cr = (int) (pl - countRes);
    Fplaces.setText(String.valueOf(cr));
}

@Override
public void onCancelled(@NonNull DatabaseError databaseError) {
    places = "Error";
}
});
```

On every change of the available parking spaces, the method above (code: setting the listener to change the number of free parking spaces) sets the textView value on the main activity via the `setText` method, so the button always contains the current number of available spaces on the parking lot. When tapping this button, a new activity is run. It contains listView, which informs the driver about current occupancy of the individual parking spaces on the parking lot. The same activity is run also upon entering the parking lot after the request to open the entry gate, so the driver has an overview of the available spaces. For this purpose, the app uses, similarly to the previous case, the data stored in the database, whose changes are monitored by the listener. The data about the occupancy of the individual spaces are stored in the database via NodeRED in the form of a string “0000110100110010”, which contains sixteen bits: “1” or “0”. If the given position has the value of “1”, it means that the space is occupied. Otherwise, the space is available. The `getOccupancy()` method (code: filling a text field based on database data) in this activity fills the `OCCUPANCY[]` array with the values “FREE” or “OCCUPIED”.

```
public void getOccupancy(){
    for(int i=0;i < 8;i++){
        System.out.println(places.substring(i, i + 1));
        if(places.substring(i, i + 1).equals("0")){OCCUPANCY[i] = "FREE";}
        if(places.substring(i, i + 1).equals("1")){OCCUPANCY[i] = "OCCUPIED";}
        if(places.substring(i + 8, i + 9).equals("0")){OCCUPANCY[i + 8] = "FREE";}
        if(places.substring(i + 8, i + 9).equals("1")){OCCUPANCY[i + 8] = "OCCUPIED";}
        NUMBERS[i] = i + 1;
    }
}
```

Afterwards, these values are in the adapter using listView passed to individual textView (code: filling text boxes and setting font color based on content), as is shown in the image (Figure 16).

FREE	8	FREE
FREE	7	FREE
OCCUPIED	6	FREE
FREE	5	OCCUPIED
FREE	4	FREE
OCCUPIED	3	FREE
FREE	2	OCCUPIED
FREE	1	FREE

FIGURE 16: Parking occupancy is displayed.

```

public View getView(int i, View view, ViewGroup
viewGroup) {
    view-
    = getLayoutInflater().inflate(R.layout.customlayout,
    null);
    TextView
    tvNumbers = view.findViewById(R.id.tvNumbers);
    TextView
    tvOccupancy = view.findViewById(R.id.tvOccupancy);
    TextView
    tvOccupancy1 = view.findViewById(R.id.tvOccupancy1) ;
    tvNumbers.setText(String.valueOf(NUMBERS
[i]));
    tvOccupancy.setText(String.valueOf(OCCU-
PANCY[i]));
    tvOccupancy1.setText(String.valueOf(OCCU-
PANCY[i+8]));
    if(OCCUPANCY[i].equals("FREE")){tvOccu-
pancy.setText(Color.parseColor("#00ff00"));}
    if(OCCUPANCY[i].equals("OCCUPIED")){tvOccu-
pancy.setText(Color.parseColor("#ff0000"));}
    if(OCCUPANCY[i+8].equals("FREE")){tvOccu-
pancy1.setText(Color.parseColor("#00ff00"));}
    if(OCCUPANCY[i+8].equals("OCCUPIED")){tvOc-
cupancy1.setText(Color.parseColor("#ff0000"));}
    return view;
}
}

```

5.10. *Creating a Parking Space Reservation.* Every driver can make one short-term reservation of one parking space. For this purpose, the app uses the Reservation.java class, which has three attributes:

id—item ID generated by the Firebase database

androidID—unique 64-bit number generated by the Android OS  
time—the time when the reservation is created

Before creating a reservation, based on the Android ID, the app checks whether the user is already saved in the database (has a valid reservation or is already on the parking lot) (Sample 14) and if there are any spaces available for reservation on the parking lot (number of free spaces—number of valid reservations). If a reservation is possible, it asks the database for a new item id: id = myRefRes.push().getKey(). It then creates a new instance of the Reservation class: myRefRes.child(id).setValue(reservations; and finally, this newly created instance is stored in the database (Figure 17): myRefRes.child(id).setValue(reservations) (code: determining the status of a user’s reservation).

```

public void onDataChange(DataSnapshot snapshot) {
    countRes = snapshot.getChildrenCount();
    updateCountReservation();
    resIndicator = false;
    for (DataSnapshot postSnapshot: snapshot.getCh-
ildren()) {
        Reservation
        post = postSnapshot.getValue(Reservation.class);
        String resCheck = post.getAndroidID();
        if(resCheck.equals(androidID)){resIn-
dicator = true;}
    }
}

```

The state of the reservations is regularly monitored also by the mini PC via NodeRED, and if the time limit for the reservation is exceeded, it is automatically removed from the database. The reservation is removed also if a driver with a valid reservation arrives on the parking lot and sends a request to open the entry gate. The procedure for removing the reservation from the database is described later.

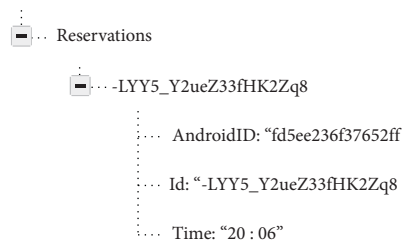


FIGURE 17: Example of saving the reservation to the database.



FIGURE 18: Record the vehicle present in the parking lot.

5.11. *Opening the Entry/Exit Gate.* To open the entry/exit gate, the app again uses the Firebase database, which contains two items:

gate: it can contain two values: 1 and 0 (entry gate open/closed)

gateID: in case the car is present on the parking lot, the app saves the androidID of the user who wants to open the exit gate

The app contains the `CarInPark.java` class, which has, similarly to the `Reservation.java` class, three attributes:

id—item ID generated by the Firebase database

androidID—unique 64-bit number generated by the Android OS

time—time of arrival on the parking lot

The same as with the requirement to create a reservation, during the requirement to open the gate, the app first checks whether the vehicle is currently present at the parking lot (has a record in the database) via androidID. Then, by comparing two GPC coordinates, it checks whether the maximum distance of the smartphone from the gate is not exceeded. If these conditions are met, by entering the value of “1” to the gate item of the Firebase database, NodeRED procures that the entry gate is open. Then, it follows with a request for a new id to save the item in the database: `String id = myRefCar.push().getKey();` then, a new instance of the `CarInPark` class is created: `carInPark = new CarInPark(id, androidID, time);` and finally, the item is saved in the database: `myRefCar.child(id).setValue(carInPark)` (Figure 18). After closing the gate, using NodeRED, a potential reservation belonging to the driver entering the parking lot is deleted.

If the vehicle is on the parking lot (user’s androidID is in the database), androidID is saved in the gateID item, and based upon this action, NodeRED opens the exit gate and removes the corresponding user’s record. The processes of opening and closing the parking lot gates using NodeRED have been described in Chapter 6.3.

## 6. Discussion

During the pilot operation, vehicle detection using a magnetometric sensor has been tested in two phases. In the first phase, unprompted detection testing has been performed. In the second phase, testing for detection of vehicles of various sizes was followed. For the first phase of the testing, an

Arduino module program was modified to count the vehicle detections. The testing was carried out for the period of 24 hours, performing a check twice per second. The sensor was placed and fixed so its move in any direction was impossible. In 24 hours, 172,800 checks were performed, and only four detections were faulty, with the error rate of 2.3%.

In the second phase, correct detection of five vehicles of different sizes (Toyota Yaris, Škoda Roomster, Škoda Octavia combi, Citroën Jumpy, and Nissan Navara) was tested. Every vehicle was placed thirty times over the magnetometric sensor. The detection success rate was very high—there has been only one faulty detection, which happened with the smallest of the vehicles (Toyota Yaris).

The automatic nearby parking lot detection has been carried out over the course of two weeks. The first week, testing for choosing the appropriate radius of the geofence was carried out, so the driver would get an information about an available parking lot in time and would be able to respond to this information easily. After one-week testing, 1,000 meters was chosen as the most suitable radius. Because of the delay described earlier, the driver in town traffic would the information about 500 to 800 meters before the parking lot. The second week, after setting the suitable radius, testing on a 10-kilometer route was carried out. On this route, five geofences were set up. Ten drivers have driven in this route ten times in total, which means that 500 tests have been performed. In three cases, the notification was not received, and in four cases, the driver received the notification in distance under 200 meters from the parking lot. This adds up to the error rate of 1.4%.

One of the important factors for successful adoption of any car parking solution is the economic efficiency. The financial costs of traditional and complex solutions, which have been stated in related works, are certainly higher than the low-cost solutions based mini PC. The final costs are also affected by the selection of individual components, so the final cost of the solution was not high. The approximate retail prices, at which the individual components of the system were purchased, are summarized in the following list:

- MPU-9250 (3 €)
- Arduino Mini (2 €)
- IQRF TR-72D (14 €)
- Battery (19 €)
- UbBoard-mini PC (90 €)
- Entrance barrier (606 €)



## 7. Conclusion

The presented solution has been used for pilot deployment, and in case the solution was to be used commercially, some enhancements of its functionality would be needed. In the current state, since the time is saved in the database upon vehicle entering the parking lot, the app would be capable of calculating the parking fee if price tariffs were to be added. For the commercial use, it would be necessary to implement a way to pay the parking fee, which could be done either using a parking machine placed directly on the parking lot or implementing a connection to a payment gateway to the app. It would also be suitable to also develop an iOS app, so that the iPhone users could use the system as well. Another option would be to develop a web app for communication with the system. The app would run directly in a smartphone web browser, and therefore, the system would be cross-platform. The majority of the system parts and the mobile app have been designed in the way that would allow future development of more functionalities. The structure of the data stored in the database makes it possible to add additional parking lots, and the automatic parking lot availability detection enables to display notifications about more than one parking lot.

Therefore, after some modifications, the system could be used by, for example, owners of permanent parking lots, also during large occasional events. Considering its low expenses, the system could not only help the drivers solve their problems with searching for empty parking spaces and improve the traffic in the towns and cities, but it could also help to deal with the problems with the drivers who avoid paying the parking fees, especially on the open parking lots with the parking machines.

## Data Availability

The measured data used to support the findings of this study are available from the corresponding author upon request.

## Conflicts of Interest

The authors declare that they have no conflicts of interest.

## Acknowledgments

This work was supported by a Specific Research Project, Faculty of Informatics and Management, University of Hradec Kralove, Czech Republic. We would like to thank Mrs. H. Svecova, a doctoral student, and Mr. J. Dian, a graduate, of Faculty of Management and Informatics, University of Hradec Kralove, for the practical verification of the proposed solutions and close cooperation in the solution.

## References

- [1] A. Khanna and R. Anand, "IoT based smart parking system," in *Proceedings of International Conference on Internet of Things and Applications (IOTA)*, pp. 266–270, Pune, India, January 2016.
- [2] I. Chatzigiannakis, A. Vitaletti, and A. Pyrgelis, "A privacy-preserving smart parking system using an IoT elliptic curve based security platform," *Computer Communications*, vol. 89–90, pp. 165–177, 2016.
- [3] S. Kubler, J. Robert, A. Hefnawy, C. Cherifi, A. Bouras, and K. Främling, "IoT-based smart parking system for sporting event management," in *Proceedings of the 13th International Conference on Mobile and Ubiquitous Systems: Computing, Networking and Services-MOBIQUITOUS 2016 [online]*, pp. 104–114, New York, USA, November 2016.
- [4] H. Arasteh et al., "IoT-based smart cities: a survey," in *Proceedings of IEEE 16th International Conference on Environment and Electrical Engineering (EEEIC)*, pp. 1–6, Florence, Italy, June 2016.
- [5] MF. Tsai, Y. C. Kiong, and A. Sinn, "Smart service relying on internet of things technology in parking systems," *The Journal of Supercomputing*, vol. 74, no. 9, pp. 4315–4338, 2018.
- [6] C. Roman, R. Liao, P. Ball, S. Ou, and M. de Heaver, "Detecting on-street parking spaces in smart cities: performance evaluation of fixed and mobile sensing systems," *IEEE Transactions on Intelligent Transportation Systems*, vol. 19, no. 7, pp. 2234–2245, 2018.
- [7] I. Calvo, J. M. Gil-García, I. Recio, A. López, and J. Quesada, "Building IoT applications with raspberry Pi and low power IQRf communication modules," *Electronics*, vol. 5, no. 4, p. 54, 2016.
- [8] V. Jan, P. Martin, and R. Hajovsky, "Wireless measurement of carbon dioxide by use of IQRf technology," *IFAC-PapersOnLine*, vol. 51, no. 6, pp. 78–83, 2018.
- [9] J. Skovranek, P. Martin, and R. Hajovsky, "Use of the IQRf and Node-RED technology for control and visualization in an IQMESH network," *IFAC-PapersOnLine*, vol. 51, no. 6, pp. 295–300, 2018.
- [10] M. Pies and R. Hajovsky, "Using the IQRf technology for the internet of things: case studies," in *Mobile and Wireless Technologies 2017. ICMWT 2017. Lecture Notes in Electrical Engineering*, K. Kim and N. Joukov, Eds., vol. 425, Singapore, Springer, 2017.
- [11] J. Kopják and G. Sebestyén, "Comparison of data collecting methods in wireless mesh sensor networks," in *Proceedings of IEEE 16th World Symposium on Applied Machine Intelligence and Informatics (Sami)*, pp. 000155–000160, Kosice, Slovakia, February 2018.
- [12] O. Vondrouš, Z. Kocur, T. Hégr, and O. Slavíček, "Performance evaluation of IoT mesh networking technology in ISM frequency band," in *Proceedings of 17th International Conference on Mechatronics-Mechatronika (ME)*, pp. 1–8, Prague, Czech Republic, December 2016.
- [13] IQRf Tech sro, *IQRf DPA framework Technical Guide*, Vol. 10, IQRf Tech, Jičín, Czech Republic, 2018.

## Research Article

# Smart Radio Resource Management for Content Delivery Services in 5G and Beyond Networks

**Dominik Neznik, Lubomir Dobos, and Jan Papaj** 

*Department of Electronics and Multimedia Communications, Faculty of Electrical Engineering and Informatics, Technical University of Kosice, Bozeny Nemcovej 32, Kosice, Slovakia*

Correspondence should be addressed to Jan Papaj; [jan.papaj@tuke.sk](mailto:jan.papaj@tuke.sk)

Received 26 April 2020; Revised 22 May 2020; Accepted 25 July 2020; Published 17 August 2020

Academic Editor: Ondrej Krejcar

Copyright © 2020 Dominik Neznik et al. This is an open access article distributed under the Creative Commons Attribution License, which permits unrestricted use, distribution, and reproduction in any medium, provided the original work is properly cited.

In 5G networks, the spectrum allocation techniques play a very important part of the quality of content delivery services. The processes of channelling and device selection are important in the 5G technology and beyond with many access devices in networks to improve the quality of services. In this paper, we propose a method based on Fuzzy Logic, Game Theory, and Smart Method (which is a combination of Fuzzy Logic and Game Theory). These methods are suitable to improve the speed and quality of links of data routing in networks. The paper shows that effective spectrum allocation to devices is not an option but a requirement in a huge data flow environment of the wireless communications, if one wants to ensure acceptable speed and quality of the connection and to provide adequate quality of the services. Each of the selected methods for radio resource management has some advantages and disadvantages in the evaluation of results. The paper describes the process of channel allocation with different methods for IEEE 802.11xx networks that are in the focus of our research in the sphere of wireless communication. Companies use cloud computing to provide services and to share information, but there needs to be some radio resource management to effectively use the services in the wireless mobile environment because the number of different types of devices being connected to the wireless networks to create smart homes and smart cities is growing.

## 1. Introduction

The 5G technology, mobile ad hoc networks, or other types of wireless networks take into account communication control information between devices and obtain this information to select suitable channels to increase the quality of the network. The main aim is to allocate channels to improve the quality of the services, which leads to a speed improvement and decrease the interference. The efficiency is used for the optimization of the channel selection in wireless networks to improve the quality of the device connection. Furthermore, smartphones are very significant devices in the modern era of the wireless networks and their constantly increasing processing, communication, and sensing capabilities lead to the expansion of their application in various fields of the services. The available spectrum in the way that is used today is not effective. It is more effective to use a free

channel for communication without interference (trying to minimize interference) while serving a huge number of wireless devices. For this purpose, the cognitive radio technology is suitable, because it enables spectrum switching based on a set of measurable parameters. Also, the cognitive radio allows a channel to be changed even if communication on the selected channel is insufficient due to interference caused by an adjacent device communicating on an inappropriate communication channel. The 5G technology will be able to support all communication needs as a low power Local Area Network (LAN) used as a home network, for Wide Area Networks (WAN), with the right latency and speed settings. The technology will be able to communicate with the broad variety of modern wireless and mobile networks (IEEE 802.11xx, Z-Wave, LoRa, 3G, 4G, etc.). Where there is a communication, there also needs to be the channel allocation mainly in networks with many types of devices such as the

Internet of Things [1]. It should be a smart channel allocation and the process should be able to adapt to the environmental conditions in order to prevent radio interference.

## 2. Spectrum Allocation in Modern Wireless Networks

If there is an imminent threat, whether natural or artificial, people prefer to work from home, usually operating from local home networks for some period of time. In such a situation, every provider in the world faces a problem of a large amount of people staying at home all day long and using their services with a huge data flow [2]. This is a situation requiring fast, secure, and low interference forwarding of the data on the Internet in the time when vast numbers of people need to work from local Internet providers. One can see how some Internet providers decrease the quality of their services (e.g., video streams) to be able to serve every customer watching films, listening to music, playing video games, and so forth at the same time at home. Many devices and data streams are connected to the same access point with the same selected channel. The design of the method for channel allocation needs to take into account a spectrum sensing to obtain availability information from the radio environment for each associated device [3–7].

The spectrum sensing method helps to measure individual parameters, for instance, the intensity of the received signal (received signal strength (RSS)), the interference from surrounding devices, and their communication channels currently in use. Another important parameter is the ratio of signals (signal-to-interference ratio (SIR)). This parameter indicates the ratio of useful signal and interference caused by the transmission of neighbouring devices within the radio range. Certainly, it is not effective to select a channel with the high traffic/network data load. A more suitable approach would be to select channels with average, low, or no traffic at all. An important parameter representing the quality of the network connection is the SIR ratio.

*2.1. Game Theory as a Method for Channel Allocation.* The Game Theory (GT) was originally designed for economic and social research, but nowadays it is used in much more disciplines. This method can also be applied in wireless communication to the channel allocation [8]. The method can be defined as a study of mathematical models of conflict and cooperation between intelligent rational decision-makers.

Game is defined as the set  $Q = 1, 2, \dots, N$ , which is a nonempty set. Elements of this set are individual players. In addition to this set, we also have a set of  $N$  sets  $\chi_1, \chi_2, \dots, \chi_N$  and  $N$  real functions  $M_1(x_1, x_2, \dots, x_N), \dots, M_N(x_1, x_2, \dots, x_N)$  defined on the set  $\chi_1, \chi_2, \dots, \chi_N$ . Then a normal game holds two sets:

$$\left\{ Q; \chi_1, \chi_2, \dots, \chi_N \right\}, \quad (1)$$

$$\left\{ M_1(x_1, x_2, \dots, x_N), \dots, M_N(x_1, x_2, \dots, x_N) \right\},$$

where the set  $Q$  means a set of players,  $\chi_n$  represents the set of strategies for the  $n$ -th player, and  $M_n$  is a gain function (pay-

off function) of the  $n$ -th player. Also, each player has a strategy set  $s_1, s_2, s_3, \dots, s_p$ , where  $p$  represents the total number of players [8].

The GT provides general mathematical techniques for analysing situations in which two or more players make decisions and influence other players [9]. It is a method for channel allocation, which uses input parameters to select a suitable type of game with a suitable strategy to improve the pay-off for channels used in the network [10].

The input parameters are priority parameters and they define the quality of services on each channel. The problem in the channel allocation is the cooperation in game strategy (channel choices) to improve the quality of the affected channel and network. The quality of the network for better communication should be the main aim, rather than the communication between two individual devices. We decided to use the Game Theory based on the game with the name ‘‘prisoner’s dilemma’’ for the channel selection in D2D networks. The prisoner’s dilemma presents a situation where two players are separated and are unable to communicate with each other. Each of them must choose between cooperating or not with the other player. The highest reward for each part occurs when both parts choose to cooperate. The same strategy can be used to select the best available channel to increase the quality of the link. When the quality of the network increases, it also means that the quality of the channel is better. In the situation where one player betrays another one, the quality of channel is increased only for a dominant player. The remaining player is forced to select one of the inferior channels. Thus, mutual cooperation is a key strategy for an optimal channel allocation. Therefore, the quality of network services can be optimal on both sides. The GT consists of players and strategies to improve the probability of winning the game. In a network, devices represent players playing the game. A typical wireless network consists of several equivalent devices. Because of that, the channel distribution is distributed equally. If a scenario regarding cognitive radio network consists of a particular number of primary and secondary devices, these devices are not equivalent (they are not treated equally) [11–15]. This scenario has a hierarchy, where the primary device has higher access rights to a transfer medium than the secondary device.

*2.2. Fuzzy Logic as a Method for Channel Allocation.* A method based on Fuzzy Logic (FL) is used for a more accurate evaluation of the channel selection. The advantage of FL is in the interval of values and not just in the definition of a parameter as suitable or unsuitable [16]. Figure 1 shows how the method works, with each parameter defined by its affinity function. As one can see in Figure 1, the process of the channel selection includes the fuzzification and defuzzification processes [17]. The fuzzification is the process of changing a real scalar value into a fuzzy value. This is achieved with the different types of functions (membership functions). The types of membership functions (MF) provided by the Fuzzy Logic Toolbox in Matlab are shown in Figure 2 and the simplest one is formed by the straight lines to create a triangle, which is the basic shape of a membership function [18, 19].

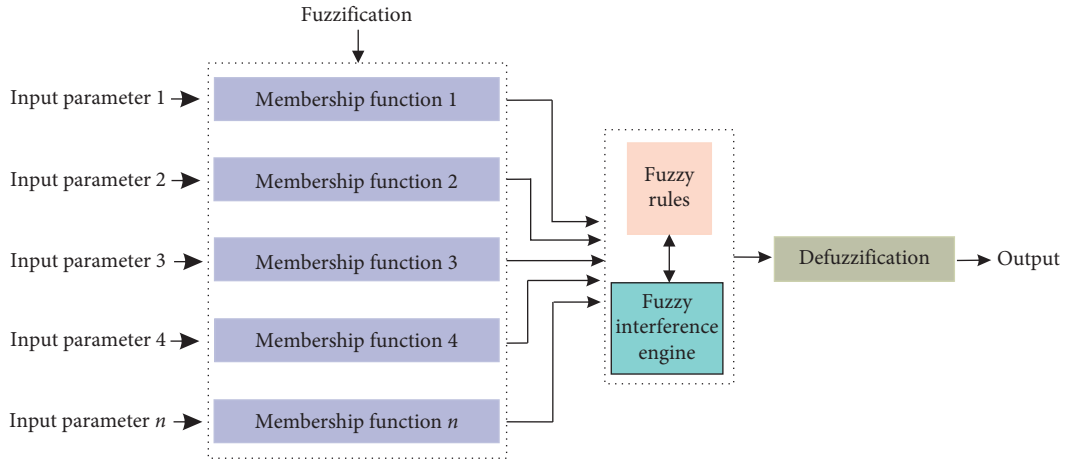


FIGURE 1: Process of Fuzzy Logic method to obtain output value of channels.

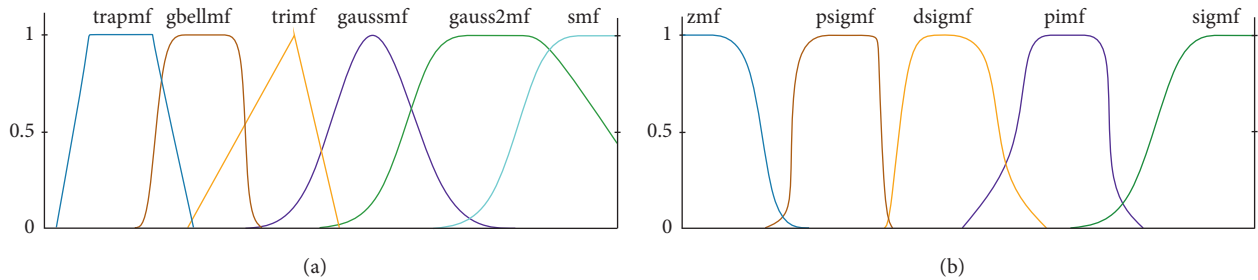


FIGURE 2: Available types of membership functions in Fuzzy Logic Toolbox in Matlab.

The fuzzification process determines the degree to which input data belong to each appropriate fuzzy set via the membership functions. The shapes of these functions can be diverse and various. For each input and each output, a variable member function needs to be selected. Typically, there are three, but the final number of functions can vary.

The defuzzification process obtains a single number from an output of the aggregated fuzzy set. The most commonly used defuzzification method is “the centre of the area method,” also commonly referred to as the centroid method. Figure 3 shows the number of input parameters (IP); one needs to define several rules for each combination of the parameter sets.

Table 1 contains possible fuzzy operations for OR and AND operators on these sets, comparatively. The most frequently used operations for OR and AND operators are max and min, respectively. Let  $\mu_A$  and  $\mu_B$  represent the membership functions for fuzzy sets A and B. For complement (NOT) operation, equation (2) is used for the fuzzy sets [17]:

$$\mu_{\bar{A}}(\chi) = 1 - \mu_A(\chi). \quad (2)$$

The output from the FL is the rank of each channel. The Fuzzy Inference System consists of two methods, which have different consequences of fuzzy rules and also different impacts on output values.

The Mamdani method [20] uses the trimming of the output membership function to rank input membership

```

IP_1 is suitable
&
If IP_2 is suitable    then output is very suitable
&
IP_3 is suitable
    
```

FIGURE 3: Fuzzy Logic rule with three input parameters.

TABLE 1: Fuzzy set operations.

<i>OR (union)</i>	
MAX	$\max\{\mu_A(\chi), \mu_B(\chi)\}$
ASUM	$\mu_A(\chi) + \mu_B(\chi) - \mu_A(\chi)\mu_B(\chi)$
BSUM	$\min\{1, \mu_A(\chi) + \mu_B(\chi)\}$
<i>AND (intersection)</i>	
MIN	$\min\{1, \mu_A(\chi), \mu_B(\chi)\}$
PROD	$\mu_A(\chi)\mu_B(\chi)$
BDIF	$\max\{0, \mu_A(\chi) + \mu_B(\chi) - 1\}$

value. This method was originally designed to imitate the performance of the human operators in charge of controlling certain processes in an industrial environment. This system is composed of If-Then rules of the following form: If X is A Then Y is B, where X and Y are parameters and A and B are sets of these parameters. As an example in our scenario, it can be as follows: If traffic is “low” then a channel is “suitable.” The If part X is A is called the *antecedent* of the rule, and the Then part Y is B is called the *consequent* of the rule. The Mamdani systems are universal approximators and



they can include knowledge in the form of linguistic rules that can be used for local fine-tuning [21].

The Sugeno method is the system that was first proposed by Takagi and Sugeno in 1985 [22], and the next version of the method was proposed by Sugeno and Kang in 1988. This method is also known as the Takagi-Sugeno-Kang (TSK) fuzzy model or the Sugeno model. The main feature of the Takagi-Sugeno fuzzy model is to express the local dynamics of each fuzzy implication (rule) by a linear system model. Also, this model is a universal approximator of any smooth nonlinear system [23].

The main difference between these two methods is that the Mamdani method is intuitive, it has widespread acceptance, and it is well suited to a human input. On the other hand, the Sugeno controller has more adjustable parameters compared to the Mamdani method controller. The Sugeno method is computationally efficient, it works well with linear techniques, and it also works well with optimization and adaptive techniques [23].

### 3. Proposed Algorithms for Channel Allocation

In this section, we present algorithms for channel allocations based on three methods (Game Theory, Fuzzy Logic, and Smart Method). In our algorithm, we consider a situation in which 13 wireless channels exist. These channels work as communication medium based on IEEE 802.11xx technology [24]. Every proposed method works autonomously on every device, but we define a parameter *ID\_value* for the order of channel allocation in the algorithm. This parameter is based on the total number of devices in the algorithm. First of all, every device needs to power on and to be able to connect to the network. The next step is the spectrum sensing which has a capability to collect important information about QoS of the links between neighbouring devices and the device itself, as well as the information about already selected channels in the radio range. The device can start a process of communication or it can stay idle if the device has no data to transfer. After this initial process, when the device has all information about the neighbored channel, the allocation method is used. The priority is to distribute available channels with no repetition in the radio range, as it is in a random distribution. Beyond these parameters of QoS for proposed methods, we also need to define the initial parameters, such as the position and radio range in the investigation area of each device (see Table 2). Devices share information about neighbours in the radio range and they can create a topology of the network. The network topology is created by links between devices. There is no localization algorithm that defines the position of each device in the network [25]. These parameters are shown in Table 3. Also for our algorithm, we need the priority parameters to define the quality of services on each channel.

The quality of the selected channel is based on interference from the environment in the radio range. We need to define how many of these priority parameters are enough to define the adequate quality of the link. We determine three main priority parameters: the first is the parameter of *SIR\_value* which shows the communication suitability of the

TABLE 2: Example of position matrix of device location in network topology.

Device ID_	1	2	3	4	5	...	<i>n</i>
<i>x</i>	50	373	402	423	100	...	350
<i>y</i>	50	33	468	408	323	...	350

TABLE 3: Parameters of simulations.

Parameters names	Values
Area (m)	500 × 500
Radio range of device (m)	100
Number of nodes	40
Number of iterations	
(Game Theory)	20
(Fuzzy Logic)	2
(Smart Method)	20
Simulation duration (min)	20

channel in the present environment, the second is the parameter of *RSS\_value* which selects the more suitable channel for the device in a lower distance, and the third is the parameter representing the current amount of network traffic in order to determine how much capacity of the channel is being used. We select these three parameters to define the quality of the channel, but, with more parameters for the device, we need more time to obtain information. Also, the method with many parameters needs more time to evaluate the output value for each channel. The main focus of the suitability of channel is based on the *SIR\_value* and only channels with the suitable value of this parameter are considered as appropriate channels for communication. Table 4 shows all possible sets of the selected input parameters for the proposed algorithms. We use the *RSS\_value* to calculate the *SIR\_value*, because the distance between two devices influences the available channel difference. It is possible to calculate the *SIR\_value* as the ratio of used signal and interference from other devices in the radio range [26]. Small distance influences connection more than long distance on the edge of the radio range. The value of the RSS parameter is determined by the strength of the received signal from the device in the radio range. Mobile devices can measure and determine the *RSS\_value* based on the received signal strength [27, 28]. So we assume that the device can determine this value, and, therefore, we only use the distance of two devices to define the value of this parameter for the algorithm process. The value of the SIR parameter is determined by the radio range of devices and their channels used. The intensity of this influence is according to their distance. A device is more influenced by the closer device. We select the path from Source device *ID\_1* to the Destination device *ID\_40*. The path is selected using Dijkstra's algorithm for determining the shortest path between the two devices, based on the connecting links in the network for devices in the radio range. Every device in the network with our algorithm has at start initial channel set to 1 as a channel to share the information between devices. Every device, when it makes a game move, exchanges information about the channel selection from devices with lower ID numbers.



TABLE 4: Sets of input parameters for proposed algorithms.

Parameter	SIR	RSS	Traffic
	Suitable	Low	No traffic
	Nonsuitable	Normal	Low traffic
		High	Normal traffic
			High traffic

The device does not have to analyse every device; it needs to analyse only devices in radio range and neighbours of neighbours to secure no interference. If there is a situation when there are no available channels, the device has two options. The first one is to wait until at least one available channel appears, and the second option is to choose some of the already used channels. The second option has some disadvantages but we can decrease the interference to a minimum and choose the channel with the lowest interference.

In the algorithm,  $ID\_value$  indicates the order in which devices run the method. The first game move is made by the device with  $ID\_1$  to allocate channels for all neighbours of this device. A device with  $ID\_1$  also allocates channels to each device in radio range based on  $ID\_value$  from the lower one of the highest. After the device with  $ID\_1$  selects channels for all neighbours, the next device can start the process of allocation. The next device in order is the device with the value  $ID\_2$  and the process is the same; only the device with  $ID\_2$  needs to consider selected channels by a device with  $ID\_1$  and optimize the channel allocation to this selection. Every device has a list of available channels that can be used. If the previous device uses some channels and it is in the radio range, then the device will discard this channel from the available list. If the device has no neighbours, there is no need to start the process of channel allocation, and it is possible to skip to another device with a higher  $ID\_value$ . The network topology consists of channel allocation for each link in the network, but it only represents preparation for demand on new data transfer between devices to select a suitable channel. The change of these channels takes place at each time slot of the movement. The proposed methods optimize channel allocations with a different number of iterations. The second iteration of the algorithm is about channel allocation and optimization of the network link quality based on the selected allocation method. During the next iterations, the optimum channel for connection between two devices is selected. Another attribute is the final channel allocation for each device, which is the last iteration of each method. The channel selected in the last iteration is to be used for the D2D connection in the radio range. The main idea of the proposed methods is presented in Figure 4 with main blocks for channel allocation. After parameter initialization based on the selected method, rules, and  $threshold\_value$ , the algorithm decides if a device has the new better channel to be used or the previous channel is more suitable to be used. Each method based on a number of iterations changes channels multiple times, but the final channel allocations for the D2D connections come from the last iterations. What is suitable for one method is not suitable for another method. Also, this influences the total number of

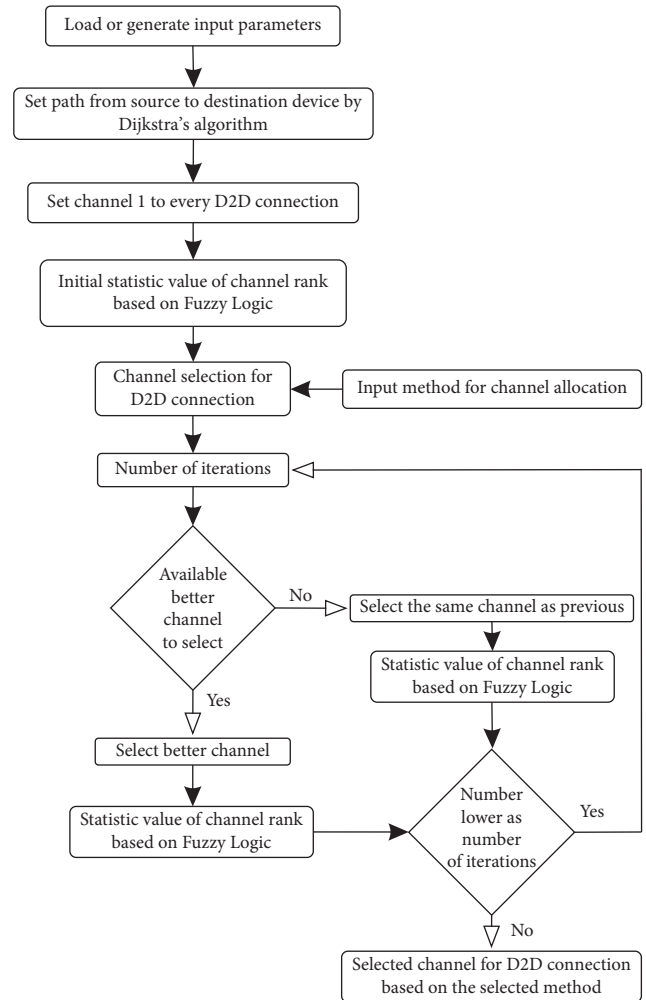


FIGURE 4: The main idea of proposed methods for channel allocation for the D2D network.

iterations necessary for the channel allocations optimization in the D2D network.

3.1. Method Based on the Game Theory Principle. There exist many different types of games that can be used, as well as information that can improve channel selection for devices in the network [29–31]. If devices want to cooperate to improve the quality of the network, then it is possible to achieve the best possible communication quality in the network. Improvement of network communication should be the main aim, rather than the communication between two individual devices. We suggest using the game type similar to the game with two prisoners. The main purpose is to reach an agreement sufficient for all players. Each device selects a channel based on previous game moves on a device with a lower ID number. The principle of the game is that one player makes a game move and other players need to react to this movement and to implement an appropriate strategy for this movement. The pseudocode of the algorithm is shown by Figure 5. We use functions such as  $SIR\_rank\_value$  to evaluate SIR ratio for each channel; also

```

input: load or generate Position_matrix, Number_of_Devices, Radio_range, ...
set path by dijkstra_algorithm from device ID_1 to device ID_40
generate channel_allocation to each links in radio range to 1;
Number_of_Iterations = 20;

Initial_parameters for method
for ID_value ← 1 to ID_value ← Number_of_Devices - 1 do
if distance of ID_value & ID_value+1 is lower as Radio_Range do
  device_connection (ID_value, ID_value + 1) = 1;
  set initial_first_value for each devices;
  SIR_rank_channel_initial calculate with RSS as influence ratio;
  RSS_value_device_initial calculate by distance;
  Traffic_value of channel set to 10;
end
end
input to fuzzy logic: SIR_rank_channel, RSS_value_of_device, Traffic_matrix;
rules_for_each_parameter_sets;
output Fuzzy_logic_out_value for channel rank on selected link and iteration;
channel_rank_iteration (1, :, :) = Fuzzy_logic_out_value;

for Number_of_Iterations ← 2 to Number_of_Iterations do
for ID_value ← 1 to ID_value ← number_of_devices + 1 do
if device_connection (ID_value, ID_value + 1) = 1 do
for channel ← 1 to channel ← 13 do
  Call Funncions: SIR_rank_channel;
  RSS_value_device;
  Traffic_matrix;
  Device_links_by_radio_range;
end
if difference between value of channel SIR and previous selected channel SIR
value is higher as threshold_value do
if Traffic_value of channel is lower as high_traffic do
  set channel_allocation of link = channel;
else
  set channel_allocation of link = channel_allocation (Number_of_Iterations - 1);
end
end
input to fuzzy logic: SIR_rank_channel, RSS_value_of_device, Traffic_matrix;
rules_for_each_parameter_sets;
output Fuzzy_logic_out_value for channel rank on selected link and iteration;
channel_rank_iteration (Number_of_Iterations, :, ID_value) = Fuzzy_logic_out_value;
end
end
end

```

FIGURE 5: Pseudocode of the proposed method based on Game Theory.

input to this function is *RSS\_value*. The distance of two devices with *RSS\_values* influences how strong the interference to other channels is and if that can be used as the channel for communication. The *Traffic\_matrix* influences how suitable the channel is. However, the main aim is to evaluate the channel's suitability based on the *SIR\_value*. A device selects the channel if the difference between the selected channel *SIR\_value* from the previous iteration and the *SIR\_value* of the best channel in the current iteration is higher than the *threshold\_value*. If this difference is lower than selected *threshold\_value*, the device will use the channel from the previous iteration. The last step of each iteration is to rank the channel used in this iteration. The channel rank is based on FL method and the output of this method is used as the channel rank, due to the fact that the channel rank value in the FL is defined as the degree of suitability. This value is from the interval 0 to 100, where 0 is the worst value and 100 is the best one.

Game Theory operates autonomously on each device and every device uses the cooperation strategy to share information with the other neighbours in the radio range to increase the effective distribution of channels. But, in our simulation, we set the order of channel allocations by the ID value. There exist many types of games to be implemented in our scenario, but we have decided to simulate a scenario with the cooperation of all devices in the network and we use the "prisoner's dilemma" game type. The "prisoner's dilemma"

game aims to obtain pay-off not for one of the players but to each one of them to give the best output value. To obtain this value, players need to cooperate and play the same strategy. The same principle can be used to choose an optimal channel in the network and to improve the quality of links for each communication.

**3.2. Method Based on the Fuzzy Logic Principle.** In the FL method, we use the *RSS\_value*, *SIR\_value*, and *Traffic\_value* parameters to rank the quality of a link for each device the same way as in the GT method. Figure 6 shows FL with these selected input parameters. Also, we focus rules more to *SIR\_value* as the priority parameter that defines if the channel can be used or not. If the *SIR\_value* is suitable, then the channel is suitable to be used. Other parameters (RSS and traffic) only define how suitable this channel is. On the other hand, if the *SIR\_value* is unsuitable, no matter how high values of other parameters are, we consider this channel as unsuitable. Some examples of rules for FL are shown in Figures 7 and 8 [32]. These figures show the limited rules for input parameters. Other rules only define how suitable examined channel is for allocation. The total number of rules is defined by several input parameters and their number of sets.

A channel can be ranked as *very suitable*, *more suitable*, *suitable*, or *unsuitable*. A device can select if a channel is *suitable* or with a higher rank value, but the main aim is to select those with the highest value due to the information from the spectrum sense and obtained information from devices in the radio range. Figure 9 shows the pseudocode of the algorithm we used for the channel selection. As one can see, it is similar to the GT with the same input and initial parameters. The main difference toward GT is in the decision. The GT uses *SIR\_value* difference as an attribute to decide if the channel is suitable or not. The FL uses *Fuzzy\_logic\_value* as an output from FL not only to rank each channel but also to decide if the channel can be used. The difference of previous iteration *Fuzzy\_logic\_value* and current *Fuzzy\_logic\_value* has to be higher than the *threshold\_value*. Only then can this channel be used and be allocated to link two devices. It is not effective to use a channel with a nonsuitable value of the SIR parameter, due to the fact that this channel has high interference, which means also low speed, more errors of packet delivery, and so on. The first process of each device is to allocate the channel to be able to communicate with other devices and to send control information, channel selection of other devices, and other information about the quality of links in the radio range.

**3.3. Smart Method for Channel Allocation.** The Smart Method is based on a combination of the GT and the FL. Attributes from the GT are the cooperation and more iterations to obtain optimal channels for each device. The process of this method is autonomous on each device in a one-time slot, where devices are not moving. The devices move in the simulation area with some social attributes but within one-time slot step simulation complete evaluation to

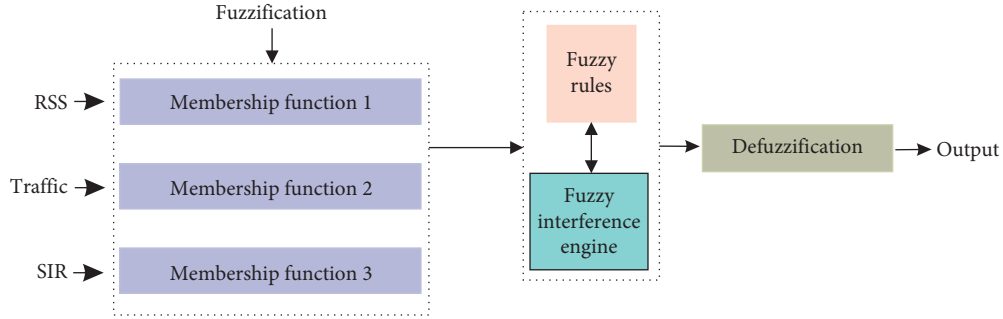


FIGURE 6: Fuzzy Logic with input parameters used for channel allocation.

Traffic is **low**  
 &  
**If** RSS is **high**      **then** output is **very suitable**  
 &  
 SIR is **suitable**

FIGURE 7: FL rule with suitable SIR value used for channel allocation.

Traffic is **low**  
 &  
**If** RSS is **high**      **then** output is **nonsuitable**  
 &  
 SIR is **nonsuitable**

FIGURE 8: FL rule with nonsuitable SIR value for channel allocation.

verify which channel is suitable to select in each iteration [33]. The FL is used as a complete unit; we only add attributes from the GT. The principle of decision is the same as the FL method, only with more iterations, where each device can react to other device selections. The player makes a game move and then the next player makes a game move but every player needs to consider the previous player’s selection. The channel rank is defined by the FL method for each iteration. The algorithm for this method is shown in Figure 10, where, in comparison with a method based on the FL, the only differences are the number of iterations and the strategy. The devices are able to change a channel multiple times, when it is possible to make it due to *threshold\_value* condition. If the channel is the same for more than one iteration, it means that there is no suitable channel to improve channel rank with consideration to the *threshold\_value*.

The multiple-channel selection by each device improves the channel allocation in the network, where a player makes a game move and the other player needs to react to this game move with the suitable game moves. The device sequence of selections of the suitable channel is by the device ID (IDentification number). The device with the lowest ID number uses this method as the first [34]. This method is used for each device separately, but again it is necessary to maintain a certain order in the algorithm. The first player by *ID\_value*, after analysis of available channels at each iteration, selects if a suitable channel is available based on a threshold condition. If this threshold condition is not valid, then the device uses the same channel as in the previous

**input:** load or generate *Position\_matrix*, *Number\_of\_Devices*, *Radio\_range*, ...  
**set** path by dijkstra\_algorithm from device ID\_1 to device ID\_40  
 generate *channel\_allocation* to each links in radio range to 1;  
*Number\_of\_Iterations* = 2;

**Initial\_parameters** for method

**for** *ID\_value* ← 1 to *ID\_value* ← *Number\_of\_Devices*-1 **do**  
**if** distance of *ID\_value* & *ID\_value*+1 is **lower** as *Radio\_Range* **do**  
   *device\_connection* (*ID\_value*, *ID\_value* + 1) = 1;  
   **set** initial\_first\_value for each devices;  
   *SIR\_rank\_channel\_initial* calculate with RSS as influence ratio;  
   *RSS\_value\_device\_initial* calculate by distance;  
   *Traffic\_value* of channel set to 10;  
   **end**  
**end**

**input to fuzzy logic:** *SIR\_rank\_channel*, *RSS\_value\_of\_device*, *Traffic\_matrix*;  
*rules\_for\_each\_parameter\_sets*;  
**output** *Fuzzy\_logic\_out\_value* for channel rank on selected link and iteration;  
*channel\_rank\_iteration* (1, :, :) = *Fuzzy\_logic\_out\_value*;

**for** *Number\_of\_Iterations* ← 2 to *Number\_of\_Iterations* **do**  
**for** *ID\_value* ← 1 to *ID\_value* ← *number\_of\_devices* + 1 **do**  
**if** *device\_connection* (*ID\_value*, *ID\_value* + 1) = 1 **do**  
   **for** *channel* ← 1 to *channel* ← 13 **do**  
     Call Funncions: *SIR\_rank\_channel*;  
                   *RSS\_value\_device*;  
                   *Traffic\_matrix*;  
                   *Device\_links\_by\_radio\_range*;  
   **end**  
   **if** difference between value of channel SIR and previous selected channel SIR  
   value is higher as *threshold\_value* **do**  
     **if** *Traffic\_value* of channel is lower as *high\_traffic* **do**  
       **set** *channel\_allocation* of link = *channel*;  
     **else**  
       **set** *channel\_allocation* of link = *channel\_allocation* (*Number\_of\_Iterations* - 1);  
     **end**  
   **end**  
**end**  
**input to fuzzy logic:** *SIR\_rank\_channel*, *RSS\_value\_of\_device*, *Traffic\_matrix*;  
*rules\_for\_each\_parameter\_sets*;  
**output** *Fuzzy\_logic\_out\_value* for channel rank on selected link and iteration;  
*channel\_rank\_iteration* (*Number\_of\_Iterations*, :, *ID\_value*) = *Fuzzy\_logic\_out\_value*;  
**end**  
**end**  
**end**

FIGURE 9: Pseudocode of the proposed method based on Fuzzy Logic.

iteration. Based on the strategy of device, one iteration is appropriate to select the best available channel for this device or improve also networks’ quality of links. Also, this change of channel is based on received information from other devices in network and the spectrum sensing from the radio range. If the device in the radio range chooses a channel, the device being investigated receives another suitable channel for reassessment; for this reason, the FL should be used multiple times and react to these allocations by other devices. The GT is represented in this Smart Method by the cooperation of each device and by sharing their information about channel selection. Also, the GT typically uses more iterations than one in a total time of evaluation to obtain the output value of the method. The disadvantage of this method

```

input: load or generate Position_matrix, Number_of_Devices, Radio_range, ...
set path by dijkstra_algorithm from device ID_1 to device ID_40
generate channel_allocation to each links in radio range to 1;
Number_of_Iterations = 21;

Initial_parameters for method
for ID_value ← 1 to ID_value ← Number_of_Devices-1 do
if distance of ID_value & ID_value + 1 is lower as Radio_Range do
  device_connection (ID_value,ID_value + 1) = 1;
  set initial_first_value for each devices;
  SIR_rank_channel_initial calculate with RSS as influence ratio;
  RSS_value_device_initial calculate by distance;
  Traffic_value of channel set to 10;
end
end

input to fuzzy logic: SIR_rank_channel, RSS_value_of_device, Traffic_matrix;
rules_for_each_parameter_sets;
output Fuzzy_logic_out_value for channel rank on selected link and iteration;
channel_rank_iteration (1, :, :) = Fuzzy_logic_out_value;

for Number_of_Iterations ← 2 to Number_of_Iterations do
for ID_value ← 1 to ID_value ← number_of_devices + 1 do
if device_connection(ID_value,ID_value + 1) = 1 do
  for channel ← 1 to channel ← 13 do
    Call Functions: SIR_rank_channel;
                   RSS_value_device;
                   Traffic_matrix;
                   Device_links_by_radio_range;
  end
end

input to fuzzy logic: SIR_rank_channel, RSS_value_of_device, Traffic_matrix;
rules_for_each_parameter_sets;
output Fuzzy_logic_out_value for channel rank on selected link and iteration;
channel_rank_iteration (Number_of_Iterations, :, ID_value) = Fuzzy_logic_out_value;

if difference of actual Fuzzy_logic_value and previous selected channel
  Fuzzy_logic_value is higher as threshold_value do
    set channel_allocation of link = channel;
  else
    set channel_allocation of link = channel_allocation (Number_of_Iterations-1);
  end
end
end
end

```

FIGURE 10: Pseudocode of proposed Smart Method.

with more than one iteration is the time that is needed to complete the evaluation. More iterations can enhance the suitability of using a given channel, since repetition can be used to select a more appropriate channel if this channel is available. The main aim is to optimize the network pay-off with the cooperative strategy of devices.

## 4. Simulation and Results

We simulated the proposed algorithms for channel allocation based on IEEE 802.11xx technology in the simulation program Matlab. This program is suitable to use the FL toolbox and to evaluate our definition of rules and parameters for simulations. Also, this environment is suitable for the use of the GT principle for channel selection. We can simulate our proposed Smart Method as a combination of the GT attributes with the FL method. We set an interval for RSS and traffic priority parameters from 0 to 100. We consider the best value of RSS as 100, when two devices are side by side, and the value of 0, when two devices are not within radio range. The traffic value is set at the best value 0 and the worst 100. Generally, a signal ratio is represented by *SIR\_value* of 20 dB or more. It is recommended that data networks should have the *SIR\_value* of 25 dB or more to use voice applications. We set the limit (minimum) value of *SIR\_value* to 18, which represents value in dB, and channel with the higher value is more suitable to be used. Similarly, we predict a signal strength based on the distance, where the radio range of the device is set to 100 m. We consider that the

signal is very strong if a distance between the two devices is lower than 30 m. When two devices are side by side, then the *RSS\_value* is set to 100, because their distance is very low. We consider device distance as large when it is more than 70 m. The *RSS\_value* is “low,” when the value equals 30. We consider the distance of two devices between 30 m and 70 m as “normal.” The initial *Traffic\_value* is set to 10 for the start of the algorithm. Subsequently, the *Traffic\_value* is generated in the range from 10 to 90 when a channel is changed to a link between two devices based on the selected scenario of the simulation. We simulated the channel allocation on the selected path from the Source device with *ID\_1* to the Destination device with *ID\_40*. The path from Source device to a Destination device is selected by Dijkstra’s algorithm.

### 4.1. Game Theory as the Method for Channel Allocation.

The Game Theory with final channel allocation according to this method is shown in Figure 11, where the investigated path from the Source device to the Destination device is shown by the red line. Every device allocates a channel for communication in every iteration. To show the channel change during iterations, we select this path and it is possible to show how the channel rank is changed. Also, we can show how the channel selection influences other devices in the radio range. Other devices react to these game moves and adjust the strategy to them. Each device has a finite set of actions. The GT method is more based on the cooperation of devices in the game. The strategy of the device in a typical game is to win the game. We eliminate the dominant strategy to select the best channel for the device by itself no matter if this selection increases or decreases the pay-off of the other devices and uses the strategy to optimize the channel allocation by coordination to select the channel, which increases the rank of the network. A method based on the game needs to make compromises to improve network routing. Every device is able to communicate with only one device at a one-time slot. Other allocated channels are prepared for devices in case there is a demand to set up a new connection and to start the data transfer with another neighbour device in the radio range. It is not correct and sufficient to set a value of threshold for each parameter due to changes in input parameters at each time step when the device movement occurs. The better choice is to select a threshold of difference between the previous channel rank (RSS, SIR, and traffic) and the current channel rank (RSS, SIR, and traffic). When we set the threshold with low value such as 15, it leads to more channels selection and also more iterations for the optimal channel selection in a network. The higher value of threshold such as 30 or more leads to a lower number of the total iterations for the optimal channel selection. The total number of iterations will be five or lower to allocate the final channel of link. In this scenario, we use the value of the threshold difference set to 20, due to the fact that each parameter is set to an interval from 0 to 100. If the previous channel is selected, then *SIR\_value* of this channel is set to 18, which represents that this channel is suitable to be used but only in case if there is no better channel to be selected. Another channel has a better value if there are not



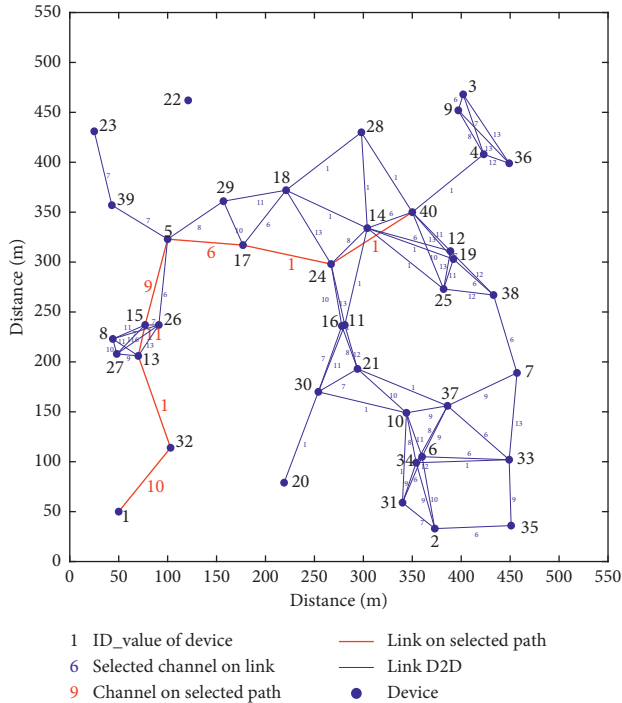


FIGURE 11: Example of the selected network topology with communications and channels allocated by Game Theory (red line represents the path from Source to Destination).

so many devices in the radio range with inappropriate (interference) channels, which influence the quality of this channel. A device with lower  $RSS\_value$  influences the lower SIR parameter compared to a device with higher RSS that influences higher  $SIR\_value$ . The reason for this is the process in which we obtain  $RSS\_value$  in our scenario. We calculate this parameter from a distance of the two devices. When the distance of the two devices is high, the value of RSS is “low,” which also means the low intensity of the signal received at this device. When two devices are close to each other, the value of the RSS is “high” and the intensity of signal strength is better. Parameter traffic is at first iteration set to value of 10. It means there is no data transfer and only this channel is used to send control frames to each device in the radio range. In the second iteration, where the device selects a better channel to communicate with other devices, the value of traffic is changed to the random value from the interval of 10 to 90. The traffic parameter is changed at every channel change, which represents the data flow at the communication channel on each device. There is no need to send packet data between devices; we simulate this transfer by this parameter. When devices make a move (physically) in a one-time slot, every parameter changes. The fixed value of the threshold is not suitable when this value needs to be different in every slot. It is not very suitable to determine a general threshold value appropriate for every possible situation of parameters values combination. This would only be possible if one of the most important parameters is determined as suitable. Only then is it possible to continue the channel rank with other parameters of the link quality. Therefore, it is preferable to

determine the  $threshold\_value$  as the difference between the previously selected channel and the current channel suitable to be used. The exact value of the threshold is at one point sufficient, but when devices make a game move or the physical movement, the same value of the threshold will be insufficient. The evaluation would be possible by additional rules and this would lead to the application of the principle of a simplified version of the FL.

Figure 12 shows the channel change based on the GT method and cooperation strategy on the selected path from the Source device to the Destination device. As we can see, there are a lot of channel changes based on the GT channel allocations in a one-time slot with 20 iterations. The device can change the channel if the  $threshold\_value$  of difference is equal to or higher than 20. Links between selected devices change channels at all possible iterations. Some devices use the same channel for more iterations, due to the fact that there is no better channel to be selected. Also, based on this figure, two links can change the channels just one time for the time slot during the simulation. This means that no better channel with a higher difference as set  $threshold\_value$  is available. If the value of the threshold is set to 20, it shows, in some cases, constant channel use for more iterations, because there is no better channel to select. Some links change channel more often based on the  $threshold\_value$ , if there is a better channel. If we select the threshold to a higher value, then the lower number of channel changes will be made. The higher value of threshold means lower number of changes to optimal channel allocation in networks. The GT method changes the channel of at least one device in every iteration. It means, for this method, to decrease the total number of channel changes, we need to increase the number of input parameters. Figure 12 shows the channel selection based on the GT and, for this selection, we evaluate the channel rank for each channel link on the selected path. We evaluate the channel rank for each method with the FL principle, which only shows statistical values for the comparison of different methods. The FL principle is suitable to be used for statistics of channel rank because the output can be defined on the interval of values based on rules and the membership functions to each parameter as the input of this method. The channel rank based on the GT is shown in Figure 13. The final channel allocation is at the last iteration of each method. Every change of channel rank influences devices in the radio range with their game move based on the strategy sets to cooperate and improve the quality in the network. The device does not change the channel, but the quality of the link decreases or increases. This change is by the channel selection of other devices in the radio range. Each device uses strategy to improve the quality of a link in the network. It means every device, when it makes a game move, uses the strategy of cooperation and selects the best channel to improve the quality, not for its higher pay-off value but to improve the pay-off of the network. The channel rank of these two methods is different due to the total number of channel changes in iterations. The GT method changes channel more often for devices based on the channel rank.



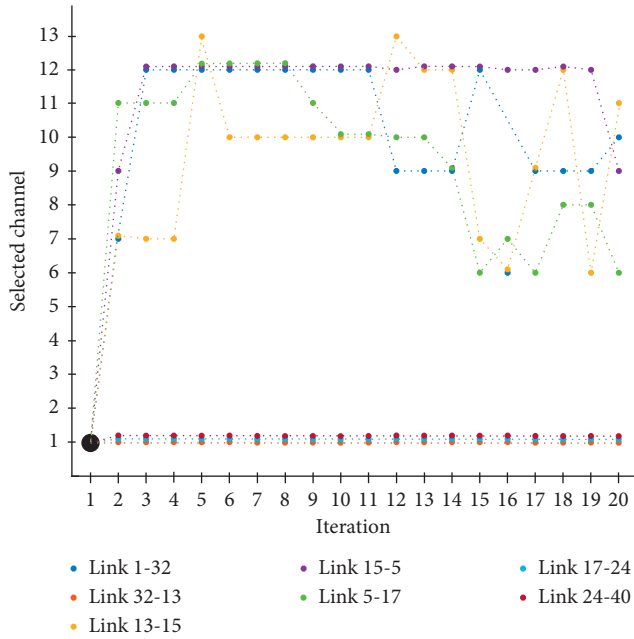


FIGURE 12: Channels determined (allocated) by Game Theory on the selected path.

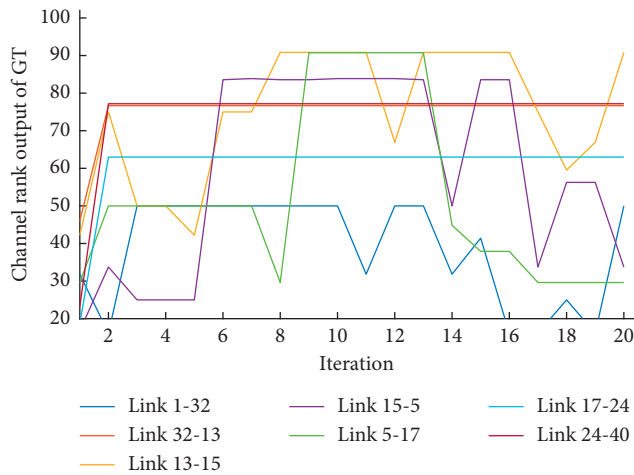


FIGURE 13: Channel rank based on Game Theory on the selected path.

4.2. Fuzzy Logic as the Method for Channel Allocation.

The Fuzzy Logic as a method for channel allocation seems to be more suitable because this is a more precise method to rank each channel based on the membership functions. On the one hand, the FL works as a ranking method, and, on the other hand, the GT works as a method that selects channels based on the strategy directly. Consideration should also be given to the case when the same channels are allocated for communication between different devices. The topology of the network is shown in Figure 14 with selected channels for each device, but at a one-time slot similar to that in GT the device can communicate only with one device. Other channels are ready for possible communication with neighbours. Membership functions use a triangular form or other forms of the functions to define individual values in

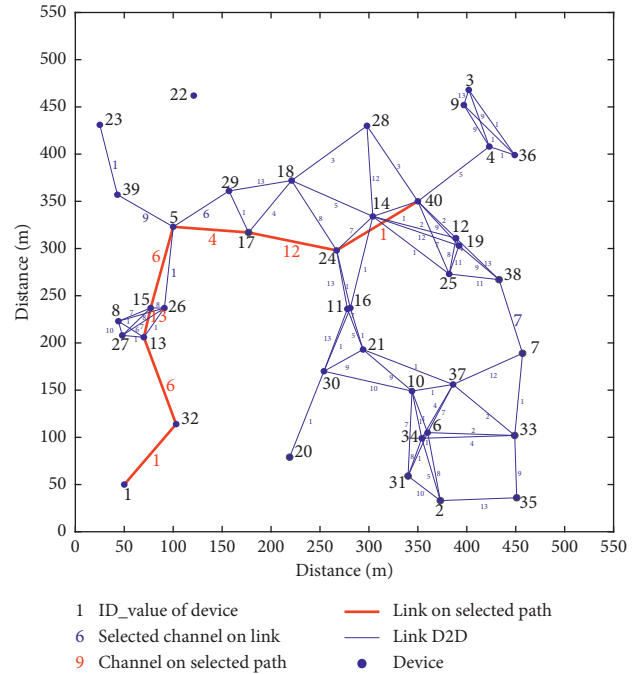


FIGURE 14: Network topology with channels allocated by Fuzzy Logic (red line represents the path from Source to Destination).

extreme cases of the interval, and the trapezoid form function is used in other parameter values. These functions can be seen in the previous subchapter on the FL principle. The FL method uses rules to determine whether a statement is true or false. In this case, we consider rules based on the values of the *RSS\_value*, traffic on a channel, and the SIR ratio of signals. Mobile devices can measure and determine the *RSS\_value* based on the received signal strength. So we assume that the device can determine this value, and therefore we only use the distance of two devices to define the value of this parameter for the simulation process. The output value of the FL based on the rules can be *very suitable*, *more suitable*, *suitable*, *less suitable*, or *nonsuitable*. Some of the rules for this method are shown in Table 5. The main aim is to choose a channel with a suitable value of SIR. Other values of parameters influence how suitable a channel to allocate is. The FL uses only one iteration to choose an optimal channel to increase the quality of the network. Figure 15 shows channel allocations based on the FL method on the selected path.

The FL method based on rules for the input parameters (RSS, traffic, and SIR) evaluates the channel selection. Each device chooses the channel with the highest value to improve the quality of the network. The FL output value is set for each channel from an interval of 0 to 100. This value represents how suitable a channel for communications is. The value represents the evaluation of the channel rank for connection between two devices based on information obtained from the surroundings as well as the transmission of information data. This value is evaluated based on the information obtained from the spectrum sensing and information that the devices share in the radio range. It means that the value is based on cooperation between devices to select a better

TABLE 5: Some rules for Fuzzy Logic used in simulation.

---

If RSS is high and traffic is nonsuitable and SIR is suitable THEN output is very suitable
If RSS is high and traffic is low and SIR is suitable THEN output is more suitable
If RSS is high and traffic is normal and SIR is suitable THEN output is suitable
If RSS is high and traffic is high and SIR is suitable THEN output is less suitable
If RSS is low and traffic is normal and SIR is nonsuitable THEN output is nonsuitable

---

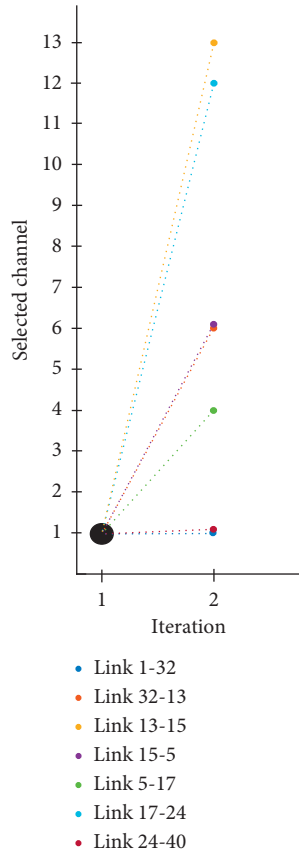


FIGURE 15: Channels determined (allocated) by Fuzzy Logic on selected path.

channel and increase the quality of the network. The rules are defined for each input parameter value to evaluate channel rank in this method. The simulation parameters are the same as those in the GT, a method with 40 devices, and the order of channel selection is based on the ID for each device. This process can be assigned to channel selection based on the MAC address, where the order of the value is determined by this address. The method has only one iteration, where each device based on the ID order selects a better channel for communication, if there is a one based on the *threshold\_value* of difference. The simulation uses *threshold\_value* set to 20. The higher or lower *threshold\_value* influences the countability of channel change. This method also uses the output value of the FL as a channel rank. The device selects a new channel if the value of the difference between the previous channel and the current best channel on the current rank is higher. If this difference is lower, the device uses the same channel. If the movement was used in the simulation, this channel selection would be

repeated at each time slot, when each device moves to a new location. Every time slot consists of channel allocation based on this method. This type of allocation is not so slow in evaluation so it can be used in every time slot with movement. However, the GT with 20 iterations will be slower than the FL to evaluate the final channel allocation for each channel at every time slot. More iterations mean FL with attributes from GT. The method works independently on each device; only channel selection is according to the order based on the ID number in our simulation. In the real operation scenario, each device obtains the necessary information and it performs the channel redistribution process using this method. To redistribute and improve the quality of the network, it is sufficient to choose this method, as the individual devices choose the optimal channel for communication from the available channels, and, at the same time, this channel is suitable for them. Each device makes a move (channel allocation) and responds to the previously selected channels by devices with a lower ID number to all neighbours in the radio range. The channels ranks are shown in Figure 16 with links between two devices on the selected path from the Source device to the Destination device. The channel rank is “low” if there is a large number of interference devices in the radio range. The channel change leads to a more suitable one and obtains a higher output of channel rank in the next iteration. The method uses an interval to define the quality of the channel and not just a Boolean-type of evaluation. Some types of the GT use Boolean logic to define parameters of the link quality. The FL, on the other side, uses the membership functions to define these parameters with mathematical functions with different shapes. Change type of membership function from one type to another one means to change the result of the output value for each defined parameter. The simulation of GT needs 20 iterations to obtain an optimal channel allocation for the network. Same *threshold\_value* and the same input parameters but a different type of membership function together mean a different number of iterations to obtain an optimal channel allocation.

#### 4.3. Smart Method as the Method for Channel Allocation.

The smart channel allocation method of simulation uses 20 iterations to obtain optimal channels for the network in a one-time step when devices do not change their location. The topology of the network is shown in Figure 17. The channel allocation is a process that evaluates the channel allocation between the movements of each device. Time is required to get the input parameters into the method, but subsequent decision-making is performed within a one-time step. The repetition of the simulation shows that the number of iterations does not have to be large, as repetition does not

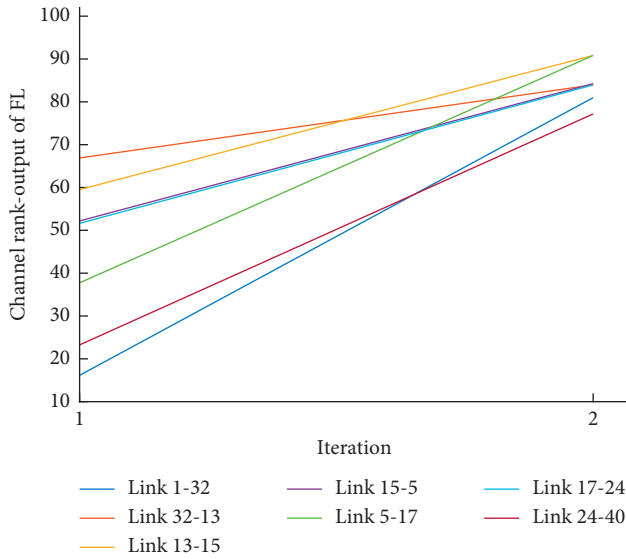


FIGURE 16: Channel rank based on Fuzzy Logic on the selected path.

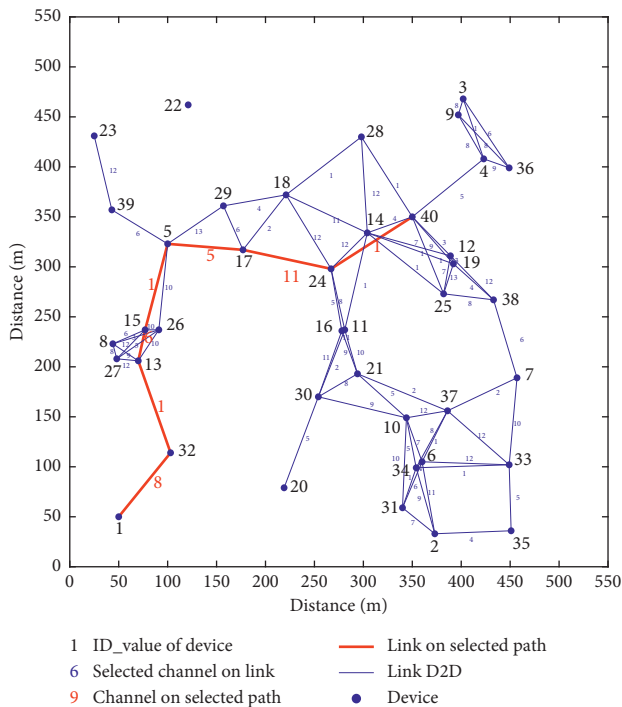


FIGURE 17: Network topology with channels allocated by Smart Method (red line represents the path from Source to Destination).

result in such drastic increases in channel rank if an appropriate decision value is selected. The biggest change of value is at the second iteration, when the allocation of communication channel 1 is changed according to the parameters to a more appropriate one using FL as the method of selection. The subsequent rank of possible channels being used is decreased due to the fact that some of the channels are already used with devices and they will not achieve such a low interference. The output from the Smart Method is the channel allocation for each device in the network, which is

shown in Figure 17. Each link of two devices has a channel for communication, but, in the one-time slot, the device can connect only to one device. So other channels are only to be ready if there is a demand to create a new connection to another device in the radio range. The red line represents the path from the Source device to the Destination device. The Smart Method uses channel rank by the FL, while also taking into account the sharing of information between devices and hence the strategy of device cooperation.

Figure 18 shows channel selection on each iteration of links between two devices on the selected path from Source device to Destination device, based on the Smart Method. It shows how devices stop changing their channels at the tenth iteration; after this iteration, there is no channel change based on the *threshold\_value*. Figure 12 shows a channel selection based on the GT. As one can see, the Smart Method needs fewer iterations steps to optimize the quality of the network. The optimal channel allocations for most of the devices is achieved by eight interactions of the Smart Method; only one link needs more iterations in this selected path to select the optimal channel for communication. After the tenth iterations, there are no more changes, so we can say that ten iterations are enough to select optimal channels for communications in the network because one link between devices 5 and 17 needs more iterations. The device is able to change the channel only if the pay-off is more than the selected threshold, which is set to 20. The threshold value of the channel rank is defined as a difference between a previously selected channel and the currently more suitable channel. The channel rank is an interval of values from 0 to 100, so difference set to 20 can be considered as a percent of change due to fact that the channel rank is without dimensional number. When we set *threshold\_value* lower than 20, it means more channels selections and also more iterations for optimal channel selection in a network. The higher value of threshold such as 30 or more means a lower number of total iterations for optimal channel selection. The total number of iterations will be five or lower to allocate the final channel of the link. A high difference in channel rank is only at the start of the simulation, where each device has a lot of free channels to select. After the first iteration, there is a lower difference between the channel ranks.

Figure 19 shows how channel ranks influence channel selection not only by the device that makes a channel selection but also with other devices in the radio range. Figure 13 shows channel rank based on the GT method. The comparison of these methods in these figures shows that the same input parameter for method influences not only the total time needed to evaluate simulation but also the total number of iterations to obtain the best channel for communication. Allocation based on the Smart Method selects a better channel if the threshold value is higher than the difference between the previous channel rank and the current channel rank. Also, other devices in the radio range negatively influence this rank with no channel change. Figure 19 shows that the channel rank of links for D2D connection can have the same value of channel rank even if the channel is unchanged. Also, this value can be changed based on other device selections in the radio range. It is a

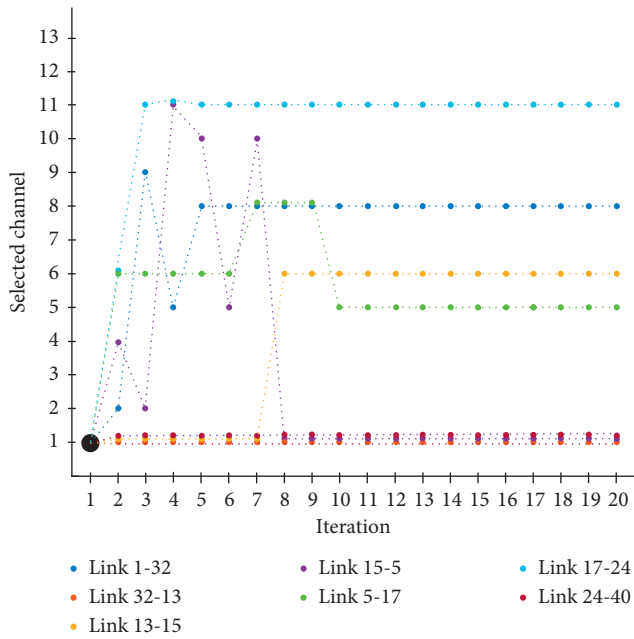


FIGURE 18: Channels determined (allocated) by Smart Method on the selected path.

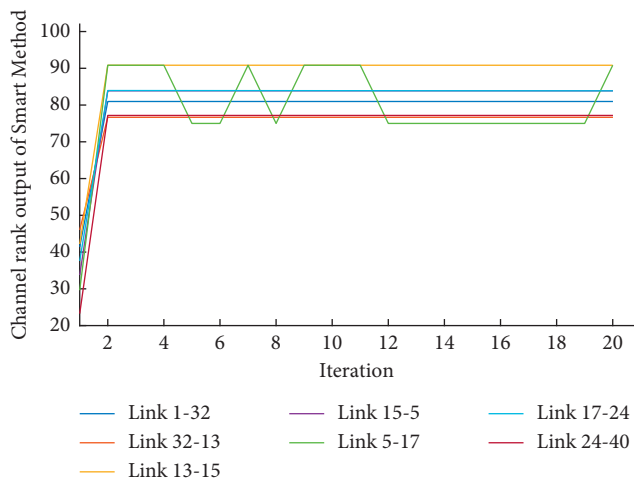


FIGURE 19: Channel rank based on Smart Method on the selected path.

case with not many devices in the radio range, which can affect individual communication on these channels. Therefore, the rank of the channel is without change. Alternatively, an adjacent device changed the channel to a more appropriate channel, and this change helped maintain the rank for the device that did not make the channel change. If the neighbour devices choose the most appropriate channel, the rank of the device will decrease or stay the same; but it is still suitable to maintain a good connection. The effort is to improve the network as a whole, and it is, therefore, possible to accept a deterioration in the evaluation of the channel used, if this value is acceptable and it does not cause a significant decrease in the quality of the connection. A comparison between the GT and the Smart Method only shows the change in rating and usage of channels on the

selected path. Every device in network topology also changes the channels used in each iteration and affects the resulting value of channel ranks on the selected path. Smart Method uses more input attributes to evaluate faster optimal channel selection. The GT is suitable as a method for channel selection, but the Smart Method with parameter definition by membership functions and attributes from the GT decreases the number of iterations needed to evaluate optimal channel selection for selected network topology.

## 5. Conclusion and Future Work

Our proposed algorithms show the effective channel allocation by a method based on Fuzzy Logic, Game Theory, and the Smart Method. For the proper function of channel allocation management, it was necessary to select the appropriate parameters that characterize the quality of the connection to a sufficient level. The Smart Method based on the FL and the GT attributes is more accurate, but the cost of this accuracy is a longer period of evaluation. These methods show that content delivery services in 5G, modern wireless, or mobile networks need radio resource management to increase channel allocation for the faster and better quality of services. As for directions for future work, we intend to aim our research at investigation and evaluation of evolution games as methods for the channel allocations. Also, the next sphere of the research could be neural networks as part of artificial intelligence.

## Data Availability

All relevant data are included within the article.

## Conflicts of Interest

The authors declare that they have no conflicts of interest.

## Acknowledgments

This work has been performed partially in the framework of the Ministry of Education of Slovak Republic under research projects APVV-17-0208, VEGA 1/0492/18, and KEGA 046TUKE-4/2018.

## References

- [1] L. Atzori, A. Iera, and G. Morabito, "The internet of things: a survey," *Computer Networks*, vol. 54, no. 15, pp. 2787–2805, 2010.
- [2] F. O. Ombongi, H. O. Absaloms, and P. L. Kibet, "Resource allocation in millimeter-wave device-to-device networks," *Mobile Information Systems*, vol. 2019, Article ID 5051360, 16 pages, 2019.
- [3] E. Hossain, M. Rasti, and L. Bao Le, *Radio Resource Management in Wireless Networks an Engineering Approach*, Cambridge University Press, Cambridge, UK, 2017.
- [4] M. Matis, D. Neznik, D. Hrabcak, L. Dobos, and J. Papaj, "Intelligent channel assigning in CR-MANET based on spectrum sensing," in *ELMAR 2017*, pp. 83–86, University of Zagreb, Zagreb, Croatia, 2017.



- [5] D. Neznik, L. Dobos, and J. Papaj, "Radio resource management for wireless networks," in *Proceedings of the Radioelektronika 2019: 29th International Conference*, pp. 317–322, Institute of Electrical and Electronics Engineers, Pardubice, Czech Republic, April 2019.
- [6] A. Raschella, L. Militano, G. Araniti, A. Orsino, and A. Iera, "Cognitive management strategies for dynamic spectrum access," in *Handbook of Cognitive Radio*, pp. 1–35, Springer, Berlin, Germany, 2017.
- [7] P. Semba Yawada and M. Trung Dong, "Performance analysis of new spectrum sensing scheme using multiantennas with multiuser diversity in cognitive radio networks," *Wireless Communications and Mobile Computing*, vol. 2018, Article ID 8560278, 13 pages, 2018.
- [8] J. Chen and Q. Zhu, "Background of game theory and network science," in *A Game-And Decision-Theoretic Approach to Resilient Interdependent Network Analysis and Design*, pp. 5–11, Springer, Cham, Switzerland, 2020.
- [9] R. B. Myerson, *Game Theory Analysis of Conflict*, Harvard University Press, Cambridge, MA, USA, 1997.
- [10] T. Başar and G. Zaccour, *Handbook of Dynamic Game Theory*, Springer International Publishing, New York City, NY, USA, 2018.
- [11] S. Pandit and G. Singh, *Spectrum Sharing in Cognitive Radio Networks*, Springer, Berlin, Germany, 2017.
- [12] J. Wen, S.-J. Q. Yang, and S.-J. Yoo, "Optimization of cognitive radio secondary information gathering station positioning and operating channel selection for IoT sensor networks," *Mobile Information Systems*, vol. 2018, Article ID 4721956, 12 pages, 2018.
- [13] Y. Zhang, P. Wan, S. Zhang, Y. Wang, and N. Li, "A spectrum sensing method based on signal feature and clustering algorithm in cognitive wireless multimedia sensor networks," *Advances in Multimedia*, vol. 2017, Article ID 2895680, 10 pages, 2017.
- [14] W. Zhang, *Handbook of Cognitive Radio*, Springer Nature Singapore Pte Ltd., London, UK, 2019.
- [15] L. Wang and F. Li, "Dynamic spectrum pricing with secondary user's normal demand preference," *Mobile Information Systems*, vol. 2018, Article ID 3572508, 8 pages, 2018.
- [16] E. P. Dadios, *Fuzzy Logic—Controls, Concepts, Theories and Applications*, InTech, London, UK, 2012.
- [17] 2020, [http://cs.bilkent.edu.tr/zeynep/files/short\\_fuzzy\\_logic\\_tutorial.pdf](http://cs.bilkent.edu.tr/zeynep/files/short_fuzzy_logic_tutorial.pdf).
- [18] 2020, <https://functionbay.com/documentation/onlinehelp/default.htm#!Documents/fuzzymembershipfunctions.htm>.
- [19] C. Wang, "A study of membership functions on mamdani-type fuzzy inference system for industrial decision-making," A thesis Presented to the Graduate and Research Committee of Lehigh University in Candidacy for the Degree of Masters of Science in Mechanical Engineering and Mechanics, Lehigh University, Bethlehem, PA, USA, 2015.
- [20] E. H. Mamdani and S. Assilina, "An experiment in linguistic synthesis with a fuzzy logic controller," *International Journal of Man-Machine Studies*, vol. 7, no. 1, pp. 1–13, 1975.
- [21] S. Izquierdo and L. R. Izquierdo, "Mamdani fuzzy systems for modelling and simulation: a critical assessment," *SSRN Electronic Journal*, vol. 21, no. 3, 2017.
- [22] T. Takagi and M. Sugeno, "Fuzzy identification of systems and its applications to modeling and control," *IEEE Transactions on Systems, Man, and Cybernetics*, vol. SMC-15, no. 1, pp. 116–132, 1985.
- [23] F. Cavallaro, "A takagi-sugeno fuzzy inference system for developing a sustainability index of biomass," *Sustainability*, vol. 7, no. 9, pp. 12359–12371, 2015.
- [24] W. Song, P. Ju, and A. L. Jin, *Protocol Design and Analysis for Cooperative Wireless Networks*, Springer International Publishing, New York City, NY, USA, 2017.
- [25] J. Machaj and P. Brida, "Optimization of rank based fingerprinting localization algorithm," in *Proceedings of the 2012 International Conference on Indoor Positioning and Indoor Navigation (IPIN)*, pp. 1–7, Sydney, Australia, November 2012.
- [26] M. Haenggi, "SIR analysis via signal fractions," 2020, <https://arxiv.org/abs/2003.03442>.
- [27] F. Afroz, R. Subramanian, R. Heidarz, K. Sandrasegaran, and S. Ahmed, "SINR, RSRP, RSSI and RSRQ measurements in long term evolution networks," *International Journal of Wireless & Mobile Networks (IJWMN)*, vol. 7, no. 4, 2015.
- [28] S. Ishida, Y. Arakawa, S. Tagashira, and A. Fukuda, "Wireless local area network signal strength measurement for sensor localization without new anchors," *Sensors and Materials*, vol. 32, no. 1, pp. 97–114, 2020.
- [29] J. B. Song, H. Li, and M. Coupechoux, *Game Theory for Networking Applications*, Springer International Publishing, New York City, NY, USA, 2019.
- [30] S. Kim, "A new cooperative dual-level game approach for operator-controlled multihop D2D communications," *Mobile Information Systems*, vol. 2019, Article ID 6276872, 11 pages, 2019.
- [31] F. Munoz-Garcia and D. Toro-Gonzalez, *Strategy and Game Theory: Practice Exercises with Answers*, Springer, Berlin, Germany, 2nd edition, 2019.
- [32] D. Neznik and L. Dobos, "Fuzzy logic based channel ranking for CR-MANET," in *Proceedings of the Radioelektronika 2018: 28th International Conference*, pp. 1–5, Institute of Electrical and Electronics Engineers, Prague, Czech Republic, April 2018.
- [33] D. Hrabcak, M. Matis, D. Neznik, L. Dobos, and J. Papaj, "Proposal of simple metrics for evaluation of social ties in mobility models for MANET networks," in *ELMAR 2017*, pp. 87–90, University of Zagreb, Zagreb, Croatia, 2017, ISBN, 978-953-184-230-3.
- [34] N. Aneja and S. Gambhir, "Profile-based ad hoc social networking using Wi-Fi direct on the top of android," *Mobile Information Systems*, vol. 2018, Article ID 9469536, 7 pages, 2018.